

https://dspace.org/

An investigation into the heat transfer aspects of transpiration cooling

Hobson, G. V

2015-08-06
http://hdl.handle.net/10539/18188

Downloaded from a DSpace repository. https://dspace.org/

UNIVERSITY OF THE WITWATERSRAND

JOHANNESBURG

SCHOOL OF MECHANICAL ENGINEERING

AN INVESTIGATION INTO THE HEAT TRANSFER ASPECTS OF TRANSPIRATION COOLING

G.V. HOBSON

A dissertation presented in fulfilment of the requirements for the Degree of Master of Science in Engineering

DECEMBER 1987

DECLARATION

I declare that this dissertation is my own, unaided work. It is being submitted for the degree of Master of Science in the University of the Witwatersrand, Johannesburg. It has not been submitted before for any degree or examination in any other University.

.....

7th day of December 1982.

ABSTRACT

Although transpiration cooling has been demonstrated to keep the metal surface temperatures, in a gas turbine, below that at which oxidation occurs even though the hot gas temperatures are in excess of the metals melting temperature, few experimental studies have been conducted on the heat transfer aspects of transpiration cooling. Especially the effect blowing has on a turbulent boundary layer that has developed over a porous surface that is heated by the mainstream. Many studies have involved the blowing or suction of the boundary layer through heated porous plates.

Transpiration cooling was experimentally investigated by making use of an existing wind tunnel which was modified so as to simulate the heat transfer phenomenon resulting from blowing coolant through a porous wall into a heated mainstream. The existing wind tunnel was designed and commissioned by Krieg (13) who considered the momentum transfer aspects of transpiration cooling. The solution of the momentum equation by Krieg forms the basis from which this investigation was developed, the original solution procedure being put forward by Cebeci and Smith (7). Krieg developed a generalised two-dimensional finite-difference computer program to solve the incompressible momentum equations describing a blown boundary layer. This program was further developed as part of this effort to solve the compressible momentum and energy equations so as to account for the heat transfer in the blown boundary layer. The program is used to predict the experimental results obtained from the literature as well as those obtained during the nine experimental runs on the wind tunnel.

Freestream flow velocities varied from 4,95 m/s to 14,95 m/s with corresponding temperatures of 44,95°C and 33,00°C respectively. The blowing fraction F, was varied from 0,0059 to a maximum of 0,01185 for the free stream velocity of approximately 10 m/s and temperature of 40°C.

The numerically calculated profiles and those obtained experimentally, as well as one set presented by another researcher, compared well. Finally, recommendations for future studies have been suggested.

ACKNOWLEDGEMENTS

I would like to thank Professor C.J. Rallis for his help and supervision throughout this research project, and the National Institute for Aeronautics and Systems Technology for the funding of this project. A special word of thanks to Mrs Alida Kühn for this mammoth typing effort. A final thank you to my wife Dianne and my parents for all the support for this effort.

CONTENTS

	Declaration	ii
	Abstracts	iii
	Acknowledgements	iv
	Contents	1
	List of Symbols	3
CHAPTER		
1	Introduction	7
2	Object	9
3	Literature Review on Transpiration Cooling	10
3.1	Introduction	10
3.2	Experimental Results	11
3.3	Analytical Development	14
4	Development of a Mathematical Model for Predicting the Boundary Layer Behaviour	23
4.1	Introduction	23
4.2	Boundary Layer Parameters	23
4.3	Formulation of Eddy Viscosity and Turbulent Prandtl Number	25
4.4	Boundary Conditions	27
4.5	Transformation of Boundary Layer and Eddy Viscosity Equations	27
5	Computational Solution of Momentum and Energy Equations	30
5.1	Introduction	30
5.2	Linearization of Momentum Equation	30
5.3	The Boundary Layer Equations in Finite Difference Form	30
5.4	The Finite Difference Grid and Finite Difference Molecule	34
5.5	Discussion of Computational Procedure	35

6	Experimental Apparatus and Procedure	40
6.1	Introduction	40
6.2	The Wind Tunnel	40
6.3	Hot wire Anemometry	44
6.4	Experimental Procedure	47
7	Discussion of Experimental Results and Computer Predictions	52
7.1	Introduction	52
7.2	Experimental Results	52
7.3	Comparison of Experimental Results with Computer Program Predictions	79
7.4	Comparison of Mickley, Ross, Squyers and Stewart Results with those Predicted by the Computer Program	92
7.5	Prediction of Stanton Number Variation with Reynolds Number Across the Porous Plate	94
8	Conclusions and Recommendations	99
8.1	Experimental Results	99
8.2	Computer Predictions	100
8.3	Recommendations for Future Study	101

APPENDICES

A1	Transformation of Energy Equation	103
A2	Finite Difference Form of Energy Equation	108
B1	Heat Transfer Through Porous Material	114
C1	Calibration Curves	129
D1	Experimental Results	131
E1	Comparison of Mickley et al Results	141
F1	Initial Temperature Profiles	143
G1	Computer Program	145
H1	Experimental Analysis	173
	List of References	176

LIST OF SYMBOLS

A	Van Driest Damping factor
A^+	Dimensionless Damping factor
B_h, b_h	Blowing parameter ($= \dot{m} / G_\infty St_0$)
C	Viscosity-density parameter ($= \rho\mu/\rho_e\mu_e$)
C_f	Coefficient of skin friction
C_p	Specific heat at constant pressure
F	Blowing parameter ($= \rho_w v_w/\rho_\infty u_\infty$)
f	Dimensionless stream function
G_∞	Mass velocity of free stream ($= \rho_e u_e$)
G	Defect-shape factor
g	Enthalpy ratio
H^*	Shape factor
H	Stagnation enthalpy ($=h + u^2/2$)
h	Specific enthalpy, heat transfer coefficient
K	Variable grid system parameter
k	Thermal conductivity
L	Reference body length
l	Mixing length
$\dot{m}$	Transpiration rate
Nu	Nusselt number
p	Pressure
Pr	Prandtl number
Pr_t	Turbulent Prandtl number
q	Heat transfer rate per unit area ($= k\, dT$ [illegible]
Re_x	Reynolds number based on distance along the plate
Re_h	Reynolds number based on enthalpy thickness
r	Recovery factor, radial distance
r_0	Radius of body of revolution
St	Stanton number
St_0	Stanton number in the absence of blowing
T	Temperature
T_1, T_∞, T_e	Free Stream temperature
T_w	Wall temperature

LIST OF SYMBOLS

A	Van Driest Damping factor
A^+	Dimensionless Damping factor
B_h, b_h	Blowing parameter ($= \dot{m} / G_\infty \, St_0$)
C	Viscosity-density parameter ($= \rho\mu / \rho_e \mu_e$)
C_f	Coefficient of skin friction
C_p	Specific heat at constant pressure
F	Blowing parameter ($= \rho_w \, v_w / \rho_\infty \, u_\infty$)
f	Dimensionless stream function
G_∞	Mass velocity of free stream ($= \rho_e u_e$)
G	Defect-shape factor
g	Enthalpy ratio
H^*	Shape factor
H	Stagnation enthalpy ($=h + u^2/2$)
h	Specific enthalpy, heat transfer coefficient
K	Variable grid system parameter
k	Thermal conductivity
L	Reference body length
l	Mixing length
$\dot{m}$	Transpiration rate
Nu	Nusselt number
p	Pressure
Pr	Prandtl number
Pr_t	Turbulent Prandtl number
q	Heat transfer rate per unit area ($= k \, dT/dy$)
Re_x	Reynolds number based on distance along the plate
Re_h	Reynolds number based on enthalpy thickness
r	Recovery factor, radial distance
r_0	Radius of body of revolution
St	Stanton number
St_0	Stanton number in the absence of blowing
T	Temperature
T_1, T_∞, T_e	Free Stream temperature
T_w	Wall temperature

T_0	Temperature of coolant on cold side of porous wall
t^+	Dimensionless temperature $= [(T-T_w)/(T_\infty-T_w)](\sqrt{C_f/2}/St)$
u	Velocity (x-direction)
u_1, u_∞, u_e	Free stream velocity
u^+	Dimensionless velocity $(= u/U_\tau)$
U_τ, u_w^*	Shear velocity $(= \sqrt{\tau_0/\rho})$
v	Velocity (y-direction)
v_w	Wall coolant velocity
x	Distance along wall
y	Distance normal to wall
y^+	Dimensionless distance from wall $(= y\, U_\tau/\nu)$
$\bar{y}$	Dimensionless distance from wall $(= y/\delta)$

GREEK SYMBOLS

β	Generalised profile factor, dimensionless velocity gradient $[= (2\xi/u_e)\ (du_e/dx)]$
γ	Intermittency factor
δ, δ^*	Displacement Thichness
δ_t	Displacement Thickness of enthalpy profile
Δ	Defect displacement thickness
ε_m	Eddy viscosity
ε^+	Dimensionless eddy viscosity $(= \varepsilon/\nu)$
ε_H, λ_t	Eddy thermal conductivity
κ	Universal mixing length constant
η	Transformed y coordinate
θ	Momentum thickness
μ	Dynamic viscosity
ν	Kinematic viscosity
ξ	Transformed x coordinate
ρ	Density
$\rho_1, \rho_\infty, \rho_e$	Free stream density
ρ_w	Coolant Density
τ	Shear stress
τ_0, τ_w	Wall shear stress
ϕ	Dimensionless mass transfer rate $[= F/(C_f/2)]$ translated stream function $(=f - \eta)$
ϕ_{Ii}	Dimensionless heat transfer rate $[= \rho_w\ v_w\ C_p/h_*]$
ψ	Dimensionless stream function
Λ	Dimensionless pressure gradient $[= (\delta^*/\nu)(du/dx)]$
ω	Coolant mass flow per unit area

SUBSCRIPTS

a	interface of laminar sublayer and outer turbulence region
e	free stream quantity
g	free stream quantity
H,h	enthalpy
i	inner laminar sublayer
m	momentum
o	outer fully turbulent region
t	turbulent
w	wall
*	absence of blowing
0	coolant initial condition (before entering the porous wall)
1	free stream quantity

SUPERSCRIPTS

'	fluctuating quantity, derivative w.r.t. η
k	flow index (= 0 two dimensional flow, = 1 axisymmetric flow)
+	non-dimensional
-	integral time averaged quantity
~	dimensionless quantity

SUBSCRIPTS

δ	interf... f lar nar sublayer and outer turbulence region
e	free tream quantity
g	free stream quantity
H,h	enthalpy
i	inner laminar sublayer
m	momentum
o	outer fully turbulent region
t	turbulent
w	wall
*	absence of blowing
0	coolant initial condition (before entering the porous wall)
1	free stream quantity

SUPERSCRIPTS

'	fluctuating quantity, derivative w.r.t. r.
*	flow index = 0 two dimensional flow, = 1 axisymmetric flow)
+	non dimensional
-	integral time averaged quantity
~	dimensionless quantity

1 INTRODUCTION

Transpiration cooling is a most effective method of keeping metal surface temperatures, in gas turbine engines that are subjected to hostile high temperature environments, well below the melting or oxidation temperature of that particular material. Far less coolant is needed to achieve this, than conventional cooling techniques, such as film cooling that has to date been used in the hot end of gas turbine engines. Transpiration cooling has been demonstrated to keep the metal surface temperatures, in a gas turbine, below that at which oxidation occurs even though the hot gas temperatures are in excess of the metals melting temperature.

As a result of these features of transpiration cooling, much research has been devoted to the study of this phenomenon. However, little experimental work has been conducted, and documented, on the heat transfer aspects or the effect blowing has on a turbulent boundary layer that has developed over a porous surface that is heated by the mainstream. Many studies, the results of which are discussed, have involved the blowing or suction of the boundary layer through heated porous plates.

Transpiration cooling was experimentally investigated by making use of an existing wind tunnel which was modified so as to simulate the heat transfer phenomenon resulting from blowing coolant through a porous wall into a heated mainstream. The existing wind tunnel was designed and commissioned by Krieg (13) who considered the momentum transfer aspects of transpiration cooling. The solution of the momentum equation by Krieg forms the basis from which this investigation was developed, the original solution procedure being put forward by Cebeci and Smith (7). Krieg developed a generalised two-dimensional finite-difference computer program to solve the incompressible momentum equations describing a blown boundary layer. This program was further developed as part of this effort to solve

the compressible momentum and energy equations so as to account for the heat transfer in the blown boundary layer. The program is used to predict the experimental results obtained from the literature as well as those obtained during the nine experimental runs on the wind tunnel.

Conclusions were made and recommendations for future research are put forward so as to ultimately enable the successful implementations of transpiration cooling in gas turbine designs that need cooling of heated surfaces. This can only be achieved if both the momentum and heat transfer aspects of transpiration cooling can be accurately predicted.

2 OBJECT

Transpiration cooling has long been considered as the most effective method to cool components in a hostile high temperature environment. Film cooling has become an integral part in the design of first stage stator vanes, rotor blades and combustion chambers of existing modern gas turbine engines. Transpiration cooling has been successfully employed to cool gas turbine engine components in rotating test rigs (Curtiss Wright publications) and stationary combustion rigs (Bayley).

Even though the practical application of transpiration cooling has been developed to a mature state, very little experimental work has been done especially on the heat transfer aspects of a blown boundary layer. A great deal of research has been done in the field of transpiration cooling although most studies have involved the blowing or suction of the boundary layer through heated porous plates. Thus inverse transpiration cooling, actually transpiration heating, was investigated. The inverse temperature profile acts as a turbulence inhibiter, thus affecting the heat transfer mechanism. Thus it was felt that tests should be conducted over a porous flat plate with a heated mainstream.

Use was made of an existing experimental rig which enabled tests to be carried out on a flat plate in 2-D flow. The rig was modified by inserting a heating system into the mainstream air so as to raise its temperature. A set of data for uniform blowing of a hot turbulent boundary was to be established with which computed results could be compared.

The heat transfer phenomenon within the porous material is also of interest and as such will be considered important.

3 LITERATURE REVIEW ON TRANSPIRATION COOLING

3.1 Introduction

The transpired boundary layer may be laminar or turbulent. The laminar boundary layer with transpiration has been extensively studied, resulting in a large number of exact mathematical solutions for certain fundamental cases where similarity in velocity profiles, and in temperature profiles, is obtained. In 1947 Yuan presented a paper on a theoretical investigation of flow of a hot fluid over a sweat-cooled porous plate. He considered laminar, incompressible flow of both the mainstream and coolant flows which were assumed to have the same viscosities. Soon after this an experimental study of transpiration cooling was reported on by Duwez and Wheeler (1948). The authors investigated a high speed, high temperature (300 m/s; 1000°C) axial flow within a cylindrical duct of porous material through the walls of which coolant was injected.

The pioneering study of Mickley et al (1956) involved the study of heat, mass and momentum transfer of flow over a flat plate with blowing or suction. This has long been regarded as the basic experimental study in this field, and is the only one which covered blowing and suction over any appreciable range of conditions. The validity of these data was questioned, in 1957, by Mickley himself, in a second report. Mickley's second study did not report any heat-transfer data, focusing entirely on the hydrodynamic problem. Nevertheless the initially reported data is still used for qualifying rigs and for comparison with analytical or computer profiles.

The review will be dealt with in two parts:

(a) Experimental Results

(b) Theoretical Developments

With Internal Heat Transfer (within the porous material) being dealt with in Appendix B.

Experimental work in turbulent boundary layer studies has always preceeded the theoretical progress, thus these titles will be dealt with in their historical order.

3.2 Experimental Results

A review of the literature shows that although, the problem of heat transfer through a turbulent boundary layer with uniform blowing, uniform surface temperature, and uniform free-stream velocity has been extensively studied, no similar study of a heated free-stream, to this investigation has been undertaken. Nevertheless the various publications on the above topic have been used as an initial test for the proposed computer program which should be able to predict the various cases considered.

As already mentioned, Mickley et al (1954) carried out extensive experimental measurements of velocity and temperature profiles and of friction and heat transfer coefficients for a wide range of flow conditions. Main-stream velocity was varied between 2 and 20 m/s, and a length Reynolds number range from 6 500 to 3 300 000 was covered.

The experimental apparatus used enabled the simulation of flow over a porous flat plate with acceleration or deceleration of the main flow and for sucking or blowing of a gas through the flat plate out of or into the main stream. The flow in the tunnel was laminar at the lowest velocity and turbulent at the highest velocity. At the intermediate velocity the flow was generally laminar in suction runs and turbulent in blowing runs (supporting the fact that transpiration cooling is turbulence promoting). Direct heat transfer measurements were made at points ranging from 75 mm to 2,5 meters from the leading edge. Data were obtained with mass transfer through the test-wall sections adjusted to give both constant velocity and constant dimensionless mass transfer rate ($v_w \propto 1/\sqrt{x}$ in laminar regime, and $v_w \propto 1/x^{0,2}$ in turbulent regime) with both blowing and suction. Constant velocity runs were made

with v_w varying from 0,04 to -0,04 m/sec and constant ϕ runs were made with ϕ_H (dimensionless heat transfer rate) varying from 1,2 to -3,6.

Temperature profile measurements were conducted under similar conditions. The dimensionless temperature, $\theta_H = (T_w-T)/(T_w-T_G)$ was plotted as a function of the dimensionless distance ratio y/ξ for the cases where the boundary layer was turbulent. The curves represented data obtained at several different traversing stations and consequently represented a wide variation in downstream distance. A few temperature profiles were compared directly with their corresponding velocity profiles which were found to be similar except in the region very close to the wall. The best similarity of the profiles were found in the runs with no mass transfer. In the runs with constant blowing velocity, a slight change in the shape of the velocity and temperature profiles with distance from the leading edge was noticed. This was possibly due to the change in the value of the dimensionless heat transfer rate (ϕ_H).

The turbulent profiles were examined on logarithmic coordinates to investigate their tendency to follow a power-law distribution. The resulting plots could be fitted by a straight line although they may better be fitted by a line with some upward curvature, but the precision of the data was felt not to be good enough to justify trying to fit such a curve to the results

Heat transfer coefficients were measured at various, x, stations along the porous plate for different test runs. These were plotted on logarithmic axes with the laminar region being predicted by boundary layer theory, which tended to give low values, the turbulent region being compared with the predictions of the Chilton-Colburn empirical relation

$$\frac{h_*}{u_\infty \rho_\infty C_p} \left(\frac{C_p \mu}{k}\right)^{2/3} = \frac{0,0288}{(Re_x)^{0,2}} \qquad \ldots 3.2.1$$

which gave good agreement with the experimental data.

The experimental results described by Kays and Moffat are all derived from the Stanford University apparatus which was used by various authors who modified the tunnel to permit studies of accelerating and decelerating flows. Figures of Stanton number as a function of x-Reynold's number for uniform blowing and suction where presented (for values of blowing fraction F varying from -0,0076 to + 0,0096). Blowing drove the Stanton number towards zero as the blowing fraction increased whereas suction tended to force the Stanton number to an asymptotic value numerically equal to the negative blowing fraction value (-F).

The data showed that the quantity St/St_0, denoting the ratio of the Stanton number with blowing to that without blowing (at the same Reynolds number), is a function of the blowing parameter. The relation being;

$$\frac{St}{St_0}_{Re_x} = \frac{\ln (1 + B_h)}{B_h} \qquad \ldots 3.2.2$$

Where $B_h = \frac{\dot{m}}{C_p S_t}$ ($\dot{m}$ = mass injection rate, u_∞ = free stream velocity of the ... stream)

A local descriptor of the boundary layer behaviour was sought and emphasis was focused upon the relationship between Stanton number and enthalpy thickness Reynolds number. By combining the two-dimensional energy integral equation with the relation described by equation 3.2.2 and with an equation describing the variation of St_0 with Re_x the following expression was presented:

$$\left.\frac{St}{St_0}\right|_{Re_h} = \left[\frac{\ln (1 + B_h)}{B_h}\right]^{1.25} (1+B_h)^{0.25} \qquad \ldots [3.2.3]$$

Implicit in equation 3.2.3 is the notion of local equilibrium: it is presumed that knowledge of Re_h and B_h will fix St/St_0, regardless of the upstream history. This was tested by experiments in the vicinity of a step change in blowing: the boundary layer was found to respond very rapidly to the step, with Stanton number dropping almost all the way from the unblown value to the uniformly blown value within a distance of 10 centimeters of the porous section.

Velocity and temperature profiles for the case of constant velocity (approximately 10 m/s), constant wall temperature (ΔT about 25°F) with injection of air into air were presented on the so-called "inner layer" coordinates, $u^+ (= u/U_\tau)$ and $y^+ (= y U_\tau/\nu)$ [where $U_\tau = \sqrt{\tau_0/\rho}$]. The temperature parameter t^+ being defined as follows:

$$t^+ = \frac{T - T_w}{T_\infty - T_w} \frac{\sqrt{\frac{C_f}{2}}}{St} \qquad \ldots [3.2.4]$$

which includes $C_f/2$ as well as St and hence is sensitive to the hydrodynamics as well as the heat transfer. This form follows from a Couette-flow analysis in which the terms are made dimensionless using U_τ. The fact that t^+ includes both $C_f/2$ and St means that t^+ profiles have inherently more scatter than u^+ profiles thus more caution should be exercised in attributing significance to the details of t^+ variations than to u^+ variations because of the added uncertainty involved.

3.3 Analytical Development

Rubesin in 1954 presented an analytical estimation of the heat transfer and skin friction characteristics by solving the continuity, momentum and energy Navier - Stokes equations for turbulent flow. These "turbulent flow" equations

are time averaged and the usual boundary-layer assumptions are imposed. The equations are:

$$\frac{\partial}{\partial x}(\bar{\rho}\bar{u}) + \frac{\partial}{\partial y}(\bar{\rho}\bar{v} + \overline{\rho' v'}) = 0 \qquad \ldots|3.3.1|$$

$$\bar{\rho}\bar{u}\frac{\partial \bar{u}}{\partial x} + (\bar{\rho}\bar{v} + \overline{\rho' v'})\frac{\partial \bar{u}}{\partial y} = \frac{\partial}{\partial y}(\bar{\mu}\frac{\partial \bar{u}}{\partial y} - \bar{\rho}\overline{u'v'}) \qquad \ldots|3.3.2|$$

$$\bar{\rho}\bar{u}\frac{\partial}{\partial x}(C_p\bar{T} + \frac{\bar{u}^2}{2}) + (\bar{\rho}\bar{v} + \overline{\rho' v'})\frac{\partial}{\partial y}(C_p\bar{T} + \frac{\bar{u}^2}{2}) =$$

$$\frac{\partial}{\partial y}(\bar{k}\frac{\partial \bar{T}}{\partial y} + \bar{\mu}\bar{u}\frac{\partial \bar{u}}{\partial y} - \bar{\rho}C_p\overline{v'T'} - \bar{u}\,\bar{\rho}\,\overline{u'v'}) \qquad \ldots|3.3.3|$$

The basic equations were reduced to ordinary differential equations and applied to the fully turbulent region by omitting all the terms based on molecular transport. In the laminar sublayer all the terms based on eddy transport were omitted.

The analysis was divided into two parts, in the first the Prandtl number and turbulent Prandtl number were both assumed to be equal to unity. This resulted in a direct relationship between the temperature and velocity, thus it was not necessary to solve the energy equation. A relationship was thus obtained between the local skin-friction coefficient and Reynolds number with the momentum thickness as the characteristic dimension. The expression obtained was as follows:

$$\ln\left\{\frac{K\sqrt{\frac{C_f}{2}\left(\frac{C_f}{2} + \frac{\rho_w v_w}{\rho_1 u_1}\right)}Re_x}{y_a^+}\right\} = G \qquad \ldots|3.3.4|$$

where

$$G = \frac{2K\left(\frac{T_1}{T_w}\right)^{\frac{1}{2}}}{A\sqrt{\frac{\rho_w v_w}{\rho_1 u_1}}\sqrt{B-\alpha}}\left\{F\left[k_m, \phi_m(\tilde{u}_a)\right] - F\left[k_m, \phi(1)\right]\right\}$$

$$k_m^2 = \frac{B+\alpha}{B-\alpha} < 1 \quad ; \quad A = \sqrt{\frac{\left[(\gamma-1)/2\right] M_1^2}{(T_w/T)}}$$

$$\sin^2\phi_m = \frac{B-\tilde{u}}{B+\alpha} \quad ; \quad B = \frac{1+\left[(\gamma-1)/2\right]M_1^2}{(T_w/T)} - 1$$

$$\alpha = \frac{B - \sqrt{B^2+4A^2}}{2A^2} \qquad \ldots|3.3.5|$$

$$\beta = \frac{B + \sqrt{B^2+4A^2}}{2A^2}$$

$$G = \frac{(C_f/2)}{\sqrt{\left(\frac{\rho_w v_w}{\rho_1 u_1}\right)}}$$

The term $F(k,\phi)$ is an elliptic integral of the first kind.

The second part of the analysis recognised that the local heat transfer coefficient is dependent on Pr and Pr_t and that a relationship between the local Stanton number and local skin friction coefficient was determined. The momentum [illegible] and energy [illegible] equations were integrated to give the following result:

$$\rho_w v_w u = (\mu + \varepsilon_m)\frac{du}{dy} + C_1 \qquad \ldots|3.3.6|$$

$$\rho_w v_w \left(C_p T + \frac{u^2}{2}\right) = \left(\frac{\mu}{Pr} + \frac{\varepsilon_m}{Pr_t}\right)\frac{d}{dy}\left(C_p T\right) + (\mu+\varepsilon_m)\frac{d}{dy}\left(\frac{u^2}{2}\right) + C_2 \qquad \ldots|3.3.7|$$

once the following substitutions were made

$$\varepsilon_m = - \frac{\bar{\rho} \overline{u'v'}}{\frac{d\bar{u}}{dy}} \qquad \ldots|3.3.8|$$

$$\varepsilon_H = \frac{\varepsilon_m C_p}{Pr_t} = - \frac{\bar{\rho} C_p \overline{v'T'}}{\frac{dT}{dy}} \qquad \ldots|3.3.9|$$

and the bars representing time-averaged quantities dropped as all the terms remaining are mean values. (C_1 and C_2 are arbitrary constraints). Once the following boundary conditions were applied, namely that at

$$\ldots|3\ 3.10|$$

$$y = 0$$

$$u = 0$$

$$\varepsilon_m = 0$$

$$T = T_w$$

$$\tau_w = \mu \left.\frac{du}{dy}\right|_w$$

$$q_w = -k \left.\frac{dT}{dy}\right|_w = - \frac{\mu}{Pr} \left.\frac{d(C_p T)}{dy}\right|_w$$

the constants can be evaluated as

$$C_1 = -\tau_w \qquad \ldots|3.3.11|$$

$$C_2 = q_w + \tau_w v_w C_p T_w \qquad \ldots|3.3.12|$$

Thus equations 3.3.6 and 3.3.7 could be written as

$$\rho_w v_w u + \tau_w = (\mu + \varepsilon_m) \frac{du}{dy} \qquad \ldots|3.3.13|$$

$$\rho_w v_w \left|C_p(T-T_w) + \frac{u^2}{2}\right| - q_w = \left(\frac{\mu}{Pr} + \frac{\varepsilon_m}{Pr_t}\right) \frac{d}{dy}(C_p T) + (\mu+\varepsilon_m) u \frac{du}{dy} \qquad |3.3.14|$$

The terms of equation 3.3.14 were divided into the terms of equation 3.3.13 to give

$$\frac{\rho_w v_w \left[C_p (T - T_w) + \frac{u^2}{2}\right] - q_w}{\rho_w v_w u + \tau_w} = \frac{\left(\frac{\mu}{Pr} + \frac{\varepsilon_m}{Pr_t}\right)}{(\mu + \varepsilon_m)} \frac{d}{du}(C_p T) + u \quad \ldots |3.3.15|$$

Equation 3.3.15 is integrated in two stages with the results combined at the sublayer - outer turbulent layer interface where $u = u_a \left(= \frac{u_a}{u_1}\right)$. The resulting solution was given as follows:

$$\frac{q_w}{\rho_1 u_1} = \frac{(C_p T - C_p T_1 - r \frac{u_1^2}{2}) \frac{\rho_w v_w}{\rho_1 u_1}}{\frac{C_f}{2} Pr \left(\frac{\rho_w v_w}{\rho_1 u_1} \tilde{u}_a + \frac{C_f}{2}\right) + Pr_t \left(\frac{\rho_w v_w}{\rho_1 u_1} + \frac{C_f}{2}\right)^{Pr_t - 1}} \quad |3.3.16|$$

The heat transfer coefficient is defined as

$$h = \frac{q_w}{T_w - T_1 - r \frac{u_1^2}{2C_p}} \quad \ldots |3.3.17|$$

where r is the recovery factor.

The final relationship obtained between heat transfer and skin friction is

$$\frac{C_f}{2} = \frac{\left(\frac{\rho_w v_w}{\rho_1 u_1}\right)}{\frac{1-Pr}{Pr-Pr_t} \left(\frac{\rho_w v_w}{\rho_1 u_1} + \frac{C_f}{2}\right) + Pr_t} - \frac{C_f}{2} \quad \ldots |3.3.18|$$

Despite a large number of experimental and theoretical investigations have been devoted to obtaining the eddy viscosity (ε_m), only a few studies have been made of the turbulent Prandtl number, with only one experimental study by Simpson, Whitten and Moffat in 1970 on the effect of blowing or suction on Pr_t. The authors concluded that the assumption of $Pr_t = 1$ throughout the boundary does not hold, especially near the wall where $Pr_t < 1$ as the small scale turbulence is strongly affected by molecular kinematic viscocity. In the outer region it was found that $Pr_t > 1$ where the kinematic viscosity has little influence.

Jenkins, (11) devised a model to account for the unequal loss of momentum and thermal energy from an eddy in flight between mixing points for a fluid with the Prandtl number not equal to unity. He argued that if the temperature of the eddy did not change in flight. then the definition of the mixing length

$$l = \frac{\sqrt{(\tau_t/\rho)}}{\frac{du}{dy}} \qquad \ldots|3.3.19|$$

$$\text{plus} \quad \varepsilon_H \frac{dT}{dy} = \overline{v'T'} \qquad \ldots|3.3.$$

$$\text{would produce} \quad \varepsilon_H = l\, v' \qquad \ldots|3.3.21|$$

since $|T'| = l \frac{dT}{dy}$. However if heat were lost, the fluctuation temperature would be less because of molecular thermal conductivity and thus

$$\varepsilon_H = l\, |v'| \frac{(T_f - T_i)}{l \left(\frac{dT}{dy}\right)} \qquad \ldots|3.3.22|$$

where T_i and T_f are the initial and final eddy mean temperatures. By treating the effects of molecular viscosity on an eddy in flight in the same manner as the effects of molecular thermal conductivity he obtained the following results

$$Pr_t = \frac{1}{Pr} \left\{ \frac{\frac{2}{15} - \frac{12}{\pi^6} \left(\frac{\varepsilon}{\nu}\right) \sum_{n=1}^{\infty} \frac{1}{n^6} \left(1 - \exp - \frac{n^2 \pi^2}{\varepsilon / \nu}\right)}{\frac{2}{15} - \frac{12}{\pi^6} \left(\frac{\varepsilon}{\nu}\right) \sum_{n=1}^{\infty} \frac{1}{n^6} \left(1 - \exp - \frac{n^2 \pi^2}{\left(\frac{\varepsilon}{\nu}\right) Pr}\right)} \right\}$$

This model agrees well with experimental results near the wall, as it should as the small scale turbulence effects are governed by molecular properties (near wall), but fails in the outer region because the model fails to acccunt for the larger eddy motion in the outer region.

For the outer region Hinze (10) in 1959 suggested that the diffusion of heat might be a combination of gradient and large eddy transport of the form

$$\frac{\dot{q}_t''}{\rho C_p (T_w - T_\infty)} = \varepsilon_m \frac{d\bar{T}}{dy} + \frac{\overline{V_E T'}}{(T_w - T_\infty)} \qquad \ldots |3.3.24|$$

where $|V_E| = V_p$ is the effective velocity at which the turbulence energy is transported in the y direction by eddy motion and $\dot{q}_t''$ is the heat flux.

Bradshaw et al (3) in 1967 suggested that V_p varies roughly linearly from zero to V_{p_∞} throughout the boundary layer. If it is assumed that

$$|T'| = l \frac{dT}{dy} \qquad \ldots |3.3.25|$$

$$\text{then } \overline{V_E T'} = V_{p_\infty} \eta l \frac{dT}{dy} \qquad \ldots |3.3.26|$$

where η is the dimensionless distance (y/δ)

Hence equation 3.3.24 becomes

$$\frac{\dot{q}_t''}{\rho C_p u_\tau (T_w - T_\infty)} = (\varepsilon_m + V_{p_\infty} \eta l) \frac{d\bar{T}}{dy} \qquad \ldots |3.3.27|$$

Thus $\varepsilon_H = \varepsilon_m + V_{p_\infty} \eta l$ $\qquad \ldots |3.3.28|$

$$\text{and} \quad Pr_t = \frac{\varepsilon_m}{\varepsilon_m + V_{p_\infty} \eta l} \qquad \ldots |3.3.29|$$

In the outer region the hypothesis of large eddy transport of heat but not of momentum is seen to account for $Pr_t < 1$ and to adequately describe the variation of Pr_t as this agrees with experimental results presented by Simpson et al (21).

Rotta (18) suggested an empirical distribution, which combines both equations 3.3.29 and 3.3.23 to describe the variation of Pr_t in both the inner and outer regions. The relationship has the following form for an unblown boundary layer.

$$Pr_t = 0,95 - 0,45\eta^2 \qquad \ldots |3.3.30|$$

Cebeci and Smith (5) presented a finite-difference method for solving laminar and turbulent boundary-layer equations for compressible two dimensional or axisymmetric flows. An implicit finite difference technique was employed to solve the linearized momentum equation and energy equation. A mixing length formulation based on Van Driest (22) was used for the sublayer and the blending region, and a formulation using intermittency for the fully turbulent region.

Cebeci (5) extended Van Driest's theory, which provided for a continuous velocity and shear distribution for turbulent flow near a non-porous wall, to turbulent flow near a porous wall.

The Van Driest velocity gradient relationship was extended to flows with injection

$$\frac{du^+}{dy^+} = \frac{2(v_w^+ u^+ + 1)}{1 + \{1+4 (v_w^+ u^+ + 1)\cdot^2 (y^+)^2 [1 - \exp(-y^+/A^+)]\cdot^{1/2}} \qquad \ldots |3.3.31|$$

Kays and Moffat (12) looked at the behaviour of the transpired boundary layer in general. Both the momentum and energy (or thermal) boundary layer development for both injection and suction in accelerating, decelerating and constant mainstream flows were discussed. Particular emphasis being placed on equilibrium boundary layers, that is flows where the rates of transpiration and variations of free stream velocity along the test plate are adjusted so that the boundary layer structure remains virtually the same as the flow develops. In this way, effects of transpiration (and

pressure gradient) may be studied free from the effects of upstream disturbances.

It was concluded that it is possible to have inner region similarity (although the outer region may extend over most of the boundary layer). The energy integral equation of the boundary layer was presented in the following form

$$\frac{dRe_h}{U_\infty \, dx/\nu} = St + \frac{v_w}{U_\infty} \qquad \ldots |3.3.32|$$

which has no pressure gradient term. For a turbulent thermal boundary layer over a constant temperature surface with constant free stream velocity outer region similarity can also be deduced.

A solution of the energy equation, to mathematically model the boundary layer, was discussed. Two different empirical equations were presented for the variation of turbulent Prandtl number through the boundary layer,

$$Pr_t = 1{,}42 - 0{,}17\, y^{+\,1/4} \qquad \ldots |3.3.32|$$

(if $Pr_t < 0{,}86$; $Pr_t = 0{,}86$)

$$\begin{aligned} Pr_t &= 0{,}90 + 0{,}35\,(1 + \cos(\pi y^+/37)) \; ; \; y^+ < 37 \\ &= 0{,}90 \; ; \; y^+ > 37 \qquad \ldots |3.3.34| \\ &= 0{,}60 \; ; \; y^+ > (\delta t_{,up}/h) \end{aligned}$$

which have been used by the authors with reasonable success to more accurately predict temperatures profiles.

Most authors have stated that the theoretical and experimental investigations of the thermal distribution in a transpiration cooled boundary have not been systematically explored. However, presented above are a few of the papers written on the subject. The review is by no means comprehensive or up to date, but hopefully will serve as an sufficient introduction for the present investigation.

4 DEVELOPMENT OF A MATHEMATICAL MODEL FOR PREDICTING THE BOUNDARY LAYER BEHAVIOUR

4.1 Introduction

The compressible turbulent boundary layer equations for two-dimensional flow can be written as

Momentum

$$\rho u \frac{\partial u}{\partial x} + (\rho v + \overline{\rho' v'}) \frac{\partial u}{\partial y} = \frac{\partial \tau}{\partial x} + \frac{\partial}{\partial y} (\mu \frac{\partial u}{\partial y} - \rho \overline{u'v'}) \quad \ldots |4.1.1|$$

Energy

$$\rho u \frac{\partial H}{\partial x} + (\rho v + \overline{\rho' v'}) \frac{\partial H}{\partial y} = \frac{\partial}{\partial y} (\frac{\mu}{Pr} \cdot \frac{\partial H}{\partial y} - \rho \overline{v'H'} + \mu (1 - \frac{1}{Pr}) u \frac{\partial u}{\partial y}) \ldots |4.1.2|$$

and Continuity

$$\frac{\partial}{\partial x} (\rho u) + \frac{\partial}{\partial y} (\rho v + \rho' \overline{v'}) = 0 \quad \ldots |4.1.3|$$

The bar denotes time averaged quantities and the prime denotes instantaneous quantities.

The analysis for the solution of the above equations is based on the classical treatment by Prandtl who replaced the fluctuating quantities by an eddy viscosity and turbulent Prandtl number in the momentum and energy equations respectively. The eddy viscosity is based on Prandtl's mixing length theory.

4.2 Boundary Layer Parameters

Once the velocity and temperature profiles have been determined, the following boundary layer parameters, which accurately described the flow situation can be calculated. Some of these parameters are listed below.

Displacement thickness, (the mass flow deficit which occurs in the boundary layer due to the reduction in velocity at the surface)

$$\delta^* = \int_0^{\infty} \left(1 - \frac{\rho u}{\rho_\infty u_\infty}\right) dy \qquad \ldots |4.2.1|$$

Momentum thickness (the deficit in momentum)

$$\theta = \int_0^{\infty} \frac{\rho u}{\rho_\infty u_\infty} \left(1 - \frac{u}{u_\infty}\right) dy \qquad \ldots |4.2.2|$$

Shear stress at the wall

$$\tau_w = \mu_w \left(\frac{\partial u}{\partial y}\right)_w \qquad \ldots |4.2.3|$$

and the local skin-friction coefficient

$$C_f = \frac{\tau_w}{\frac{1}{2}\rho_\infty u_\infty^2} \qquad \ldots |4.2.4|$$

Heat transfer rate to the wall

$$-q_w = \frac{k_w}{C_p} \left(\frac{\partial h}{\partial y}\right)_w \qquad \ldots |4.2.5|$$

Stanton number

$$St = \frac{-q_w}{\rho_\infty u_\infty (H_\infty - H_w)} \qquad \ldots |4.2.6|$$

Shape factor (ratio of displacement to momentum thickness)

$$H^* = \frac{\delta^*}{\theta} \qquad \ldots |4.3.7|$$

Defect - shape factor

$$G = \int_0^{\infty} \left(\frac{u_\infty - u}{u_w^*}\right)^2 dy \Big/ \int_0^{\infty} \left(\frac{u_\infty - u}{u_w^*}\right) dy = \sqrt{\frac{2}{C_f}} \left(1 - \frac{1}{H}\right) \qquad \ldots |4.2.8|$$

Defect displacement thickness

$$\Delta = \int_0^{\infty} \left(\frac{u_\infty - u}{u_w^*}\right) dy = \left(\frac{2}{C_f}\right)^{\frac{1}{2}} \delta^* \qquad |4.2.9|$$

4.3 Formulation of Eddy Viscosity and Turbulent Prandtl Number

To solve equations 4.1.1 and 4.1.2 it is necessary to relate the Reynolds shear stress, $-\rho\overline{u'v'}$ and the term $-\rho\overline{v'H'}$ to mean velocity and enthalpy distributions respectively. The concept of eddy viscosity (ε_m) and eddy conductivity (λ_t) is introduced to relate the time-mean fluctuating quantities to mean velocity and enthalpy distributions. The eddy viscosity and eddy conductivity are thus defined as follows:

$$\varepsilon = -\frac{\overline{u'v'}}{\partial u/\partial y} \quad ; \quad \lambda_t = -\frac{\overline{v'H'}}{\partial H/\partial y} \qquad \ldots |4.3.1|$$

and can be related to each other as follows

$$\lambda_t = \frac{\varepsilon}{Pr_t} \qquad \ldots |4.3.2|$$

where Pr_t is the "turbulent Prandtl number".

As most authors have suggested, the eddy viscosity model within the boundary layer is divided into two regions, the inner (sublayer) region and outer (fully turbulent) region. For the inner region the eddy viscosity is based on Prandtl's mixing length theory;

$$\varepsilon_i = l^2 \frac{\partial u}{\partial y} \qquad \ldots |4.3.3|$$

where l, the mixing length, is given by $l = \kappa.y$ (where $\kappa = 0,4$). Van Driest [22] modified this to account for the viscous sublayer close to the wall by considering Stokes flow (flow over an infinite plate oscillating sinusoidally to itself). Thus

$$l = 0,4y\ (1,0 - \exp\ (-\ y/A)) \qquad \ldots |4.3.4|$$

where A is a constant for a given streamwise location in the boundary layer, dofined as

4.3 Formulation of Eddy Viscosity and Turbulent Prandtl Number

To solve equations 4 1.1 and 4.1.2 it is necessary to relate the Reynolds shear stress, $-\rho\overline{u'v'}$ and the term $-\rho\overline{v'H'}$ to mean velocity and enthalpy distributions respectively. The concept of eddy viscosity (ε_m) and eddy conductivity (λ_t) is introduced to relate the time-mean fluctuating quantities to mean velocity and enthalpy distributions. The eddy viscosity and eddy conductivity are thus defined as follows:

$$\varepsilon = -\frac{\overline{u'v'}}{\partial u/\partial y} \quad ; \quad \lambda_t = -\frac{\overline{v'H'}}{\partial H/\partial y} \qquad \ldots |4.3.1|$$

and can be related to each other as follows

$$\lambda_t = \frac{\varepsilon}{Pr_t} \qquad \ldots |4.3.2|$$

where Pr_t is the "turbulent Prandtl number".

As most authors have suggested, the eddy viscosity model within the boundary layer is divided into two regions, the inner (sublayer) region and outer (fully turbulent) region. For the inner region the eddy viscosity is based on Prandtl's mixing length theory;

$$\varepsilon_i = l^2 \frac{\partial u}{\partial y} \qquad \ldots |4.3.3|$$

where l, the mixing length, is given by $l = \kappa.y$ (where $\kappa = 0,4$). Van Driest (2) modified this to account for the viscous sublayer close to the wall by considering Stokes flow (flow over an infinite plate oscillating sinusoidally to itself). Thus

$$l = 0,4y\ (1,0 - \exp(-y/A)) \qquad \ldots |4.3.4|$$

where A is a constant for a given streamwise location in the boundary layer, defined as

$$A = 26\nu\,(\tau_w/\rho_w)^{-\frac{1}{2}} \qquad \ldots |4.3.5|$$

The expression given by equation 4.3.4 was obtained by Van Driest for a flat plate flow with no mass transfer. Cebeci (5) modified A to account for flows with pressure gradient and mass transfer. The damping constant, A^+, resulting was written as

$$A^+ = 26\,\{-(p^+/v_w^+)\,[\exp(11{,}8v_w^+) - 1{,}0] + \exp(11{,}8v_w^+)\}^{-\frac{1}{2}} \qquad \ldots |4.3.6|$$

where

$$p^+ = -\frac{dp}{dx}\cdot\frac{\nu}{\rho_w(u_w^*)^3}\,, \quad v_w^+ = \frac{v_w}{u_w^*}, \quad y^+ = \frac{yu_w^*}{\nu} \qquad \ldots |4.3.7|$$

Upon substitution of equations 4.3.6 and 4.3.4 into equation 4.3.3 the final form of the inner eddy-viscosity can be written as

$$\varepsilon_i = 0{,}16\,y^2\,[1{,}0 - \exp(-y^+/A^+)^2]\left|\frac{\partial u}{\partial y}\right| \qquad \ldots |4.3.8|$$

For the outer region a constant eddy viscosity is used

$$\varepsilon_o = \gamma u_e |\delta^*| \qquad \ldots |4.3.9|$$

where γ is Klebanoff's intermittency factor approximated by

$$\gamma = [1{,}0 + 5{,}5\,(y/\delta)^6]^{-1} \qquad \ldots 4.3.10$$

γ is a constant with a value between 0,016 and 0,02 and as such a value of 0,0168 will be used as suggested by Krieg (13).

Thus

$$\varepsilon_o = 0{,}0168\,u_e\,|\delta^*| \qquad \ldots |4.3.11|$$

The empirical equation describing the variation of turbulent Prandtl number through the boundary layer as suggested by Kays and Moffat (12) is to be used. The turbulent Prandtl number is approximated as follows:

$$Pr_t = 1{,}43 - 0.17\ (y^+)^{1/4} \qquad \ldots|4.3.12|$$

and for $Pr_t < 0{,}86$; $Pr_t = 0{,}86$

4.4 Boundary Conditions

The following boundary conditions are to be applied during the solution of equations 4.1.1, 4.1.2 and 4.1.3;

$$\text{At } y = 0: \quad \begin{aligned} u\ (x,0) &= 0 \\ v\ (x,0) &= 0 \text{ or } v_w \text{ with mass transfer} \\ H\ (x,0) &= H_w(x) \end{aligned} \qquad \ldots|4.4.1|$$

$$\lim_{y \to \infty}: \quad \begin{aligned} u\ (x,y) &= u_e(x) \\ v\ (x,y) &= 0 \\ H\ (x,y) &= H_e(x) \end{aligned} \qquad \ldots|4.4.2|$$

$$\text{and } u_e \frac{du_e}{dx} = -\frac{1}{\rho}\frac{dp}{dx} \qquad \ldots|4.4.3|$$

4.5 Transformation of Boundary-Layer and Flow-Viscosity

Application of the Probstein-Elliott /Levy-Lees transformation

$$d\xi = \rho_e \mu_e u_e\, dx \ ; \ d\eta = \frac{\rho u_e}{(2\xi)^{\frac{1}{2}}}\, dy \qquad \ldots|4.5.1|$$

and the definition of a dimensionless stream function f where

$$\psi = 2(\xi)^{\frac{1}{2}} f(\xi;\eta) \qquad \ldots|4.5.2|$$

[which satisfies the continuity equation 4.1.3 as follows

The empirical equation describing the variation of turbulent Prandtl number through the boundary layer as suggested by Kays and Moffat (12) is to be used. The turbulent Prandtl number is approximated as follows:

$$Pr_t = 1{,}43 - 0{,}17\ (y^+)^{1/4} \qquad \ldots|4.3.12|$$

and for $Pr_t < 0{,}86$; $Pr_t = 0{,}86$

4.4 Boundary Conditions

The following boundary conditions are to be applied during the solution of equations 4.1.1, 4.1.2 and 4.1.3;

$$\text{At } y = 0 \text{ ;} \quad \begin{aligned} u\ (x,0) &= 0 \\ v\ (x,0) &= 0 \text{ or } v_w \text{ with mass transfer} \\ H\ (x,0) &= H_w(x) \end{aligned} \qquad \ldots|4.4.1|$$

$$\lim_{y \to \infty} \quad \begin{aligned} u\ (x,y) &= u_e(x) \\ v\ (x,y) &= 0 \\ H\ (x,y) &= H_e(x) \end{aligned} \qquad \ldots|4.4.2|$$

$$\text{and } u_e \frac{du_e}{dx} = -\frac{1}{\rho}\frac{dp}{dx} \qquad \ldots|4.4.3|$$

4.5 Transformation of Boundary-Layer and Eddy-Viscosity

Application of the Pronstein-Elliott Levy-Lees transformation

$$d\xi = \rho_e \mu_e u_e\, dx \ ; \ d\eta = \frac{\rho u_e}{(2\xi)^{\frac{1}{2}}}\, dy \qquad \ldots|4.5.1|$$

and the definition of a dimensionless stream function f where

$$\psi = 2(\xi)^{\frac{1}{2}} f(\xi;\eta) \qquad \ldots|4.5.2|$$

which satisfies the continuity equation 4.1.3 as follows

$$\frac{\partial \psi}{\partial y} = \rho u \; ; \; \frac{\partial v}{\partial x} = -(\rho v + \overline{\rho' v'}) \;]$$

to the boundary layer equations 4.1.1 and 4.1.2 gives the following transformed momentum and energy equations (See Appendix A1 for the details of the energy equation transformation).

Momentum:

$$[\,(\quad)(\quad)^{+}\;]' + ff'' + \beta[(\quad) - (f')^2] = 2\xi\left(f'\frac{\partial f'}{\partial \xi} - f''\frac{\partial f}{\partial \xi}\right) \quad \ldots |4.5.3|$$

Energy:

$$[\,(\quad)(\quad)^{+}\;]' + (u_e^2/H_e)(1-1/Pr)f'f'']\}' + fg' =$$

$$2\xi\left(f'\frac{\partial}{\partial \xi} - \quad\frac{\partial f}{\partial \xi}\right] \quad \ldots |4.5.4|$$

where differentiation w.r.t. η and

$$\frac{2\xi}{u_e}\frac{du_e}{d\xi} \; ; \; f' = \frac{u}{u_e} \; ; \; g = \frac{H}{H_e} \; ; \; C = \frac{\rho\mu}{\rho_e \mu_e} \quad \ldots |4.5.5|$$

The Levy-Lees eddy-viscosity expression can

$$= \exp\left[-(A_1/26).Y.\right.$$

$$\ldots |4.5.6|$$

where

$$A_1 = (\rho/\rho_e).[\,(2\xi)^{\frac{1}{2}}/\mu] \; ; \; Y = \int_0^{\eta} (\rho_e/\rho)\, d\eta \quad \ldots |4.5.7|$$

And in dimensionless form, the expression for the outer eddy viscosity then becomes

$$\varepsilon_o^+ = \gamma(\rho/\mu_e)\,[(2\xi)^{\frac{1}{2}}/u]\,\Big[\int_0^{\eta_\infty}(\rho_e/\rho)(1-f')\,d\eta\Big] \qquad (4.5.8)$$

With the following boundary conditions in the $\xi;\eta$ plane

At

$$\eta = 0\ ;\quad f(\xi;0) = 0 \text{ or } -1(2\xi)^{\frac{1}{2}}\int_0^{\xi}(\rho_w v_w)/(\rho_e u_e)\,d\xi \qquad (4.5.9)$$

$$f'(\xi;0) = 0$$

$$g(\xi;0) = H_w/H_e = g_w$$

$$\lim_{\eta\to\infty} f'(\xi;\eta) = 1 \qquad (4.5.10)$$

$$\lim_{\eta\to\infty} g(\xi;\eta) = 1$$

$$\varepsilon_o^+ = \gamma(\rho/\rho_e)\,[(2\xi)^{\frac{1}{2}}/\mu]\,\left[\int_0^{\eta_\infty}(\rho_e/\rho)(1-f')\,d\eta\right] \qquad |4.5.8|$$

With the following boundary conditions in the ξ/η plane

At

$$\eta = 0\ ;\ f(\xi;0) = 0 \text{ or } -1(2\xi)^{\frac{1}{2}}\int_0^{\xi}(\rho_w v_w)/(\rho_e u_e \mu_e)\,d\xi \qquad |4.5.9|$$

$$f'(\xi;0) = 0$$

$$g(\xi;0) = H_w/H_e = g_w$$

$$\lim_{\eta\to\infty} f'(\xi;\eta) = 1 \qquad |4.5.10|$$

$$g(\xi;\eta) = 1$$

5 COMPUTATIONAL SOLUTION OF THE MOMENTUM AND ENERGY EQUATIONS

5.1 Introduction

An implicit finite-difference method for solving equations 4.5.3 and 4.5.4 is presented. The computer program to solve the momentum and energy equations includes transition from laminar to turbulent boundary layer flow, pressure gradient effects, transpiration and heat transfer for compressible flow about two dimensional geometries. Although transition is accounted for, the criteria for transition (ie critical x-direction Reynolds number) has to be predetermined and then used as an input to the program. By compressible flow is meant that both density and viscosity variations through the boundary layer are accounted for as well as the variation of the specific heat (or molecular Prandtl number).

5.2 Linearization of Momentum Equation

An additional transformation is introduced to be substituted into the momentum equation. The translated stream function ϕ is used to improve the numerical computation.

$$\begin{aligned} f &= \phi + \eta \\ f' &= \phi' + 1 \\ f'' &= \phi'' \end{aligned} \qquad \ldots (5.2.1)$$

Which when substituting 5.1.1 into 4.5.3 gives

$$\begin{aligned} &\left[C(1+t^2)\phi''\right]' + (\phi+\eta)\phi'' + \beta\left[(\rho_e/\rho) - (\phi')^2 - 2\phi' - 1\right] = \\ &2\xi\left[(\phi'+1)\left(\frac{\partial\phi'}{\partial\xi}\right) - \phi''\left(\frac{\partial\phi}{\partial\xi}\right)\right] \end{aligned} \qquad \ldots (5.2.2)$$

5.3 The Boundary Layer Equations in Finite Difference Form

For the momentum equation the streamwise derivatives are replaced by three-point finite-difference formulas. A finite difference pattern in the shape of a horizontal T

involving three points in the ξ direction and five points in the η direction is used. (See figure 5.1)

To completely linearize the momentum equation 5.2.2 it is assumed that certain terms are known from the previous iteration, that is,

$$\left[C_o(1+\varepsilon^+)_o\phi''\right]' + (\phi_o+\eta)\phi'' + \beta\left[(\rho_e/\rho)_o - \phi_o'\,\phi' - 2\phi'-1\right] =$$

$$2\xi\left[(\phi_o' + 1)\left(\frac{\partial\phi'}{\partial\xi}\right) - \phi_o''\left(\frac{\partial\phi}{\partial\xi}\right)\right] \qquad \ldots [5.3.1]$$

the subscript o indicating that the function has been obtained from a previous iteration.

The iteration process is initiated by equating the assumed value to that of the previous ξ stations, and completed when the latest value approaches that of the previous iteration

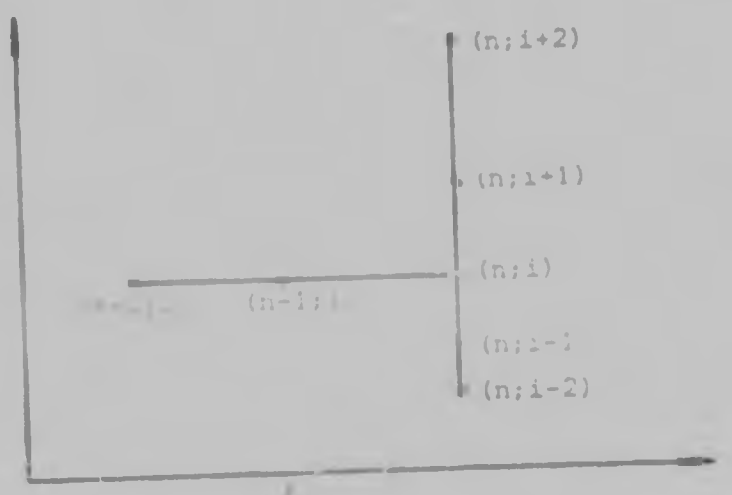

FIG 5.1 FINITE DIFFERENCE MOLECULE FOR THE MOMENTUM EQUATION

The resulting finite difference equation is in the form

$$\phi_{n;i-2}\,A_i+\phi_{n,i-1}\,B_i+\phi_{n;i}\,C_i+\phi_{n;i+1}\,D_i+\phi_{n;i+2}\,E_i = F_i \quad . \quad |5.3.2|$$

or in matric form

$$\{A\}\,\{\phi\} = B \qquad i = 3 \text{ to } i = N-2 \qquad \ldots \quad |5.3.3|$$

(The complete form being presented by Kreig [13].

For the energy equation a similar method is used except that only three points in the r direction are needed because the equation is second order. The final complete finite difference form which has been derived is as follows. (See Appendix A2 for the complete derivation).

$$\theta_{n;i-1}\{(D+A.b)(C_{n;i_0}/Pr)\left[1+(\varepsilon^+Pr/Pr_t)_{n;i_0}\right]+A^2(C_{n;i-1_0}/Pr)$$

$$\left[1+(\varepsilon^+Pr/Pr_t)_{n;i-1_0}\right]$$

$$+A.C(C_{n;i+1_0}/Pr)\left[1+(\varepsilon^+Pr/Pr_t)_{n;i+1_0}\right]+A(\phi_{n;i_0}+\eta_i)$$

$$+2\xi_n.A.(L.\phi_{n-2;i}+M.\phi_{n-1;i}+N.\phi_{n;i})\}+$$

$$\theta_{n;i}\{(E+B^2)(C_{n;i_0}/Pr)\left[1+(\varepsilon^+Pr/Pr_t)_{n;i_0}\right]+B.A(C_{n;i-1_0}/Pr)$$

$$\left[1+(\varepsilon^+Pr/Pr_t)_{n;i-1_0}\right]$$

$$+B.C(C_{n;i+1_0}/Pr)\left[1+(\varepsilon^+Pr/Pr_t)_{n;i+1_0}\right]+B(\phi_{n;i_0}+\eta_i)$$

$$+2\xi_n B(L.\phi_{n-2;i}+M._{n-1;i}+N.\phi_{n;i})-2\xi_n.N(\phi'_{n;i_0}+1))+$$

$$\theta_{n;i+1}\{(F+C.B)(C_{n;i_0}/Pr)\left[1+(\varepsilon^+Pr/Pr_t)_{n;i_0}\right]+C.A(C_{n;i-1_0}/Pr)$$

$$\left[1+(\varepsilon^+Pr/Pr_t)_{n;i-1_0}\right]$$

$$+C^2(C_{n;i+1_0}/Pr)\left[1+(\varepsilon^+Pr/Pr_t)_{n;i+1_0}\right]+C(\phi_{n;i_0}+\eta_i)$$

$$+2\xi_n.C.(L.\phi_{n-2;i}+M.\phi_{n-1;i}+N\phi_{n;i})\} =$$

$$2\xi_1\ \phi'_{n;i_0+1})(L.\theta_{n-2;i}+M.\theta_{n-1;i}) -$$

$$A.C_{n;i-1_0}(u_e^2/H_e)\left[1-(1/Pr)\right](\phi'_{n;i-1_0}+1)\phi''_{n;i-1_0} -$$

$$B.C_{n;i_0}(u_e^2/H_e)\left[1-(1/Pr)\right](\phi'_{n;i_0}+1)\phi''_{n;i_0} -$$

$$C.C_{n;i+1_0}(u_e^2/H_e)\left[1-(1/Pr)\right](\phi'_{n;i+1_0}+1)\phi''_{n;i+1_0} \quad \ldots |5.3.4|$$

Lumping the coefficients into single constants reduces 5.3.4 to

$$P_i\theta_{n;i-1}+Q_i\theta_{n;i}+R_i\theta_{n;i+1} = S_i \quad (i=1 \text{ denotes } n=0) \quad \ldots |5.3.5|$$

A system of linear simultaneous equations can be written starting with i = 2. If N is the number of η steps, a total of N - 2 equations can be set up (because 5.3.5 must end with N - 1). There are thus N unknowns and N - 2 equations. Using boundary conditions θ_1 and θ_n can be determined.

$$\theta_{n;1}P_2+\theta_{n;2}Q_2+\theta_{n;3}R_2+0+0 \quad \ldots 0 = S_2$$

$$0+\ldots+\theta_{n;2}P_3+\theta_{n;3}Q_3+\theta_{n;4}R_3+0 \quad \ldots 0 = S_3$$

$$0+\ldots+0+\theta_{n;3}P_4+\theta_{n;4}Q_4+\theta_{n;5}R_4 \quad \ldots 0 = S_4$$

$$0+\ldots\theta_{n;N-2}P_{N-1}+\theta_{n;N-1}Q_{N-1}+\theta_{n;N}R_{N-1} = S_{N-1} \quad \ldots |5.3.6|$$

Because $\theta_{n;1}$ is known it can be taken to the right hand side, ie.

$$\theta_{n;2}Q_2+\theta_{n;3}R_2 = S_2-\theta_{n;1}P_2 \quad \ldots |5.3.7|$$

Since from the boundary conditions

$$\lim_{\eta \to \infty} \theta(\xi;\eta) = 1 \quad \text{thus} \quad \theta_{n;N} = 1 \qquad \ldots|5.3.8|$$

thus equation N-1 becomes

$$\theta_{n;N-2}.F_{N-1} + \theta_{n;N-1}Q_{N-1} = S_{N-1} - R_{N-1} \qquad \ldots|5.3.9|$$

The general equation may be stated

$$|R| \{\theta\} = \{Q\} \quad (i = 2 \text{ to } N-1) \qquad \ldots|5.3.10|$$

5.4 The Finite Difference Grid and Finite Difference Molecule

To solve for ϕ and θ at station n, it is necessary to know the values of ϕ, θ, ϕ', and ϕ'' at stations n-2 and n-1. Two initially generated profiles are therefore required to start the solution at the third station. The program then marches to the n+1 station and uses the n and n-1 station value on the right hand side to solve the momentum and energy equations. The iteration procedure is based on the convergence of the momentum equations parameters ϕ'' and β, once this is obtained the energy equation is solved.

The step lengths normal to the wall are to increase from very small, near the wall in the region of rapid changes in velocity to a maximum at the outer edge of the boundary layer. Cebeci and Smith (6) suggested a grid of the form

$$\Delta\eta_i = K.\Delta\eta_{i-1} \qquad \ldots|5.4.1|$$

$\Delta\eta_i$ is the general step length, and for K 1, this step length is larger than the previous step. If the first step length is h, the distance to the ith grid point is

$$\eta_i = h \frac{(K^{i-1} - 1)}{K - 1} \qquad \ldots|5.4.2|$$

The program allows for the variation of the initial step length, h, as an input as well as accomodating the specification of the factor K.

Thus the finite difference grid can be represented as follows

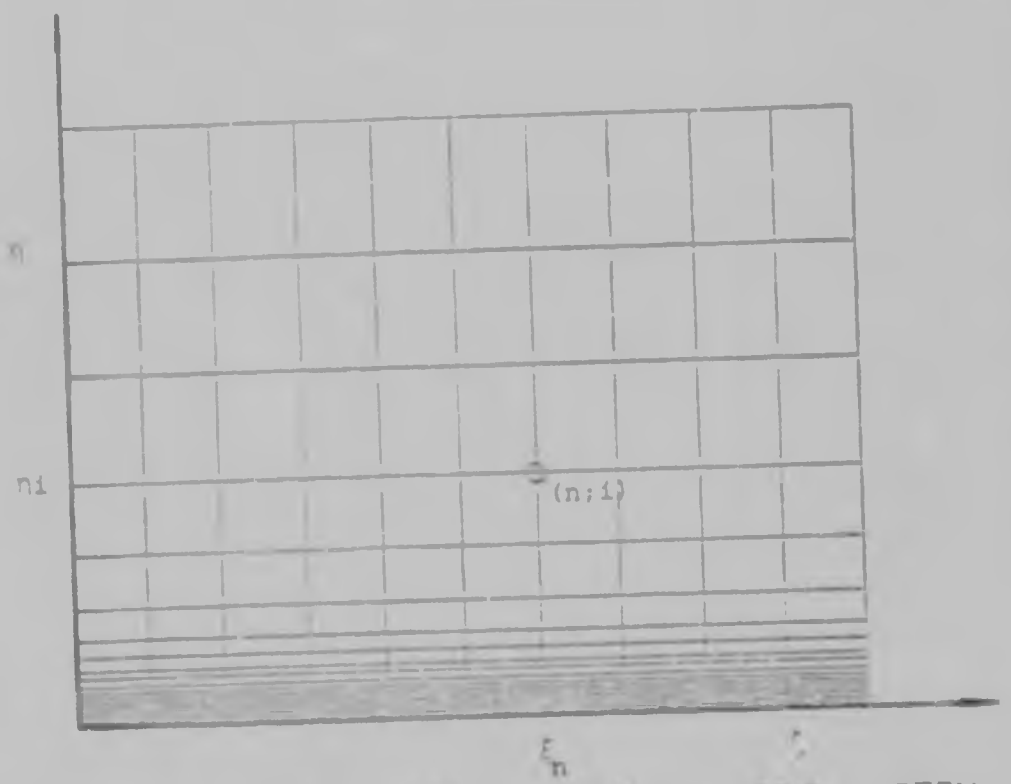

FIG 5.2 THE FINITE DIFFERENCE VARIABLE GRID SYSTEM

5.5 Discussion of Computational Procedure

Figure 5.3 gives the flow chart representing the computer program. As can be seen the program begins by generating the finite difference grid and calculating the free stream and wall boundary conditions. The option for laminar or turbulent flow then leads on to the generation of the two initial velocity and temperature profiles. The program then enters the main forward-step solution with the iteration procedure based on the convergence of δ^* and ϕ''.

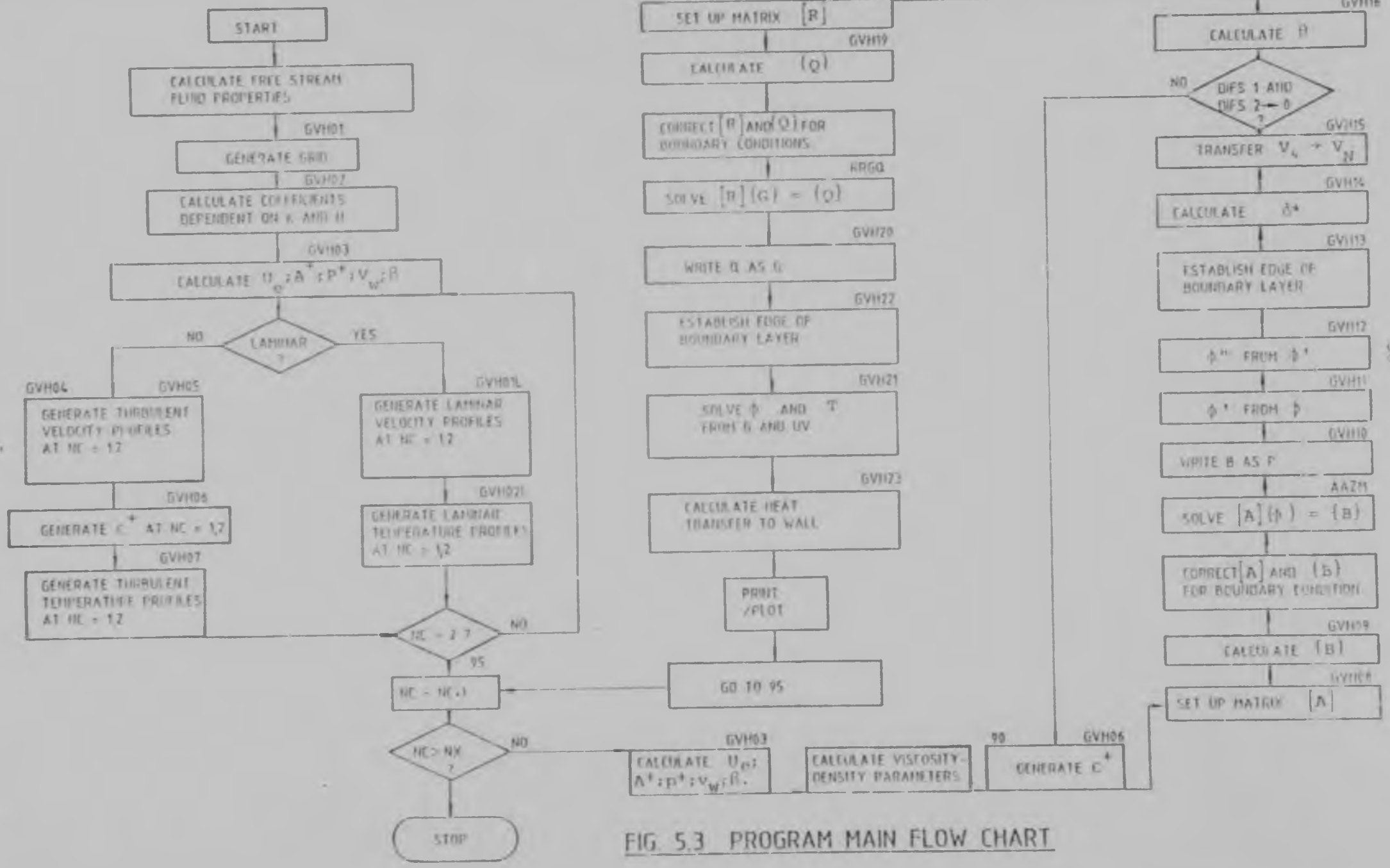

FIG 5.3 PROGRAM MAIN FLOW CHART

5.5.1 Initial Profiles

The distance along the flat plate is used as a criterion for laminar or turbulent flow.

The laminar profiles are suggested from the equations given by Grimson (9).

Momentum

$$\frac{u}{u_e} = \bar{y}(2-2\bar{y}^2+\bar{y}^3) + [(\Lambda\bar{y})/6](1-3\bar{y} + 3\bar{y}^2 - \bar{y}^3) \qquad \ldots|5.5.1|$$

where

$$\bar{y} = y/\delta \qquad \ldots|5.5.2|$$

$$\Lambda = \frac{\delta^2}{\nu} \cdot \frac{du}{dx} \qquad \ldots|5.5.3|$$

and energy

$$\frac{T-T_e}{T_w-T_e} = 1 - 2\eta_t + 2\eta_t^3 - \eta_t^4 \qquad \ldots|5.5.4|$$

where

$$\eta_t = y/\delta_t \qquad \ldots|5.5.5|$$

$$\delta_t/\delta \approx (Pr)^{-1/3} \qquad \ldots|5.5.6|$$

The turbulent momentum profiles are generated, using Van Driest's mixing length theory (22). This is similar to equation 3.3.31 but is simplified by setting $v_w = 0$ and thus the velocity can be written as follows:

$$u^+ = \int_0^{y^+} \frac{2\,dy}{1 + \sqrt{1 + 4\kappa^2 y^{+2} [1 - \exp(-y^+/A^+)]^2}} \qquad \ldots|5.5.7|$$

with the wall coefficient of friction C_f, to be used to convert u^+ to u/u_e, being evaluated from the following simplified equation

$$C_f = 0{,}0595/(Re_x)^{0,2} \qquad \ldots 5.5.8$$

The turbulent enthalpy profiles generated are also according to Van Driest (22). He introduced the concept of a mixed Prandtl number Pr_m which contains both the molecular and turbulent Prandtl numbers:

$$Pr_m = \frac{\mu + \varepsilon}{(\mu/Pr) + (\varepsilon/Pr_t)}$$

The enthalpy profile is given as follows

$$H(U_*) = H(0)-[H(0)-1][S(u_*)/S(1)]+(u_e^2/He)\{[S(u_*)R(1)/S(1)]-R(u_*)\} \qquad \ldots 5.5.9$$

where

$$H = H/H_e \; ; \; u_* = u/u_e \qquad \ldots 5.5.10$$

The functions $S(u_*)$ and $R(u_*)$ were given as

$$S(u_*) = \int_0^{u_*} Pr_m . \exp\left[-\int_{\tau(0)}^{\tau} (1-Pr_m)(d\tau/\tau)\right] du_* \qquad \ldots 5.5.11$$

$$R(u_*) = \int_0^{u_*} Pr_m . \exp\left[-\int_{\tau(0)}^{\tau} (1-Pr_m)(d\tau/\tau)\right] \cdot \left\{\int_0^{u_*} \exp\left[-\int_{\tau(\rho)}^{\tau} (1-Pr_m)(d\tau/\tau)\right] du_*\right\} du_* \qquad \ldots 5.5.12$$

where

$$\tau = (\mu+\varepsilon)\frac{du}{dy} = 1-\exp\left[1-(\kappa/\sqrt{C_f/2})(1-u_*)\right] \qquad \ldots 5.5.13$$

and the final integrals are as follows

$$S(1) = \int_0^1 Pr_m . \exp\left[-\int_{\tau(0)}^{\tau} (1 - Pr_m)(d\tau/\tau)\right] du_* \qquad \ldots|5.5.14|$$

$$R(1) = \int_0^1 Pr_m . \exp\left[-\int_{\tau(0)}^{\tau} (1-Pr_m)(d\tau/\tau)\right] \left\{\int_0^{u_*} \exp \int_{\tau(0)}^{\tau} (1-Pr_m)(d\tau/\tau)\, du_*\right\} du_*$$

$$\ldots|5.5.15|$$

Fluid Properties

Air is treated as a perfect gas and the fluid properties μ and [illegible] are assumed to be functions of specific enthalpy only, the specific heat capacity of air at constant pressure, C_p, being assumed to be a function of total enthalpy. The viscosity is obtained from Sutherland's law expressed as

$$\frac{\mu}{\mu_\infty} = \left(\frac{h}{h_\infty}\right)^{0,667} \frac{h_\infty + 1.19493 \times 10^5}{h + 1.19493 \times 10^5} \qquad \ldots|5.5.16|$$

6 EXPERIMENTAL APPARATUS AND PROCEDURE

6.1 Introduction

The object of the experiment was to obtain a number of mean temperature profiles on a porous flat plate preceded by a solid flat plate. The temperature of the coolant was also measured so to determine the heat transfer through the porous plate. An existing wind tunnel used by Krieg [1] was modified to suit the requirements for these experiments.

6.2 The Wind Tunnel

The wind tunnel used was of the open circuit type being driven by a Sirrocco centrifugal fan which in turn was driven by a 22 kW Siemens A C induction motor. The tunnel flow-rate could be adjusted by varying the opening of a trap door just after the fan through which air could be extracted from the system. The mainstream air was then lead to the working section through a series of ducts consisting of a diffuser, settling chamber and contraction. Honeycomb sections straightened the flow in the settling chamber region.

Just aft of the diffuser region the modification to the wind tunnel took place. Fifteen electrical heater elements each absorbing approximately 2.2 kW electric power were installed across the widest section of the tunnel. These elements were independently connected to the main laboratory electrical supply thus the option existed of being able to vary the mainstream crosswise temperature profile by switching on certain heater elements. These heater elements were able to heat the mainstream air to a maximum of 45°C at a free-stream velocity of approximately 5 m/s. At the maximum freestream velocity of 15 m/s the heated air had a temperature of approximately 32°C.

The working section consists of a rectangular section 209 x 496 mm with the side walls of perspex, the upper and lower (solid) walls of aluminium. The lower wall consists of a porous insert, of sintered bronze, which is preceded by a 797 mm flat plate section with a boundary layer bleed installed below it so as to allow for a uniform velocity distribution in front of the plates leading edge.

Figure 6.1 gives a view of the tunnel working section and instrumentation during the experiments.

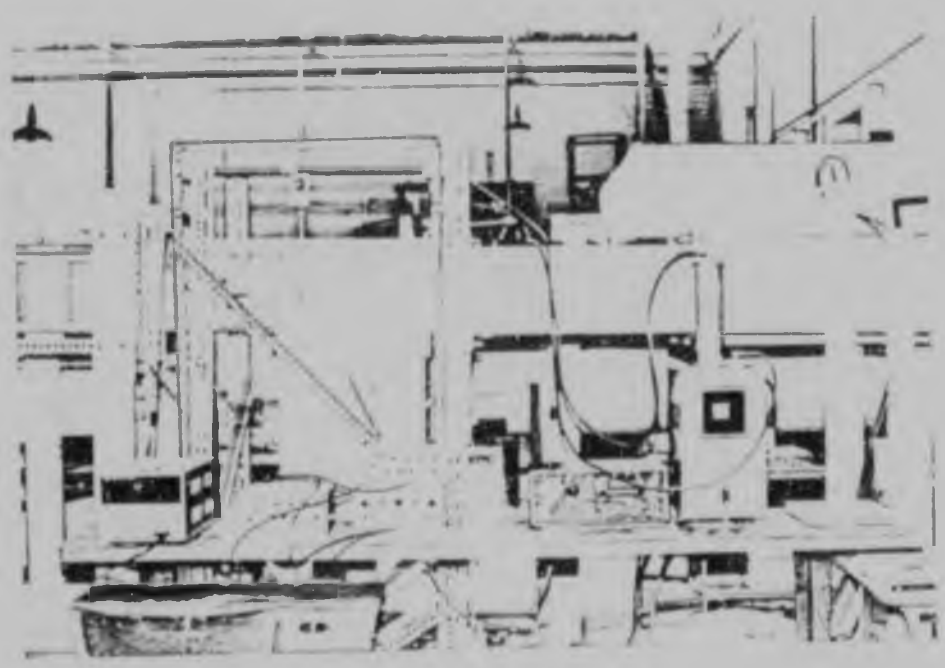

FIGURE 6.1: WIND TUNNEL WORKING SECTION AND INSTRUMENTATION

A traversing mechanism, which holds the probe, is mounted above the working section on a 4 degree of freedom rig, with the probe arm passing through a slit in the upper wall down to the lower plate surface. Figure 6.2 shows the traversing mechanism in more detail.

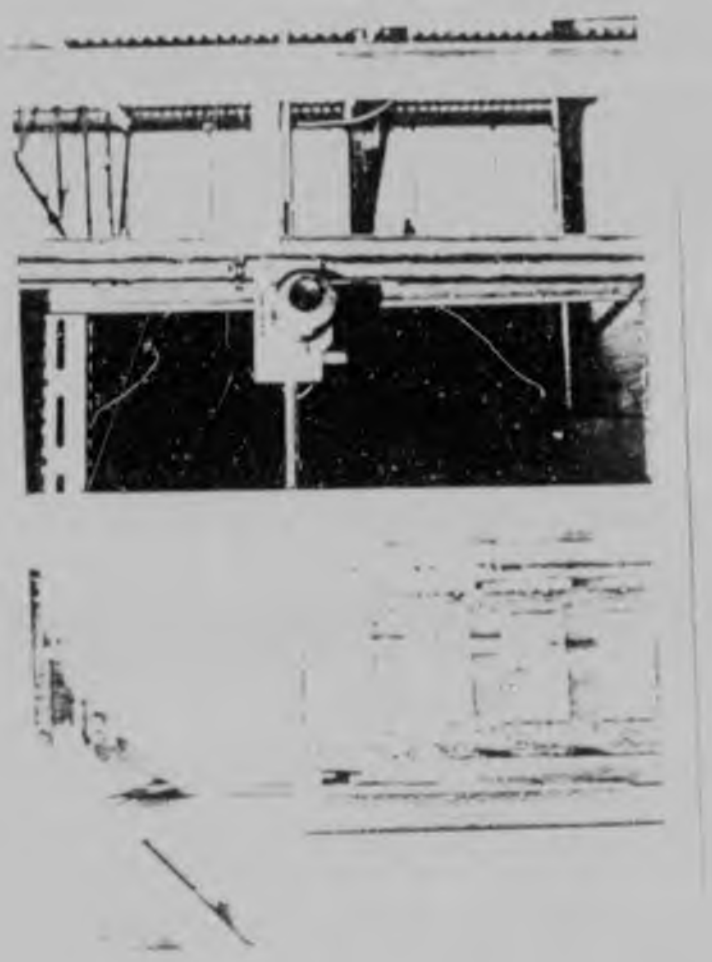

FIGURE 6.2 : TRAVERSING MECHANISM WITH PROBE HOLDER AND PROBE ABOVE AT THE WORKING SECTION

Measurements of both velocity and temperature were carried out thus a double hot wire probe had to be used and as the points of velocity and temperature measurement had to be as close as possible the probe had to be mounted on the probe holder as shown on figure 6.3. This resulted in the biggest drawback of the successful measurement of turbulent temperature profiles as the probe could not be brought closer than 1 mm to the wall. As this is the region where most changes, especially velocity, take place, the experimental results obtained were not completely satisfactory.

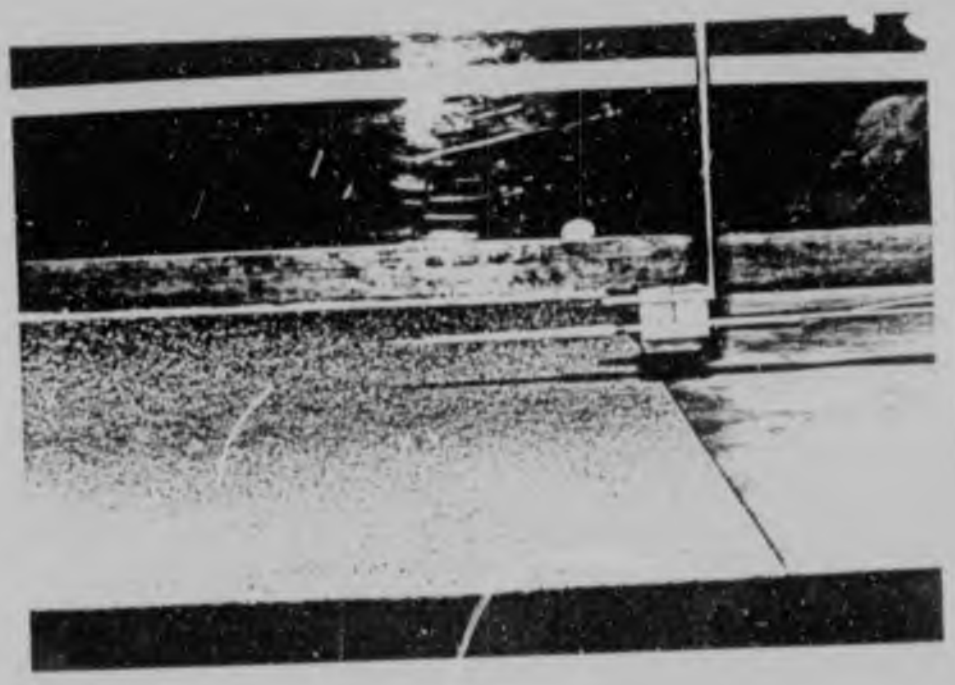

FIGURE 6.3: PROBE MOUNTED IN PROBE HOLDER ABOVE POROUS PLATE

The table below gives the stations, over the porous section where the profiles were measured, and their coordinates (the porous section began at x = 0,797 m and ended at x = 1,097 m)

TABLE 6.1: STATIONS AT WHICH TEMPERATURE PROFILES WERE MEASURED

STATION	DISTANCE FROM LEADING EDGE (m)
1	0,847
2	0,897
3	0,947
4	0,997
5	1,047

At each one of these stations thermocouples were inserted into the porous plate from the bottom to fit flush with the plate's upper surfaces. These thermocouples gave the wall temperature which could be read, off a digital (NKC)

thermometer. The temperature, pressure and flowrate of the coolant air was also measured, this air being supplied to the flat plate via a plenum chamber from the laboratories compressed air supply.

The wind tunnel free stream velocity and temperature were monitored with a pitot static tube and thermocouple respectively, these can be seen in figure 6.4 positioned in front and above the probe so as not to disturb the boundary layer to be measured by the probe.

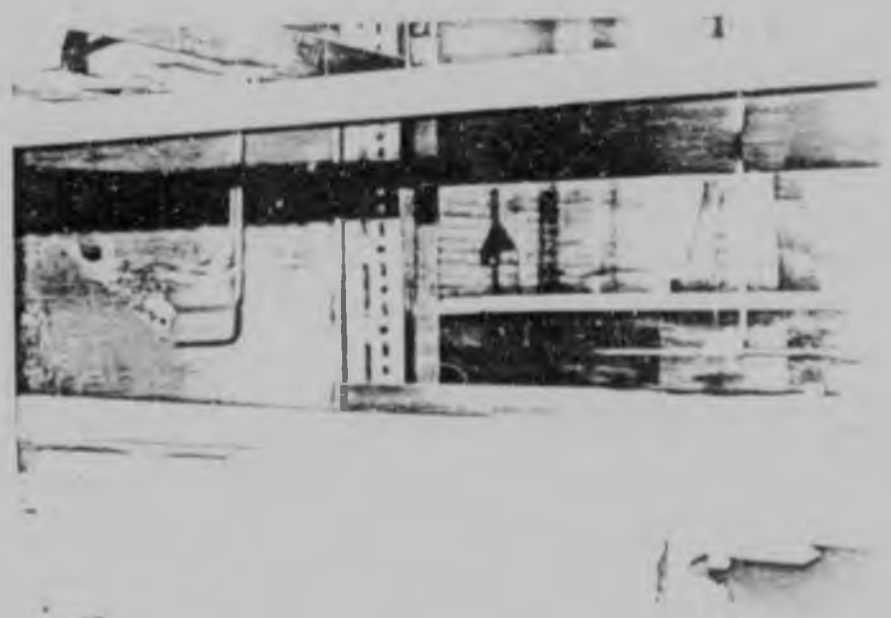

FIGURE 6.4 : WORKING SECTION, COOLING PLENUM CHAMBER (BELOW) AND MAINSTREAM PROBES

6.3 Hot Wire Anemometry

If a hot wire is placed in a flow, the heat flux from the wire is expressed as the following equation by King's law:

$$I^2 R_w = \frac{E_o^2}{R_w} + K U^n (T_{hw} - T_a) \qquad \ldots (6.3.1)$$

where I is the current flowing through the wire with resistance of R_w (at ambient conditions)

E_o is the potential difference across the wire at zero flow to heat it to ambient conditions

K is a constant

U the flow velocity

n an exponent (approximately equal to 0,5)

T_{hw} the hot wire temperature

T_a the flow temperature (or ambient temperature at zero flow)

The heat flux is proportional to both the flow velocity and temperature, so a dual probe (Disa type 55 E 30) was used. The thin hot wire probe was used to measure the heat flux predominantly effected by the velocity of the flow and the thermistor wire coil to measure the heat flux predominantly effected by the flow temperature. It was found that the flow velocity affected the thermistor reading and visa versa with the hot wire, thus it was necessary to carry out the calibration of the probe in the wind tunnel for various known flow velocities and temperatures once the hot wire had been initially calibrated in a rig to simulate flow velocity at constant temperature.

The hot wire was calibrated in a Disa type 55D90 calibration rig consisting of a [illegible] control unit, a [illegible] Nozzle unit and a 55D46 Pressure converter. A free air jet is produced by the nozzle unit, the velocity of which is controlled by the pressure control unit and measured by the pressure converter. The probe is placed in the free jet and as such can be accurately calibrated for any flow velocity.

The probe was controlled by a Disa type 55D01 Anemometer unit which supplies electric current to the probe which

where I is the current flowing through the wire with resistance of R_w (at ambient conditions)

E_o is the potential difference across the wire at zero flow to heat it to ambient conditions

K is a constant

U the flow velocity

n an exponent (approximately equal to 0,5)

T_{hw} the hot wire temperature

T_a the flow temperature (or ambient temperature at zero flow)

The heat flux is proportional to both the flow velocity and temperature, so a dual probe (Disa type 55 E 30) was used. The thin hot wire probe was used to measure the heat flux predominantly effected by the velocity of the flow and the thermistor wire coil to measure the heat flux predominantly effected by the flow temperature. It was found that the flow velocity affected the thermistor reading, and visa versa with the hot wire, thus it was necessary to carry out the calibration of the probe in the wind tunnel for various known flow velocities and temperatures once the hot wire had been initially calibrated in a rig to simulate flow velocity at constant temperature.

The hot wire was calibrated in a Disa type 55D90 calibration rig consisting of a 55D45 Pressure control unit, a 55D47 Nozzle unit and a 55D46 Pressure converter. A free air jet is produced by the nozzle unit, the velocity of which is controlled by the pressure control unit and measured by the pressure converter. The probe is placed in the free jet and as such can be accurately calibrated for any flow velocity.

The probe was controlled by a Disa type 55D01 Anemometer unit which supplies electric current to the probe which

heats the wire to a desired temperature. The temperature is kept virtually constant by a servo control system (or D C amplifier) which balances a Wheatstone bridge of which the probe forms part of one side of the bridge. The instantaneous value of the electric power applied may therefore be assumed to equal the instantaneous thermal loss to the surroundings which in this case is dependent on the flow velocity.

Because the output voltage of the anemometer unit is a nonlinear function of the flow velocity, use is made of a Disa 55D10 Linearizer which can automatically linearize the anemometer output electronically. The linearized output is fed to a Hewlett Packard Digital voltmeter with the gain on the output so that the voltage read out can be directly related to velocity, ie, 10 m/s is equal to 10 volts etc.

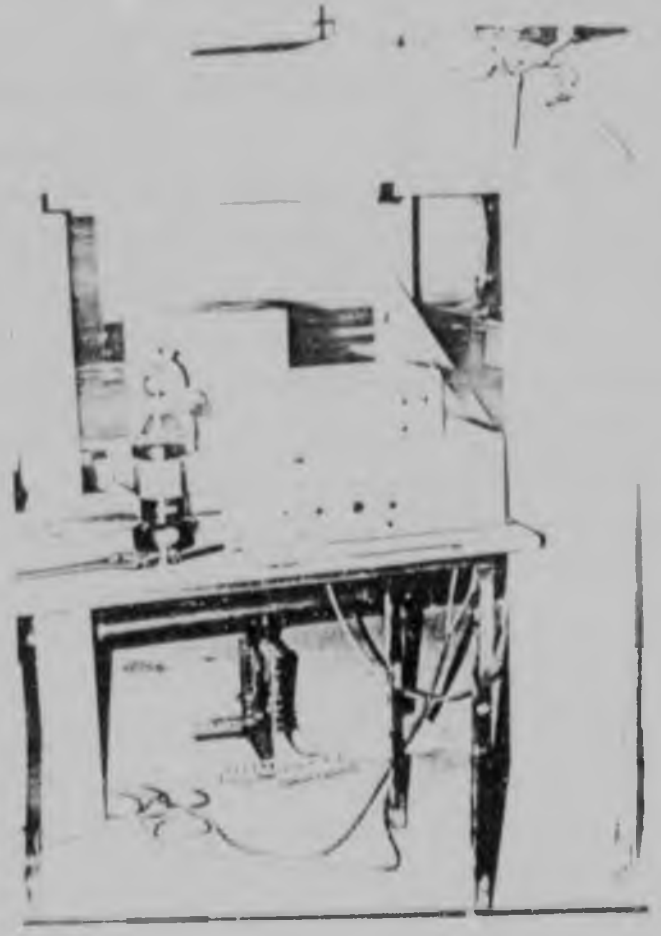

FIGURE 6.5 DISA TYPE 55D90 CALIBRATION RIG WITH COMPRESSED AIR SUPPLY

The temperature of a hot wire, hot film or thermistor can be measured indirectly by balancing the Wheatstone bridge of an Anemometer unit, one arm of which consists of the probe. This is performed by varying the resistance of the adjacent arm of the bridge until bridge balance is obtained. The resulting varied resistance is then proportional to the probes temperature (or resistance in the case of a thermistor).

The thermistor leads of the dual probe were thus connected to a Disa type 55D01 Anemometer unit and the bridge balanced in the temperature measurement mode by varying the bridge resistance.

6.4 Experimental Procedure

The hot wire was calibrated in the Disa rig as described above before the wind tunnel was set into operation. Care had to be taken that the anemometer unit and linearizer were not switched off whilst transferring the probe from the calibration rig to the wind tunnel.

The wind tunnel was then started up by first switching on the fan with the by pass trap door open which was closed to the desired setting once the electric motor had reached full speed. Next the electric heaters were switched on so as to heat up the mainstream. Approximately one hour had to be allowed for the tunnel temperature to stabilise due to heat convection to and conduction through the tunnel walls. Because of the long set up times and large power consumption of the tunnel, only nine runs were performed during which time temperature profiles and other parameters were measured.

The complete probe could now be calibrated in the wind tunnel by measuring the hot wire effective velocity (as this was previously calibrated for constant temperature flow) and thermistor resistance for various free stream flow velocities

and temperatures which were monitored by the pitot static tube and thermocouple as shown in figure 6.4.

The calibration curve obtained is shown in Appendix C1

Temperature profiles were then measured at five stations along the porous plate during which time free stream and coolant flow parameters were also monitored. The mainstream flow velocity being measured with a pitot static tube connected to a water manometer and a free stream temperature with a thermocouple connected to a NKC thermometer as were the thermocouples embedded in the porous plate. Coolant flowrate was measured by taking the differential pressure across an orifice plate in the compressed air supply pipe. The plenum chamber pressure was also monitored on the digital Furness manometer connected to a pressure tapping in the chambers side. The coolant flow plenum chamber temperature was also measured with a thermocouple connected to the thermometer which could accomodate thirteen channels with each reading being available at the push of that particular channels switch.

Freestream flow velocities varied from 4,95 m/s to 14,95 m/s with corresponding temperatures of 44,95°C and 33,00°C respectively. The blowing fraction F was varied from 0,0 to a maximum of [illegible] for the freestream velocity of approximately 15 m/s and temperature of 4[illegible]C (See Appendix for experimental results).

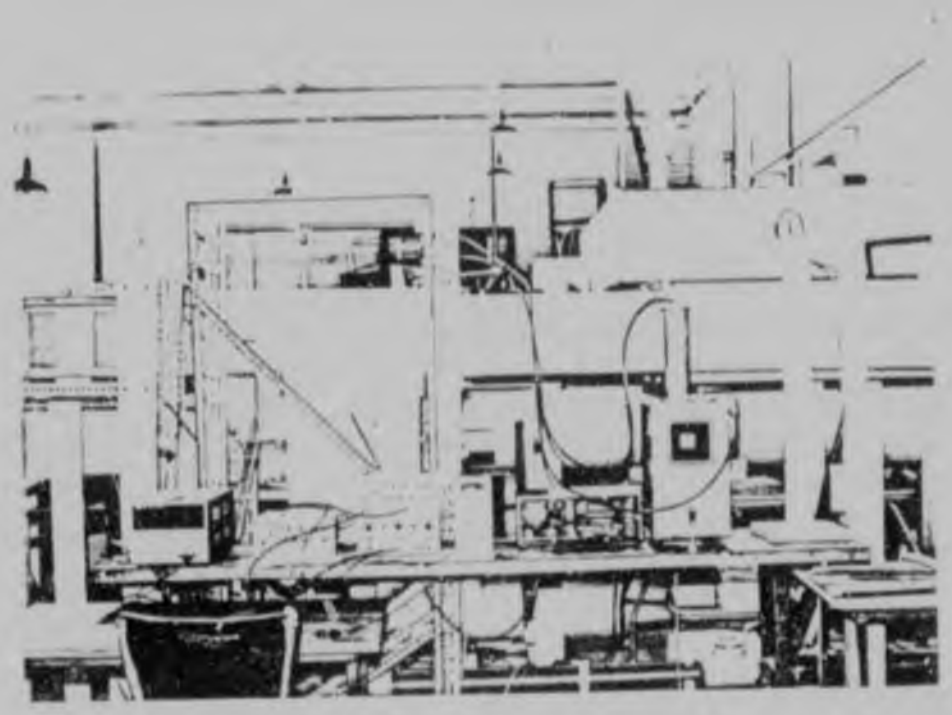

FIGURE 6.6 : EXPERIMENTAL APPARATUS FROM LEFT TO RIGHT

HEWITT PACKARD DIGITAL VOLTMETER

DISA 55D01 ANEMOMETER UNIT (CONNECTED TO THERMISTOR)

TOP:DISA 55D01 ANEMOMETER UNIT (CONNECTED TO HOT WIRE)

BOTTOM: DISA 55D1 LINEARIZER UNIT

FURNESS DIGITAL MANOMETER

WATER MANOMETER (FLOW VELOCITY)

MERCURY MANOMETER (COOLANT FLOWRATE)

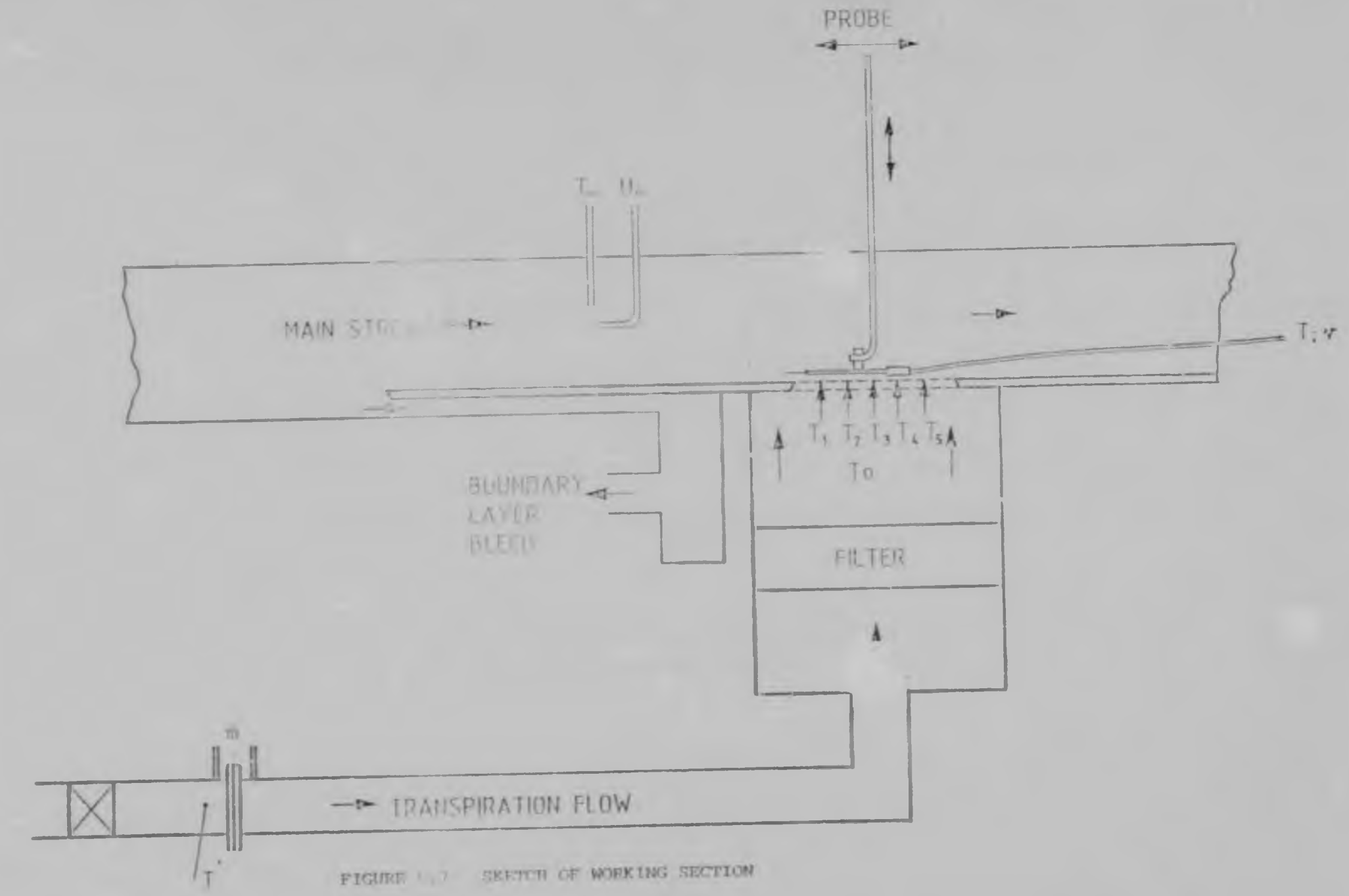

FIGURE 4.7 SKETCH OF WORKING SECTION

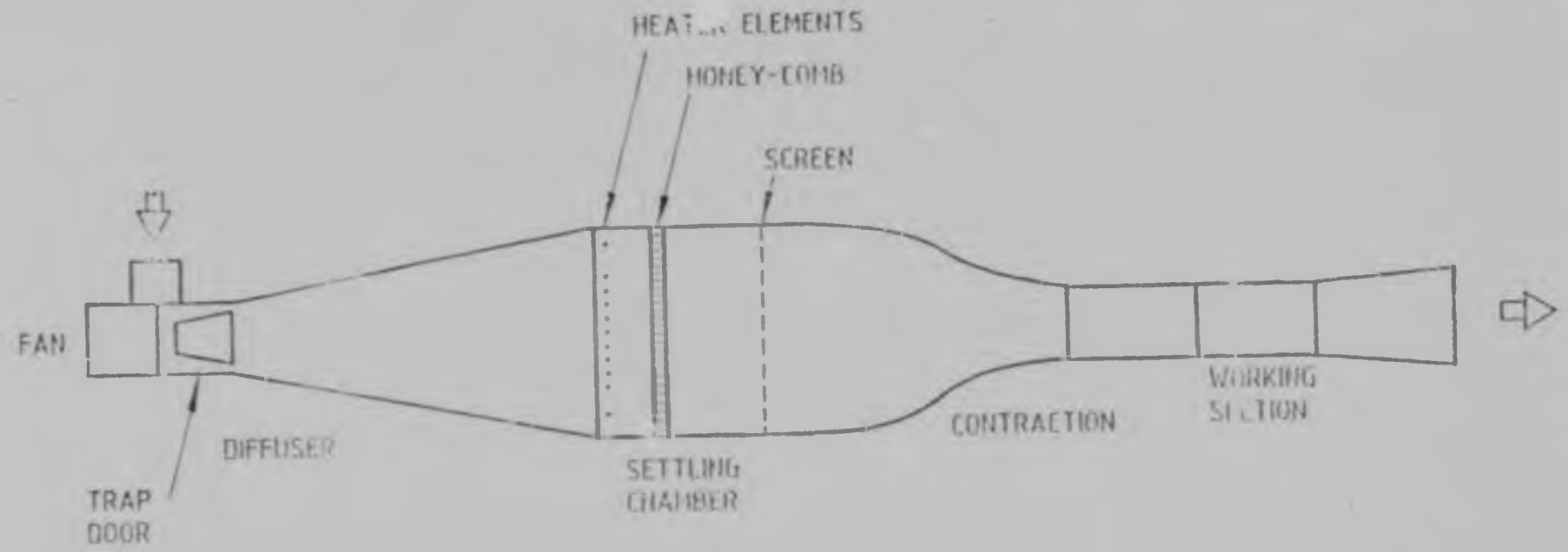

FIGURE 6.1 PLAN VIEW OF WIND TUNNEL.

7 DISCUSSION OF EXPERIMENTAL RESULTS AND COMPUTER PREDICTIONS

7.1 Introduction

This section will be divided in four parts: the experimental results, the comparison of the experimental results with those predicted by the computer program, the comparison of some of Mickley et al (17) results with those predicted by the program, and finally the heat transfer or Stanton number prediction of the experimental results by the program.

The modification of the wind tunnel by inserting electric heater elements vertically across the width of the wind tunnel downstream of the diffuser, was not completely successful. Initially only nine heater elements were installed across the widest section of the tunnel upstream of the flow straighteners.

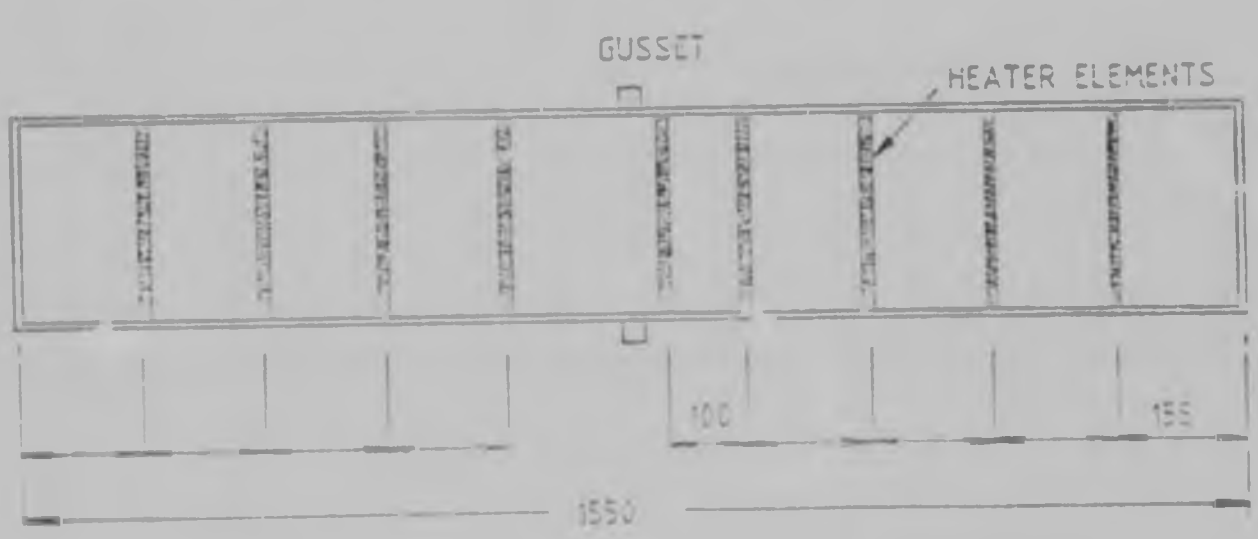

FIG. 7.1 CROSSECTION OF WIND TUNNEL AT STATION OF HEATER ELEMENTS.

As can be seen from the figure above, which indicates the location of the heaters, this section is not symmetrical.

The middle heater element had to be installed off centre so as to clear the reinforcing gusset on the outer wind tunnel surface. This resulted in an uneven spanwise temperature distribution at the working section of the wind tunnel (even though the spanwise velocity distribution was uniform). The spanwise temperature distribution peaked at two locations, each close to the side walls, with a trough of minimum temperature at the working section centre line. The profile was also skewed as can be expected from the above heater element arrangement.

To overcome this five additional heaters were installed to firstly correct the uneven temperature profile as well as raising the overall free stream temperature. The additional elements were installed in the central region and are shown below by dotted lines.

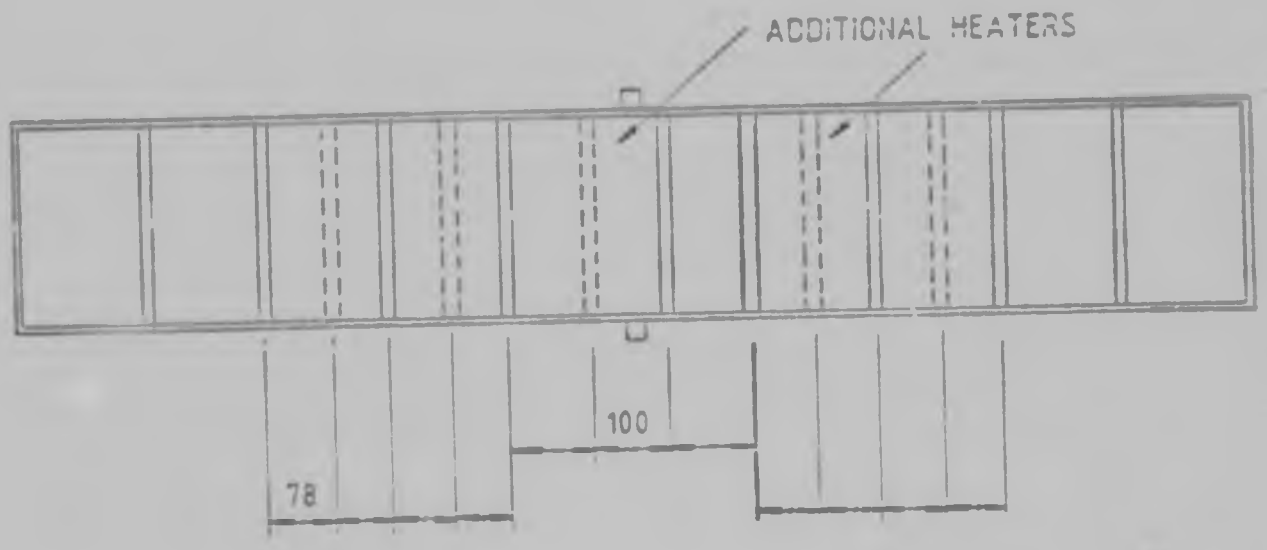

FIG. 7.2 FINAL HEATER ELEMENT ARRANGEMENT

This resulted in a more symmetric arrangement although the problem of a minimum temperature at the working section still persisted. This is obvious from the

observation that by adding the additional heaters, the two regions adjacent to the centre section have closer spaced elements. The results of a temperature traverse of this final arrangement is given in figure 7.3. Although this situation is not completely acceptable, it was felt that meaningful results could be obtained by assuming the flow to be two-dimensional. This is not unrealistic, as initial vertical temperature measurements (without blowing) once the wind tunnel had been running for approximately one hour, showed that the profile was uniform in this direction. The tunnel walls and free stream temperatures were almost the same, ie, the tunnel was in thermal equilibrium.

The maximum free stream temperature obtained, at a flow velocity of 5 m/s, was 45°C. At the maximum free stream velocity of 15 m/s the heated air at the working section centreline was approximately 32°C.

For the experimental results, flow over a flat plate, with little density (or viscosity) variations across the boundary layer resulted. However, provision has been made for the computer program to handle two-dimensional, or axisymmetric flow with variation of fluid properties across the boundary layer with an imposed pressure gradient.

7.2 Experimental Results

7.2.1 Temperature Profiles

The summary of the experimental results obtained for the nine runs is given in table 7.1. These runs are divided into three groups according to the flow conditions. The criteria used for this grouping is similar free stream velocity and temperature, with each group being represented by increasing blowing rate at the porous wall. The first

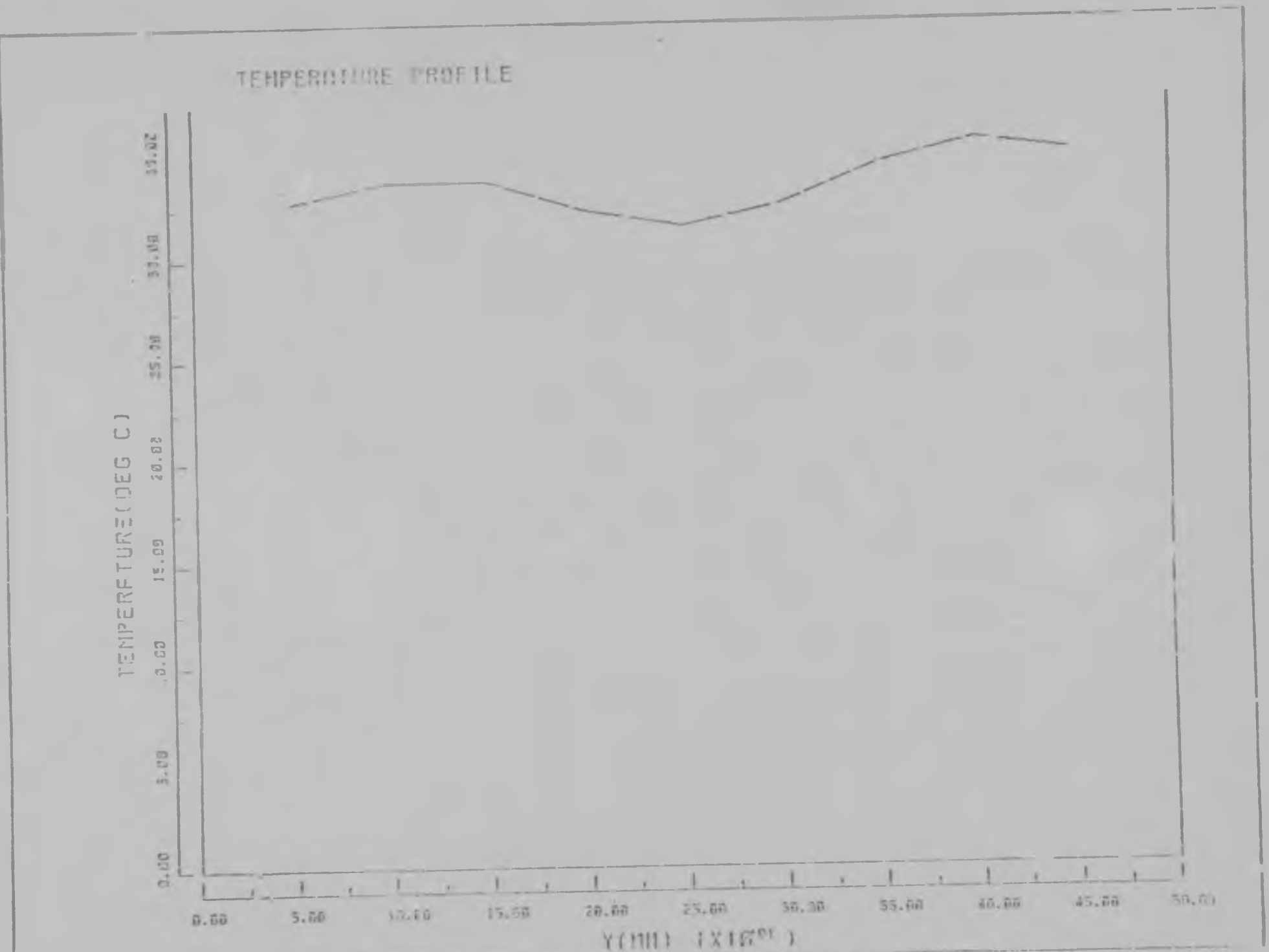

FIGURE 7.3 SPANWISE TEMPERATURE DISTRIBUTION ACROSS WORKING SECTION

group represents free stream flow velocity of 14,95 m/s and free stream temperature of approximately 33°C for which three runs of increasing blowing rate were carried out for which temperature profiles were measured. The next four runs are for a free stream flow velocity of 10,85 m/s and free stream flow temperature of approximately 40°C. The final two runs were for flow velocity and temperature of approximately 5 m/s and 45°C respectively.

The data points for each experimental run are shown on graphs 7.4 through 7.12. Linear axes are used so as to represent the profiles in their actual form (the discussion of the profile will be dealt with when considering semi-logarithmic plots of the profiles in the next section). All the profiles obtained at the five measuring stations are superimposed on one another so as to illustrate the development of the thermal boundary layer of the porous section of the flat plate. Each profile being represented by a different symbol on the graphs plotted.

Appendix D1 contains the full set of experimental results obtained during the nine runs.

TABLE 7.1 SUMMARY OF EXPERIMENTAL RESULTS

EXPERIMENT RUN	u_∞ (m/s)	T_∞ (°C)	v_w (m/s)	T_w (°C)	F	T_0 °C
1	14,95	33,01	0,064	25,00	0,00428	24,5
2	14,95	33,14	0,088	23,64	0,00589	23,0
3	14,95	34,10	0,113	23,05	0,00756	22,9
4	10,85	39,02	0,064	26,50	0,00590	26,3
5	10,85	39,21	0,088	26,25	0,00811	26,1
6	10,85	39,54	0,112	26,13	0,01032	26,0
7	10,80	40,01	0,128	25,89	0,01185	25,7
8	4,95	44,89	0,021	26,12	0,00424	25,5
9	5,01	44,95	0,045	25,95	0,00849	25,5

KEY TO SYMBOLS OF FIGURES 7.4 THROUGH 7.12

SYMBOL		STATION
○	-	1
△	-	2
+	-	3
×	-	4
◇	-	5

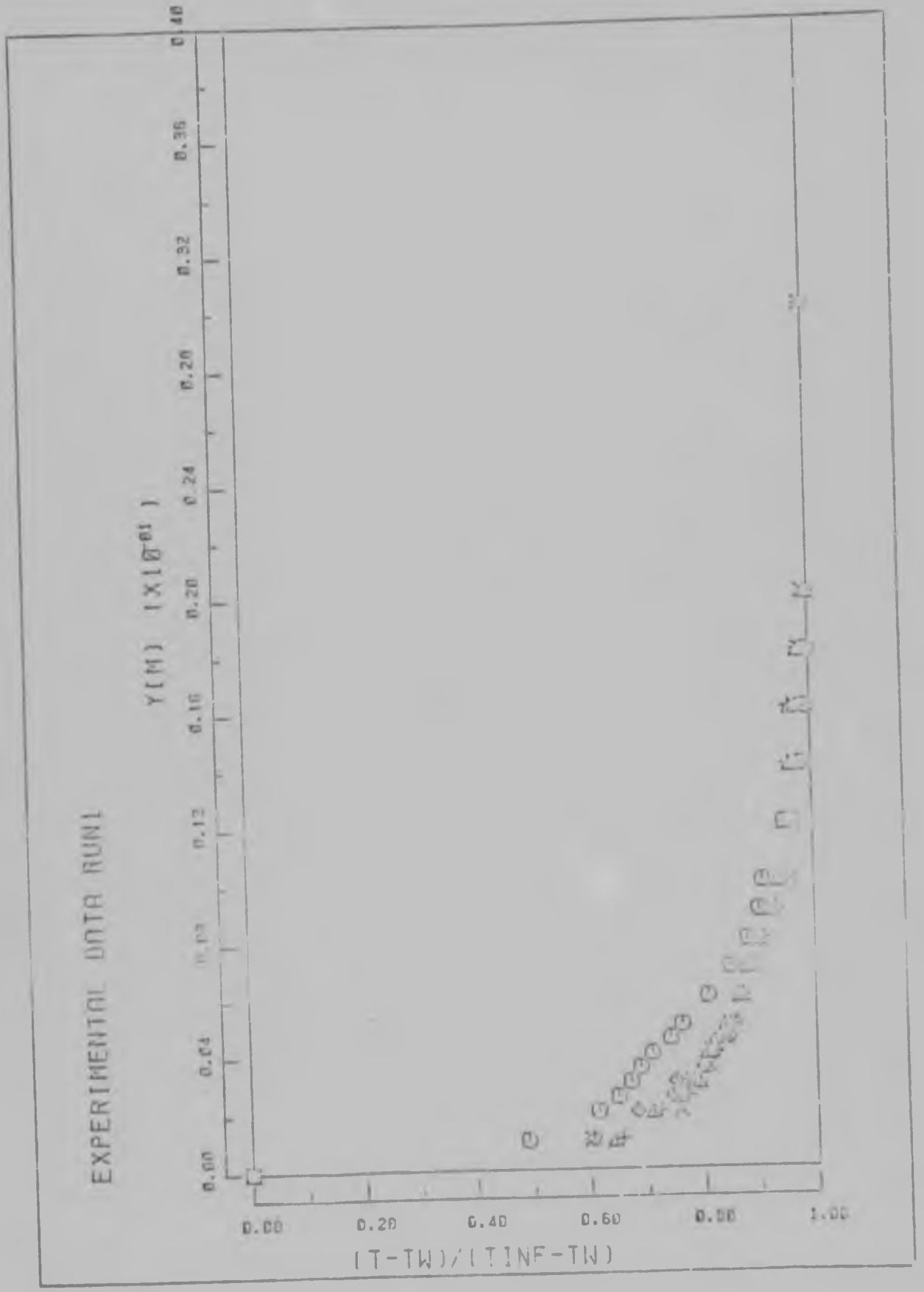
EXPERIMENTAL DATA RUN1
Y(M) (X10⁻⁰¹)
0.00
0.04
0.08
0.12
0.16
0.20
0.24
0.28
0.32
0.36
0.40
0.00
0.20
0.40
0.60
0.80
1.00
(T-TW)/(TINF-TW)

FIGURE 7.4

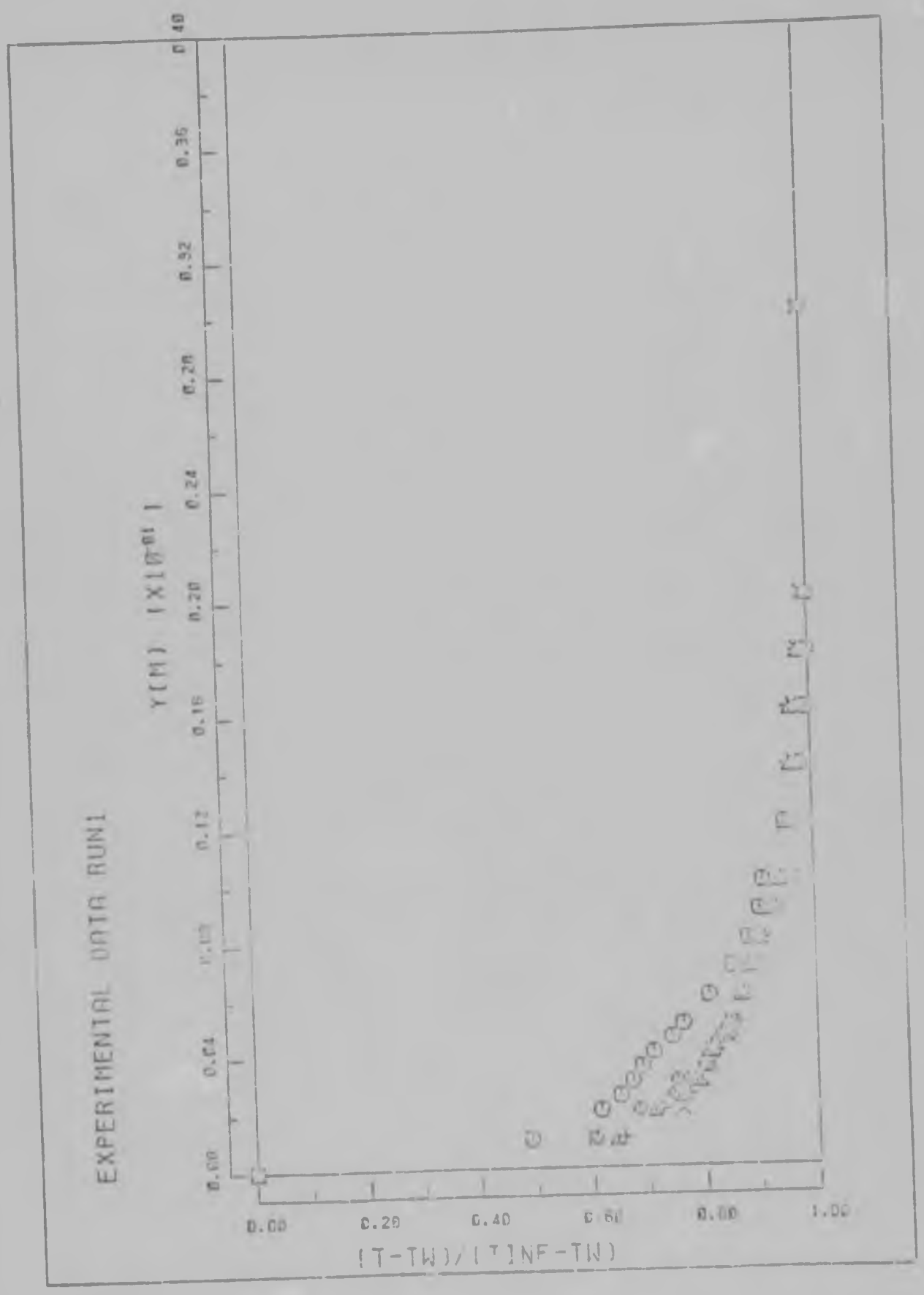
EXPERIMENTAL DATA RUN1
Y(M) (X10**01)
0.00
0.04
0.08
0.12
0.16
0.20
0.24
0.28
0.32
0.36
0.40
0.00
0.20
0.40
0.60
0.80
1.00
(T-TW)/(TINF-TW)

FIGURE 7.4

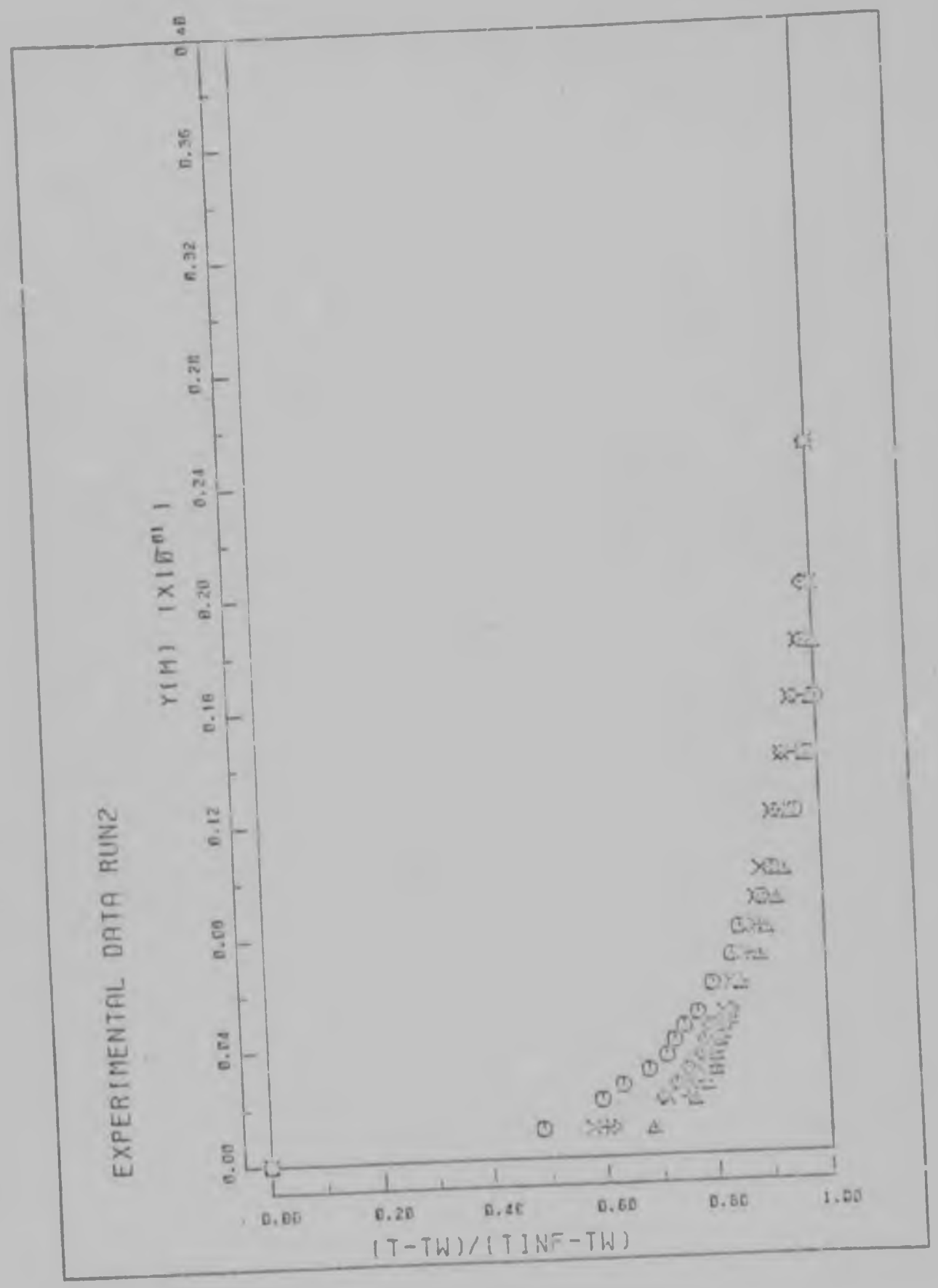
EXPERIMENTAL DATA RUN2
Y(M) (X10**01)
0.00
0.04
0.08
0.12
0.16
0.20
0.24
0.28
0.32
0.36
0.40
0.00
0.20
0.40
0.60
0.80
1.00
(T-TW)/(TINF-TW)

FIGURE 7.5

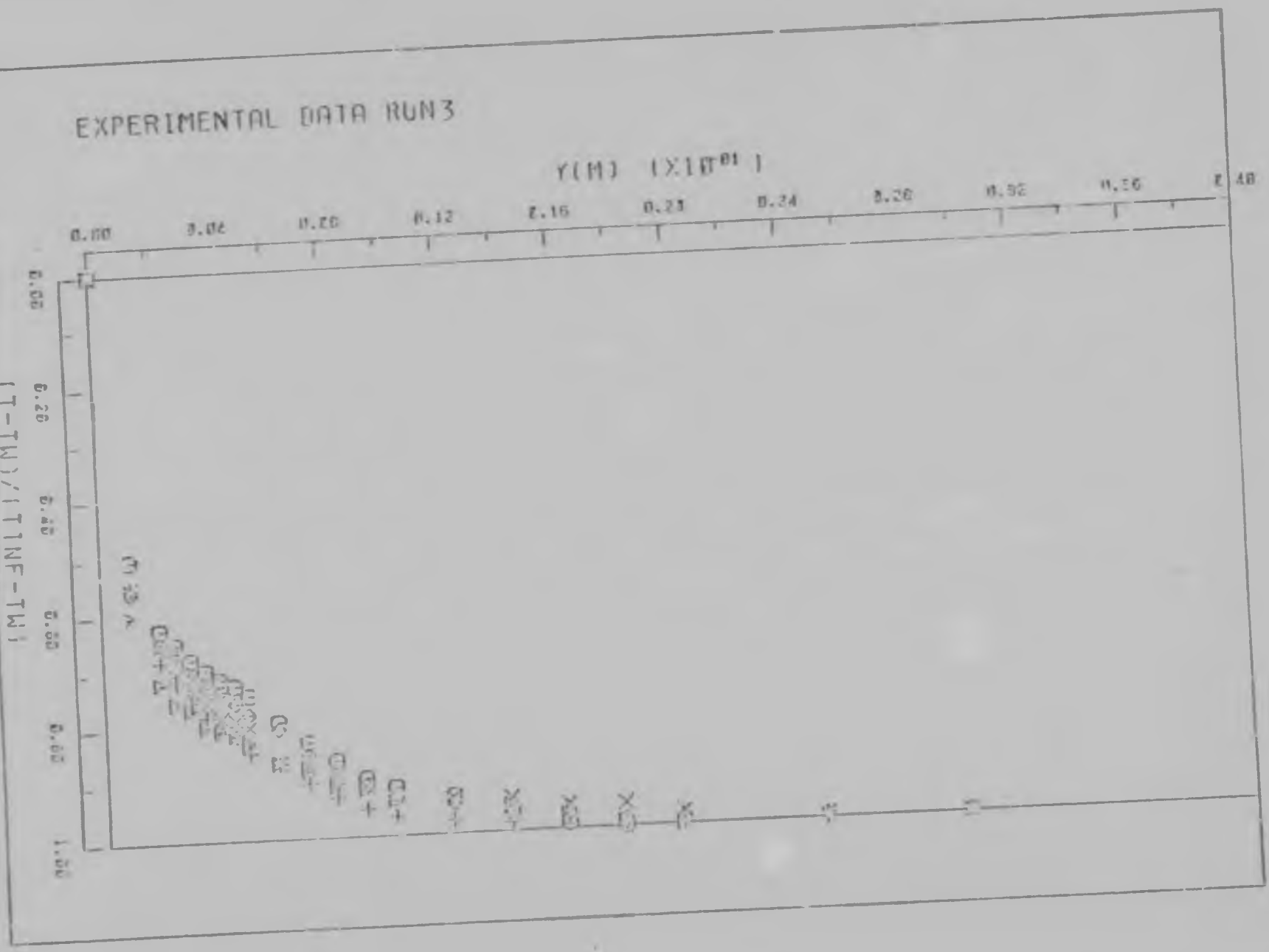
EXPERIMENTAL DATA RUN3
Y(M) (X10^01)
0.00
0.04
0.08
0.12
0.16
0.20
0.24
0.28
0.32
0.36
0.40
0.00
0.20
0.40
0.60
0.80
1.00
(T-TINF)/(TW-TINF)

FIGURE 7.6

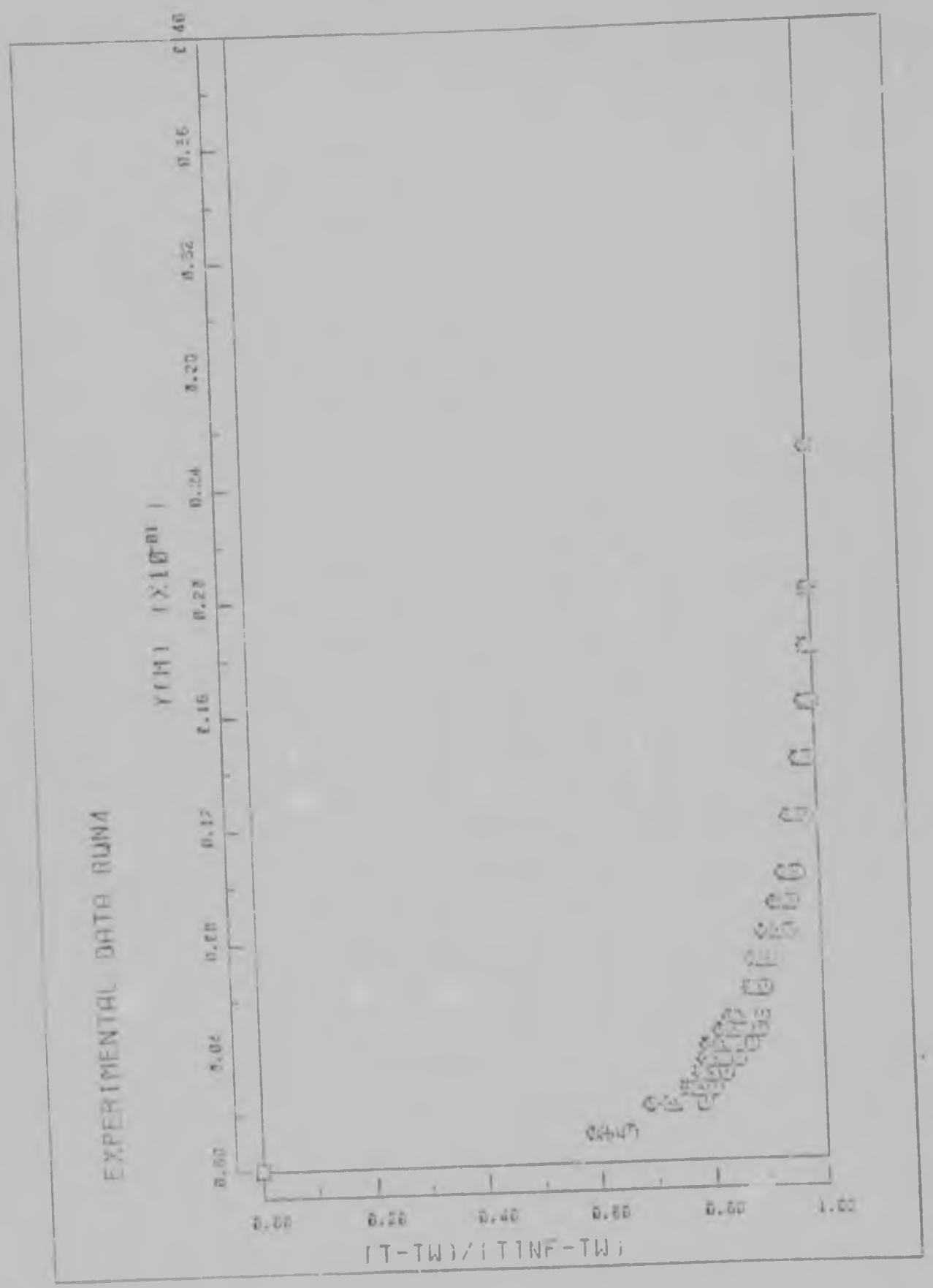
EXPERIMENTAL DATA RUN4
0.00
0.04
0.08
0.12
0.16
0.20
0.24
0.28
0.32
0.36
0.40
0.00
0.20
0.40
0.60
0.80
1.00
(T-TW)/(TINF-TW)

FIGURE 7.7

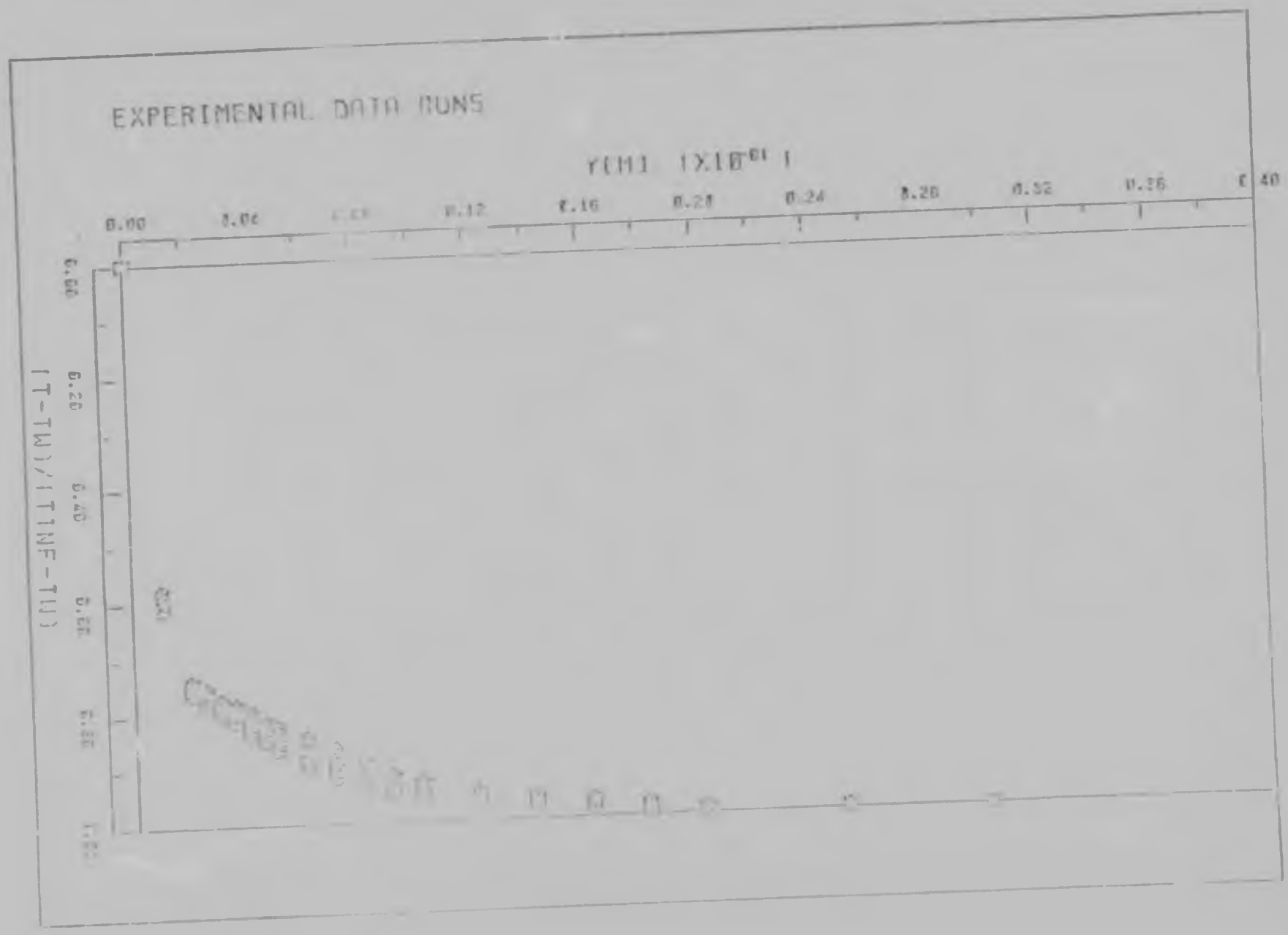
EXPERIMENTAL DATA RUNS
Y(M) 1X10^01
0.00
0.04
0.08
0.12
0.16
0.20
0.24
0.28
0.32
0.36
0.40
0.00
0.20
0.40
0.60
0.80
1.00
(T-TW)/(TINF-TW)

FIGURE 7.8

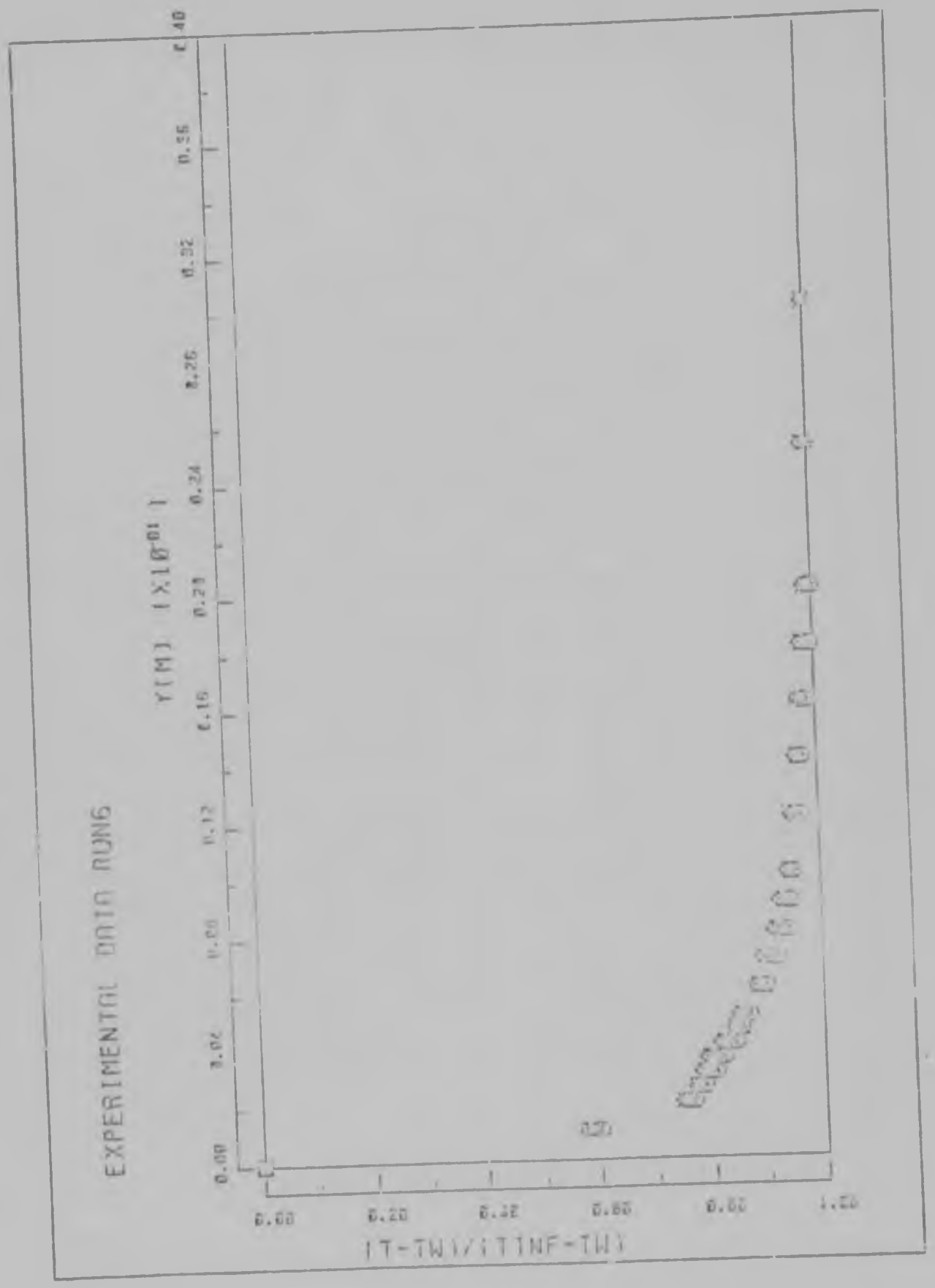
EXPERIMENTAL DATA RUNS
Y[M] (X10^01)
0.00
0.04
0.08
0.12
0.16
0.20
0.24
0.28
0.32
0.36
0.40
0.00
0.20
0.40
0.60
0.80
1.00
(T-TW)/(TINF-TW)

FIGURE 7.9

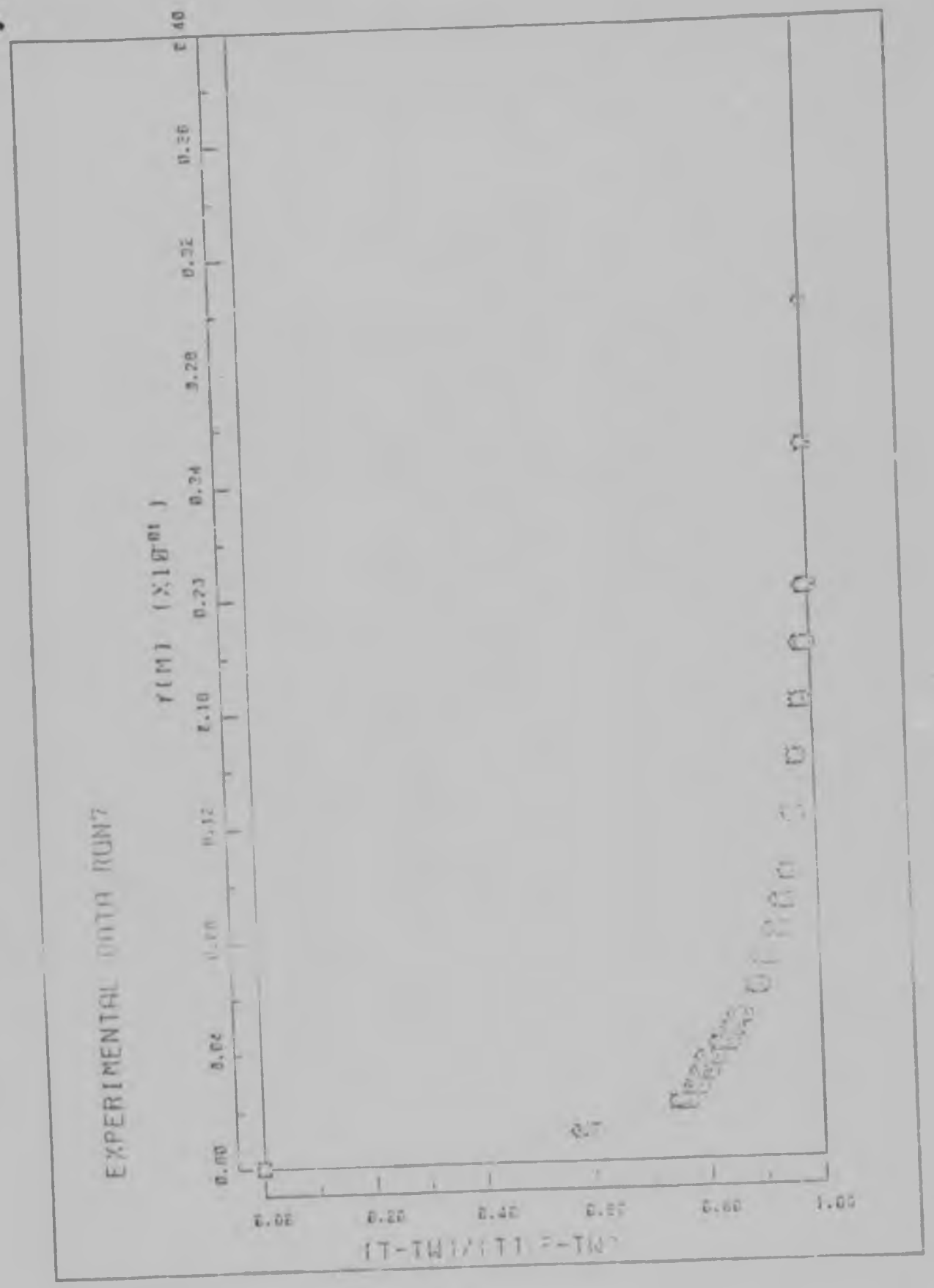
EXPERIMENTAL DATA RUN7
0.00
0.08
0.16
0.24
0.32
0.40
0.48
0.56
0.64
0.72
0.80
0.88
0.96
1.04
0.00
0.20
0.40
0.60
0.80
1.00

FIGURE 7.10

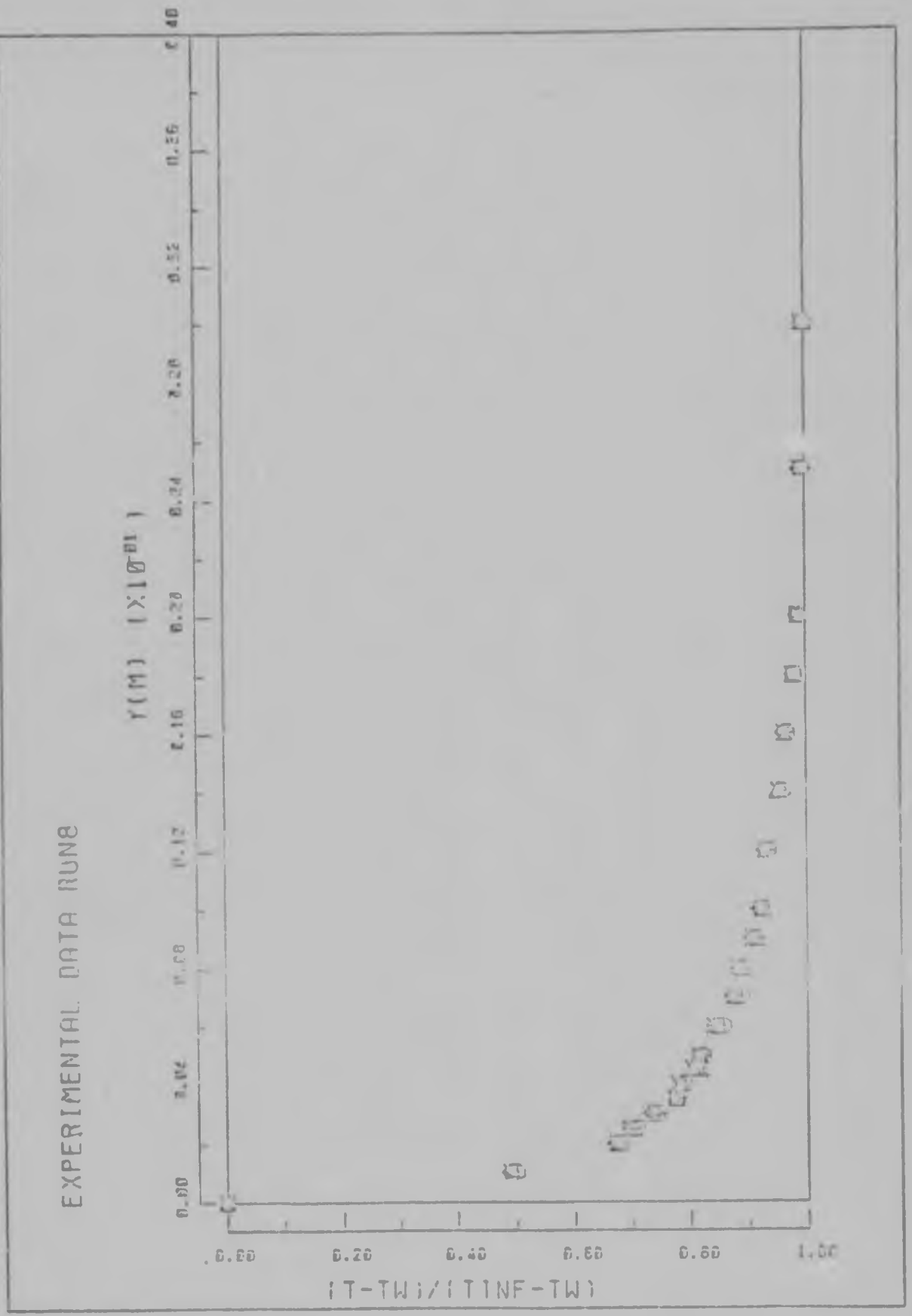
EXPERIMENTAL DATA RUN8
Y(M) (X10**01)
0.00
0.04
0.08
0.12
0.16
0.20
0.24
0.28
0.32
0.36
0.40
0.00
0.20
0.40
0.60
0.80
1.00
(T-TW)/(TINF-TW)

FIGURE 7.11

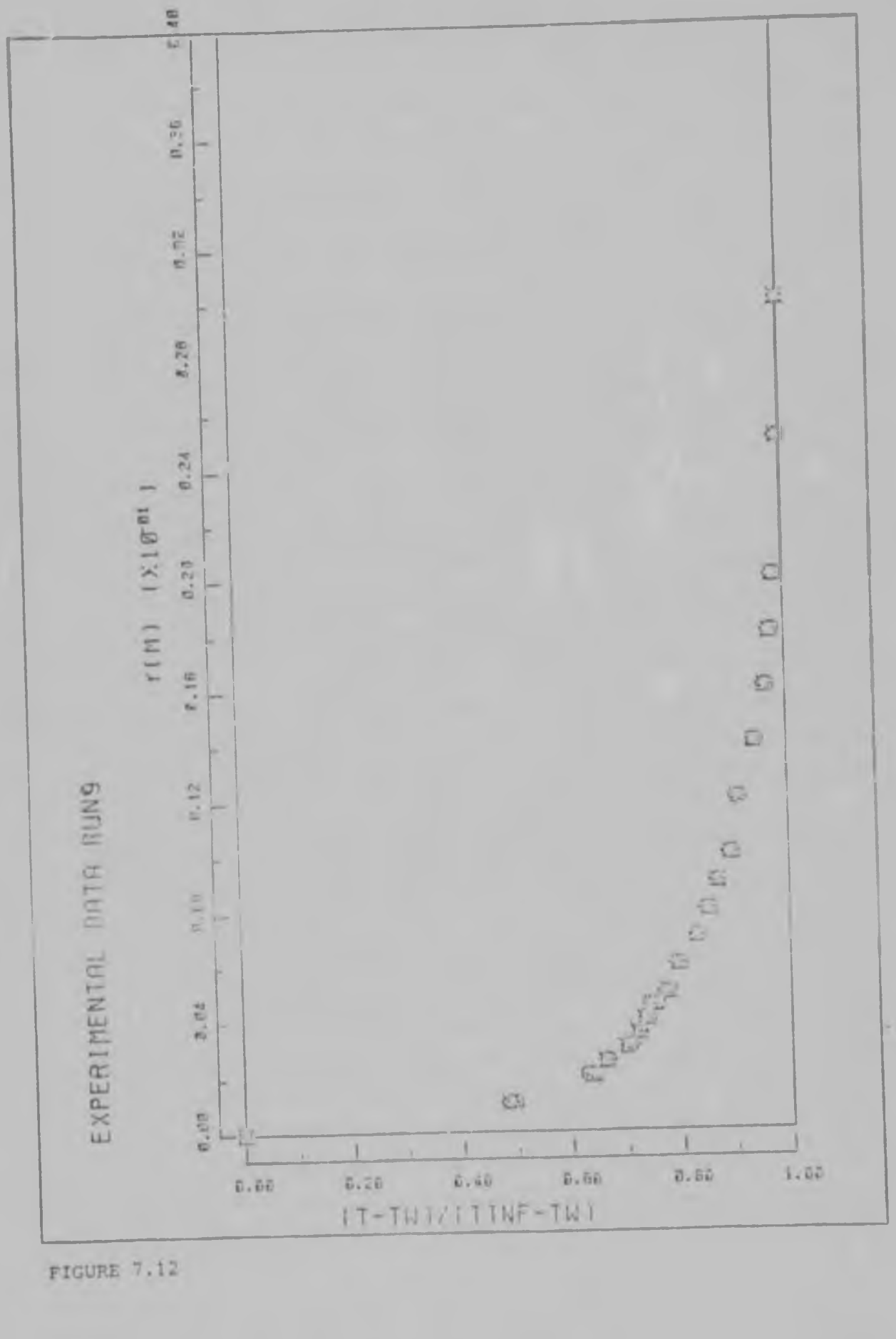
EXPERIMENTAL DATA RUN9
R(M) (X10**01)
0.00
0.04
0.08
0.12
0.16
0.20
0.24
0.28
0.32
0.36
0.40
0.00
0.20
0.40
0.60
0.80
1.00
(T-TW)/(TINF-TW)

FIGURE 7.12

7.2.2 Semi-Logarithmic Temperature Profiles

The temperature profiles obtained were also plotted on the so called "inner layer" coordinates with the lower axis in logarithmic form. These coordinates are used so as to investigate the similarity of the profiles due to constant free stream velocity and temperature with constant blowing.

As can be seen from these graphs (figs 7.13 through 7.21) it is only possible to measure the outer region or fully turbulent region, of the thermal boundary layer, and as such only outer layer similarity will be able to be investigated.

The first three figures (7.13, 7.14 and 7.15) can be considered together. In all these three runs the free stream velocities and temperatures were approximately the same, ie 14,95 m/s and 33°C, with increasing blowing.

Outer layer similarity is only evident in the last four profiles measured during run 1 (fig 7.13) which is most probably due to the step change in blowing from the unblown flat plate to the porous section. The boundary layer does not seem to have fully adjusted to this blowing condition during the first 100 mm of the porous section after which a similar situation results but due to the increased blowing the boundary layer seems to have settled down in a shorter distance along the porous section. For a blowing rate of F = 0,0076 the boundary layer settles down before the first measuring station (at 50 mm from the leading edge of the porous section). As mentioned by Kays and Moffat (12) the temperature profiles have significant scatter when plotted on semi-log coordinates using the dimensionless quantities t^+ and y^+ where

$$t^+ = \frac{T - T_w}{T_\infty - T_w} \frac{\sqrt{C_f/2}}{St} \qquad \ldots|7.2.1|$$

This scatter can be explained by the fact that t^+ includes both $C_f/2$ and St and thus inherently has more scatter than u^+ velocity profiles that are only dependent on the shear velocity U_τ ($u^+ = u/U_\tau, U_\tau = \sqrt{\tau_0/\rho}$)

The next four figures, 7.15 to 7.18, represent runs of 10 m/s free stream velocity and 40°C free stream temperature at increasing blowing rates for each run. Similarity of the profiles is evident in all these runs suggesting that the slower free stream velocity and higher temperature difference between the free stream and the porous wall enhances the idea of equilibrium profiles. There is a certain amount of scatter amongst the profiles but not as much as for the first three runs. All the profiles being the same could also mean that the boundary layer adjusted to flow conditions before the first station of measurement. The flow being slower than the initial three runs, most probably gave the boundary layer more time to settle down before measurements were taken. Nevertheless the adjustment of the boundary layer to blowing conditions in the first three runs is felt to be acceptable as Kays and Moffat [12] also reported adjustment of the boundary layer to a step change in blowing to take approximately 100 mm. These observations were made by measuring the heat transfer coefficient or Stanton number variation over a step change in blowing, from no blowing, F = 0, to blowing of F = 0,004.

Unlike the profiles presented by Kays and Moffat, which showed more scatter towards the edge of the boundary layer, the profiles presented so far have shown little if no scatter at the edge of the boundary layer. Most of the uncertainty being observed to occur at the beginning of the outer turbulent region. The inner region of the boundary layer unfortunately was not sufficiently

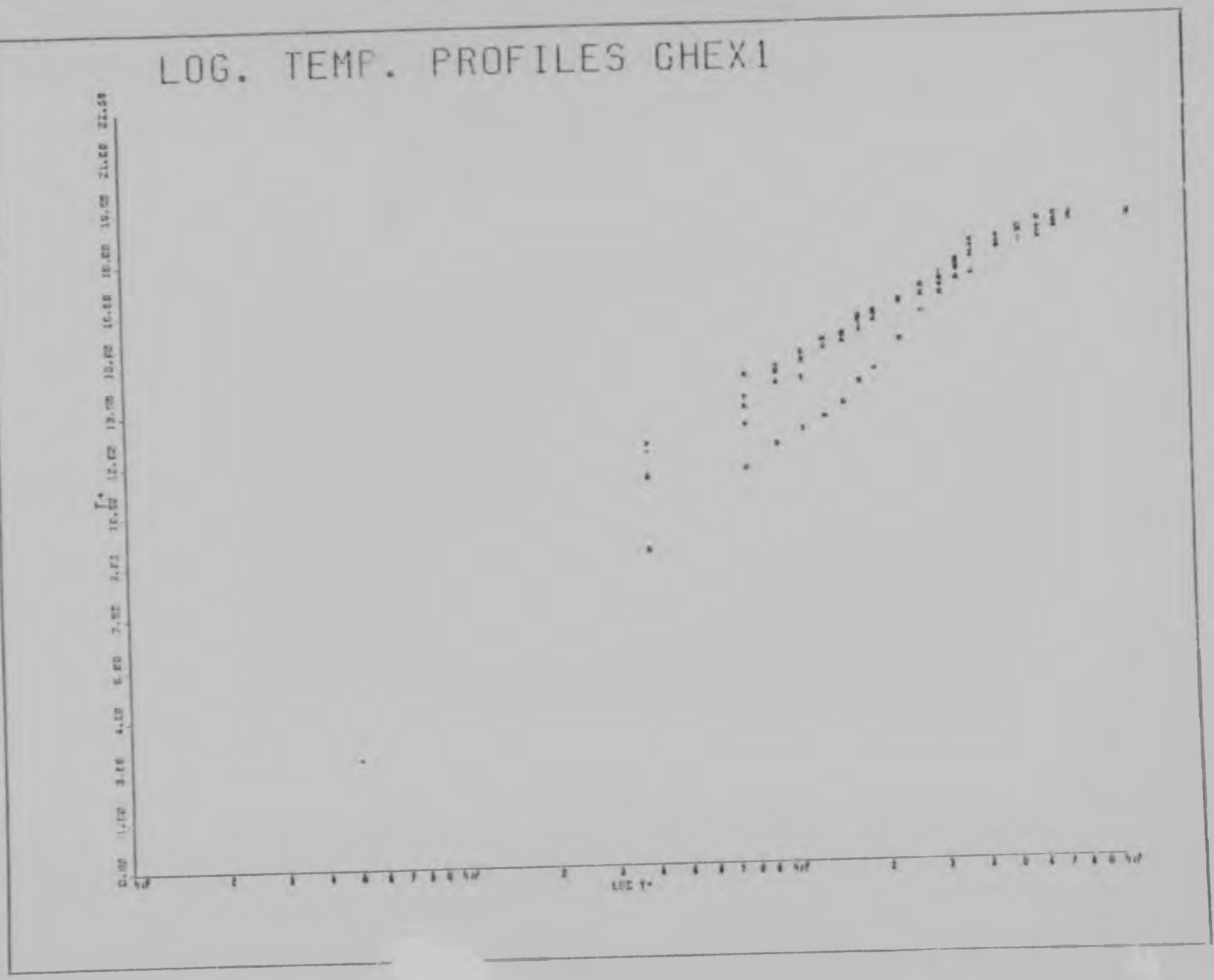

FIGURE 7.13

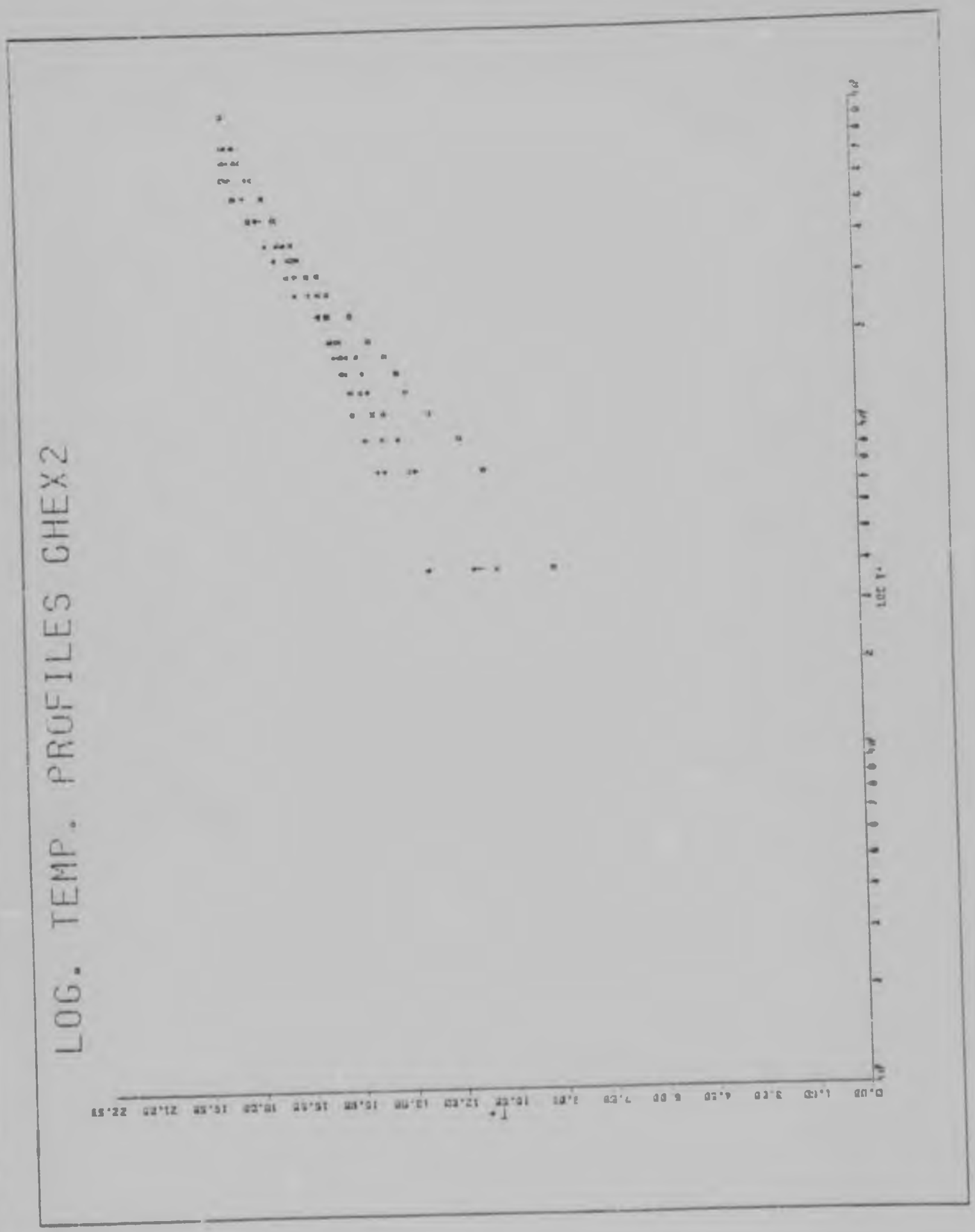

FIGURE 7.14

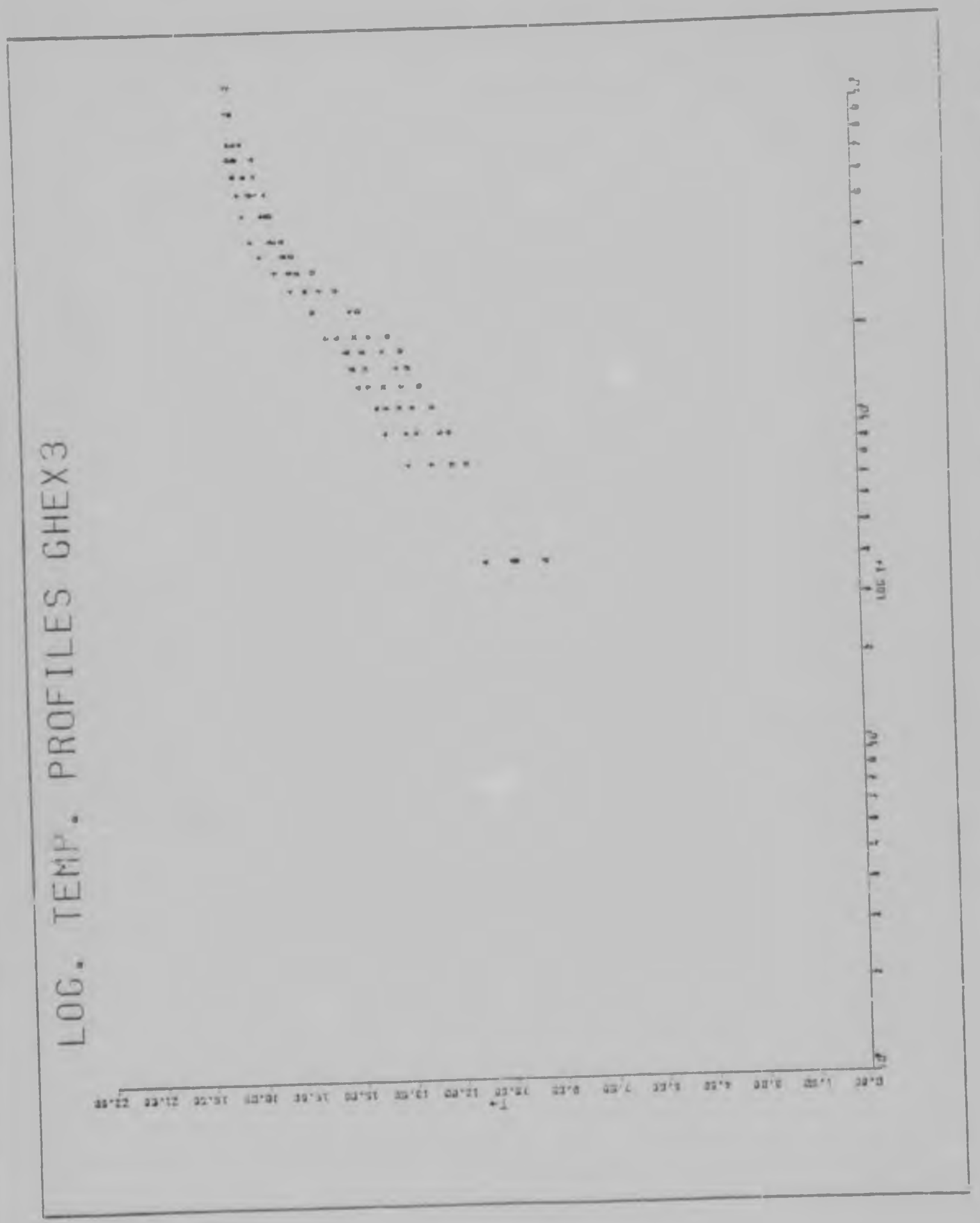

FIGURE 7.15

LOG. TEMP. PROFILES GHEX4



FIGURE 7.16

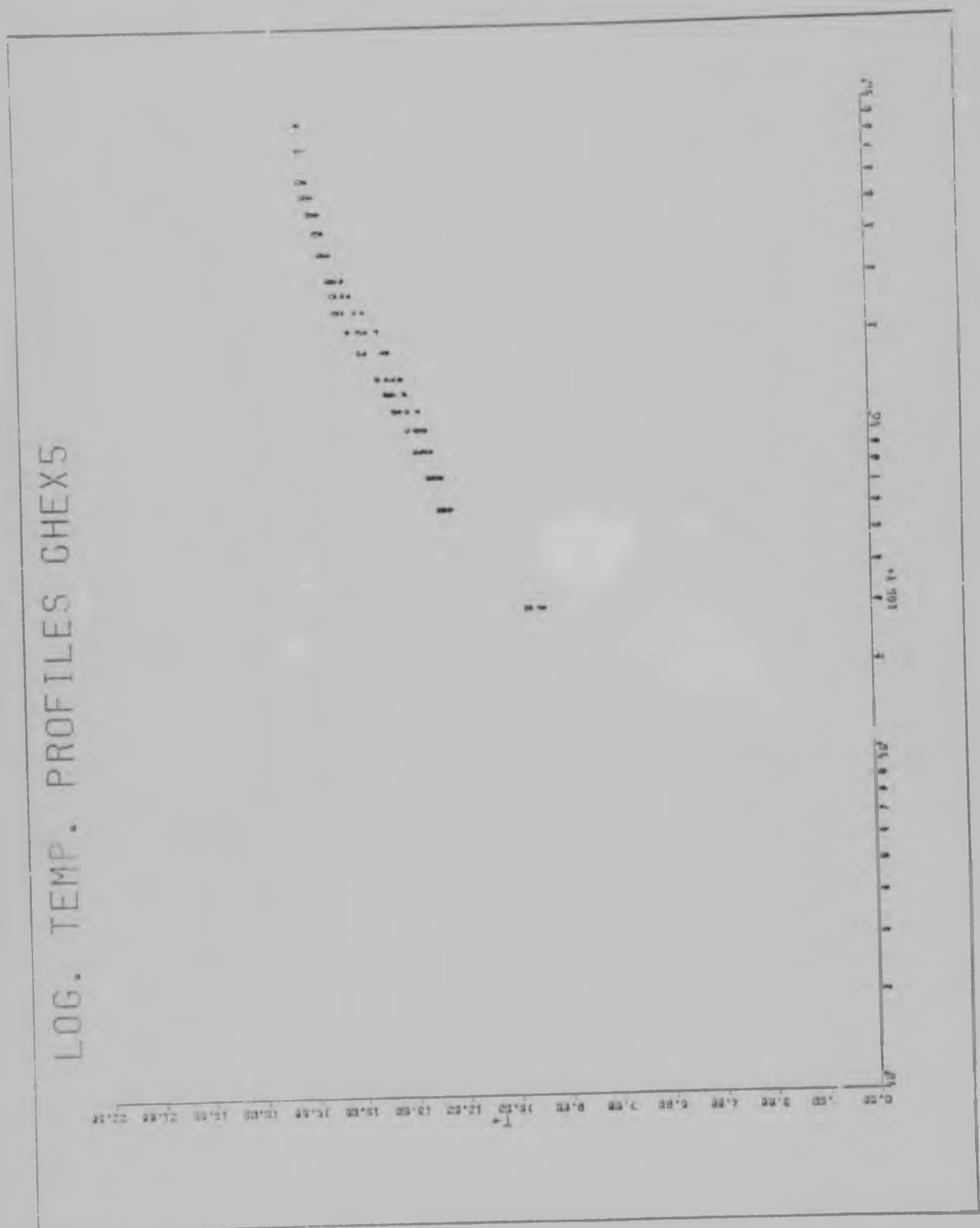

FIGURE 7.17

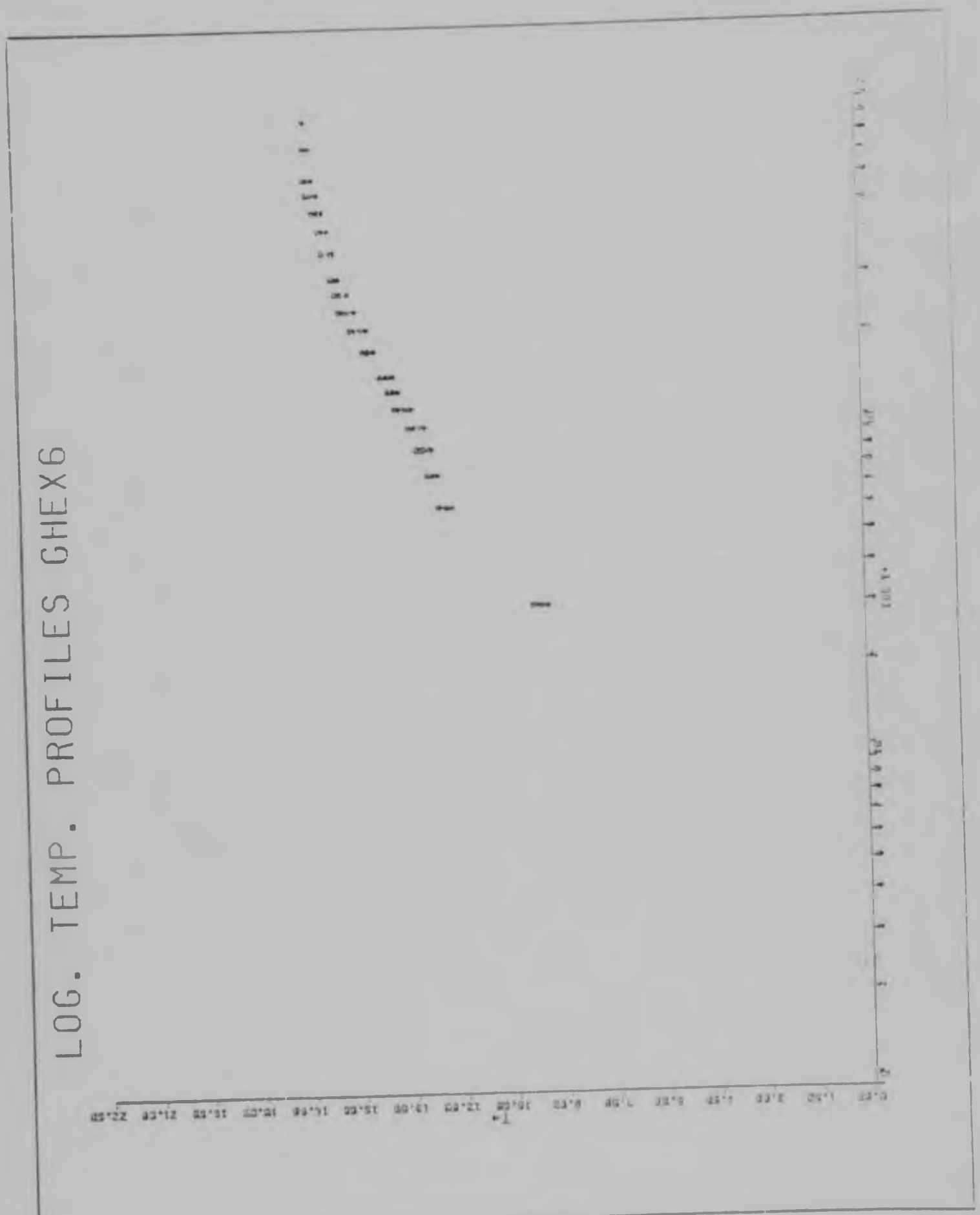

FIGURE 7.18

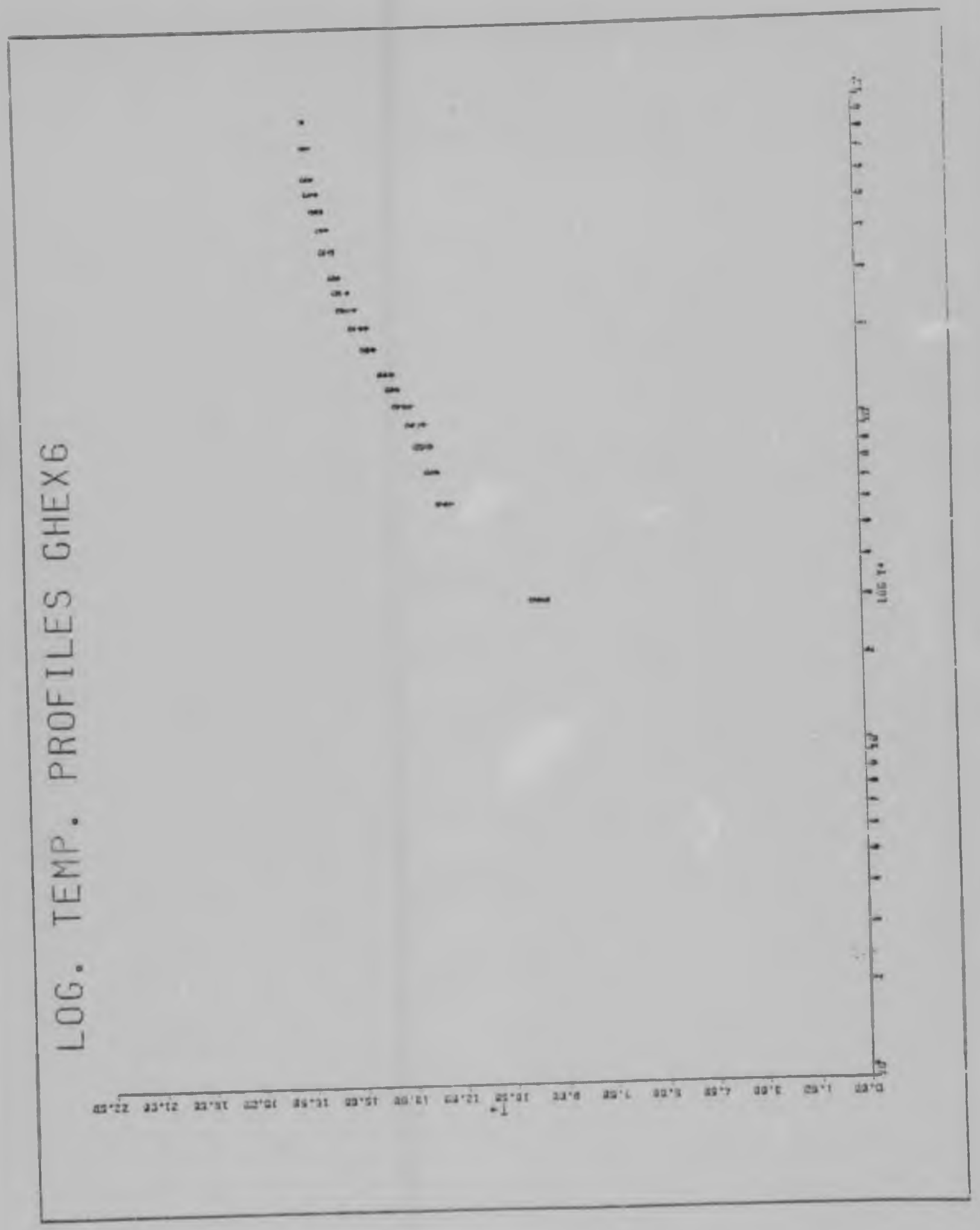

FIGURE 7.18

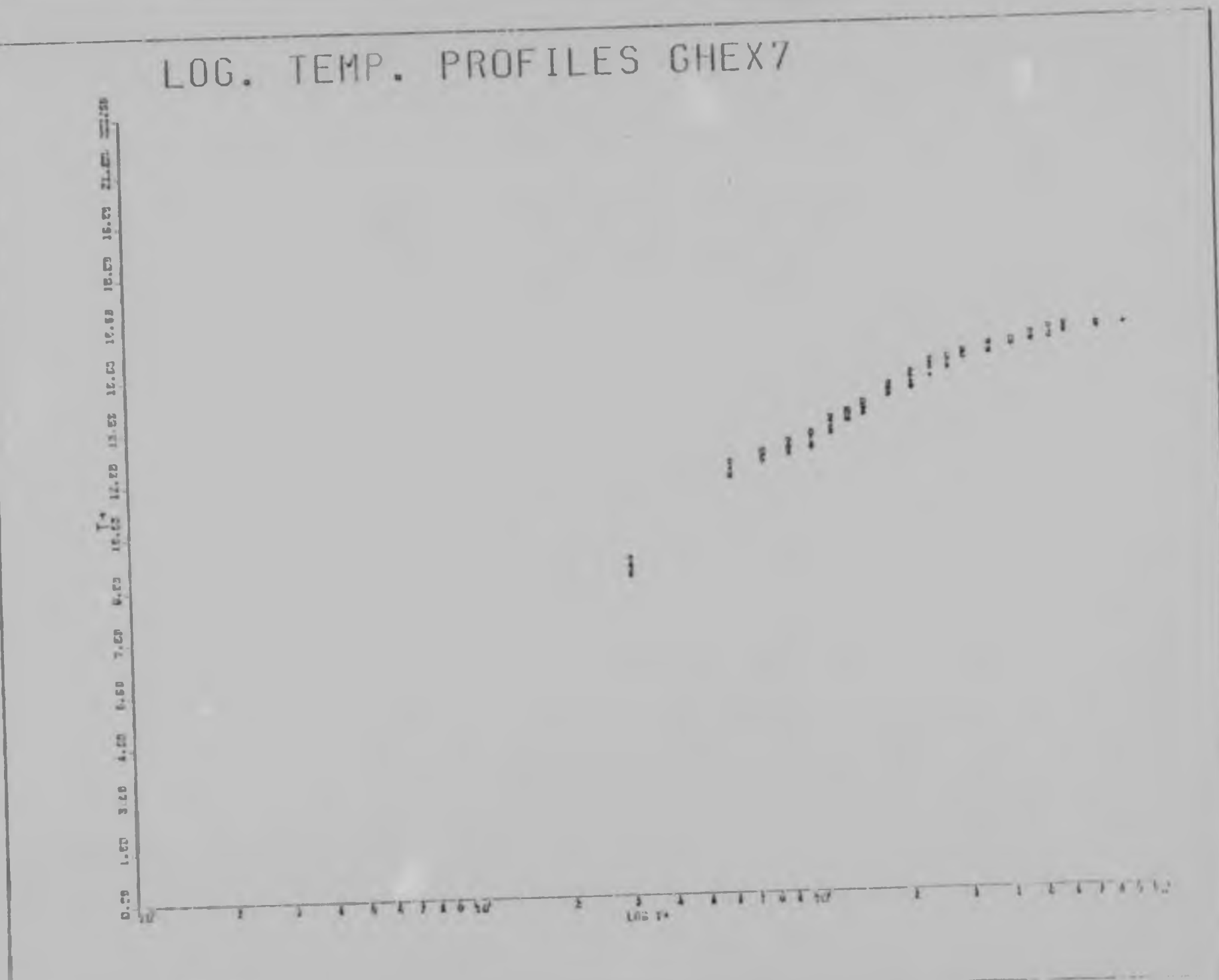

FIGURE 7.19

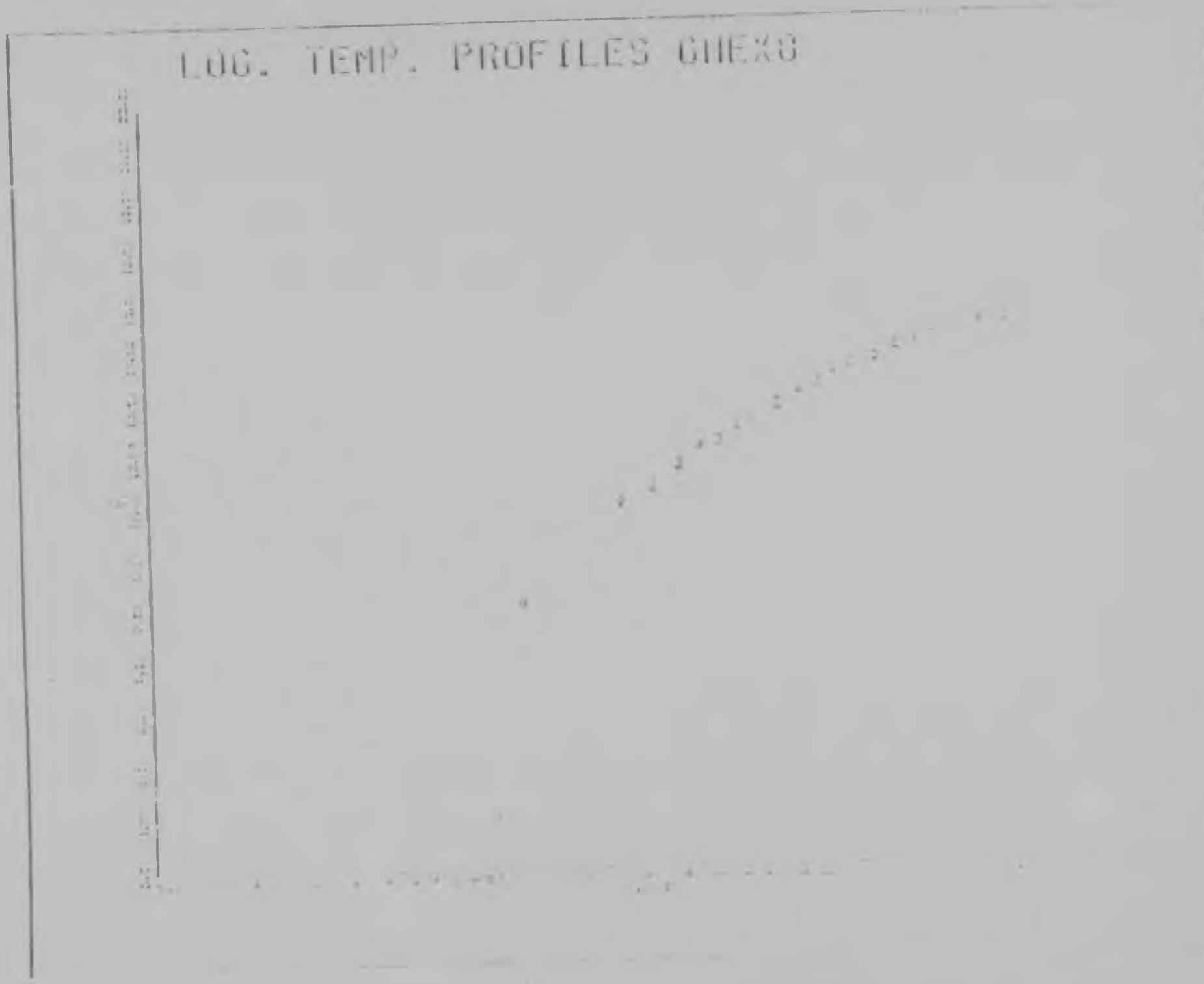

FIGURE 7.20

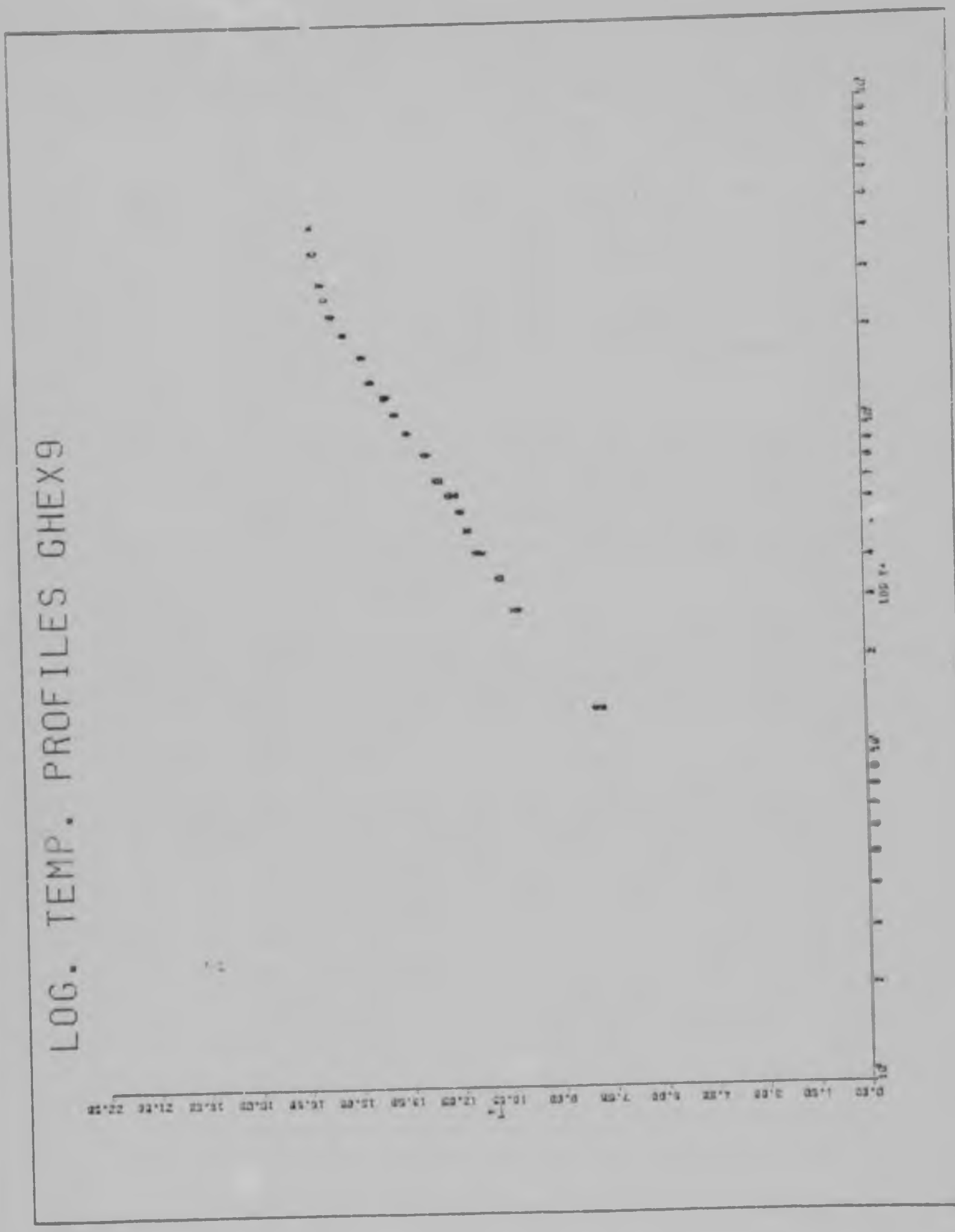

FIGURE 7.21

investigated so as to make any meaningful observations. The general trend of all the profiles measured as represented on the following figures agrees with those presented by Kays and Moffat. The outer region of the thermal boundary layer shows a linear upward trend with a slight upsweep of the profile points at the edge of the boundary layer followed by a levelling off of the points at the extremities. Once again the parabolic nature of the inner region can not be commented on as not enough points were obtained in this region.

The final two figures, 7.19 and 7.20, are for the runs of minimum free stream velocity and maximum free stream temperature. These two runs display very good similarity of the fully turbulent region, with only slight scatter of the data points as measured.

The profiles obtained during these two runs also showed outer region linear variation as well as the slight deviation from this linear trend at the edge of the boundary layer.

When air is the working fluid of both the mainstream and coolant flow, the values of Prandtl number and Turbulent Prandtl number are both near unity, especially at the beginning of the fully turbulent region. Thus it can be expected that u^+ and t^+ would be similarly distributed within the boundary layer in a constant velocity flow (which exhibits velocity profile similarity). It is reasonable to expect t^+ to vary like u^+ within the boundary layer.

If throughout the boundary layer the normalised velocity and temperature profiles are assumed to be completely similar, i.e :

$$\frac{u}{u_\infty} = \frac{T - T_w}{T - T_w} \qquad \ldots|7.2.2|$$

then from the definition of u^+ and t^+ (equation 7.2.1) the

$$t^+ = u^+ \left(\frac{C_f/2}{St}\right) \qquad \ldots|7.2.3|$$

Thus the temperature profile can be approximated as proportional to the velocity profile for constant free stream velocity and temperature.

7.3 Comparison of Experimental Results with Computer Program Predictions

Once the experimental results were obtained the computer program was employed so as to predict the measured flow situation.

The main stream and coolant flow parameters were used as inputs to the program, so that the flow conditions as measured and as predicted would have the same boundary conditions. The parameters used were free stream velocity, u_∞; free stream temperature T_∞; wall temperature, T_w; coolant flow velocity out of the wall, v_w; and the flow static pressure over the flat plate, p. The free stream flow parameters remained constant over the full length of the flat plate, however, the wall temperature and coolant flow velocity had to be adjusted at the beginning of the porous section. The wall temperature dropped from that of the free stream temperature (as the tunnel was in thermal equilibrium after running for approximately one hour) to the temperature as measured by the embedded thermocouples in the porous section. The blowing rate varied from no blowing to that as set by the coolant flow system at the beginning of the porous section and then reduced to no blowing at the end of the porous section.

$$\frac{u}{u_\infty} \equiv \frac{T - T_w}{T - T_w} \qquad \ldots|7.2.2|$$

then from the definition of u^+ and t^+ (equation 7.2.1) the

$$t^+ = u^+ \left(\frac{C_f/2}{St}\right) \qquad \ldots|7.2.3|$$

Thus the temperature profile can be approximated as proportional to the velocity profile for constant free stream velocity and temperature.

7.3 Comparison of Experimental Results with Computer Program Predictions

Once the experimental results were obtained the computer program was employed so as to predict the measured flow situation.

The main stream and coolant flow parameters were used as inputs to the program, so that the flow conditions as measured and as predicted would have the same boundary conditions. The parameters used were free stream velocity, u_∞; free stream temperature T_∞; wall temperature, T_w; coolant flow velocity out of the wall, v_w; and the flow static pressure over the flat plate, p. The free stream flow parameters remained constant over the full length of the flat plate, however, the wall temperature and coolant flow velocity had to be adjusted at the beginning of the porous section. The wall temperature dropped from that of the free stream temperature (as the tunnel was in thermal equilibrium after running for approximately one hour) to the temperature as measured by the embedded thermocouples in the porous section. The blowing rate varied from no blowing to that as set by the coolant flow system at the beginning of the porous section and then reduced to no blowing at the end of the porous section.

$$\frac{u}{u_\infty} \equiv \frac{T - T_w}{T - T_w} \qquad \ldots|7.2.2|$$

then from the definition of u^+ and t^+ (equation 7.2.1) the

$$t^+ \equiv u^+ \left(\frac{C_f/2}{St}\right) \qquad \ldots|7.2.3|$$

Thus the temperature profile can be approximated as proportional to the velocity profile for constant free stream velocity and temperature.

7.3 Comparison of Experimental Results with Computer Program Predictions

Once the experimental results were obtained the computer program was employed so as to predict the measured flow situation.

The main stream and coolant flow parameters were used as inputs to the program, so that the flow conditions as measured and as predicted would have the same boundary conditions. The parameters used were free stream velocity, u_∞; free stream temperature T_∞; wall temperature, T_w; coolant flow velocity out of the wall, v_w; and the flow static pressure over the flat plate, p. The free stream flow parameters remained constant over the full length of the flat plate, however, the wall temperature and coolant flow velocity had to be adjusted at the beginning of the porous section. The wall temperature dropped from that of the free stream temperature (as the tunnel was in thermal equilibrium after running for approximately one hour) to the temperature as measured by the embedded thermocouples in the porous section. The blowing rate varied from no blowing to that as set by the coolant flow system at the beginning of the porous section and then reduced to no blowing at the end of the porous section.

A total of eleven profiles were calculated at the following x-stations: 0,547; 0,597; 0,647; 0,697; 0,747, 0,797; 0,847; 0,897; 0,947; 0,997; 1,047. This gave an even spacing for the forward step solution that the program used. The initial points had to be moved rearward, to x_1 = 0,600; x_2 = 0,65 etc, for the runs at the slowest free stream velocity so as to satisfy the solution of only turbulent boundary layer flow. The option of transition from laminar to turbulent flow was not used in the following predictions, as transition could not be predicted. Six profiles were computed before the porous section, and measuring stations. These were adequate in that any irregularities that may have been introduced, especially in the generation of the initial two profiles to start the computational procedure, would be smoothed out by the time the profiles to be predicted had been reached computationally.

Figure 7.22 gives the comparison between the experimental and computational results for run 1 where the main stream flow velocity is 14,95 m/s and temperature is 33°C with a wall temperature of 25°C at a blowing rate of 0,064 m/s. The program is able to predict the transition of the profiles from unblown to blown wall conditions as can be seen by the change in the shape of the porfile especially in the outer turbulent region. The first three profiles are accurately predicted whereas the last two profiles predicted by the program tend to indicate a larger deficit of the profiles as measured in the region of transition from the inner sub-layer to the outer fully turbulent region. The slope of the curve at the wall corresponds to the slope of a line between the first two measuring points, this indicates that the heat transfer rate to the wall can be predicted computationally. The prediction of the edge of the thermal boundary layer for all five stations correspond

well to those measured during the experimental procedure.

The prediction of the profiles resulting from similar main stream conditions but with an increase in blowing rate, to 0,088 m/s giving a wall temperature of 23,64°C, are shown in figure 7.23. For this case the first two profiles were predicted whereas the final three profiles the program prediction showed a deficit in the lower fully trubulent region, after which the profiles cross, and the program prediction bulges beyond the measured points. The heat transfer, or slope at the wall, and edge of the thermal boundary layer as predicted by the program correspond to the measured profiles.

For the final run, figure 7.24 at a free stream velocity of 14,95 m/s with the following flow parameters: free stream temperature 34,1°C; wall temperature 23,0°C and a blowing rate of 0,113 m/s the correlation between the measured and predicted results is good for all five profiles. This seems to suggest that flows of high flow velocities are more accurately predicted by the program. This observation is more evident when considering the rest of the runs as illustrated by figures 7.25 through 7.30.

By decreasing the free stream flow velocity to 10,85 m/s and increasing the free stream temperature to 39,0°C the profiles calculated, although satisfactory, did not correspond to the measured points in the region close to the wall. The theoretical prediction of the heat transfer rate to the wall is thus less than the actual measured value. This is illustrated in figure 7.25 where the wall temperature resulting was 26,5°C with a blowing rate of 0,064 m/s.

Figure 7.26 gives the prediction for similar flow conditions except that the blowing rate is increased to 0,088 m/s.

Here the lack of correspondence between predicted and measured results is more evident especially in the latter profiles where the computational procedure is not able to predict the effect of the increased blowing on the inner thermal boundary layer. However, the outer layer predictions correspond to the measured results.

As the blowing rate increases this inaccuracy of the prediction of the profiles close to the wall, resulting in lower predicted heat transfer rates, increases as illustrated in figure 7.27. For a flow velocity of 10,85 m/s and temperature of 39,54°C the blowing rate is increased to 0,112 m/s to give a wall temperature of 26,13°C. The initial profiles predicted correspond with the measured results at the first stations, the shortcoming of the program to accurately predict the final profiles could be attributed to either the effect the blowing rate has on the complete solution of the profiles (where the largest effect would be on the region closest to the wall) or the effect the blowing rate has on the turbulent Prandtl number. The turbulent Prandtl number is modelled according to investigations carried out on a blown boundary layer but, similar to the shortcomings of these experimental results, insufficient data is available as to the behaviour of the turbulent Prandtl number close to the wall. The effect of varying the turbulent Prandtl number significantly effects the prediction of the profiles in the region closest to the wall and as such the turbulent Prandtl number variation closest to the wall should be further investigated.

As the free stream flow velocity is decreased, and the free stream temperature and blowing rate increased as in the flows represented in figures 7.27 through 7.30 this inaccuracy at the wall becomes more pronounced. However, the prediction of the outer boundary layer is more accurate, the height of the predicted boundary layer corresponding to the height of the measured boundary layer.

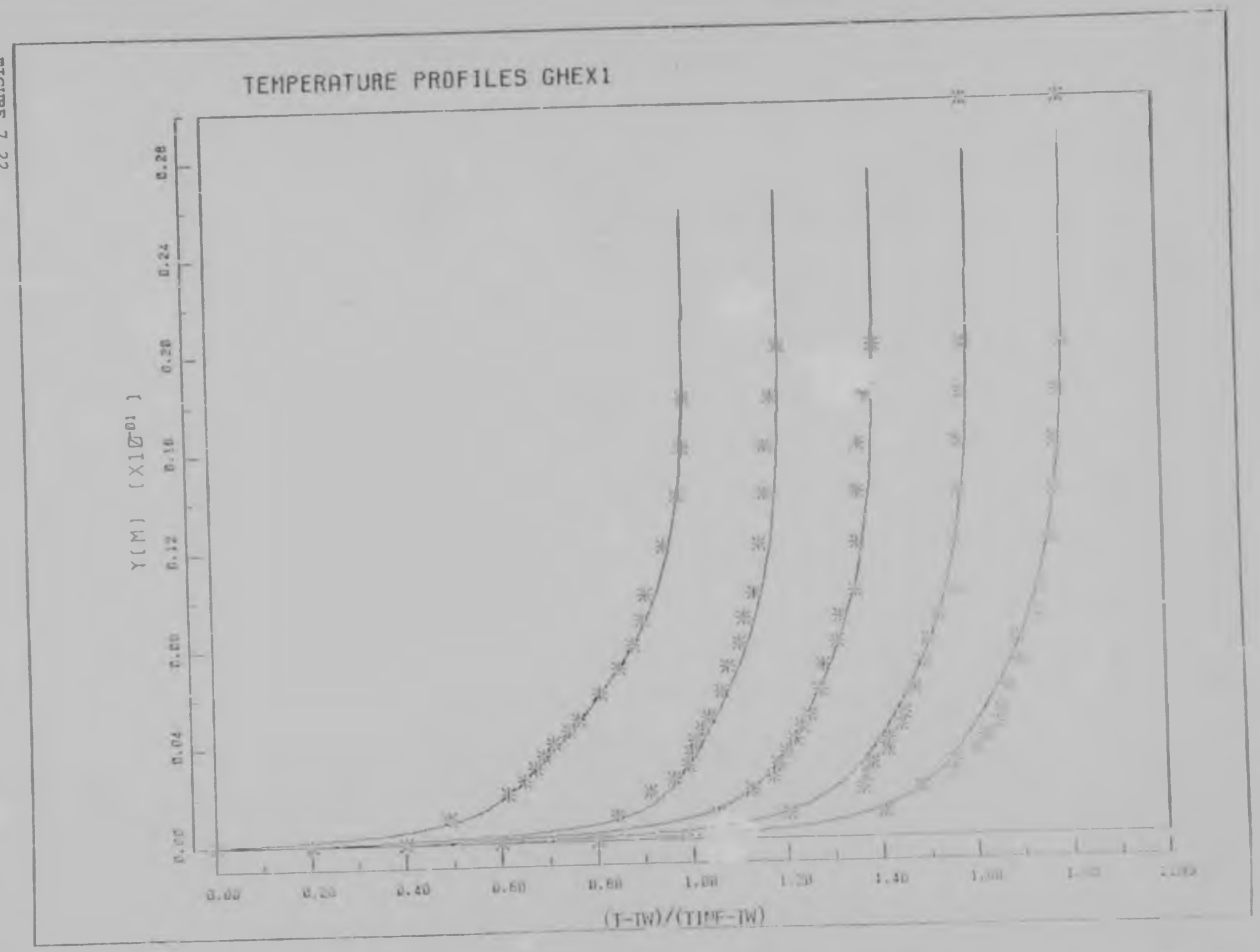
TEMPERATURE PROFILES GHEX1
Y(M) (X10^-01)
0.00
0.04
0.08
0.12
0.16
0.20
0.24
0.28
0.00
0.20
0.40
0.60
0.80
1.00
1.20
1.40
(T-TW)/(TINF-TW)

FIGURE 7.22

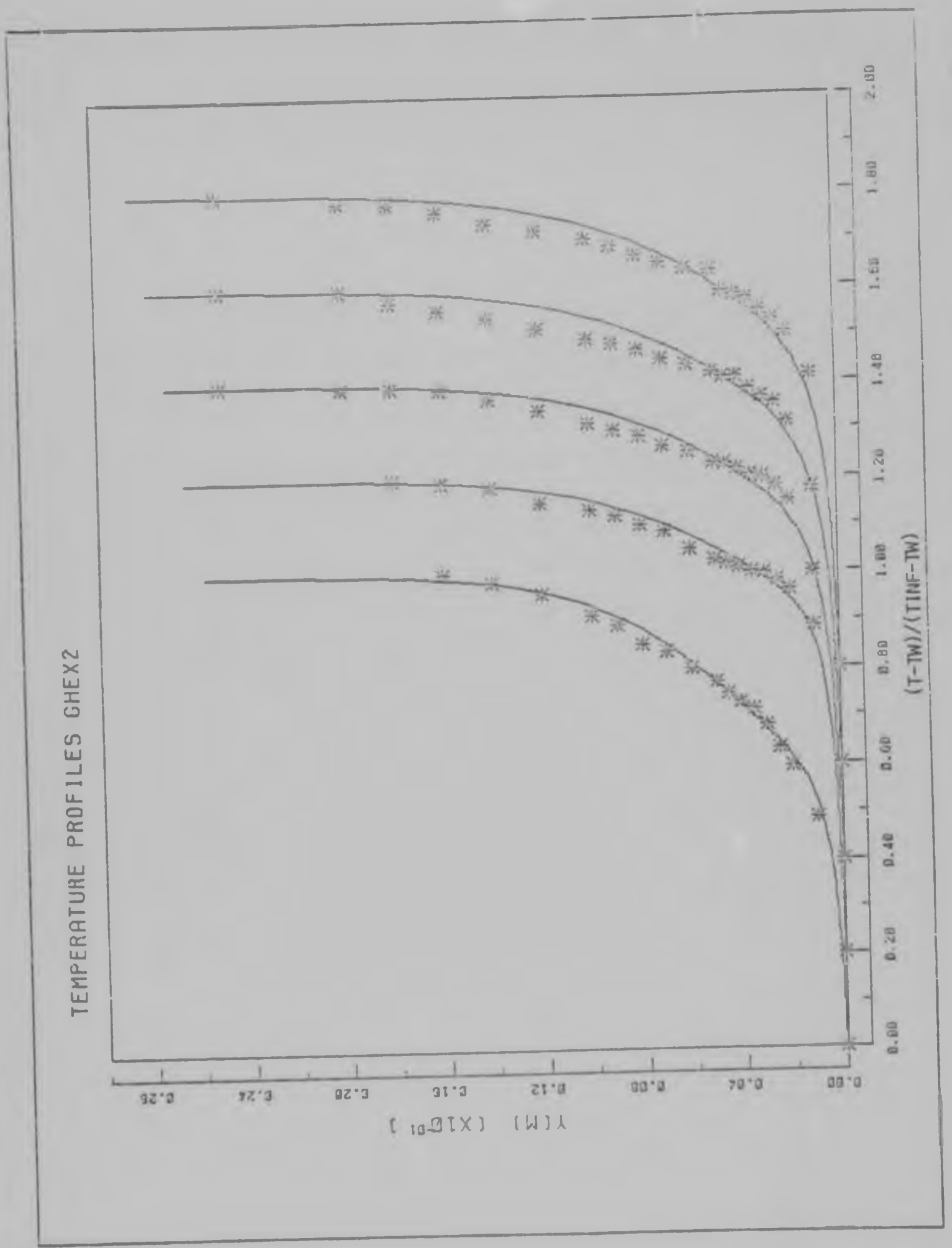
TEMPERATURE PROFILES GHEX2
Y(M) (X10E-01)
0.00
0.04
0.08
0.12
0.16
0.20
0.24
0.28
(T-TW)/(TINF-TW)
0.00
0.20
0.40
0.60
0.80
1.00
1.20
1.40
1.60
1.80
2.00

FIGURE 7.23

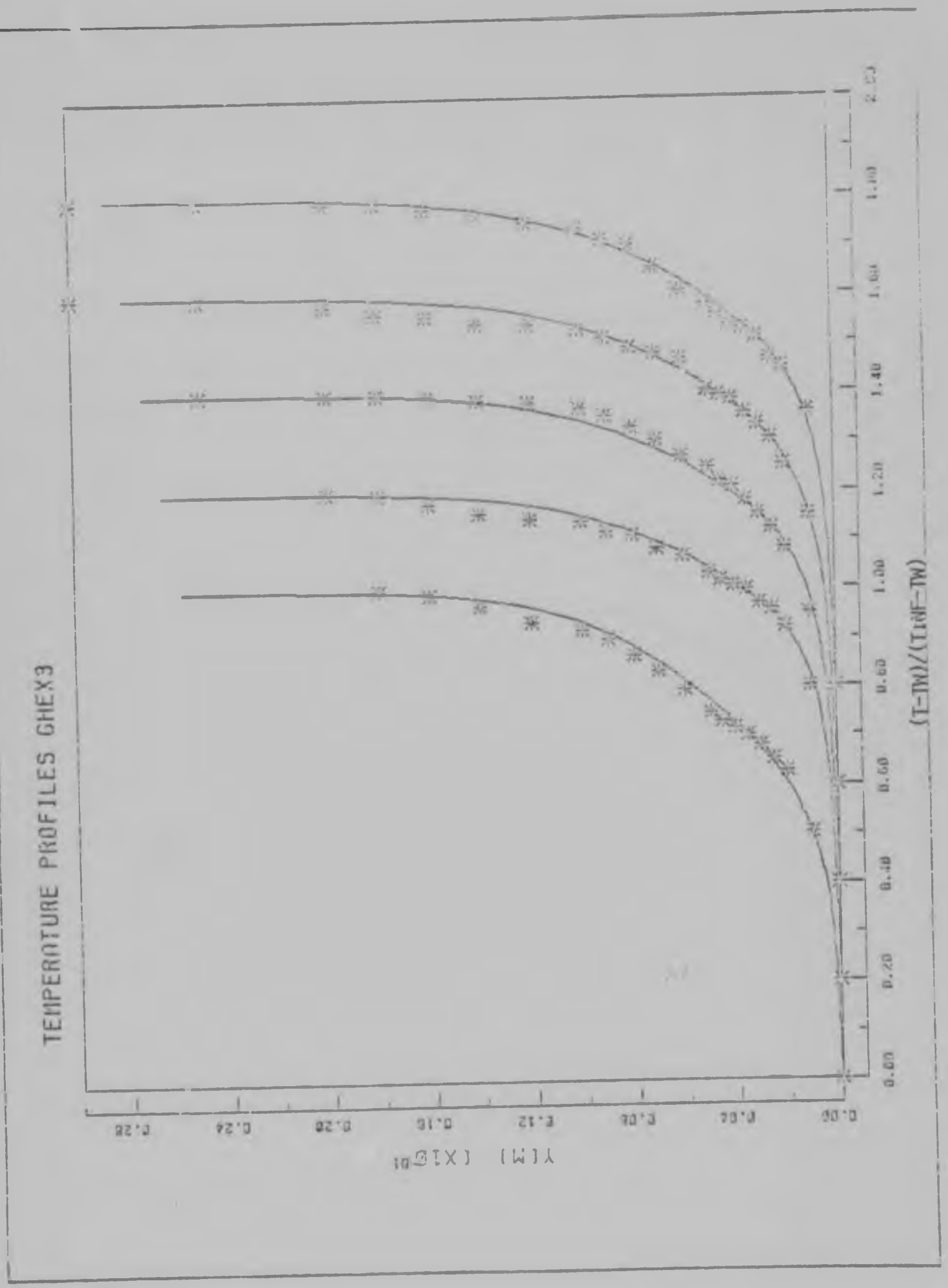
TEMPERATURE PROFILES GHEX3
Y[M] (X10**-01
0.00
0.04
0.08
0.12
0.16
0.20
0.24
0.28
0.00
0.20
0.40
0.60
0.80
1.00
1.20
1.40
1.60
1.80
2.00
(T-TW)/(TINF-TW)

FIGURE 7.24

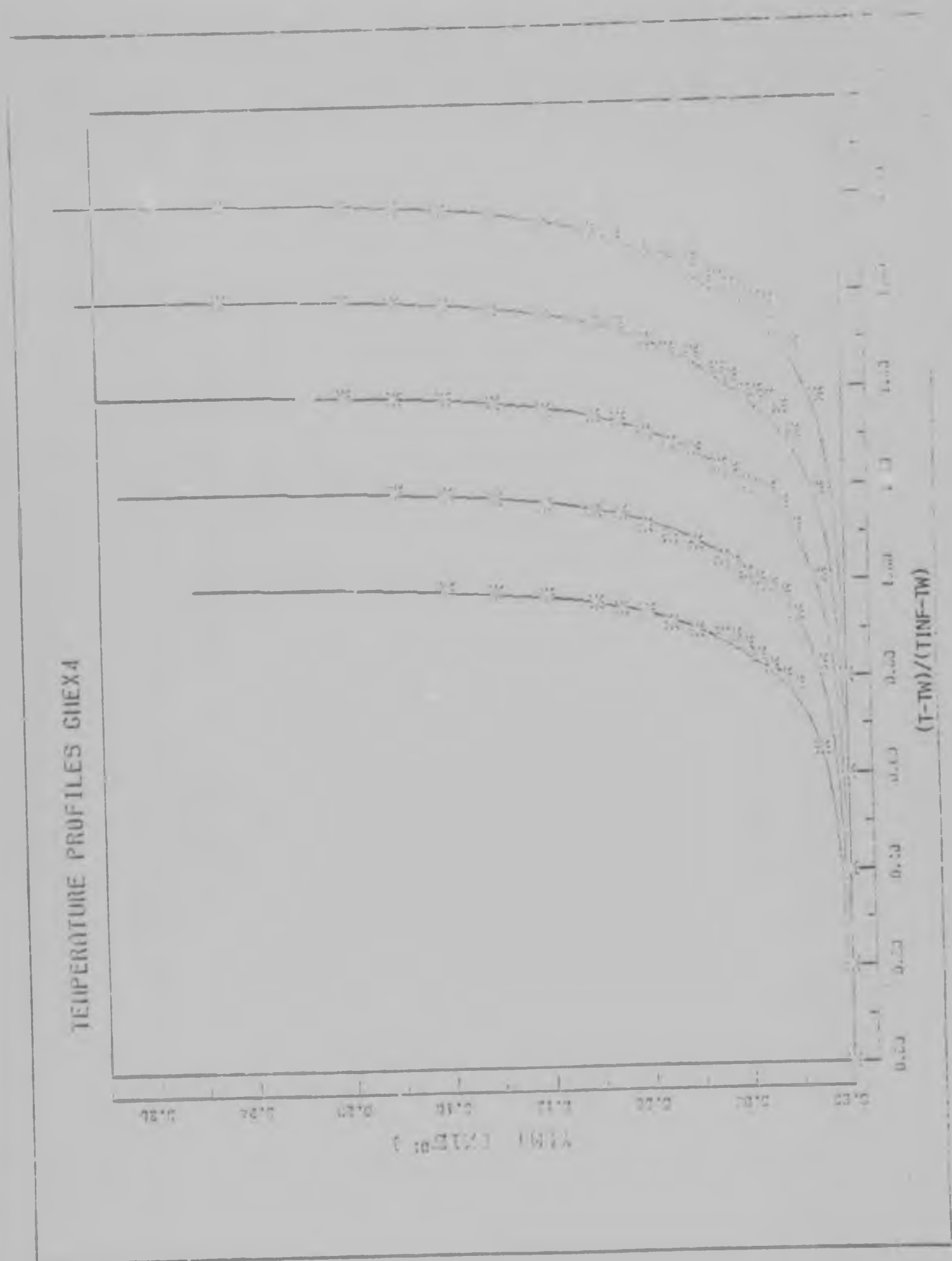

FIGURE 7.25

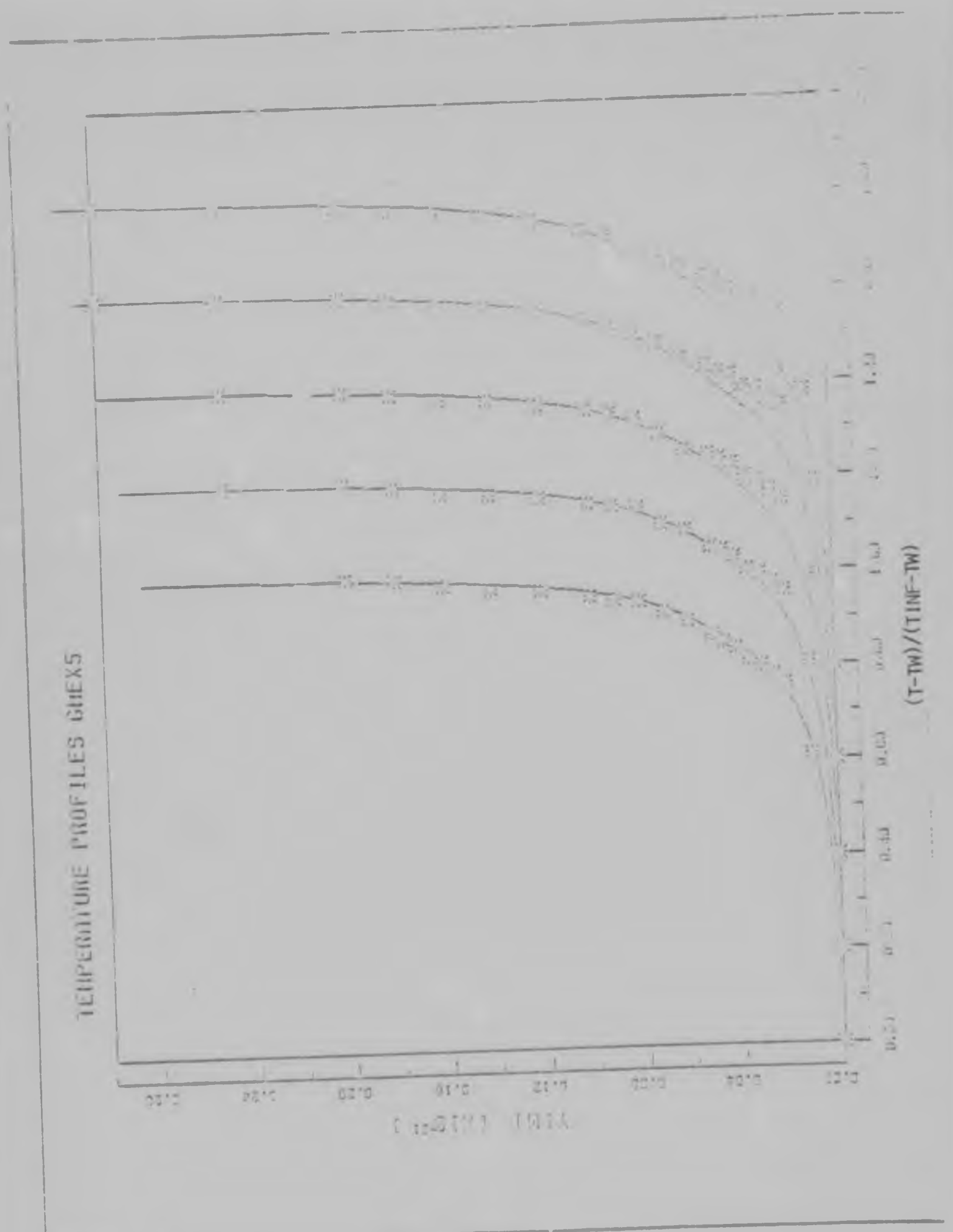

FIGURE 7.26

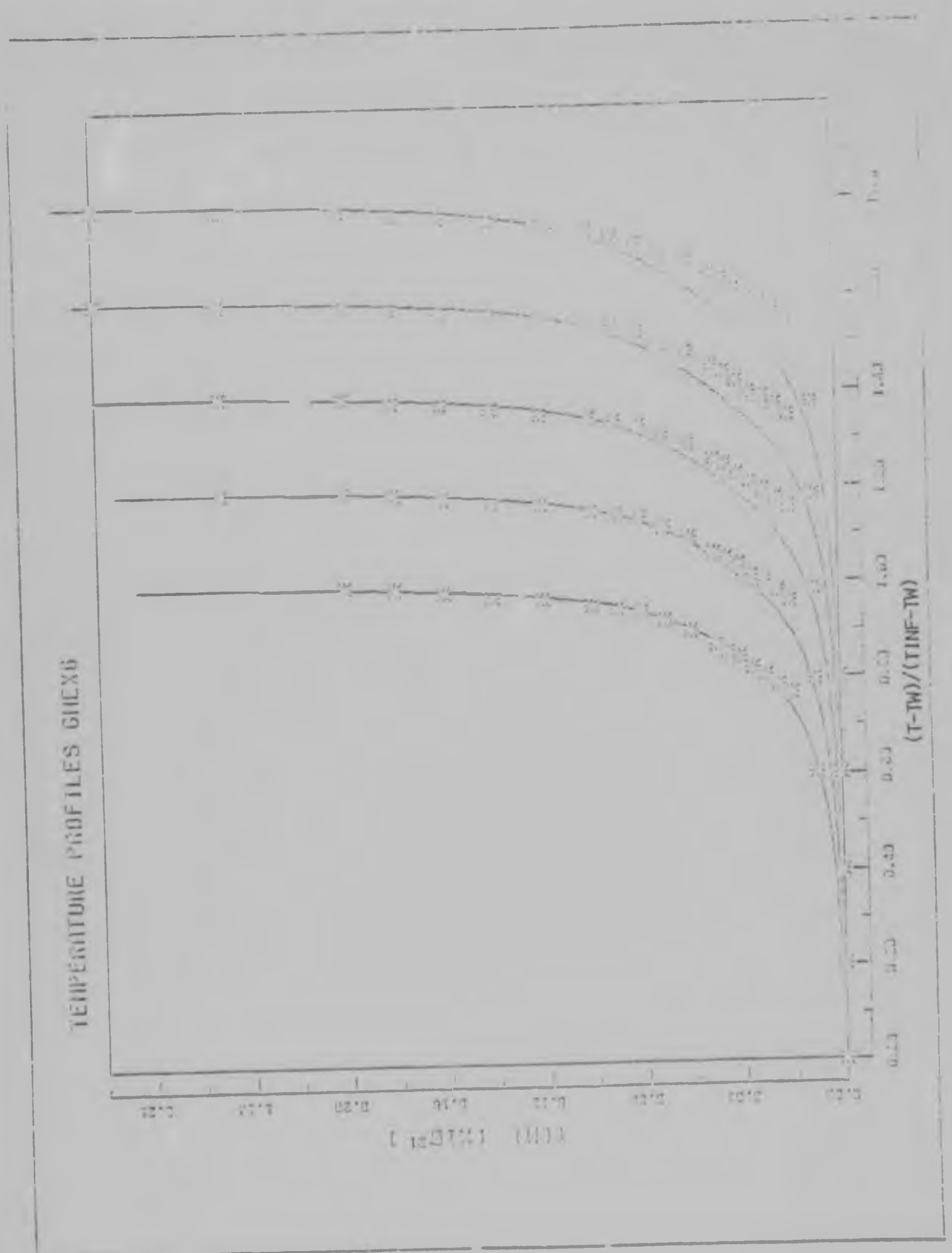

FIGURE 7.27

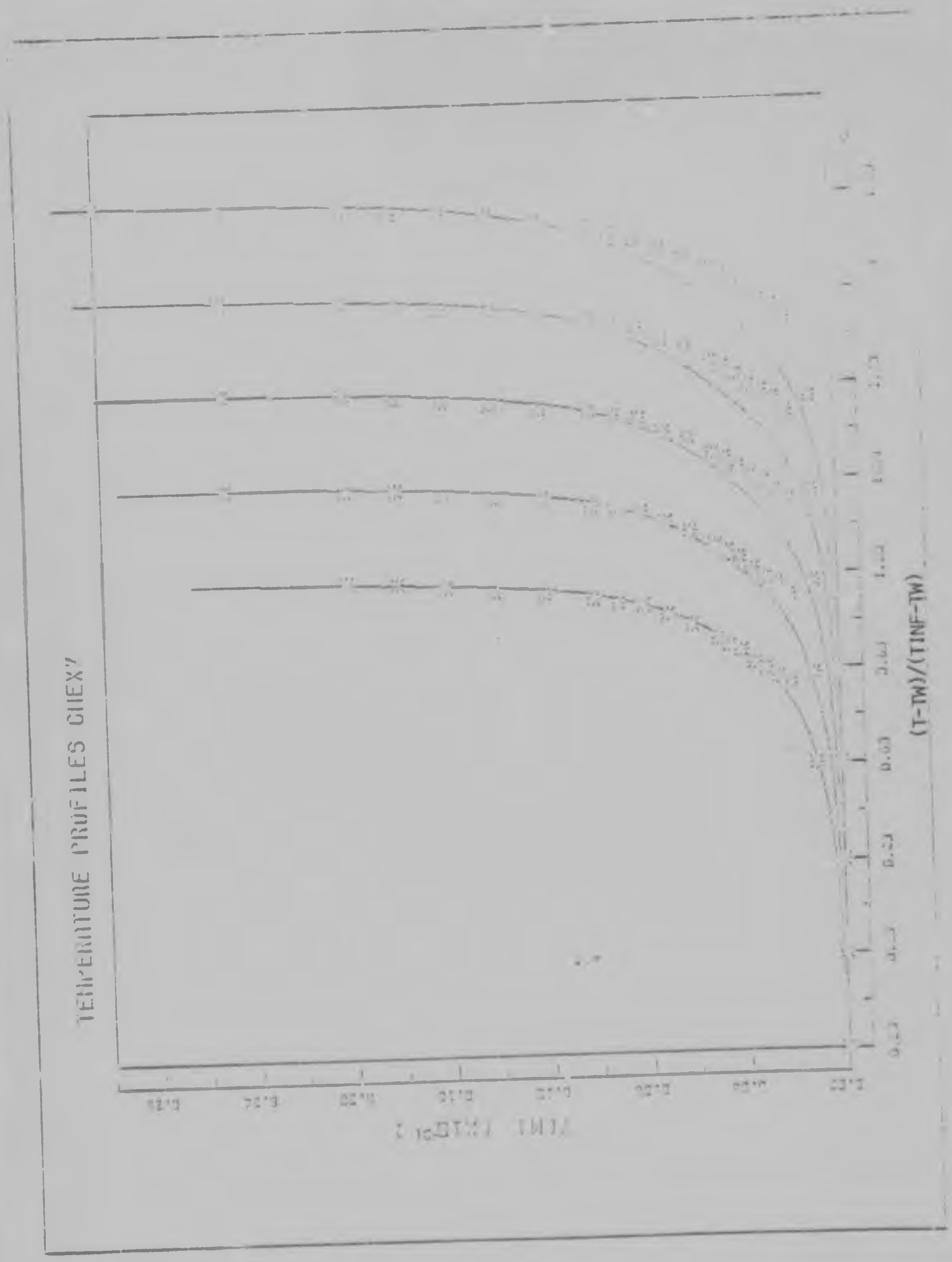

FIGURE 7.28

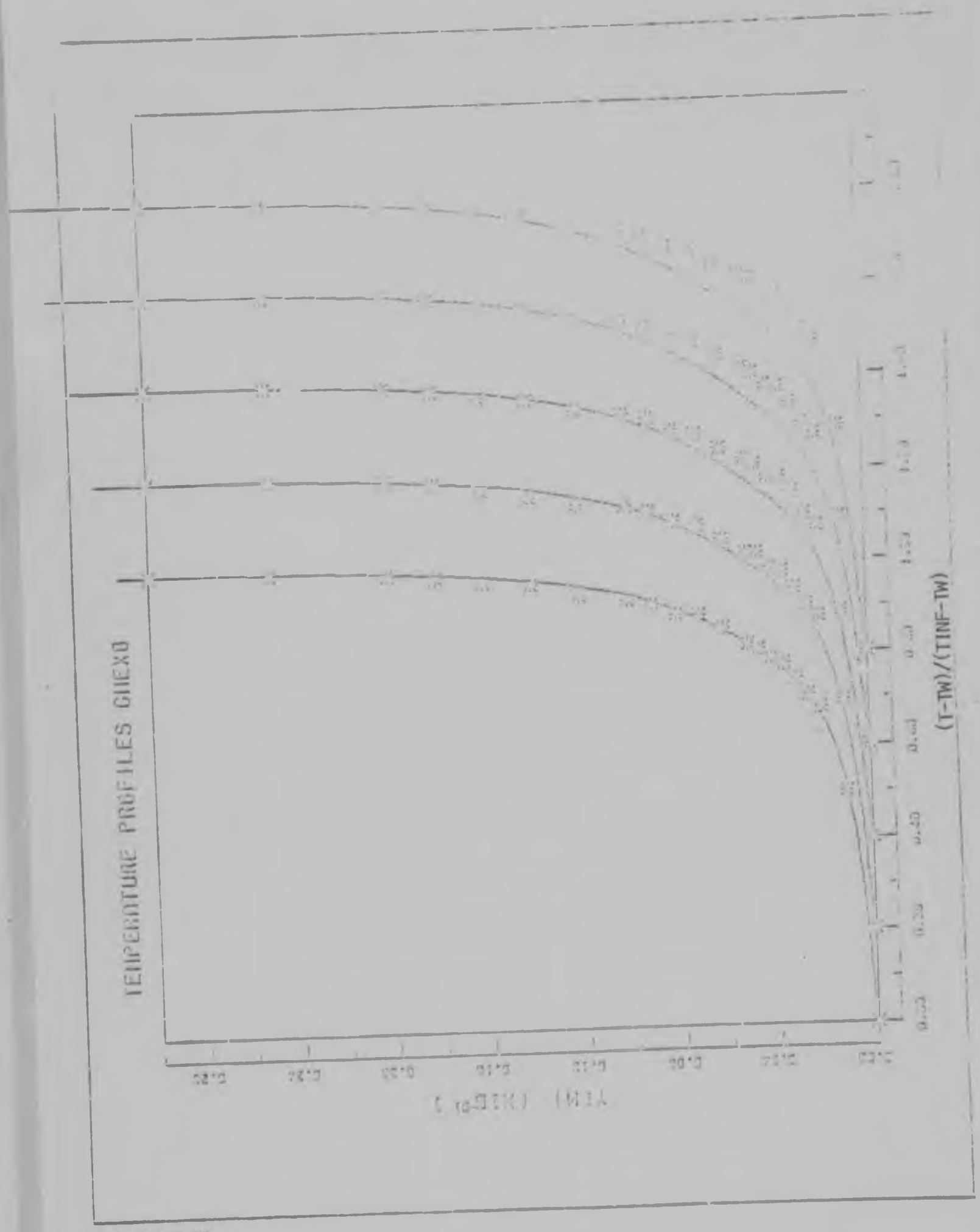

FIGURE 7.29

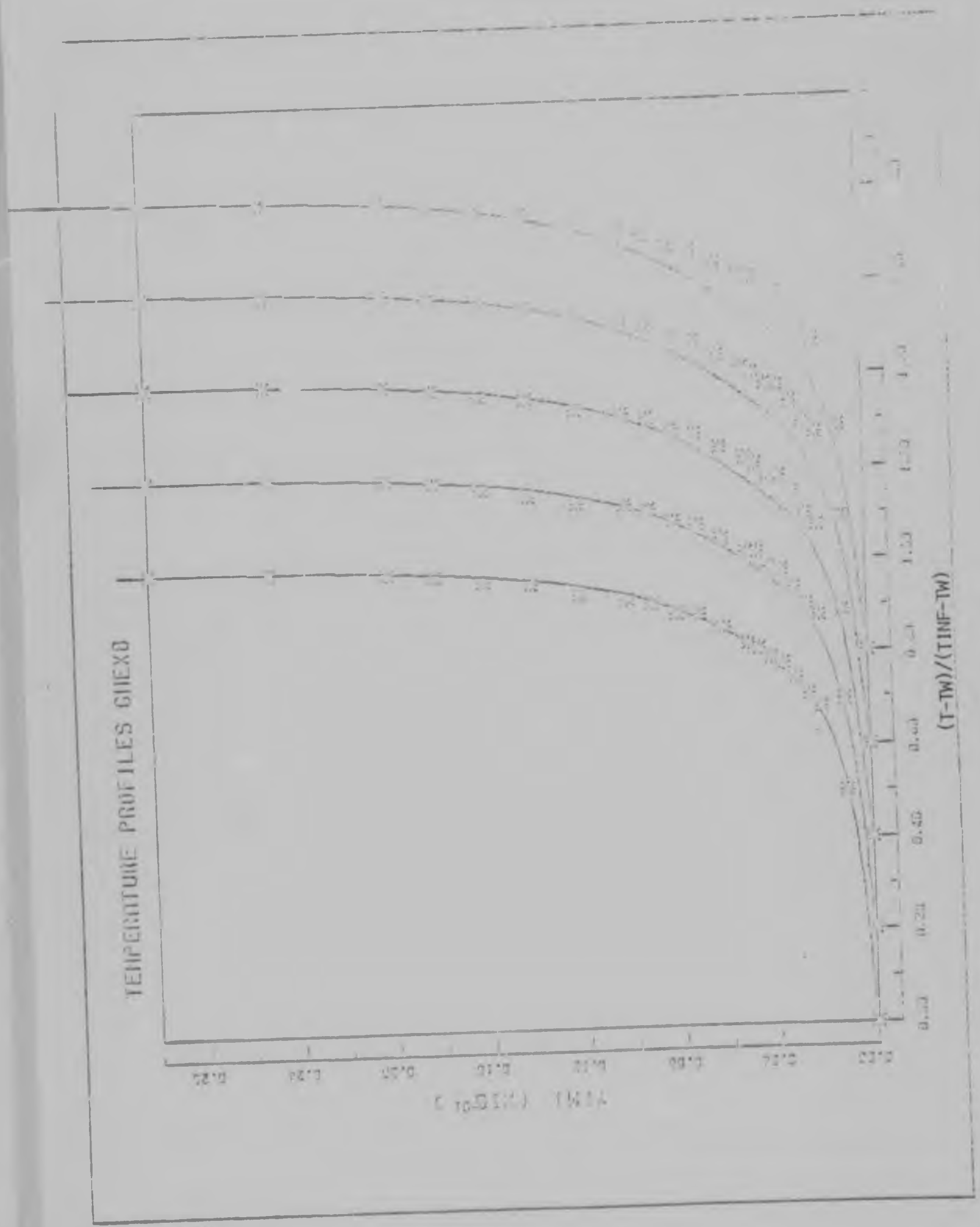

FIGURE 7.29

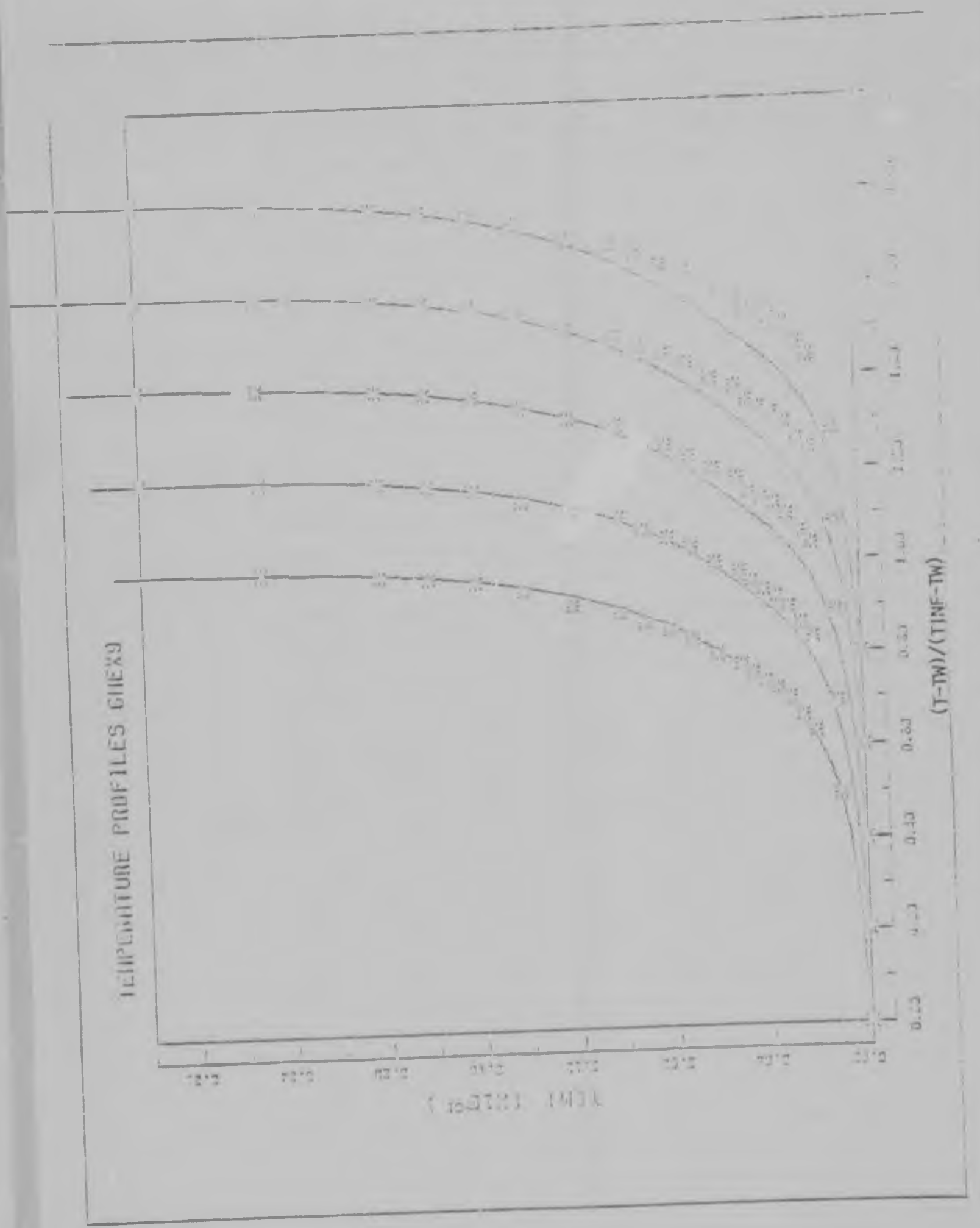

FIGURE 7.30

7.4 Comparison of Mickley, Ross, Squyers and Stewart Results (17) with Those Predicted by the Computer Program

An attempt was made to predict the experimental results as reported by Mickley et al (17) in their report on the heat, mass and momentum transfer for flow over a flat plate with blowing. Unfortunately only one set of experimental data, resulting from run H-17a, was able to be adequately predicted by the computer program. Several sets of data were however, investigated but the predictions of these experimental runs is felt to be unsatisfactory.

The validity of this data has been questioned by the authors themselves in an erratum attached to the beginning of the report. Mention is only made of erroneous local friction coefficient in the order of 15 to 30 percent, with no mention of the heat transfer characteristics. The data reported in this technical note was so comprehensively documented that it was possible to use the boundary conditions presented as inputs to the current computer program so as to predict the final reported temperature profiles. Due to the lack of any other documented data points these results were used although not much emphasis should be placed on the program's ability or inability to predict these results.

A similar method of drawing up the inputs to the program was used as described in the previous section on the prediction of the present experimental results. The free stream flow parameters and wall coolant flow parameters were used. Eleven profiles were generated by the program with the final five representing the actual measured profiles. The initial profiles being used once again to allow for any irregularities to be smoothed out by the implicit finite difference scheme. As stated earlier the porous wall was electrically heated and thus an inverse temperature gradient resulted, which the program is able to predict

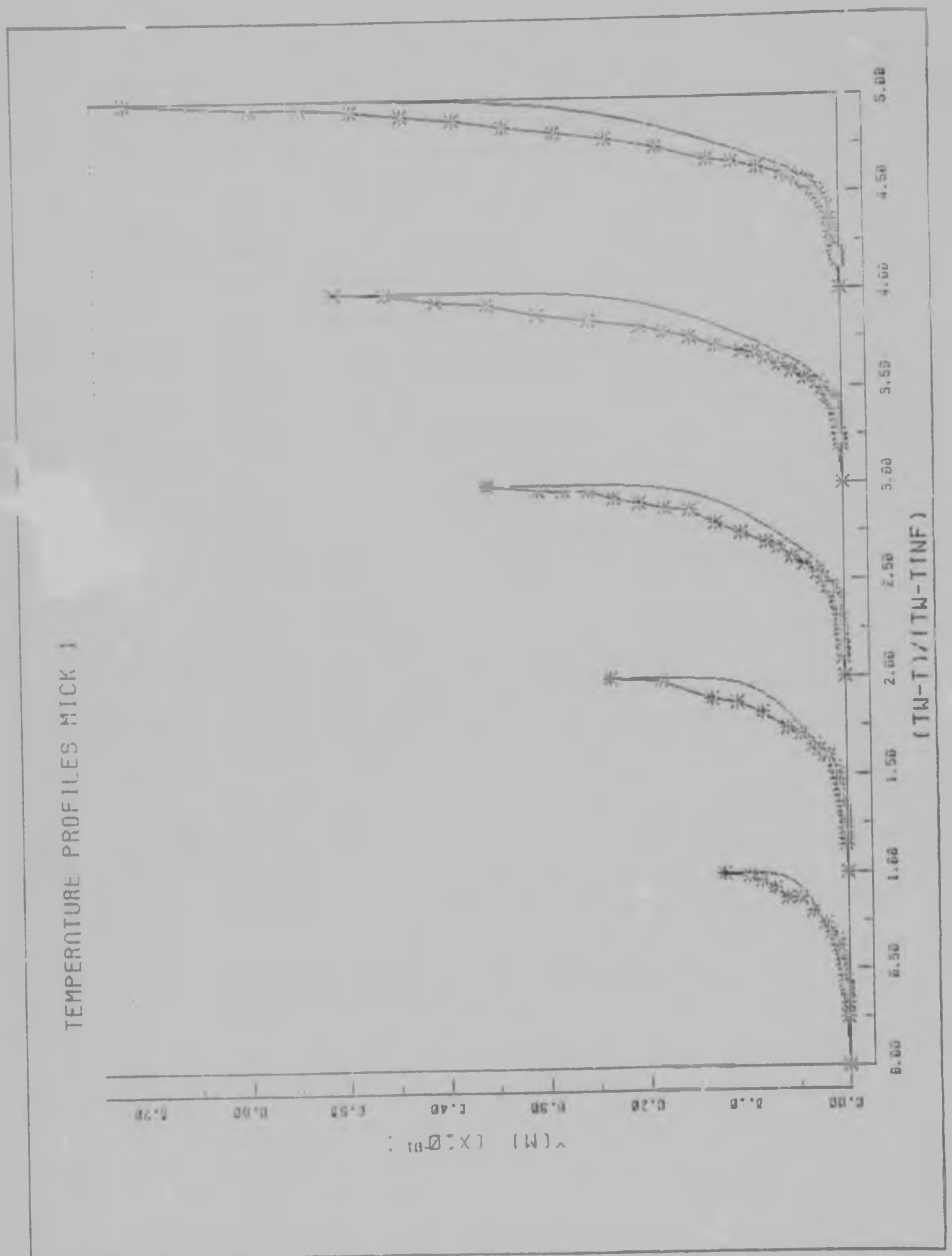

FIGURE 7.31 - COMPARISON OF MICKLEY ET AL RESULTS RUN H-17a WITH THE COMPUTED RESULTS

provided a few internal adjustments are made, mainly to the definition of the dimensionless temperature $(T - T_w)/(T_\infty - T_w$ that appears throughout the program. Coolant flow is provided for the full length of the flat plate thus a wall temperature and coolant flow velocity transition point did not have to be incorporated. However, the initial two profiles that are generated separately from the finite difference scheme can not accomodate wall blowing and as such it is hoped that this irregularity is accounted for by the time the profiles to be predicted are reached computationally and spatially.

Figure 7.31 gives the comparison of the profiles generated by the program to those as measured by Mickley and his co-workers. For all the profiles good correlation is evident at the wall, meaning that the heat transfer rate to the wall should correspond in both cases. The edge of the thermal boundary layer as predicted also corresponds to the measured points, however, the profile is "over predicted" in the fully turbulent region ie the predicted profile bulges past the measured points.

For the unsuccessful predictions this "over prediction" is far more pronounced and the edge of the boundary does not correspond for the predicted and measured results. The results of these attempts are illustrated in Appendix E1.

7.5 Prediction of Stanton Number Variation with Reynolds Number Across the Porous Plate

The program was also used to predict the heat transfer rate or flow Stanton number to the wall at the various measuring stations. Although it was not possible to obtain temperature profile measurements closer than 1 mm to the wall, so as to experimentally determine the heat transfer from the mainstream flow, meaningful observation can be made as to the

general trend of the program predictions.

Figure 7.32 gives the Stanton number variation with Reynolds number for the first three runs at the maximum free stream velocity and free stream temperature of approximately 33°C. Firstly the effect of blowing (increasing F) is evident in that the heat transfer rate to the wall is decreased. The observation can be made, when considering the logarithmic profiles in section 7.2.2 that the variation of Stanton number with Reynolds number for this flow situation is hyperbolic in nature. This suggests a transition region once blowing has commenced before the thermal boundary layer settles down to an equilibrium state.

Once again the effect of increasing blowing is evident for the following four runs in figure 7.33 where the free stream conditions were approximately constant. For these runs, as noted earlier, the thermal boundary layer was in equilibrium over all the five measuring stations and thus a linear variation of Stanton number with Reynolds number results.

For figure 7.34 the same observation can be made for the logarithmic profiles presented for the final two runs, where equilibrium profiles resulted for minimum free stream velocity and maximum free stream temperature.

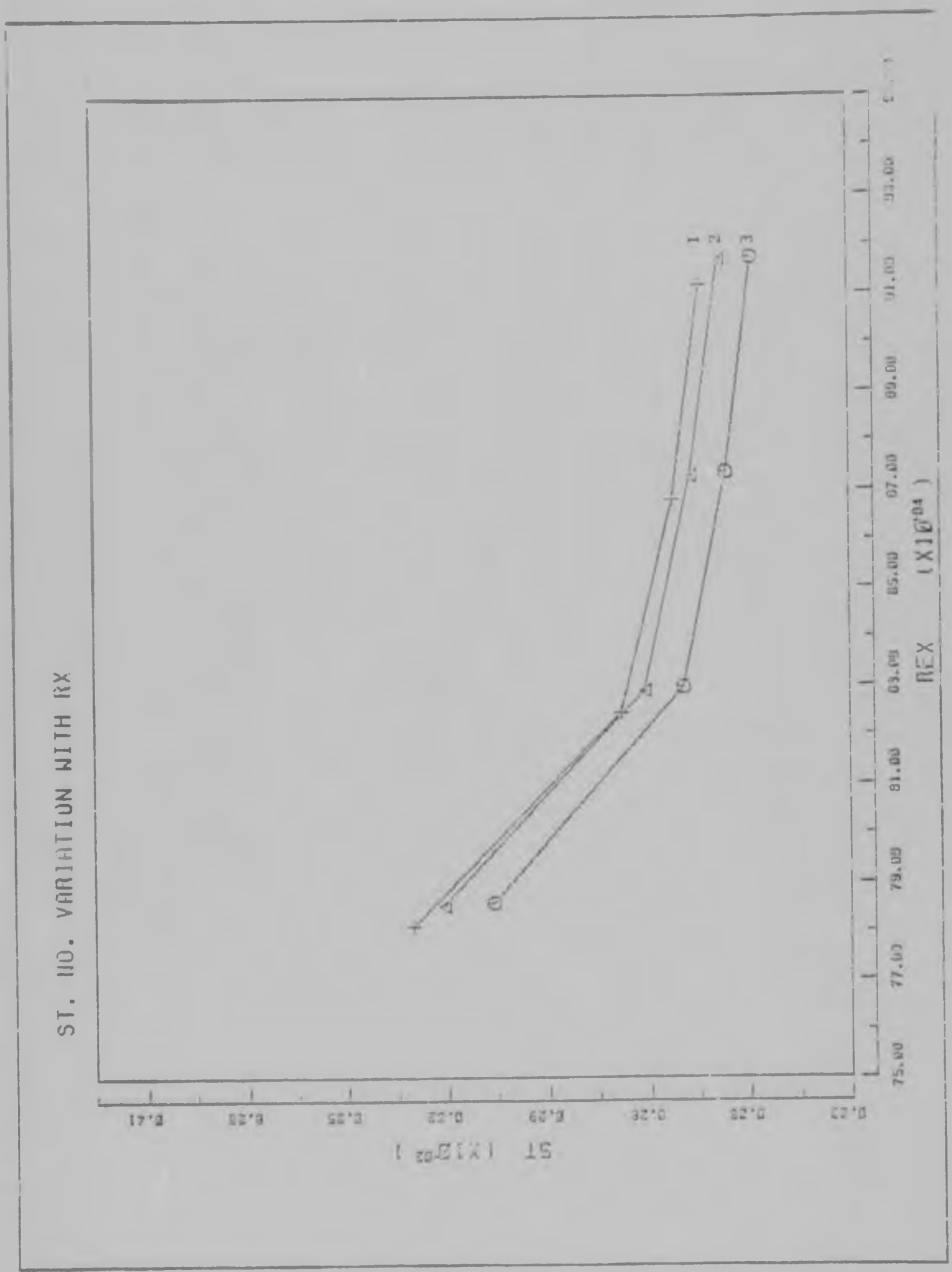

FIGURE 7.32 COMPUTER PREDICTIONS OF STANTON NO VARIATION WITH REYNOLDS NO FOR RUNS 1,2 AND 3

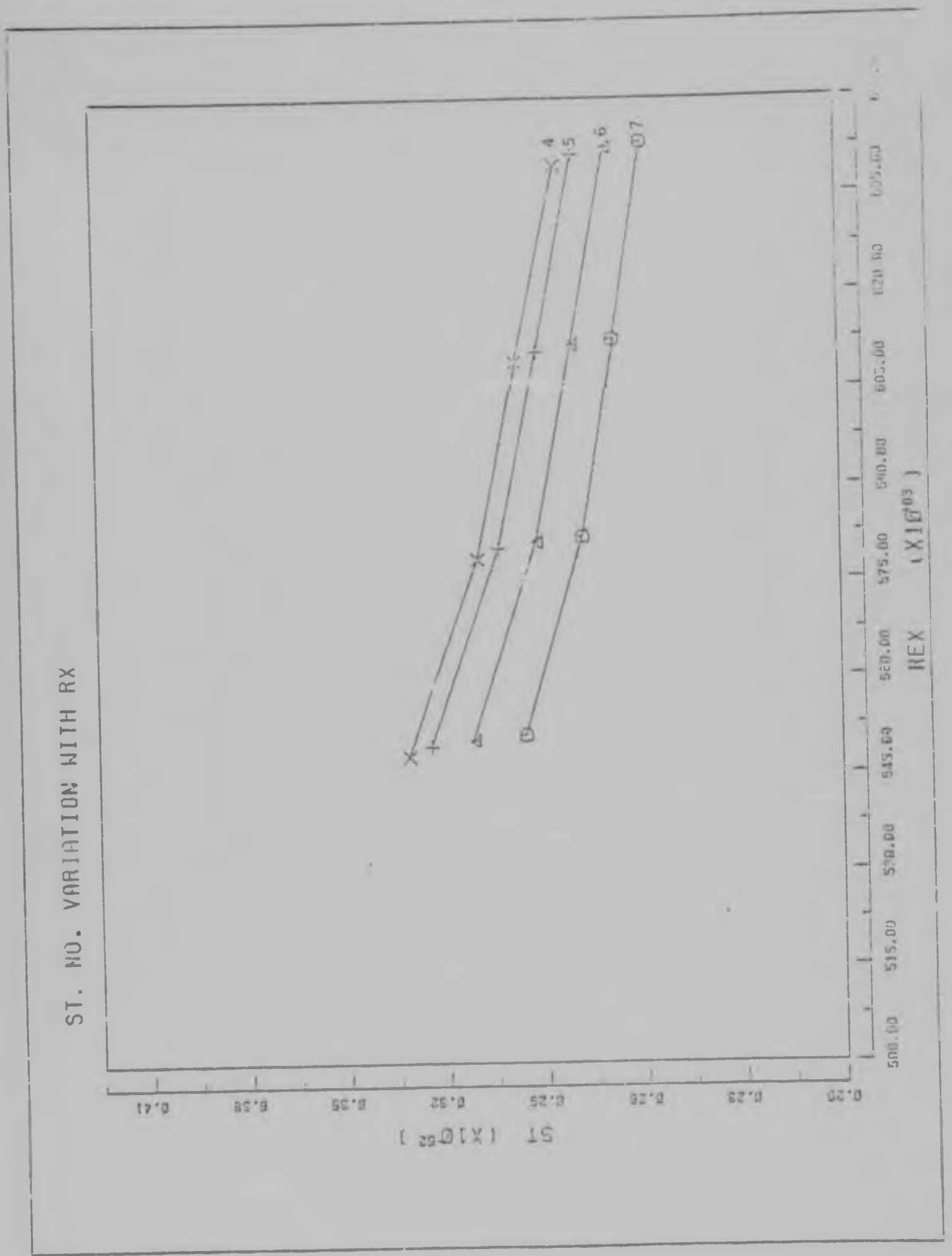

FIGURE 7.33 COMPUTER PREDICTIONS OF STANTON NO VARIATION WITH REYNOLDS NO FOR RUNS 4 THROUGH 7

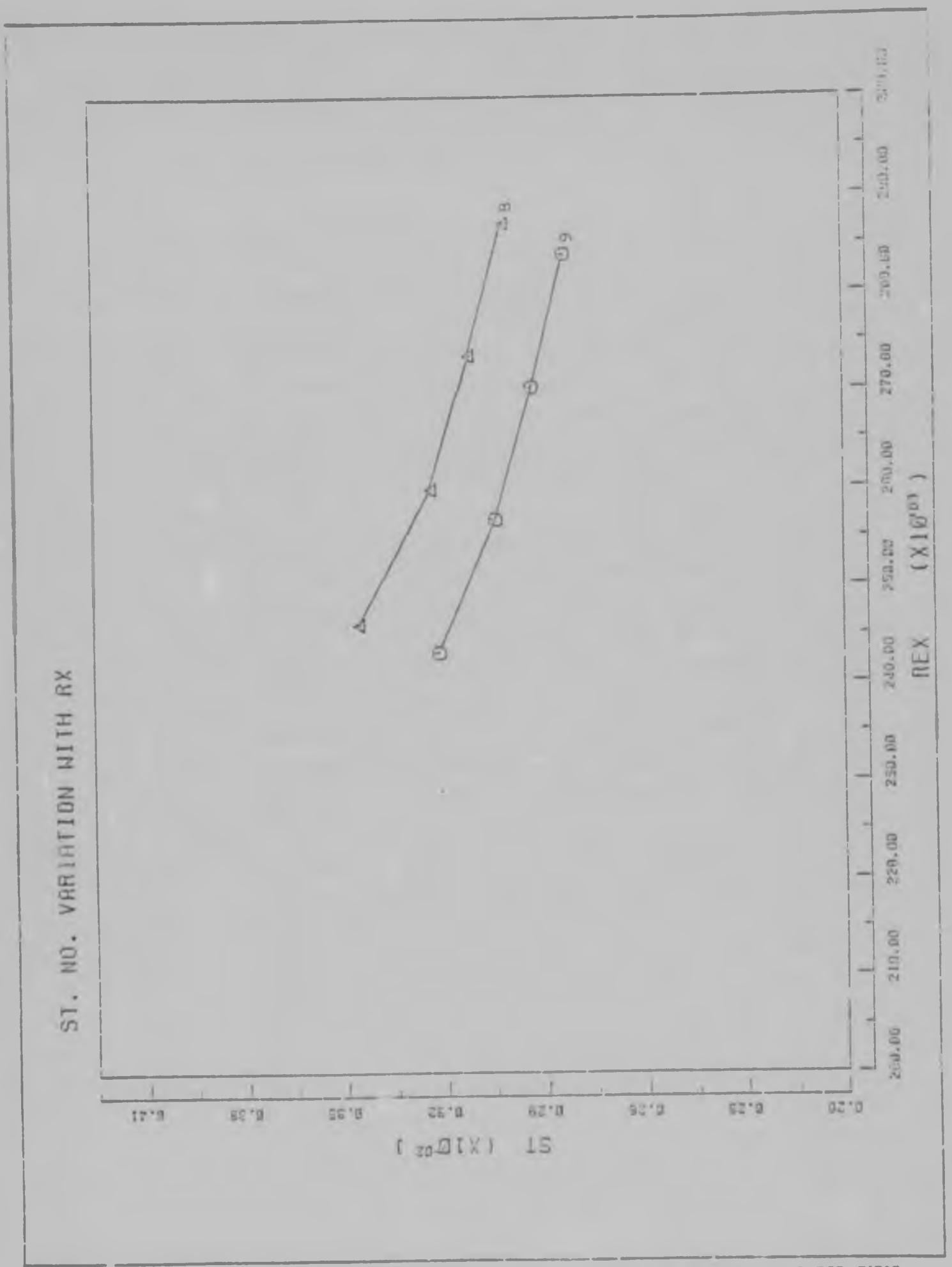

FIGURE 7.34 COMPUTER PREDICTIONS OF STANTON NO VARIATION WITH REYNOLDS NO FOR RUNS 8 and 9.

8 CONCLUSIONS AND RECOMMENDATIONS

8.1 Experimental Results

Nine experimental runs were performed, during which temperature profiles were obtained at the five measuring stations. These experimental runs were carried out once the wind tunnel had been recommissioned and modified by placing heater elements in the main stream flow. The addition of the heaters did not result in a uniform temperature distribution across the working section, however, the unblown temperature profiles normal to the flat plate were uniform and thus the approximation of two dimensional flow was made.

The experimental runs were divided into three sections depending on that run's particular free stream velocity. The free stream velocities measured were approximately 14, 95 m/s, 10,85 m/s and 5,00 m/s with the blowing fraction varying from 0,00424 to 0,01185. The maximum free stream temperature recorded was 44,95° with a corresponding wall temperature of 25,95°C (19°C temperature difference). At the maximum free stream velocity of 14,95 m/s the free stream temperature was 33,01°C and wall temperature was 25,00°C.

The measured temperature profiles were presented on linear and semi-logarithmic axes. The presentation of the profiles on the linear axes gave an indication as to the turbulent shape of the profiles. At the high free stream velocity the transition of the flow (as it adjusts to blowing) is evident in that the profiles seem to be adjusting over the first few measuring stations, to equilibrium or similar profiles. This is more evident when considering the profiles plotted on the semi logarithmic axes where the similarity is verified when the plotted points for the different profile fall on top of one another. Similarity of the profiles is

evident at the low free stream flow velocity and high free stream temperature runs. The idea of similar profiles resulting from flows of constant free stream temperature and velocity and constant wall temperature with blowing is enhanced by these results. However, only outer region similarity can be accurately commented on as due to restrictions, of moving the probe closer than 1 mm to the wall, measurements were taken in mainly the fully turbulent outer region.

The profiles when plotted on the semi-logarithmic axes, resulted in a linear form in the fully turbulent region as can be expected from turbulent profiles. The slight deviation from this linear trend at the edge of the thermal boundary layer was also noticed. More uncertainty of the points was measured in the laminar to turbulent transitions region than at the edge of the boundary layer.

8.2 Computer Prediction

The computer program that was written to solve the momentum and energy equations describing the particular flow situation that was studied was used to predict the temperature profiles as measured. With the successful prediction of these results it is hoped that the prediction of the heat transfer to the porous wall will be accurate.

The comparison of the predicted and measured results for the free stream flow velocity of 14,95 m/s was very good, which seems to indicate that the program will be able to accurately predict the heat transfer resulting from flows of high free stream velocity as are usually encountered in gas turbine engines. For the slow velocities and high temperature differences between the free stream and the wall the computed results were less accurate with the computed profile having a smaller enthalpy thickness.

The program was also used to predict the results measured by Mickley et al(17) [illegible] one set of profiles were satisfactorily predicted. Two runs were considered with the successful prediction of run H-17a being presented.

Finally the program was used to predict the heat transfer, or Stanton number, variation along the porous section as a function of Reynolds number based on distance along the flat plate. This was done so as to determine the effect blowing has on the heat transfer for different flow conditions. As measurements of the temperature profiles could not be made close enough to the wall no experiment results could be compared to these predictions.

8.3 Recommendations for Future Study

1 The modification to the wind tunnel should be refined so that a uniform temperature distribution arrives at the working section.

2 The effect of pressure gradient on the momentum and thermal boundary layer should be investigated experimentally and computationally.

3 The aerodynamic effects of transpiration cooling on a cascade or blade (as in a turbine) should be studied.

4 The program should be improved to allow for enclosed flows as well as being able to predict three dimensional flows which are experienced in gas turbine engines.

5 For combustion chamber analysis this should include the effects of radiation, combustion, dilution holes and three dimensional flows.

6 More realistic flow velocities and temperatures, similar to those experienced in gas turbine engines, should be investigated. This will require the use of a rig using either combustion or very large electrical power so as to heat the working fluid.

7 The variation of the turbulent Prandtl number throughout (especially close to the wall) the blown boundary layer should be further investigated.

APPENDIX A

A1 TRANSFORMATION OF THE ENERGY EQUATION

To solve equations 4.1.1 and 4.1.2 they first have to be transformed to a coordinate system that removes the [illegible] $x = 0$ and stretches the coordinates normal to the flow direction. Firstly these equations are placed in an almost two dimensional form by the Probstein-Elliott transformation.

Probstein-Elliot Trarsformation:

$$d\bar{x} = \left[\frac{r_0(x)}{L}\right]^{2k} dx \; ; \; d\bar{y} = \left[\frac{r(x;y)}{L}\right]^{k} dy \qquad \ldots |A.1.1|$$

where $r_0(x)$ specifies the body shape over which the boundary layer forms and $r(x;y)$ is given by

$$r(x;y) = r_0(x) + y \cos \alpha \qquad \ldots |A.1.1|$$

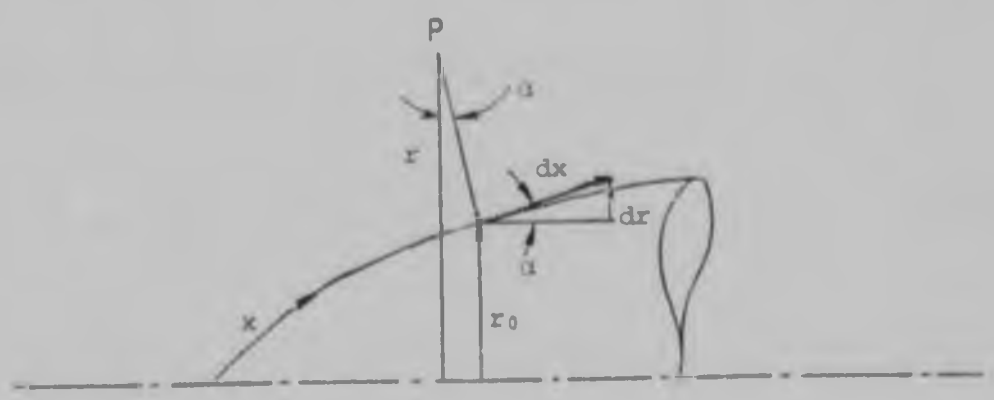

FIG. A1 COMPUTATIONAL AXES

Thus from equation A.1.1

$$\frac{\partial}{\partial x} = \frac{\partial \bar{x}}{\partial x} \cdot \frac{\partial}{\partial \bar{x}} + \frac{\partial \bar{y}}{\partial x} \cdot \frac{\partial}{\partial \bar{y}} = \left(\frac{r_o}{L}\right)^{2k} \cdot \frac{\partial}{\partial \bar{x}} + \frac{\partial \bar{y}}{\partial x} \cdot \frac{\partial}{\partial \bar{y}} \quad \ldots|A.1.3|$$

and

$$\frac{\partial}{\partial y} = \frac{\partial \bar{y}}{\partial y} \cdot \frac{\partial}{\partial \bar{y}} = \left(\frac{r}{L}\right)^{k} \frac{\partial}{\partial \bar{y}} \quad \ldots|A.1.4|$$

A stream function ψ is defined that satisfies the continuity equation 4.1.3 resulting in the following

$$\frac{\partial \psi}{\partial y} = r^{k} \rho u; \quad \frac{\partial \psi}{\partial x} = -r^{k} (\rho v + \overline{\rho' v'}) \quad \ldots|A.1.5|$$

$$\ldots|A.1.6|$$

By letting $\bar{\psi} = \frac{\psi}{L^{k}}$; $\bar{v} = v$; $\bar{u} = u$; $\overline{\rho' v'} = \overline{\overline{\rho' v'}}$

the continuity equation can be written as;

$$\frac{\partial}{\partial \bar{x}} (\rho \bar{u}) + \frac{\partial}{\partial \bar{y}} (\rho \bar{v} + \overline{\overline{\rho' v'}}) = 0 \quad \ldots|A.1.7|$$

the stream function that satisfies this equation is

$$\frac{\partial \psi}{\partial \bar{y}} = \rho \bar{u} ; \quad \frac{\partial \psi}{\partial \bar{x}} = -(\rho \bar{v} + \overline{\overline{\rho' v'}}) \quad \ldots|A.1.8|$$

Using equations A.1.3; A.1.4; A.1.6 and A.1.8 equation A.1.5 becomes

$$\rho u = \left(\frac{L}{r}\right)^{k} \frac{\partial \bar{\psi}}{\partial y} = \left(\frac{L}{r}\right)^{k} \left[\left(\frac{r}{L}\right)^{k} \frac{\partial \bar{\psi}}{\partial \bar{y}}\right] = \frac{\partial \bar{\psi}}{\partial \bar{y}} \qquad \ldots |A.1.9|$$

$$\rho \overline{u'v'} = -\left(\frac{L}{r}\right)^{k} \frac{\partial \bar{\psi}}{\partial x} = -\left(\frac{L}{r}\right)^{k} \left[\left(\frac{r_0}{L}\right)^{2k} \frac{\partial \bar{\psi}}{\partial \bar{x}} + \frac{\partial \bar{y}}{\partial x} \cdot \frac{\partial \bar{\psi}}{\partial \bar{y}}\right] \ldots A\text{-}1\text{-}10$$

Upon substitution of the above into equation 4.1.2 the energy equation becomes

$$\frac{\partial \bar{\psi}}{\partial \bar{y}} \left(\frac{r_0}{L}\right)^{2k} \frac{\partial H}{\partial \bar{x}} + \frac{\partial \bar{y}}{\partial x} \cdot \frac{\partial H}{\partial \bar{y}} \Big] - \left(\frac{L}{r}\right)^{k} \left[\left(\frac{r}{L}\right)^{\kappa} \frac{\partial \bar{\psi}}{\partial \bar{x}} + \frac{\partial \bar{y}}{\partial x} \frac{\partial \bar{\psi}}{\partial \bar{y}}\right] \left(\frac{r}{L}\right)^{k} \frac{\partial H}{\partial y} =$$

$$\frac{1}{r^{k}} \left(\frac{r}{L}\right)^{k} \frac{\partial}{\partial \bar{y}} \left[r^{k} \left(\frac{\mu}{Pr}\right) \left(\frac{r}{L}\right)^{k} \frac{\partial H}{\partial \bar{y}} + \frac{\mu e}{Pr_t} \left(\frac{r}{L}\right)^{k} \frac{\partial H}{\partial \bar{y}} + u\left(1 - \frac{1}{Pr}\right) \frac{1}{2} \cdot \frac{\partial \psi}{\partial \bar{y}}\right.$$

$$\left(\frac{r}{L}\right)^{k} \frac{\partial}{\partial \bar{y}} \left(\frac{1}{\rho} \frac{\partial \bar{\psi}}{\partial \bar{y}}\right)\Big) \Big] \qquad \ldots |A.1.11|$$

which can be multiplied out as follows

$$\left(\frac{r_0}{L}\right)^{2k} \frac{\partial \bar{\psi}}{\partial \bar{y}} \cdot \frac{\partial H}{\partial \bar{x}} + \frac{\partial \bar{y}}{\partial x} \cdot \frac{\partial H}{\partial \bar{y}} \cdot \frac{\partial \bar{\psi}}{\partial \bar{y}} - \left(\frac{r_0}{L}\right)^{2k} \frac{\partial \bar{\psi}}{\partial \bar{x}} \cdot \frac{\partial H}{\partial \bar{y}} - \frac{\partial \bar{y}}{\partial x} \cdot \frac{\partial \bar{\psi}}{\partial \bar{y}} \cdot \frac{\partial H}{\partial \bar{y}} =$$

$$\frac{1}{L^{k}} \frac{\partial}{\partial \bar{y}} \left[r^{k} \left[\left(\frac{r}{L}\right)^{k} \cdot \frac{\mu}{Pr} \cdot \left(1 + \frac{\epsilon^{+} Pr}{Pr_t}\right) \frac{\partial H}{\partial \bar{y}} + \frac{\mu}{\rho} \left(1 - \frac{1}{Pr}\right) \frac{\partial \bar{\psi}}{\partial \bar{y}} \cdot \frac{\partial}{\partial \bar{y}} \left(\frac{1}{\rho} \frac{\partial \bar{\psi}}{\partial \bar{y}}\right)\right]\right]$$

$$\ldots |A.1.12|$$

Finally resulting in

$$\frac{\partial\bar{\psi}}{\partial\bar{y}} \cdot \frac{\partial H}{\partial\bar{x}} - \frac{\partial\bar{\psi}}{\partial\bar{x}} \cdot \frac{\partial H}{\partial\bar{y}} = \frac{\partial}{\partial\bar{y}} \left\{ (1+t)^{2k} \left[\left(\frac{\mu}{Pr}\right) \left(1 + \frac{\varepsilon^{+} Pr}{Pr_t}\right) \frac{\partial H}{\partial\bar{y}} + \right.\right.$$

$$\left.\left. \frac{\mu}{\rho} \left(1 - \frac{1}{Pr}\right) \frac{\partial\bar{\psi}}{\partial\bar{y}} \cdot \frac{\partial}{\partial\bar{y}} \left(\frac{1}{\rho} \cdot \frac{\partial\bar{\psi}}{\partial\bar{y}}\right) \right] \right\} \qquad \ldots (A.1.13)$$

Levy-Lees Transformation:

The Levy-Lees transformation is used in order to remove the singularity at $\bar{x} = 0$ and stretch the coordinates in the $\bar{y}$ direction.

$$d\xi = \rho_e \mu_e u_e \, d\bar{x} \; ; \; d\eta = \frac{\rho u_e}{(2\xi)^{\frac{1}{2}}} \, d\bar{y} \qquad \ldots (A.1.14)$$

Once again a dimensionless stream function f is defined and related to $\bar{\psi}$ as follows

$$\bar{\psi} = (2\xi)^{\frac{1}{2}} f(\xi;\eta) \qquad \ldots (A.1.15)$$

Therefore

$$\frac{\partial}{\partial\bar{x}} = \rho_e \mu_e u_e \left(\frac{\partial}{\partial\xi} + \frac{\partial\eta}{\partial\xi} \cdot \frac{\partial}{\partial\eta}\right) \qquad \ldots (A.1.16)$$

and

$$\frac{\partial}{\partial\bar{y}} = \frac{\rho_e u_e}{(2\xi)^{\frac{1}{2}}} \frac{\partial}{\partial\eta} \qquad \ldots (A.1.17)$$

$$\frac{\partial\bar{\psi}}{\partial\xi} = (2\xi)^{\frac{1}{2}} \left(\frac{f}{2\xi} + \frac{\partial f}{\partial\xi}\right) \qquad \ldots (A.1.18)$$

$$\frac{\partial\bar{\psi}}{\partial\eta} = (2\xi)^{\frac{1}{2}} f' \qquad \ldots (A.1.19)$$

(where $f' = \frac{\partial f}{\partial \eta}$)

$$\frac{\partial \bar{\psi}}{\partial \bar{y}} = \frac{\rho u_e}{(2\xi)^{\frac{1}{2}}} \frac{\partial \bar{\psi}}{\partial \eta} = \rho u_e f' \qquad \ldots|A.1.20|$$

$$\frac{\partial \bar{\psi}}{\partial \bar{x}} = \rho_e \mu_e u_e \left(\frac{\partial \bar{\psi}}{\partial \xi} + \frac{\partial \eta}{\partial \xi} \cdot \frac{\partial \bar{\psi}}{\partial \eta}\right) = \rho_e \mu_e u_e (2\xi)^{\frac{1}{2}} \left[\frac{f}{2\xi} + \frac{\partial f}{\partial \xi} + \frac{\partial \eta}{\partial \xi} \cdot f'\right]$$

$$\ldots|A.1.21|$$

By substituting equation A.1.14 through A.1.21 into equation A.1.13 the following results:

$$\rho u_e f' \left[\rho_e \mu_e u_e \left(\frac{\partial H}{\partial \xi} + \frac{\partial \eta}{\partial \xi} \cdot \frac{\partial H}{\partial \eta}\right)\right] - \rho_e \mu_e u_e (2\xi)^{\frac{1}{2}} \left[\frac{f}{2\xi} + \frac{\partial f}{\partial \xi} + \frac{\partial \eta}{\partial \xi} \cdot f'\right] \frac{\rho u_e}{(2\xi)^{\frac{1}{2}}} \frac{\partial H}{\partial \eta}$$

$$= \frac{\rho u_e}{(2\xi)^{\frac{1}{2}}} \frac{\partial}{\partial \eta} \left[(1+t)^{2k} \frac{\mu}{Pr} \left(1 + \frac{\varepsilon^+ Pr}{Pr_t}\right) \frac{\rho u_e}{(2\xi)^{\frac{1}{2}}} \frac{\partial H}{\partial \eta} + \right.$$

$$\left. \frac{\mu}{\rho} \left(1 - \frac{1}{Pr}\right) \rho u_e f' \cdot \frac{\rho u_e}{(2\xi)^{\frac{1}{2}}} \frac{\partial}{\partial \eta} \left(\frac{1}{\rho} \cdot \rho u_e f'\right)\right]\} \qquad \ldots|A.1.22|$$

Upon simplification this finally results in

$$\{(1+t)^{2k} C \left[\left(1 + \frac{\varepsilon^+ Pr}{Pr_t}\right) \frac{g'}{Pr} + \frac{u_e^2}{H_e} \left(1 - \frac{1}{Pr}\right) f' f''\right]\}' + fg' =$$

$$2\xi \left[f' \frac{\partial g}{\partial \xi} - g' \frac{\partial f}{\partial \xi}\right] \qquad \ldots|A.1.23|$$

where $g = H/H_e$

$$C = \rho\mu/\rho_e \mu_e \qquad \ldots|A.1.24|$$

A2 FINITE DIFFERENCE FORM OF ENERGY EQUATION

By considering a Taylor's Series expansion of a function f at grid points i - 2; i - 1; i : ..... etc which have different spacings between them,

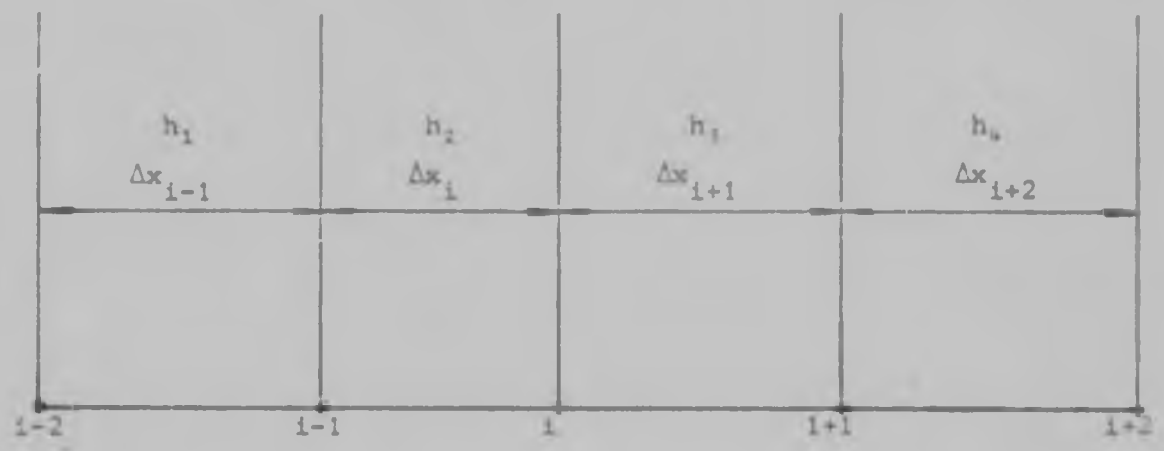

the functions at (i + 1) and (i - 1) can be expressed as follows

$$f(x_{i+1}) = f(x_i) + h_3 f'(x_i) + \frac{h_3^2}{2!} f''(x_i) + O(h_3^3) \quad \ldots|A.2.1|$$

$$f(x_{i-1}) = f(x_i) - h_2 f'(x_i) + \frac{h_2^2}{2!} f''(x_i) + O(h_2^3) \quad \ldots|A.2.2|$$

By multiplying equation A.2.1 by h_2^2 and A.2.2 by h_3^2 and subtracting the one from the other the following results

$$f'(x_i) = \frac{-h_3 f(x_{i-1})}{h_2(h_2 + h_3)} - \frac{(h_2 - h_3)}{h_2 h_3} f(x_i + \frac{h_2 f(x_{i+1})}{h_3(h_2 + h_3)} + O(h^2)$$

$$\ldots|A.2.3|$$

Where the error is expressed as an order of h^2 if $h_2 \neq h_3$

If A.2.1. is multiplied by h_2 and added to the product of A.2.2 and h_3 a solution of $f''(x_i)$ is found.

A2 FINITE DIFFERENCE FORM OF ENERGY EQUATION

By considering a Taylor's Series expansion of a function f at grid points i - 2; i - 1; i ; ..... etc which have different spacings between them,

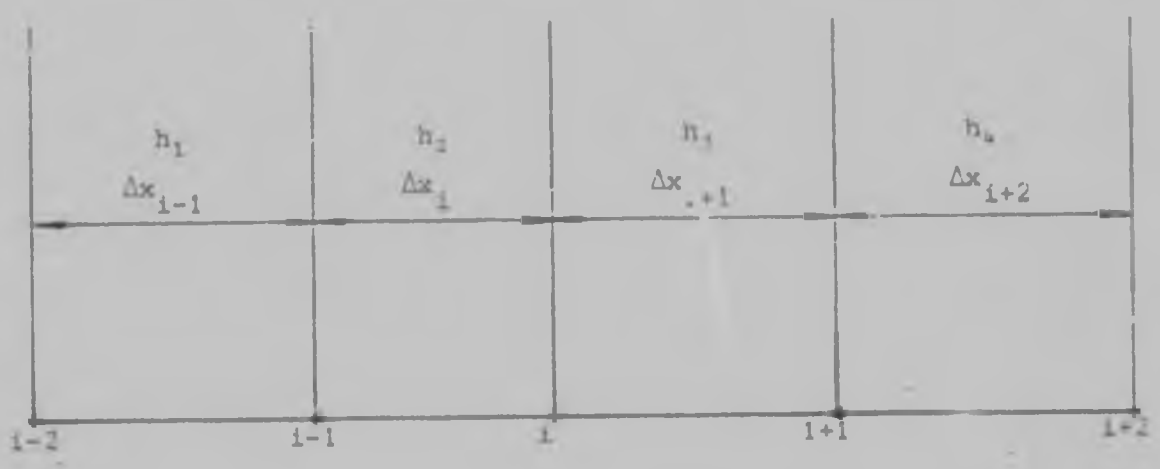

the functions at (i + 1) and (i - 1) can be expressed as follows

$$f(x_{i+1}) = f(x_i) + h_3 f'(x_i) + \frac{h_3^2}{2!} f''(x_i) + O(h_3^3) \quad \ldots |A.2.1|$$

$$f(x_{i-1}) = f(x_i) - h_2 f'(x_i) + \frac{h_2^2}{2!} f''(x_i) + O(h_2^3) \quad \ldots |A.2.2|$$

By multiplying equation A.2.1 by h_2^2 and A.2.2 by h_3^2 and subtracting the one from the other the following results

$$f'(x_i) = \frac{-h_3 f(x_{i-1})}{h_2(h_2 + h_3)} - \frac{(h_2 - h_3)}{h_2 h_3} f(x_i) + \frac{h_2 f(x_{i+1})}{h_3(h_2 + h_3)} + O(h^2)$$

$$\ldots |A.2.3|$$

Where the error is expressed as an order of h^2 if $h_2 \approx h_3$

If A.2.1. is multiplied by h_2 and added to the product of A.2.2 and h_3 a solution of $f''(x_i)$ is found.

$$f''(x_i) = \frac{2\,f(x_{i-1})}{h_2(h_3+h_2)} - \frac{2\,f(x_i)}{h_2\,h_3} + \frac{2\,f(x_{i+1})}{h_3(h_3+h_2)} + O(h) \quad \ldots|A.2.4|$$

The error of order h in this case is more than in equation A.2.3 and thus equation A.2.4 is less accurate.

If the spacing between the grid points is such that they can be written as follows;

$$\begin{aligned} h_1 &= \Delta x_{i-1} = h\,K^{i-3} \\ h_2 &= \Delta x_i = h\,K^{i-2} \\ h_3 &= \Delta x_{i+1} = h\,K^{i-1} \\ h_4 &= \Delta x_{i+2} = h\,K^{i} \end{aligned} \quad \ldots|A.2.5|$$

Each term in equations A.2.3 and A.2.4 can be divided into three parts namely; function f; a constant K and h. Thus for example the first term of equation A.2.3 can be simplified as follows

$$-\frac{h_3\,f(x_{i-1})}{h_2(h_2+h_3)} = \frac{-K^{i-1}f(x_{i-1})}{hK^{i-2}(K^{i-2}+K^{i-1})} = \frac{-f(x_{i-1})}{hK^{i-3}(1+K)} = A\,f(x_{i-1})$$

$$\ldots|A.2.6|$$

$$\text{where } A = \frac{-K^3}{h(1+K)K^i}$$

Similarly the following derivatives can be expressed as

$$f'(x_i) = A\,f(x_{i-1}) + B\,f(x_i) + C\,f(x_{i+1}) \quad \ldots|A.2.7|$$

$$f''(x_i) = D\,f(x_{i-1}) + E\,f(x_i) + F\,f(x_{i+1}) \quad \ldots|A.2.8|$$

$$f''(x_{i-1}) = X1\, f(x_{i-2}) + X2\, f(x_{i-1}) + X3\, f(x_i) \qquad \ldots|A.2.9|$$

$$f''(x_{i+1}) = X4\, f(x_i) + X5\, f(x_{i+1}) + X6\, f(x_{i+2}) \qquad \ldots|A.2.10|$$

where $A = -K^3/[h(1+K)\,K^i]$

$B = -[(1-K)K]/(h.K^i)$

$C = K/[h(1+K)\,K^i]$

$D = 2K^4/[h^2(1+K)\,K^{2i}]$

$E = -2K^3/(h^2.K^{2i})$

$F = 2K^3/[h^2(1+K).K^{2i}]$

$X1 = 2K^6/[h^2(1+K).\,K^{2i}]$ $\qquad \ldots|A.2.11|$

$X2 = -2K^5/(h^2.K^{2i})$

$X3 = 2K^5/[h^2(1+K)\,K^{2i}]$

$X4 = 2K^2/[h^2(1+K)\,K^{2i}]$

$X5 = -2K/[h^2(1+K)\,K^{2i}]$

$X6 = 2K/[h^2(1+K)\,K^{2i}]$

The streamwise derivatives are calculated as follows

$$\left.\frac{\partial\phi_i}{\partial\xi}\right|_n = L\,\phi_{n-2;i} + M\,\phi_{n-1;i} + N\,\phi_{n;i} \qquad \ldots|A.2.12|$$

$$\left.\frac{\partial\phi_i}{\partial\xi}\right|_n = L\,\phi'_{n-2;i} + M\,\phi'_{n-1;i} + N\,\phi'_{n;i} \qquad \ldots|A.2.13|$$

where

$$L = \frac{\Delta\xi_n}{\Delta\xi_{n-1}\,(\Delta\xi_n + \Delta\xi_{n-1})}$$

$$M = -\frac{(\Delta\xi_n + \Delta\xi_{n-1})}{\Delta\xi_n\,\Delta\xi_{n-1}} \qquad \ldots|A.2.14|$$

$$N = \frac{2\Delta\xi_n + \Delta\xi_{n-1}}{\Delta\xi_n(\Delta\xi_n + \Delta\xi_{n-1})}$$

By using the following equation to linearise the momentum equation and change g to θ as follows;

$$\begin{aligned} f &= \phi + \eta \\ f' &= \phi' + 1 \\ f'' &= \phi'' \end{aligned} \qquad \ldots A.2.15$$

$$\begin{aligned} g &= \theta \\ g' &= \theta' \\ g'' &= \theta'' \end{aligned} \qquad \ldots|A.2.16|$$

the energy equation A.1.23 can be written in finite difference form

$$\left((1+t)^{2k} C_{n;i}\left[\left(1+\frac{\varepsilon^{+}Pr}{Pr_t}\right)_{n;i}\frac{\theta'_{n;i}}{Pr} + \frac{u_e^2}{H_e}\left(1-\frac{1}{Pr}\right)(\phi'_{n;i_0}+1)\phi''_{n;i}\right]\right)' +$$

$$\left[\phi_{n;i_0} + \eta_i\right]\theta'_{n;i} = 2\xi_n\left[(\phi'_{n;i_0}+1)\left.\frac{\partial\theta}{\partial\xi}\right|_{n;i} - \theta'_{n;i}\left.\frac{\partial\phi}{\partial\xi}\right|_{n;i}\right]$$

$\ldots|A.2.17|$

Term 1 of A.2.17 becomes

$$\{(1+t)^{2k} C_{n;i}\,'(1+(\frac{\varepsilon^{+}Pr}{Pr_t})_{n;i}) \frac{\theta'_{n;i}}{Pr}\}' + \{(1+t)^{2k} C_{n;i_0} (\frac{u_e^2}{H_e})(1-\frac{1}{Pr})$$

$$(\phi'_{n;i_0}+1)\phi''_{n;i}\}$$

$$= (1+t)^{2k} C_{n;i}(1+(\frac{\varepsilon^{+}Pr}{Pr_t})_{n;i}) \frac{\theta''_{n;i}}{Pr} + [(1+t)^{2k} C_{n;i}(1+(\frac{\varepsilon^{+}Pr}{Pr_t})_{n;i}]' \frac{\theta'_{n;i}}{Pr} + P_5$$

[where $P_5 = \{(1+t)^{2k} C_{n;i} (\frac{u_e^2}{H_e})(1-\frac{1}{Pr})(\phi'_{n;i_0}+1)\phi''_{n;i_0}\}']$

$$= (1+t)^{2k} (\frac{C_{n;i_0}}{Pr})(1+(\frac{\varepsilon^{+}Pr}{Pr_t})_{n;i_0}) [D\theta_{n;i-2} + E\theta_{n;i} + F_{n;i+1}] +$$

$$\{A(1+t)^{2k} (\frac{C_{n;i-1_0}}{Pr})(1+(\frac{\varepsilon^{+}Pr}{Pr_t})_{n;i-1_0}) + B(1+t)^{2k}(\frac{C_{n;i_0}}{Pr})(1+(\frac{\varepsilon^{+}Pr}{Pr_t})_{n;i_0}) +$$

$$C(1+t)^{2k}(\frac{C_{n;i+1_0}}{Pr})(1+\frac{\varepsilon^{+}Pr}{Pr_t})_{n;i+1_0})\}\{.A.\theta_{n;i-1} + B.\theta_{n;i} + C.\theta_{n;i+1}\}$$

$$+ P_5 = \theta_{n;i-1}\{(D+A.B)(1+t)^{2k}(\frac{C_{n;i_0}}{Pr})(1+(\frac{\varepsilon^{+}Pr}{Pr_t})_{n;i_0}) + A^2(1+t)^{2k}(\frac{C_{n;i-1_0}}{Pr})$$

$$(1+(\frac{\varepsilon^{+}Pr}{Pr_t})_{n;i-1_0}) + A.C.(1+t)^{2k}(\frac{C_{n;i+1_0}}{Pr})(1+(\frac{\varepsilon^{+}Pr}{Pr_t})_{n;i+1_0})\} +$$

$$\theta_{n;i}\{(E+B^2)(1+t)^{2k}(\frac{C_{n;i_0}}{Pr})(1+(\frac{\varepsilon^{+}Pr}{Pr_t})_{n;i_0}) + B.A.(1+t)^{2k}(\frac{C_{n;i-1}}{Pr})$$

$$(1+(\frac{\varepsilon^{+}Pr}{Pr_t})_{n;i-1_0}) + B.C(1+t)^{2k}(\frac{C_{n;i+1_0}}{Pr})(1+(\frac{\varepsilon^{+}Pr}{Pr_t})_{n;i+1}) +$$

$$\theta_{n;i+1}\{(F+C.B)(1+t)^{2k}(\frac{C_{n;i_0}}{Pr})(1+(\frac{\varepsilon^{+}Pr}{Pr_t})_{n;i_0}) + C.A.(1+t)^{2k}(\frac{C_{n;i-1_0}}{Pr})$$

$$(1+(\frac{\varepsilon^{+}Pr}{Pr_t})_{n;i-1_0}) + C.^2(1+t)^{2k}(\frac{C_{n;i+1_0}}{Pr})(1+(\frac{\varepsilon^{+}Pr}{Pr_t})_{n;i+1}) + P_5 \quad \ldots(A.2.18)$$

Term 2 of equation A.1.17 becomes

$$(\phi_{n;i_0}+\eta_i)(A.\theta_{n;i-1} + B.\theta_{n.i} + C.\theta_{n;i+1}) =$$

$$\theta_{n;i-1}\ [A(\phi_{n;i_0} + \eta_i)] \ +$$

$$\theta_{n;i}\ [B\ (\phi_{n;i_0} + \eta_i)] \ +$$

$$\theta_{n;i+1}\ [C(\phi_{n;i_0} + \eta_i)] \qquad \ldots |A.2.19|$$

Term 3 of equation A.2.17 becomes

$$2\xi_n(\phi'_{n;i_0} + 1)(L.\theta_{n-2;i} + M.\theta_{n-1;i} + N.\theta_{n;i}) =$$

$$\theta_{n;i}|2\xi_n.N.(\phi'_{n;i_0} + 1)| \ + 2\xi_n(\phi'_{n;i_0} + 1)(L.\theta_{n-2;i} + M.\theta_{n-1;i}) \qquad \ldots |A.2.20|$$

Term 4 of equation A.2.17 becomes

$$-2\xi_n\phi'_{n;i}\ \frac{\partial\phi}{\partial\xi}\Big|_{n;i} = -2\xi_n(A.\theta_{n;i-1} + B.\theta_{n;i} + C.\theta_{n;i+1})$$

$$(L.\phi_{n-2;i} + M.\phi_{n-1;i} + N.\phi_{n;i})$$

$$= -2\xi_n\theta_{n;i-1}\ \{A.(L.\phi_{n-2;i} + M\phi_{n-1;i} + N\phi_{n;i})\} \ +$$

$$-2\xi_n\theta_{n;i}\ \{B.(L.\phi_{n-2;i} + M\phi_{n-1;i} + N\phi_{n;i})\} \ +$$

$$-2\xi_n\theta_{n;i+1}\ \{C.(L.\phi_{n-2;i} + M.\phi_{n-1;i} + N.\phi_{n;i})\} \qquad \ldots \text{A.2.21}$$

Term 2 of equation A.1.17 becomes

$$(\phi_{n;i_0}+\eta_i)(A.\theta_{n;i-1} + B.\theta_{n;i} + C.\theta_{n;i+1}) =$$

$$\theta_{n;i-1}\ [A(\phi_{n;i_0} + \eta_i)] \ +$$

$$\theta_{n;i}\ [B\ (\phi_{n;i_0} + \eta_i)] \ +$$

$$\theta_{n;i+1}\ \ [C(\phi_{n;i_0} + \eta_i)] \qquad \ldots|A.2.19|$$

Term 3 of equation A.2.17 becomes

$$2\xi_n(\phi'_{n;i_0} + 1)(L.\theta_{n-2;i} + M.\theta_{n-1;i} + N.\theta_{n;i}) =$$

$$\theta_{n;i}|2\xi_n.N.(\phi'_{n;i_0} + 1)| \ + 2\xi_n(\phi'_{n;i_0} + 1)(L.\theta_{n-2;i} + M.\theta_{n-1;i})$$

$$\ldots|A.2.20|$$

Term 4 of equation A.2.17 becomes

$$-2\xi_n\theta'_{n;i}\ \left.\frac{\partial\phi}{\partial\xi}\right|_{n;i} = -2\xi_n(A.\theta_{n;i-1} + B.\theta_{n;i} + C.\theta_{n;i+1})$$

$$(L.\phi_{n-2;i} + M.\phi_{n-1;i} + N.\phi_{n;i})$$

$$= -2\xi_n\theta_{n;i-1}\ \{A.(L.\phi_{n-2;i} + M\phi_{n-1;i} + N\phi_{n;i})\} \ +$$

$$-2\xi_n\theta_{n;i}\ \ \{B.(L.\phi_{n-2;i} + M\phi_{n-1;i} + N\phi_{n;i})\} \ +$$

$$-2\xi_n\theta_{n;i+1}\ \{C.(L.\phi_{n-2;i} + M.\phi_{n-1;i} + N.\phi_{n;i})\} \qquad \ldots\ A.2.21$$

APPENDIX B

B1 HEAT TRANSFER THROUGH POROUS MATERIAL

B1.1 INTRODUCTION

A simplified model of transpiration cooling can be considered.

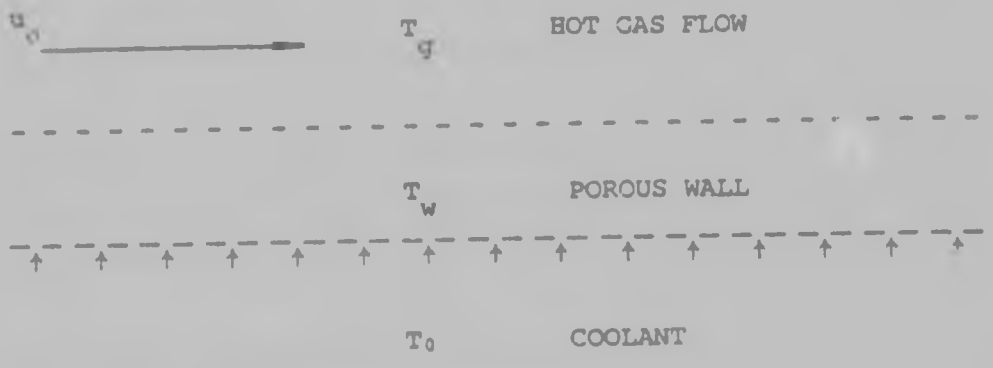

FIGURE B1: SIMPLIFIED TRANSPIRATION COOLING

The convective heat transfer to the porous wall is equal to the increase in enthalpy of the cooling fluid.(assuming that the cooling fluid is at the same temperature as the porous wall and there is no conduction of heat along the wall's length)

$$h(T_g - T_w) = \dot{\omega} C_p (T_w - T_0) \qquad \ldots|B.1.1|$$

where h is the forced convection heat transfer coefficient; $\dot{\omega}$ the coolant mass flow per unit area and C_p the specific heat, at constant pressure, of the coolant.

Using equation B.1.1 the temperature of the wall can be predicted provided the mass flowrate of coolant is known and the temperature of the mainstream and coolant is fixed.

The estimation of the heat transfer coefficient is complicated in that it is dependent on the wall temperature. The forced convection correlation equation;

$$Nu = 0{,}292\ (Re)^{\frac{4}{5}}\ (Pr)^{1/3} \qquad \ldots\ B.1.2$$

for turbulent flow over a flat plate will not give accurate values of the heat transfer coefficient because this correlation equation does not take into account the effect of the blowing of the coolant through the porous wall which reduces the heat transfer to the wall.

Kutateladze and Leontev (14) have put forward a theoretical-empirical correlation whereby blowing can be accounted for, this correlation will be discussed at a later stage.

B1.2 THEORETICAL PREDICTION OF WALL TEMPERATURE FOR THE TRANSPIRATION COOLED FLAT PLATE

The theoretical prediction of the wall and coolant temperatures for transpiration flow in a porous flat plate will be discussed with reference to the following figure.

The conduction within the metal (porous) can be expressed as follows by the Fourier equation:

$$q = k_m \frac{dc}{dx} \qquad \ldots|B.2.1|$$

The convection of energy from the metal to the coolant (within the pores) is:

$$dq = h_i\ (t - T)\ dx \qquad \ldots|B.2.2|$$

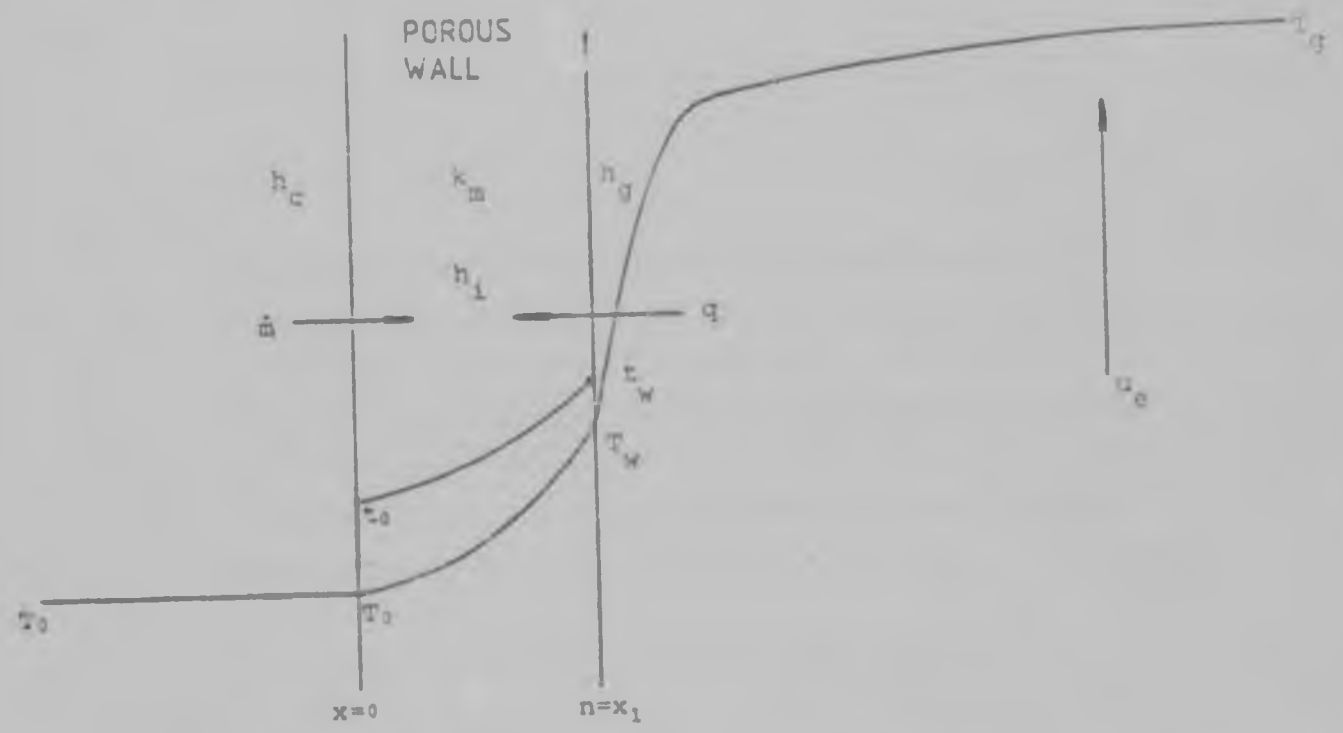

FIG 32:TEMPERATURE DISTRIBUTION THROUGH POROUS WALL AND ADJACENT FLOW FIELDS.

[t is the metal temperature and T the coolant temperature]. This convective heat transfer raises the enthalpy of the coolant according to the following relationship.

$$dq = \dot{\omega} C_p dT \qquad \ldots \text{B.2.3}$$

Thus setting equation B.2.2 equal to B.2.3 gives

$$\dot{\omega} C_p \frac{dT}{dx} = h_1(t-T) \qquad \ldots \text{B.2.4}$$

Differentiating equation B.2.1 w.r.t.x gives

$$dq = k_m \frac{d^2t}{dx^2} \cdot dx \qquad \ldots|B.2.5|$$

Setting equation B.2.5 equal to equation B.2.3 gives

$$k_m \frac{d^2t}{dx^2} = \dot{\omega} C_p \frac{dT}{dx} \qquad \ldots|B.2.6|$$

The equations(B.2.6 and B.2.4) are the one-dimensional equations describing the heat flow within the interior of an elemental volume of the porous wall. The internal volumetric heat transfer coefficient for the porous wall, h_i, is a function principally of the mass flow of coolant through the wall, and the mass flowrate, $\dot{\omega}$ and internal thermal conductivity, k_m, are both per unit area quantities.

Equations B.2.6 and B.2.4 have the following solution

$$T = \alpha + \beta \exp\left[(B-A/2)x\right] + \gamma \exp\left[-(B+A)/2x\right| \qquad \ldots|B.2.7|$$

$$t = \alpha + \left(\frac{1}{2} + \frac{B}{A}\right)\beta \exp\left[(B-A/2)x\right] + \left(\frac{1}{2} - \frac{B}{A}\right)\gamma \exp\left[-(B+A)/2x\right| \qquad \ldots|B.2.8|$$

where

$$A = h_i/\dot{\omega} C_p \text{ and } B = \left[(h_i/k_m) + (A/2)^2\right]^{\frac{1}{2}} \qquad \ldots|B.2.9|$$

For the prediction of the wall temperatures the following boundary conditions are applied to the above equations. For this the heat transfer coefficients h_g and h_c and the radiation fluxes R_g and R_c have to be specified on the hot gas and coolant sides respectively. Thus the boundary conditions are;

$$k_m \left(\frac{dt}{dx}\right)_{x=x_1} = -h_g (t_1 - T_g) + R_g \qquad \ldots|B.2.10|$$

$$k_m \left(\frac{dt}{dx}\right)_{x=0} = h_c (t_0 - T_0) + R_c \qquad \ldots|B.2.11|$$

The incorporation of these boundary conditions, as well as the assumption that at x = 0; T = T_0, into equations B.2.7 and B.2.8 allows the constants ($\alpha;\beta;\gamma$) to be evaluated. The final result is given below:

$$\beta = \frac{-h_g(t_w-T_g) - h_c(t_0-T_0)\exp\left[-(B+A/2)x_1\right]}{k_m A\left[(B/A)^2 - (1/4)\right]\left\{\exp\left[(B-A/2)x_1\right] - \exp\left[-(B+A/2)x_1\right]\right\}} \quad \ldots|B.2.12|$$

$$\gamma = \frac{1}{k_m A\left[(B/A)^2 - (1/4)\right]}\left\{h_c(t_0 - T_0) + \frac{h_g(t_w-T_g) + h_c(t_0-T_0)\exp\left[-(B+A/2)x_1\right]}{\exp\left[(B-A/2)x_1\right] - \exp\left[-(B+A/2)x_1\right]}\right\} \quad \ldots|B.2.13|$$

$$\alpha = T_0 - \frac{h_c(t_0 - T_0)}{k_m A\left[(B/A)^2 - (1/4)\right]} \quad \ldots|B.2.14|$$

The internal heat-transfer coefficient for sintered powder components can be determined from the following experimental relationship

$$Nu_i = 0{,}35\ Re_i \quad \ldots|B.2.15|$$

where

$$Nu_i = \frac{h_i(v/s)^2}{k}\ ;\quad Re_i = \frac{\bar{\omega}(v/s)}{\mu} \quad \ldots|B.2.16|$$

(v is the volume of the porous material; s is the internal surface area swept by the coolant).

For many calculations, particularly those involving injection in boundary layers, it has been assumed that the emerging coolant attains the outer surface metal temperature. For dense, porous metal components with convection present this assumption is usually valid but for coarse-wire compacts,

which have a low effective thermal conductivity, the coolant can emerge well below the outer surface metal temperature.

The effective thermal conductivity of the porous metal is important since low values produce large temperature gradients across the thickness of the wall. This reduces quite markedly the available temperature difference between metal and coolant (and would also set up large thermal stresses within the porous compact). Although little is known about the thermal conductivity of porous metals, particularly sintered woven wire compacts, the limited data available for sintered power components indicate the relation

$$k_m = k_s (1 - 2f) \qquad \ldots|B.2.17|$$

where k_s is the thermal conductivity of the solid compact and f is the porosity based on mass. Thus for 50% porosity k_m tends to zero.

The problem of separating the radiative and convective components of heat flux inside a combustion chamber flame, tube for instance is very complex. The luminosity of the flame, which is seen by the walls varies with temperature, emissivity and flow direction and velocity all of which are extremely difficult to predict.

Bayley, Cornforth and Turner (1) used, a simplified one-dimensional model for evaluating the radiation fluxes. The hot side radiation fluxe used is as follows

$$R_g = \sigma\left(\frac{1+e_w}{2}\right) \left| e_f T_f^4 - a_f t_1^4 \right| \qquad \ldots|B.2.18|$$

where e_w and e_f are the wall and flame emissivities, α_f is the gas absorptivity, σ the Stefan- Boltzmann constant and T_f the "effective" flame temperature.

For a transpiration cooled wall the effusing coolant reduces the convective heat flux to the surface and a sufficiently high blowing rate can reduce it to zero. For the present predictions the results of the theoretical-experimental work of Kutateladze and Leontev (14) on the quantitive reduction in heat flux will be used. From considerations of the turbulent boundary layer these authors obtained the correlation

$$\psi = \frac{St}{St_0} = \left|1 - \frac{b_h}{b_{h,cr}}\right|^3 \qquad \ldots|B.2.19|$$

The blowing parameter b_h is defined as

$$b_h = \frac{\dot{\omega}}{St_0 \rho_e u_e} \qquad \ldots|B.2.20|$$

and the critical blowing parameter, which would "blow off" the thermal boundary layer, is dependent on the wall to gas temperature ratio, ϕ, and is given by

$$b_{h,cr} = \frac{1}{1-\phi}\left(\ln\left|\frac{1 + (1-\phi)^{\frac{1}{2}}}{1 - (1-\phi)^{\frac{1}{2}}}\right|\right)^2 \qquad \ldots|B.2.21|$$

The problem of what the Stanton number without coolant injection, St_0, would be is still present and it appears in both ψ and the expression for b_h (equation B.2.20). For the prediction of this main stream flow the turbulent developed flat plate flow correlation is used in the following form:

$$Nu_g = 0{,}0292\ (Re_g)^{0{,}80}\ (Pr_g)^{0{,}33} \qquad \ldots|B.2.22|$$

with the Reynold's number evaluated using the means-mass velocity existing at that longitudinal position.

B1.3 COMPUTER PROGRAM TO SOLVE THE INTERNAL HEAT TRANSFER PROBLEM

A computer program has been developed to solve the metal and coolant temperature distributions that exist across the porous wall that is [illegible]
employs the correlation equations presented in the proceeding section.

Two iterations are performed to arrive at a final solution once the initial prediction of the wall temperatures has been made by using the simplified model that was previously considered. The first iteration updates this prediction of the external, mainstream, heat transfer coefficient by considering blowing. Once a stable solution is found the program proceeds to consider the internal heat transfer and temperature distribution which gives the external wall and coolant temperatures. These temperatures are used once more to update the model in the second and final iteration. In the first iteration the criteria for convergence is the external heat transfer coefficient whereas for the second iteration the convergence of the wall, hot side, metal temperature is used as the convergence factor.

A flow chart and listing of the program with a typical solution is presented. Unfortunately due to the low temperature difference between the coolant and mainstream gases in the wind tunnel which resulted in wall temperature distributions that were not able to be accurately measured no meaningful predictions could be made with the present program.

However, it is felt that it can be used to predict actual transpiration cooling problems as all the theory is based on existing correlation equations that have been successfully used in the past.

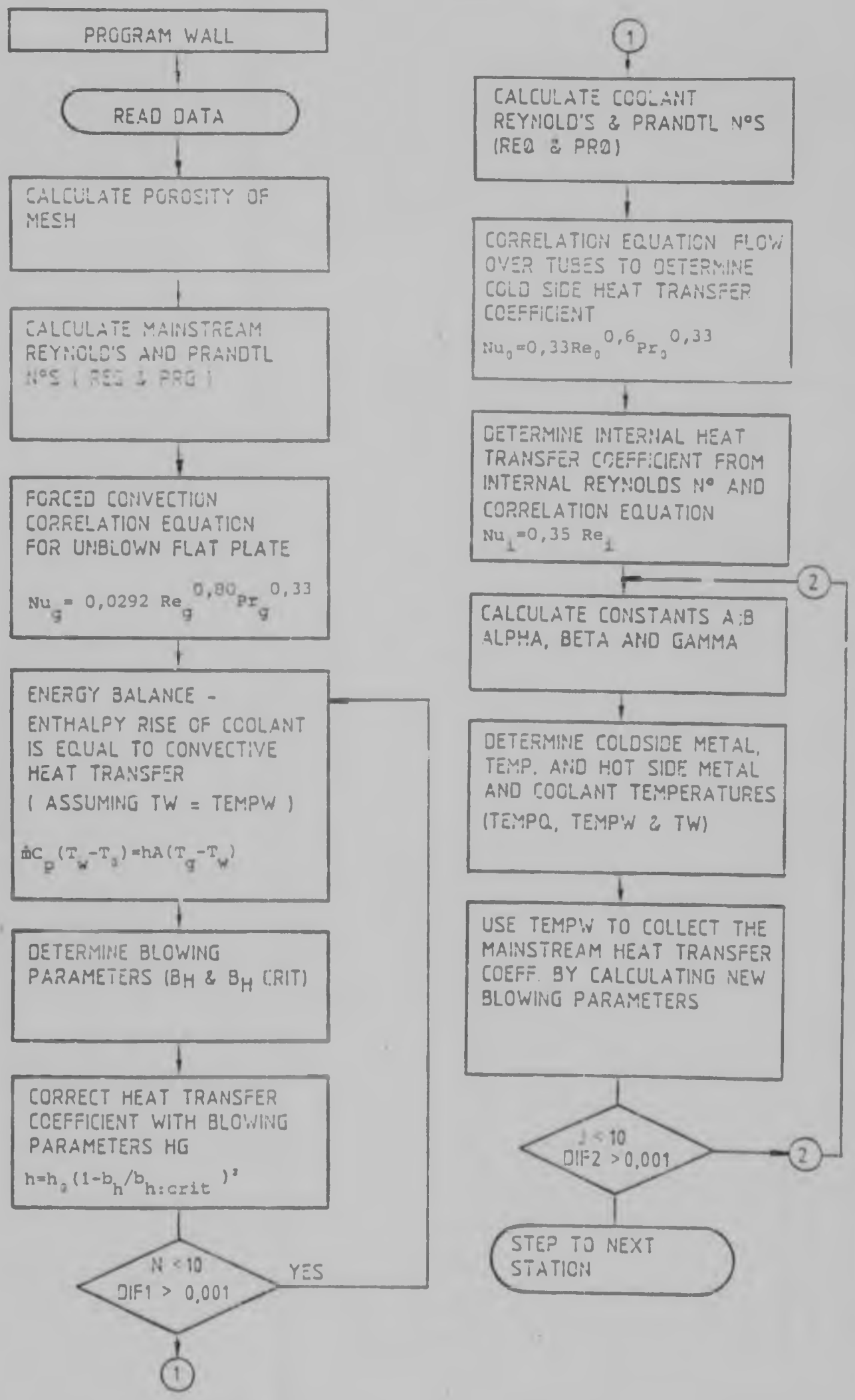
PROGRAM WALL
READ DATA
CALCULATE POROSITY OF MESH
CALCULATE MAINSTREAM REYNOLD'S AND PRANDTL N°S (REG & PRG)
FORCED CONVECTION CORRELATION EQUATION FOR UNBLOWN FLAT PLATE
$Nu_g = 0,0292\ Re_g^{0,80} Pr_g^{0,33}$
ENERGY BALANCE - ENTHALPY RISE OF COOLANT IS EQUAL TO CONVECTIVE HEAT TRANSFER (ASSUMING TW = TEMPW)
$\dot{m}C_p(T_w-T_0)=hA(T_g-T_w)$
DETERMINE BLOWING PARAMETERS (B_H & $B_{H\ CRIT}$)
CORRECT HEAT TRANSFER COEFFICIENT WITH BLOWING PARAMETERS HG
$h=h_0(1-b_h/b_{h:crit})^2$
N < 10
DIF1 > 0,001
YES
1
1
CALCULATE COOLANT REYNOLD'S & PRANDTL N°S (RE0 & PR0)
CORRELATION EQUATION FLOW OVER TUBES TO DETERMINE COLD SIDE HEAT TRANSFER COEFFICIENT
$Nu_0=0,33Re_0^{0,6}Pr_0^{0,33}$
DETERMINE INTERNAL HEAT TRANSFER COEFFICIENT FROM INTERNAL REYNOLDS N° AND CORRELATION EQUATION
$Nu_i=0,35\ Re_i$
2
CALCULATE CONSTANTS A;B ALPHA, BETA AND GAMMA
DETERMINE COLDSIDE METAL, TEMP. AND HOT SIDE METAL AND COOLANT TEMPERATURES (TEMP0, TEMPW & TW)
USE TEMPW TO COLLECT THE MAINSTREAM HEAT TRANSFER COEFF. BY CALCULATING NEW BLOWING PARAMETERS
J < 10
DIF2 > 0,001
2
STEP TO NEXT STATION

```
      PROGRAM WALL(INPUT,OUTPUT,WALLIN,WALOUT,TAPE5=WALLIN,TAPE6=WALOUT)
      REAL MUG,KG,MDOT,MAJ,MIN,NUG,KG,CM,L,NUI,KS,NUG,NUG
C
C     THIS PROGRAM PREDICTS THE WALL TEMPERATURE PROFILES FOR METAL AND
C     COOLANT IN A POROUS WALL THAT IS TRANSPIRATION COOLED
C
      NAMELIST/NAM1/TOG,UG,L,RHOG,CPG,MUG,KG,TO,CPO,MDOT,AREA,MAJ,MIN,
     *RHOG,MUG,KG,SPACE,D1,D2,KS,VS,X
C
      READ(5,NAM1)
      WRITE(6,99)
   99 FORMAT(5X,"PREDICTION OF WALL AND COOLANT TEMPERATURES FOR A",
     *" TRANSPIRATION COOLED FLAT PLATE",/5X,82("*")/)
      WRITE(6,88)TOG,TO,UG,MDOT
   88 FORMAT(5X,33H MAINSTREAM STAGNATION TEMPERATURE =,F11.4/
     *5X,33H COOLANT STAGNATION TEMPERATURE =,F11.4/
     *5X,22H MAINSTREAM VELOCITY =,F11.4/
     *5X,24H COOLANT MASS FLOWRATE =,F11.4/)
C
C     CALCULATION OF POROSITY OF MESH
C
      ATOT=SPACE*2.0*D2
      AMAT=(2.0*D2*D1)+(6.283*MAJ*MIN)
      PORO=AMAT/ATOT
      VINF=MDOT/(RHOG*AREA)
      VMAT=(1.571*D1*D1*D2)+(1.571*D2*D2*SQRT((D1+D2)**2.0+SPACE**2.0))
      VTOT=2.0*D2*SPACE*(D1+2.0*D2)
      POROUS=VMAT/VTOT
      VT=VINF/PORO
      KM=KS*(1.0-2..*POROUS)
      J=0
      N=0
      I=0
    9 DL=0.0585
      I=I+1
      WRITE(6,98)I,L
   98 FORMAT(//10X,11H AT STATION,I3/10X,11("-")//,10X,
     *36H DISTANCE FROM PLATE LEADING EDGE IS,F11.4/)
      L=L+DL
C
C     MAINSTREAM REYNOLDS AND PRANTL NUS
C
      REG=(RHOG*UG*L)/MUG
      PRG=(MUG*CPG)/KG
C
C     FORCED CONVECTION CORRELATION EQUATION
C
      NUG=0.0292*(REG**0.801)*(PRG**0.33)
C
C     INITIAL HEAT TRANSFER COEFFICIENT
C
      HG=(NUG*KG)/L
      HG1=HG
C
C     MAINSTREAM STANTON NO
C
      SG=HG/(CPG*RHOG*UG)
C
C     BLOWING PARAMETER
C
      BH=MDOT/(GREAT*SG*RHOG*UG)
      WRITE(6,110)REG,PRG,NUG,SG,BH
```

```
      PROGRAM WALL(INPUT,OUTPUT,WALLIN,WALLOUT,TAPE5=WALLIN,TAPE6=WALLOUT)
      REAL MACH,MDOT,MAIN,MCOOL,MTOT,MAJ,MIN,MEA
C
C     THIS PROGRAM PREDICTS THE WALL TEMPERATURE PROFILES FOR METAL AND
C     COOLANT IN A FORMER WALL THAT IS TRANSPIRATION COOLED
C
      PARAMETER(NSTA=11,NPTS=NSTA*10,TO=530.,PO=.1,MDOT=.0002,MEA=.1,
     *MAJ=.1,MIN=.05,DI=.02,SVSX
C
      READ(5,*)NCASES
      WRITE(6,*)
     $' PROGRAM WALL: PREDICTION OF WALL AND COOLANT TEMPERATURES FOR A',
     *' TRANSPIRATION COOLED FLAT PLATE',/5X,'CASE',I2)
      WRITE(6,*)
     $' FORMAT(//5X,20H MAIN STREAM MACH NO.=,F11.4/
     *5X,20H MAIN STREAM STAGNATION TEMPERATURE =,F11.4/
     *5X,20H MAIN STREAM VELOCITY =,F11.4/
     *5X,20H COOLANT MASS FLOWRATE =,F11.4/)
C
C     CALCULATION OF REYNOLDS NUMBER
C
      ATOT=SPACE*2.0*D2
      AMAI=(2.0*D2*D1)*(6.28*MAJ*MIN)
      FLAG=SQRT(ATOT
      VISC=SUTH(TO,PO,MACH,MAIN,MCOOL,MTOT,MAJ,MIN,MEA,SPACE,D1,D2)
      VMAI=1.5716*D1*D2*(1.5716*D2*D2+SQRT(1.5716*D2*D2+2.0*SPACE**2.0))
      VTOT=2.0*D2*SPACE*(D1+2.0*D2)
      FLOWS=VMAI/VTOT
      VT=VTOT/FLAG
      PRT=SPR(1.0-2.0*FLOWS
      J=0
      N=0
      I=0
      S=0.0
      DO 5 I=1,NSTA
      I=I+1
      WRITE(6,99)I,L
   99 FORMAT(//10X,11H AT STATION,13/10X,11(1H*)//,10X,
     *32H DISTANCE FROM PLATE LEADING EDGE (IN.F11.4/)
      L=0.
C
C     MAIN STREAM REYNOLDS AND PRANTL NOS
C
      REC=(RHO*U*L)/MU
      PRC=(MUC*CP)/K
C
C     FORCED CONVECTION CORRELATION EQUATION
C
      NUF=0.0296*(REC**0.8)*(PRC**0.33)
C
C     INITIAL HEAT TRANSFER COEFFICIENT
C
      HI=(NUF*K)/L
      HO=HI
C
C     MAIN STREAM SPARTAN NO
C
      SU=HO/(CP*RHO*VEL)
C
      DO 10 N=1,NPTS
C
      BU=MDOT/(RHO*VEL*SPACE*2.0*D1)
      WRITE(6,110)FLOWS,FLAG,VISC,BU
```

```
100 FORMAT(10X,5H REQ =,F11.2/10X,5H PRO =,F11.4/10X,6H MUO =
     *F11.4/10X,5H MO =,F11.4/10X,5H EH =,F11.4///)
      WRITE(6,111)
111   FORMAT(5X,25H HEAT TRANSFER COEFF.(HO),3X,
     *25H TUBE TEMPERATURE(TEMPW),3X,
     *20H CRITICAL ENERGY RATIO///5X,84(1H-)//)
C
C     ENTRY ENTHALPIE - ENTHALPY FLUX OF COOLANT IS EQUAL TO CONVECTIVE
C     HEAT TRANSFER
C
    2 IU (TEMPW-TEMP)*(MUO*CPO*TO)/(HO*AREA*MUO*CPO)
      TEMP=TW
C
C     CRITICAL ENERGY PARAMETER
C
    4 FHI=TEMPW/TOO
      RATIO=(1.0+SQRT(1.0+FHI))/(1.0-SQRT(1.0-FHI))
      BOILI=((RATIO)**2.0)/(1.0+FHI)
      WRITE(6,105)HO,TW,BOILI
  105 FORMAT(15X,F11.4,10X,F11.6,10X,F11.6)
C
C     CORRECTED HEAT TRANSFER COEFFICIENT
C
      HO=EH=HO*(1.0-(EH/EMERIT)**2.0
      N=N+1
      DIFF=ABS(HO-EH)
      IF(DIFF.LT.0.001)GO TO 3
      HO=EH
      IF(N.EQ.10)GO TO 3
      GO TO 2
    3 CONTINUE
      N=0
C
C     COOLANT REYNOLDS AND PRANDTL NOS
C
      REO=(RHOO*VT*((D1+D2)/2.0))/MUO
      PRO=(MUO*CPO)/KO
C
C     CORRELATION EQUATION FOR FLOW OVER TUBES
C
      NU=0.35*(REO**0.6)*(PRO**0.33)
C
      TEMP=(4.0*TO+TEMPW)/5.0
      TW=TW
C
C     COOLANT HEAT TRANSFER COEFFICIENT
C
      HC=(NU*KO)/((D1+D2)/2.0)
C
C     INTERNAL REYNOLDS NO, NUSSELT NO, AND HEAT TRANSFER COEFFICIENT
C
      REI=(MUOT*VS)/(AREA*MU)
      NU=0.35*REI
      HI=(NU*KI)/(VS**2.0)
      WRITE(6,101)HO,HI
  101 FORMAT(10X,5H HO =,F11.4/10X,5H HI =,F11.4///)
C
C     CALCULATION OF CONSTANTS A, B, ALPHA, BETA, GAMMA
C
      A=(HI*AREA)/(MUOT*CPO)
      B=SQRT((1/M)*((A/2.0)**2.0))
      E=((1/M)+2.0)-0.25)
      F=B-(A/2.0)
```

```
      U=BI(R/2.0)
      U=EXP(F*X)-(1.0/EXP(G*X))
      R=EXP(F*X)
      S=1.0/EXP(G*X)
      WRITE(5,120)
  120 FORMAT(2X,22H COLD SIDE METAL TEMP.,1X,
     *21H HOT SIDE METAL TEMP.,1X,
     *24H COLD SIDE COOLANT TEMP.,1X,
     *23H HOT SIDE COOLANT TEMP.,1X,
     *25H HEAT TRANSFER COEFF.(HG),1X,
     *7H BHCRIT/2X,1[illegible]
     / ALPHA=TO-(HC*(TEMPO-TO))/(KM*A*E)
      BETA=(-HC*(TEMPW-TOO)-HC*(TEMPO-TO)*S)/(KM*A*E*U)
      GAMMA=(HC*(TEMPO-TO)-((HG*(TEMPW-TOO)+HC*(TEMPO-TO)*S)/U))
     */(KM*A*E)
C
C     CALCULATION OF WALL TEMPERATURE
C
      TEMPW=ALPHA+(0.5+(B/A))*BETA*R*(0.5-(B/A))*GAMMA*S
      TEMPO=ALPHA+(0.5+(B/A))*BETA+(0.5-(B/A))*GAMMA
      TO=ALPHA+BETA*GAMMA
      TW=ALPHA+BETA*R*GAMMA*S
      PHI=TEMPW/TOO
      RATIO=(1.0+SQRT(1.0-PHI))/(1.0-SQRT(1.0-PHI))
      BHCRIT=((ALOG(RATIO))**2.0)/(1.0-PHI)
C
C     CORRECTED HEAT TRANSFER COEFFICIENT
C
      HG=HG1*(1.0-(BH/BHCRIT))**2.0
      WRITE(6,102)TEMPO,TEMPW,TO,TW,HG,BHCRIT
  102 FORMAT(5X,F11.6,12X,F11.6,12X,F11.6,12X,F11.6,12X,F11.6,
     *12X,F11.6)
      J=J+1
      DIF2=ABS(TW1-TW)
      IF(DIF2.LT.0.001)GO TO 6
      TW1=TW
      IF(J.EQ.10)GO TO 6
      GO TO 7
    6 CONTINUE
      J=0
      IF(L.GT.1.089)GO TO 8
      DL=0.00
      GO TO 9
    8 CONTINUE
      STEND
END OF FIL
```

PREDICTION OF WALL AND COOLANT TEMPERATURES FOR A TRANSPIRATION COOLED FLAT PLATE
****

MAINSTREAM STAGNATION TEMPERATURE = 320.0000
COOLANT STAGNATION TEMPERATURE = 290.0000
MAINSTREAM VELOCITY = 20.0000
COOLANT MASS FLOWRATE = .0222

AT STATION 1

DISTANCE FROM PLATE LEADING EDGE IS .7970

REG = [illegible]
PRG = .6973
NUG = 1399.6169
SG = .0024
BH = 3.1238

HEAT TRANSFER COEFF.(HG)	WALL TEMPERATURE(TEMPW)	CRITICAL BLOWING PARA(BHCRIT)
49.080663	297.293521	4.200152
3.225231	[illegible]	4.263473
3.509191	[illegible]	4.262958
3.506818	290.673065	4.262963

HC = 53.1802
HI =595657.4474

COLD SIDE METAL TEMP.	HOT SIDE METAL TEMP.	COLD SIDE COOLANT TEMP.	HC [illegible]LANT TEMP.	HEAT TRANSFER COEFF.(HG)	BHCRIT
[illegible]	290.632096	[illegible]	290.626214	3.503620	[illegible]
290.458614	290.458633	290.000000	290.454364	3.516171	[illegible]
290.525049	290.525067	290.000000	[illegible]	3.513282	[illegible]
290.499603	290.499621	290.000000	290.494971	3.514391	[illegible]
290.509349	290.509367	290.000000	290.501617	3.513976	[illegible]
290.505616	290.505634	290.000000	290.500929	3.5141.9	[illegible]
290.507046	290.[illegible]07664	290.000000	290.502345	3.514057	[illegible]
290.506498	290.506516	290.000000	290.501802	3.514090	[illegible]

AT STATION 2

DISTANCE FROM PLATE LEADING EDGE IS .8555

REG = 879201.93
PRG = .6973
NUG = 1475.6730
SG = .0024
BH = 3.1651

HEAT TRANSFER COEFF.(HG)	WALL TEMPERATURE(TEMPW)	CRITICAL BLOWING PARA(BHCRIT)
48.435656	297.220744	4.200831

2.944589	290.567196	4.263965
3.217152	290.618616	4.263488
3.214974	290.618209	4.263492

NC = 53.1802
NI =595657.4474

COLD SIDE METAL TEMP.	HOT SIDE METAL TEMP.	COLD SIDE COOLANT TEMP.	HOT SIDE COOLANT TEMP.	HEAT TRANSFER COEFF.(HO)	[illegible]
290.580504	290.580579	290.000000	290.575177	3.216590	[illegible]
290.421152	290.421170	290.000000	290.417250	3.223284	[illegible]
[illegible]	290.481667	290.000000	290.477382	3.220735	[illegible]
[illegible]	290.458754	290.000000	[illegible]	3.221702	[illegible]
[illegible]	290.467555	290.000000	[illegible]	3.221336	[illegible]
290.461107	290.464204	290.000000	290.459284	3.221476	4.264970
290.465463	290.465400	290.000000	290.461148	3.221423	4.264967
290.464277	290.464294	290.000000	290.460366	3.22144[illegible]	[illegible]

AT STATION 3

DISTANCE FROM PLATE LEADING EDGE IS .9140

REG = [illegible]5474.70
PRG = .6973
NUG = 1550.7609
SG = .0024
BM = 3.2046

HEAT TRANSFER COEFF.(HO)	WALL TEMPERATURE(TEMPW)	CRITICAL BLOWING PARA(BMCRIT)
47.8[illegible]384	297.152931	4.201464
2.693205	290.519612	4.264444
2.954997	290.569163	4.263966
2.952991	290.[illegible]764	4.263969

NC = 53.1802
NI =595657.4474

COLD SIDE METAL TEMP.	HOT SIDE METAL TEMP.	COLD SIDE COOLANT TEMP.	HOT SIDE COOLANT TEMP.	HEAT TRANSFER COEFF.(HO)	[illegible]
290.534148	290.534163	290.000000	290.529192	2.954408	4.264[illegible]
290.387413	290.387423	290.000000	290.[illegible]423	2.960349	4.2657[illegible]
[illegible]	290.443003	290.000000	290.438880	[illegible]	4.265184
290.421[illegible]	290.421253	290.000000	290.418026	[illegible]	4.265388
290.42[illegible]11	290.42[illegible]26	290.000000	[illegible]	[illegible]	4.265311
290.426841	290.426[illegible]	290.000000	290.422933	2.958750	4.265340
290.428035	290.428050	290.000000	290.424066	2.958704	[illegible]
290.427601	290.427617	290.000000	[illegible]	2.958721	[illegible]

AT STATION 4

DISTANCE FROM PLATE LEADING EDGE IS .9725

REG = 991747.47
PRG = .6973

NUM = 1624.9504
SG = .0023
BH = 3.2422

HEAT TRANSFER COEFF.(HG)	WALL TEMPERATURE(TEMPW)	CRITICAL BLOWING PARA(BHCRIT)
47.182746	297.029454	4.202056
2.466959	290.478655	4.254859
2.718470	290.524406	4.264279
2.717626	290.524052	4.264401

HC = 53.1802
HI =595657.4474

COLD SIDE METAL TEMP.	HOT SIDE METAL TEMP.	COLD SIDE COOLANT TEMP.	HOT SIDE COOLANT TEMP.	HEAT TRANSFER COEFF.(HG)	BHCRIT
290.492140	290.492154	290.000000	290.487574	2.717845	4.[illegible]709
290.356837	290.356901	290.000000	290.353579	2.723169	4.266017
290.407865	290.407879	290.000000	290.404083	2.721177	1.[illegible]
290.388650	290.388664	290.000000	290.385046	2.721928	4.[illegible]710
290.395892	290.395906	290.000000	290.392222	2.721645	4.2[illegible]40
290.[illegible]3162	290.393176	290.000000	290.389517	2.7[illegible]1751	4.[illegible]666
290.[illegible]4191	290.394205	290.000000	290.390537	2.721711	4.[illegible]
290.393803	290.393813	290.000000	290.390152	2.721726	4.2[illegible]660

AT STATION 5

DISTANCE FROM PLATE LEADING EDGE IS 1.0310

REG = 1048020.24
FRG = .6973
NUG = 1698.3021
SG = .0023
BH = 3.2762

HEAT TRANSFER COEFF.(HG)	WALL TEMPERATURE(TEMPW)	CRITICAL BLOWING PARA(BHCRIT)
46.763712	297.029897	.202612
2.262480	290.437733	4.265235
2.504720	290.481739	4.264791
2.502487	290.480408	4.264774

HC = 53.1802
HI =595657.4474

COLD SIDE METAL TEMP.	HOT SIDE METAL TEMP.	COLD SIDE COOLANT TEMP.	HOT SIDE COOLANT TEMP.	HEAT TRANSFER COEFF.(HG)	BHCRIT
290.453972	290.453984	290.000000	290.449760	2.503608	4.265078
290.329159	290.329172	290.000000	290.[illegible]6108	2.503313	4.266385
290.379993	290.376006	290.000000	290.372507	2.506547	4.[illegible]
290.358410	290.358431	290.000000	290.350[illegible]76	2.507210	4.[illegible]
290.365013	290.365026	290.000000	290.361629	2.506961	4.[illegible]
290.362533	290.362551	290.000000	290.359177	2.507054	4.265[illegible]
290.363467	290.363480	290.000000	290.360097	2.507019	4.[illegible]

END OF [illegible]

APPENDIX C

C1 PROBE CALIBRATION CURVES

The calibration curve is used as follows:

1 By noting the hot wire output given in volts, which are related directly to the flow velocity, the graph is entered on the x-axis.

2 The thermistor resistance (in ohms) that is needed to balance the second anemometer unit is used to determine the calibration line as given on the following graph.

3 By combining these two readings as shown the flow temperature can be read off the graph.

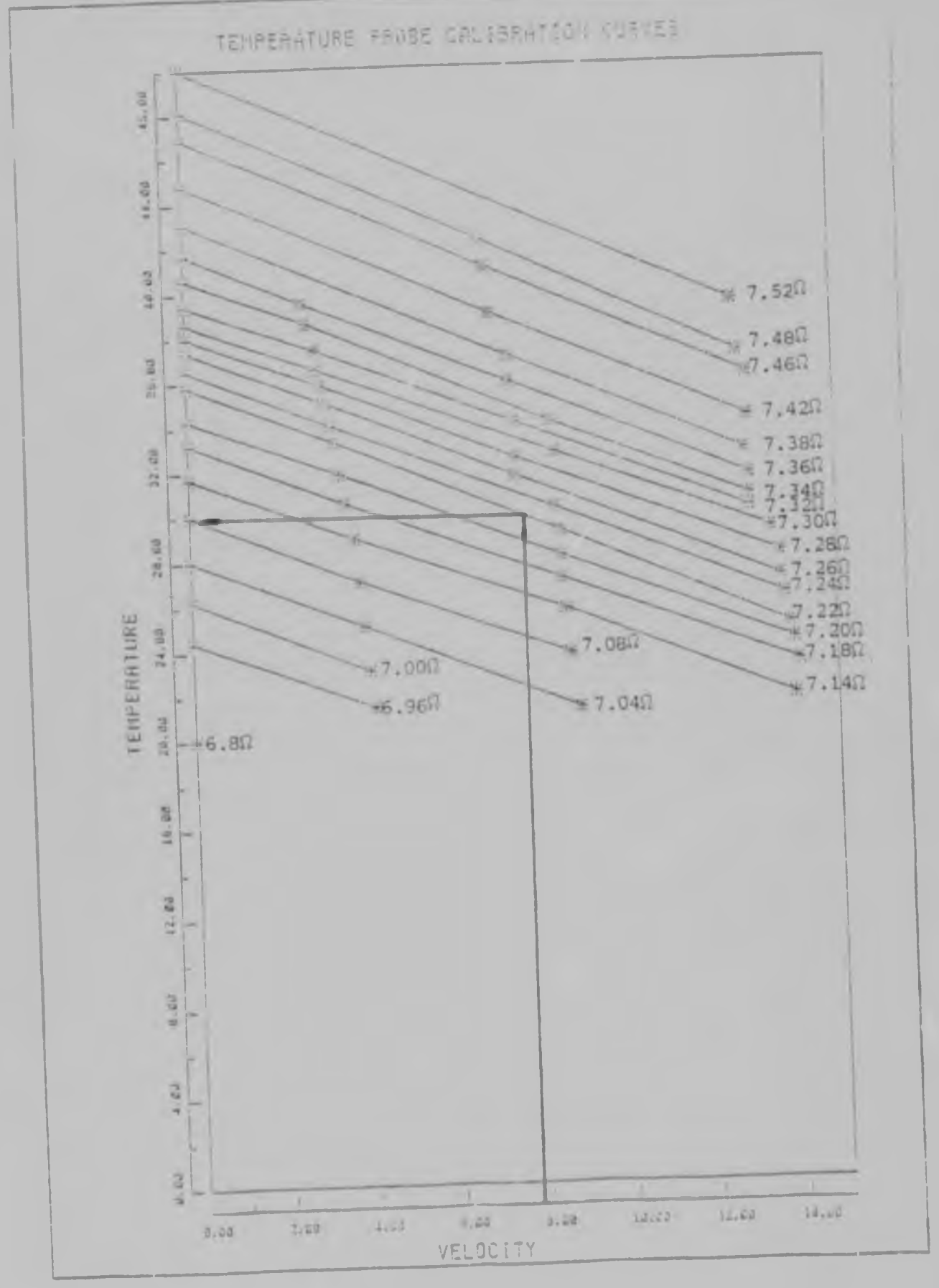
TEMPERATURE PROBE CALIBRATION CURVES
TEMPERATURE
VELOCITY
7.52Ω
7.48Ω
7.46Ω
7.42Ω
7.38Ω
7.36Ω
7.34Ω
7.32Ω
7.30Ω
7.28Ω
7.26Ω
7.24Ω
7.22Ω
7.20Ω
7.18Ω
7.14Ω
7.08Ω
7.04Ω
7.00Ω
6.96Ω
6.8Ω

APPENDIX D

E1 EXPERIMENTAL RESULTS

EXPERIMENT [illegible]

T_w = 25,00°C u_∞ = 14,95 m/s

T_∞ = 33,01°C v_w = 0,064 m/s

T_0 = 24,5 °C F = 0,00428

Y (mm)	STATION 1		STATION 2		STATION 3		STATION 4		STATION 5	
	T(°C)	$\frac{T-T_w}{T_g-T_w}$	T(°C)	$\frac{T-T_w}{T_g-T_w}$	T(°C)	$\frac{T-T_w}{T_g-T_w}$	T(°C)	$\frac{T-T_w}{T_g-T_w}$	T(°C)	$\frac{T-T_w}{T_g-T_w}$
0,0	25,00	0,000	25,00	0,000	25,00	0,000	25,00	0,000	25,00	0,000
1,0	28,92	0,490	30,14	0,642	30,24	0,655	29,82	0,602	29,84	0,605
2,0	29,92	0,615	30,69	0,711	30,80	0,725	31,07	0,754	30,46	0,682
2,5	30,20	0,650	31,10	0,762	31,18	0,772	31,10	0,762	30,97	0,746
3,0	30,38	0,672	31,34	0,793	31,26	0,782	31,23	0,779	31,02	0,752
3,5	30,52	0,690	31,40	0,800	31,40	0,800	31,49	0,811	31,39	0,799
4,0	30,70	0,712	31,46	0,808	31,54	0,817	31,53	0,816	31,57	0,821
4,5	30,96	0,745	31,59	0,824	31,65	0,831	31,72	0,840	31,78	0,847
5,0	31,13	0,765	31,72	0,840	31,79	0,849	31,79	0,849	31,84	0,855
6,0	31,47	0,809	31,93	0,866	31,98	0,872	31,97	0,871	31,94	0,868
7,0	31,80	0,850	32,03	0,879	32,05	0,881	32,12	0,890	32,15	0,894
8,0	32,05	0,881	32,23	0,904	32,29	0,911	32,20	0,900	32,14	0,892
9,0	32,22	0,902	32,32	0,915	32,34	0,917	32,40	0,925	32,45	0,931
10,0	32,28	0,910	32,50	0,937	32,61	0,951	32,68	0,960	32,54	0,942
12,0	32,60	0,950	32,60	0,950	32,66	0,957	32,70	0,963	32,73	0,966
14,0	32,85	0,981	32,70	0,963	32,67	0,959	32,78	0,972	32,80	0,975
16,0	32,94	0,993	32,73	0,966	32,70	0,962	32,78	0,972	32,83	0,979
18,0	32,99	0,999	32,85	0,981	32,84	0,980	32,86	0,983	32,91	0,989
20,0			32,98	0,998	33,00	1,000	32,93	0,991	32,99	0,999
25,0							32,98	0,998	33,00	1,000
30,0										
50,0										

EXPERIMENT : II

T_w = 23,64°C u_ω = 14,95 m/s

T_ω = 33,14°C v_w = 0,088 m/s

T_g = 23,0 °C F = 0,00589

y (mm)	STATION I		STATION 2		STATION 3		STATION 4		STATION 5	
	T(°C)	$\frac{T-T_w}{T_g-T_w}$	T(°C)	$\frac{T-T_w}{T_g-T_w}$	T(°C)	$\frac{T-T_w}{T_g-T_w}$	T(°C)	$\frac{T-T_w}{T_g-T_w}$	T(°C)	$\frac{T-T_w}{T_g-T_w}$
0,0	23,72	0,000	23,66	0,000	23,60	0,000	23,62	0,000	23,64	0,000
1,0	28,27	0,487	30,17	0,687	29,34	0,600	29,11	0,576	29,45	0,612
2,0	29,29	0,595	30,89	0,763	30,77	0,750	30,40	0,712	30,32	0,703
2,5	29,64	0,632	31,09	0,784	31,05	0,780	30,79	0,753	30,56	0,728
3,0	30,10	0,680	31,23	0,799	31,24	0,800	30,93	0,767	30,77	0,750
3,5	30,43	0,715	31,26	0,802	31,27	0,803	31,10	0,785	31,00	0,775
4,0	30,56	0,728	31,34	0,810	31,39	0,816	31,34	0,810	31,07	0,782
4,5	30,74	0,747	31,42	0,819	31,50	0,827	31,33	0,809	31,15	0,791
5,0	30,97	0,772	31,50	0,827	31,52	0,829	31,42	0,819	31,33	0,809
6,0	31,24	0,800	31,72	0,850	31,73	0,852	31,56	0,834	31,61	0,839
7,0	31,58	0,836	32,07	0,887	31,85	0,864	31,71	0,849	31,72	0,851
8,0	31,72	0,850	32,19	0,900	32,06	0,886	31,88	0,867	31,88	0,867
9,0	32,11	0,892	32,38	0,920	32,16	0,897	32,02	0,882	32,06	0,886
10,0	32,29	0,911	32,51	0,934	32,31	0,913	32,10	0,891	32,22	0,903
12,0	32,74	0,958	32,65	0,048	32,58	0,941	32,33	0,915	32,38	0,920
14,0	32,98	0,983	32,96	0,981	32,82	0,966	32,54	0,937	32,53	0,936
16,0	33,14	1,000	33,06	0,992	33,02	0,987	32,71	0,955	32,77	0,961
18,0			33,14	1,000	33,05	0,991	32,88	0,973	32,94	0,979
20,0					33,07	0,993	33,12	0,998	32,97	0,982
25,0					33,14	1,000	33,14	1,000	33,13	0,999
30,0									33,14	1,000
50,0										

EXPERIMENT : III

T_w = 23,05°C u_∞ = 14,95 m/s

T_∞ = 34,10°C ν_w = 0,113 m/s

T_0 = 22,9 °C F = 0,00756

y (mm)	STATION 1		STATION 2		STATION 3		STATION 4		STATION 5	
	T(°C)	$\frac{T-T_w}{T_g-T_w}$	T(°C)	$\frac{T-T_w}{T_g-T_w}$	T(°C)	$\frac{T-T_w}{T_g-T_w}$	T(C°)	$\frac{T-T_w}{T_g-T_w}$	T(°C)	$\frac{T-T_w}{T_g-T_w}$
0,0	23,08	0,000	23,06	0,000	23,05	0,000	23,04	0,000	23,02	0,000
1,0	28,61	0,503	29,69	0,601	29,13	0,550	29,14	0,551	29,22	0,558
2,0	29,98	0,627	31,03	0,722	30,60	0,683	30,23	0,650	30,23	0,650
2,5	30,28	0,654	31,4'	0,757	31,03	0,722	30,84	0,705	30,43	0,668
3,0	30,58	0,681	31,56	0,770	31,38	0,754	31,15	0,733	30,92	0,712
3,5	30,79	0,700	31,88	0,799	31,69	0,782	31,41	0,757	31,11	0,729
4,0	30,97	0,717	31,97	0,807	31,99	0,809	31,72	0,785	31,18	0,736
4,5	31,11	0,729	32,06	0,815	32,09	0,818	31,79	0,791	31,44	0,759
5,0	31,32	0,748	32,24	0,832	32,42	0,848	31,91	0,802	31,67	0,780
6,0	31,83	0,795	32,64	0,868	32,65	0,869	32,64	0,868	31,98	0,808
7,0	32,24	0,832	32,79	0,881	33,03	0,903	32,76	0,879	32,52	0,857
8,0	32,63	0,867	33,09	0,909	33,32	0,929	32,91	0,892	33,03	0,903
9,0	33,00	0,900	33,18	0,917	33,57	0,952	33,12	0,911	33,13	0,912
10,0	33,17	0,916	33,30	0,928	33,74	0,967	33,32	0,929	33,37	0,934
12,0	33,38	0,935	33,46	0,942	33,87	0,979	33,41	0,938	33,53	0,948
14,0	33,75	0,968	33,61	0,956	33,93	0,985	33,47	0,943	33,71	0,965
16,0	34,00	0,991	33,83	0,976	34,01	0,992	33,64	0,958	33,83	0,976
18,0	34,10	1,000	34,02	0,993	34,06	0,996	33,67	0,961	33,96	0,987
20,0			34,10	1,000	34,08	0,998	33,87	0,979	34,98	0,989
25,0					34,10	1,000	34,04	0,995	34,04	0,995
30,0							34,10	1,000	34,07	0,997
50,0										

EXPERIMENT : IV

T_w = 26,50°C $\quad u_\infty$ = 10,85 m/s

T_∞ = 39,02°C $\quad v_w$ = 0,064 m/s

T_0 = 26,3 °C $\quad F$ = 0,0059

y (mm)	STATION 1		STATION 2		STATION 3		STATION 4		STATION 5	
	T(°C)	$\frac{T-T_w}{T_g-T_w}$	T(°C)	$\frac{T-T_w}{T_g-T_w}$	T(°C)	$\frac{T-T_w}{T_g-T_w}$	T(°C)	$\frac{T-T_w}{T_g-T_w}$	T(°C)	$\frac{T-T_w}{T_g-T_w}$
0,0	26,(	0,000	26,52	0,000	26,50	0,000	26,40	0,000	26,38	0,000
1,0	34,65	0,651	34,36	0,628	34,12	0,609	33,07	0,589	33,80	0,583
2,0	36,32	0,784	35,66	0,732	35,44	0,714	35,35	0,707	35,13	0,689
2,5	36,54	0,802	36,22	0,776	36,04	0,762	35,99	0,758	35,94	0,754
3,0	36,82	0,824	36,40	0,791	36,37	0,788	36,27	0,780	36,23	0,777
3,5	37,09	0,846	36,55	0,803	36,45	0,795	36,40	0,791	36,33	0,785
4,0	37,39	0,870	36,73	0,817	36,55	0,803	36,45	0,795	36,39	0,790
4,5	37,61	0,887	37,00	0,839	36,89	0,830	36,82	0,824	36,69	0,814
5,0	37,67	0,892	37,14	0,850	37,04	0,842	37,00	0,839	36,89	0,830
6,0	37,77	0,900	37,53	0,881	37,47	0,876	37,42	0,872	37,37	0,868
7,0	37,97	0,916	37,73	0,897	37,63	0,889	37,56	0,883	37,46	0,875
8,0	38,33	0,945	38,02	0,920	37,93	0,913	37,82	0,904	37,69	0,894
9,0	38,39	0,950	38,37	0,948	38,29	0,942	38,24	0,938	37,99	0,918
10,0	38,54	0,962	38,43	0,953	38,37	0,948	38,29	0,942	38,21	0,935
12,0	38,77	0,980	38,58	0,965	38,53	0,961	38,46	0,955	38,36	0,947
14,0	38,86	0,987	38,79	0,982	38,76	0,979	38,67	0,972	38,62	0,968
16,0	38,96	0,995	38,91	0,991	38,88	0,989	38,83	0,985	38,77	0,980
18,0			38,99	0,998	38,93	0,993	38,89	0,990	38 86	0,987
20,0					39,02	1,000	38,96	0,995	38,92	0,992
25,0							38,02	1,000	38,99	0,998
30,0										
50,0										

EXPERIMENT · V

T_w = 26,25°C u_∞ = 10,85 m/s

T_∞ = 39,21°C v_w = 0,088 m/s

$\bar{T}$ = 26,1 °C F = 0,00811

y (mm)	STATION 1		STATION 2		STATION 3		STATION 4		STATION 5	
	T(°C)	$\frac{T-T_w}{t_g-T_w}$	T(°C)	$\frac{T-T_w}{T_g-T_w}$	T(°C)	$\frac{T-T_w}{T_g-T_w}$	T(°C)	$\frac{T-T_w}{T_g-T_w}$	T(°C)	$\frac{T-T_w}{T_g-T_w}$
0,0	26,31	0,000	26,25	0,000	26,24	0,000	26,23	0,000	26,21	0,000
1,0	34,16	0,610	34,08	0,604	33,87	0,588	33,83	0,585	33,77	0,580
2,0	36,13	0,762	36,07	0,758	35,97	0,750	35,94	0,748	35,87	0,742
2,5	36,36	0,780	36,31	0,776	36,22	0,769	36,11	0,761	36,07	0,758
3,0	36,62	0,800	36,54	0,794	36,49	0,790	36,41	0,784	36,29	0,775
3,5	36,80	0,814	36,66	0,803	36,59	0,798	36,49	0,790	36,41	0,784
4,0	37,10	0,837	37,01	0,830	36,97	0,827	36,80	0,814	36,57	0,796
4,5	37,28	0,851	37,21	0,846	37,11	0,838	36,88	0,820	36,84	0,817
5,0	37,47	0,866	37,28	0,851	37,24	0,848	37,10	0,837	36,94	0,825
6,0	37,88	0,897	37,77	0,889	37,33	0,855	37,27	0,850	37,21	0,846
7,0	38,15	0,918	37,94	0,902	37,84	0,894	37,75	0,887	37,46	0,865
8,0	38,43	0,940	38,39	0,937	38,26	0,927	37,98	0,905	37,78	0,890
9,0	37,20	0,945	38,48	0,944	38,41	0,938	38,25	0,926	38,10	0,914
10,0	38,59	0,952	38,54	0,948	38,50	0,945	38,42	0,939	38,26	0,927
12,0	38,78	0,967	38,73	0,963	38,69	0,960	38,65	0,957	38,56	0,950
14,0	38,87	0,974	38,83	0,971	38,83	0,971	38,80	0,968	38,70	0,961
16,0	38,98	0,982	38,91	0,977	38,89	0,975	38,85	0,972	38,78	0,967
18,0	39,15	0,995	39,09	0,991	39,04	0,987	39,02	0,985	38,92	0,978
20,0	39,21	1,000	39,18	0,998	39,13	0,994	39,11	0,992	39,05	0,988
25,0			39,21	1,000	39,21	1,000	39,16	0,996	39,15	0,995
30,0							39,21	1,000	39,21	1,000
50,0										

EXPERIMENT: VI

T_w = 26,13°C u_∞ = 10,85 m/s

T_∞ = 39,54°C v_w = 0,112 m/s

T_0 = 26,0 °C F = 0,01032

y (mm)	STATION 1		STATION 2		STATION 3		STATION 4		STATION 5	
	T(°C)	$\frac{T-T_w}{T_g-T_w}$	T(°C)	$\frac{T-T_w}{T_g-T_w}$	T(°C)	$\frac{T-T_w}{T_b-T_w}$	T(°C)	$\frac{T-T_w}{T_g-T_w}$	T(°C)	$\frac{T-T_w}{T_g-T_w}$
0,0	26,14	0,000	26,13	0,000	26,13	0,000	26,13	0,000	26,13	0,000
1,0	34,19	0,601	34,10	0,594	33,99	0,586	33,91	0,580	33,83	0,574
2,0	36,43	0,768	36,31	0,759	36,25	0,755	36,19	0,750	36,13	0,746
2,5	36,67	0,786	36,60	0,781	36,54	0,776	36,48	0,772	36,44	0,769
3,0	36,93	0,805	36,86	0,800	36,78	0,794	36,70	0,788	36,58	0,779
3,5	37,13	0,820	37,05	0,814	36,98	0,809	36,80	0,796	36,72	0,790
4,0	37,43	0,843	37,38	0,839	37,21	0,826	37,14	0,821	37,03	0,813
4,5	37,58	0,854	37,54	0,851	37,49	0,847	37,39	0,840	37,35	0,837
5,0	37,77	0,868	37,69	0,862	37,62	0,857	37,57	0,853	37,46	0,845
6,0	38,19	0,899	38,13	0,895	38,06	0,890	37,98	0,884	37,92	0,879
7,0	38,48	0,921	38,40	0,915	38,24	0,903	38,16	0,897	38,00	0,891
8,0	38,76	0,942	38,71	0,938	38,63	0,932	38,55	0,926	38,36	0,912
9,0	38,83	0,947	38,80	0,945	38,75	0,941	38,71	0,938	38,52	0,924
10,0	38,94	0,955	38,87	0,950	38,86	0,949	38,83	0,947	38,75	0,941
12,0	39,14	0,970	39,10	0,967	38,94	0,955	38,88	0,951	38,87	0,950
14,0	39,20	0,975	39,15	0,971	39,12	0,969	39,06	0,964	39,02	0,961
16,0	39,34	0,985	39,27	0,980	39,24	0,978	39,14	0,970	39,12	0,969
18,0	39,49	0,996	39,43	0,992	39,34	0,985	39,29	0,981	39,22	0,976
20,0	39,54	1,000	39,51	0,998	39,46	0,994	39,38	0,988	39,34	0,985
25,0			39,54	1,000	39,54	1,000	39,45	0,993	39,39	0,989
30,0							39,54	1,000	39,50	0,997
50,0										

EXPERIMENT : VII

T_w = 25,89°C u_∞ = 10,80 m/s

T_∞ = 40,01°C v_w = 0,128 m/s

T_0 = 25,7 °C F = 0,01185

Y (mm)	STATION 1		STATION 2		STATION 3		STATION 4		STATION 5	
	T(°C)	$\frac{T-T_w}{T_g-T_w}$	T(°C)	$\frac{T-T_w}{T_g-T_w}$	T(°C)	$\frac{T-T_w}{T_g-T_w}$	T(°C)	$\frac{T-T_w}{T_g-T_w}$	T(°C)	$\frac{T-T_w}{T_g-T_w}$
0,0	25,90	0,000	25,89	0,000	25,89	0,000	25,88	0,000	25,88	0,000
1,0	34,36	0,600	34,23	0,591	34,14	0,584	33,99	0,574	33,94	0,570
2,0	36,71	0,766	36,56	0,756	36,51	0,752	36,35	0,741	36,34	0,740
2,5	36,96	0,784	36,89	0,779	36,82	0,774	36,76	0,770	36,71	0,766
3,0	37,21	0,802	37,13	0,796	37,06	0,791	36,97	0,785	36,86	0,777
3,5	37,38	0,814	37,36	0,812	37,27	0,806	37,10	0,794	37,02	0,788
4,0	37,76	0,841	37,69	0,836	37,52	0,824	37,45	0,819	37,36	0,812
4,5	37,92	0,852	37,89	0,850	37,82	0,845	37,71	0,837	37,69	0,836
5,0	38,12	0,866	38,05	0,861	37,98	0,856	37,89	0,850	37,84	0,846
6,0	38,56	0,897	38,49	0,892	38,41	0,887	38,32	0,880	38,29	0,878
7,0	38,87	0,919	38,78	0,913	38,60	0,900	38,53	0,895	38,46	0,890
8,0	39,16	0,940	39,11	0,936	39,04	0,931	38,94	0,924	38,74	0,910
9,0	39,23	0,945	39,23	0,945	39,13	0,938	39,12	0,937	38,95	0,925
10,0	39,36	0,954	39,28	0,948	39,28	0,948	39,28	0,948	39,19	0,942
12,0	39,57	0,969	39,53	0,966	39,36	0,954	39,33	0,952	39,33	0,952
14,0	39,64	0,974	39,57	0,969	39,54	0,967	39,53	0,966	39,52	0,965
16,0	39,81	0,986	39,70	0,978	39,67	0,976	39,63	0,973	39,61	0,972
18,0	39,94	0,995	39,88	0,991	39,80	0,985	39,77	0,983	39,66	0,975
20,0	40,01	1,000	39,95	0,996	39,97	0,997	39,88	0,991	39,81	0,986
25,0			40,0.	1,000	40,01	1,000	39,98	0,998	39,91	0,993
30,0									40,01	1,000
50,0										

```
C
      RETURN
      END
C
C     ***********************************************************************
      SUBROUTINE OVHO7(ETA,X,XI,TAU,KL,MU,RHO,FD,IY,NC,NDEL,UE,T,Q,CF,
     *LAMBDA,NDELT,DELT,PRT,EP,TW,TINF,TINFS,TO)
C     ***********************************************************************
C     SUBROUTINE TO CALCULATE THE INITIAL TURBULENT TEMPERATURE PROFILES
C
      REAL ETA(100),X(60),XI(60),Y(100),YODELT(100)
      REAL TAU,KL,MU(100),RHO(100)
      REAL FD(100),UE,T(100),Q(4,100),TW,TINF,TINFS,TO(100),GS(100)
      REAL CP(100),LAMBDA(100),DELT,PRT,EP(100),PR(100),INTGL3(100)
      REAL PRM(100),STRESS(100),INTGL1(100),INTGL2(100),FUNC(100)
      REAL S(100),RS(100),THETA(100)
C
      S(1)=0.00
      RS(1)=0.00
      INTGL3(1)=0.00
      INTGL2(1)=0.00
      GS(1)=TW/TINFS
      CF=TAU/(0.50*RHO(IY)*UE*UE)
      PR(IY)=MU(IY)*C      )/LAMBDA(IY)
      WRITE(6,193)PR    )
  193 FORMAT(T5,"PR(..)  ",E13.6)
      DO 1 I=1,IY
      PRM(I)=(MU(IY)+EP(I))/(MU(IY)/PR(IY)+EP(I)/PRT)
    1 CONTINUE
      DO 2 J=1,IY
      STRESS(J)=1.00-EXP(1.00-(KL/(SQRT(CF/2.0)))*(1.0-FD(J)))
    2 CONTINUE
      DO 3 I=2,IY
      J=I-1
      FUNC(J)=(1.0-PRM(J))/STRESS(J)
      FUNC(I)=(1.0-PRM(I))/STRESS(I)
      INTGL3(I)=INTGL3(J)+(FUNC(I)+FUNC(J))*(STRESS(I)-STRESS(J))/2.00
    3 CONTINUE
      DO 20 I=1,IY
      INTGL1(I)=EXP(-INTGL3(I))
   20 CONTINUE
      DO 4 J=2,IY
      I=J-1
      S(J)=S(I)+(PRM(J)*INTGL1(J)+PRM(I)*INTGL1(I))*(FD(J)-FD(I))/2.00
      INTGL2(J)=INTGL2(I)+((EXP(INTGL3(J))+(EXP(INTGL3(I))))*
     *(FD(J)-FD(I))/2.
    4 CONTINUE
      DO 5 I=2,IY
      J=I-1
      RS(I)=RS(J)+(PRM(I)*INTGL1(I)*INTGL2(I)+PRM(J)*INTGL1(J)*
     *INTGL2(J))*(FD(I)-FD(J))/2.00
    5 CONTINUE
C
C
C     ENTHALPY PROFILE
      DO 6 I=2,IY
      GS(I)=GS(I)+(GS(I)-1.00)*(S(I)/S(IY))+((UE*UE)/(CP(IY)*TINFS))*
     *((S(I)/S(IY))*RS(IY)-RS(I))
    6 CONTINUE
      DO 7 J=1,IY
      T(J)=GS(J)*TINFS
      TO(J)=T(J)+UE*UE/(2.00*CP(IY))
      G(NC,J)=TO(J)/TINF
```

EXPERIMENT : VIII

T_w = 26,12°C u_∞ = 4,95 m/s

T_∞ = 44,84°C u_w = 0,021 m/s

T_0 = 25,5 °C F = 0,00424

y (mm)	STATION 1		STATION 2		STATION 3		STATION 4		STATION 5	
	T(°C)	$\frac{T-T_w}{T_g-T_w}$	T(°C)	$\frac{T-T_w}{T_g-T_w}$	T(°C)	$\frac{T-T_w}{T_g-T_w}$	T(°C)	$\frac{T-T_w}{T_g-T_w}$	T(°C)	$\frac{T-T_w}{T_g-T_w}$
0,0	26,12	0,000	26,12	0,000	26,12	0,000	26,12	0,000	26,11	0,000
1,0	35,51	0,500	35,43	0,496	35,32	0,490	35,34	0,491	35,26	0,487
2,0	38,90	0,681	38,85	0,678	38,79	0,675	38,75	0,673	38,70	0,670
2,5	39,43	0,709	39,33	0,704	39,26	0,700	39,18	0,696	39,17	0,695
3,0	40,10	0,745	40,01	0,740	40,16	0,748	39,97	0,738	39,90	0,734
3,5	40,69	0,776	40,70	0,777	40,78	0,781	40,67	0,775	40,69	0,776
4,0	40,97	0,791	40,85	0,785	40,84	0,784	40,87	0,786	40,85	0,785
4,5	41,30	0,809	41,49	0,819	41,29	0,808	41,23	0,805	41,34	0,811
5,0	41,51	0,820	41,49	0,819	41,55	0,822	41,44	0,816	41,42	0,815
6,0	42,17	0,855	42,06	0,849	41,98	0,845	41,92	0,842	41,89	0,840
7,0	42,75	0,886	42,62	0,879	42,56	0,876	42,51	0,873	42,47	0,871
8,0	42,83	0,890	42,81	0,889	42,73	0,885	42,68	0,882	42,66	0,881
9,0	43,22	0,911	43,29	0,915	43,20	0,910	43,16	0,908	43,11	0,905
10,0	43,44	0,923	43,46	0,924	43,43	0,922	43,41	0,921	43,33	0,917
12,0	43,67	0,935	43,58	0,930	43,59	0,931	43,56	0,929	43,50	0,926
14,0	44,12	0,959	43,93	0,949	44,06	0,956	43,99	0,952	44,05	0,955
16,0	44,29	0,968	44,23	0,965	44,23	0,965	44,18	0,962	44,16	0,961
18,0	44,51	0,980	44,55	0,982	44,48	0,978	44,48	0,978	44,46	0,977
20,0	44,66	0,988	44,70	0,990	44,70	0,990	44,65	0,987	44,63	0,986
25,0	44,80	0,995	44,83	0,997	44,85	0,998	44,76	,993	44,72	0,991
30,0	44,89	1,000	44,89	1,000	44,89	1,000	44,80	0,995	44,81	0,996
50,0							44,89	1,000	44,89	1,000

EXPERIMENT : VIII

T_w = 26,12°C u_∞ = 4,95 m/s

T_∞ = 44,84°C u_w = 0,021 m/s

T_0 = 25,5 °C F = 0,00424

y (mm)	STATION 1		STATION 2		STATION 3		STATION 4		STATION 5	
	T(°C)	$\frac{T-T_w}{T_g-T_w}$	T(°C)	$\frac{T-T_w}{T_g-T_w}$	T(°C)	$\frac{T-T_w}{T_g-T_w}$	T(°C)	$\frac{T-T_w}{T_g-T_w}$	T(°C)	$\frac{T-T_w}{T_g-T_w}$
0,0	26,12	0,000	26,12	0,000	26,12	0,000	26,12	0,000	26,11	0,000
1,0	35,51	0,500	35,43	0,496	35,32	0,490	35,34	0,491	35,26	0,487
2,0	38,90	0,681	38,85	0,678	38,79	0,675	38,75	0,673	38,70	0,670
2,5	39,43	0,709	39,33	0,704	39,26	0,700	39,18	0,696	39,17	0,695
3,0	40,10	0,745	40,01	0,740	40,16	0,748	39,97	0,738	39,90	0,734
3,5	40,69	0,776	40,70	0,777	40,78	0,781	40,67	0,775	40,69	0,776
4,0	40,97	0,791	40,85	0,785	40,84	0,784	40,87	0,786	40,85	0,785
4,5	41,30	0,809	41,49	0,819	41,29	0,808	41,23	0,805	41,34	0,811
5,0	41,51	0,820	41,49	0,819	41,55	0,822	41,44	0,816	41,42	0,815
6,0	42,17	0,855	42,06	0,849	41,98	0,845	41,92	0,842	41,89	0,840
7,0	42,75	0,886	42,62	0,879	42,56	0,876	42,51	0,873	42,47	0,871
8,0	42,83	0,890	42,81	0,889	42,73	0,885	42,68	0,882	42,66	0,881
9,0	43,22	0,911	43,29	0,915	43,20	0,910	43,16	0,908	43,11	0,905
10,0	43,44	0,923	43,46	0,924	43,43	0,922	43,41	0,921	43,33	0,917
12,0	43,67	0,935	43,58	0,930	43,59	0,931	43,56	0,929	43,50	0,926
14,0	44,12	0,959	43,93	0,949	44,06	0,956	43,99	0,952	44,05	0,955
16,0	44,29	0,968	44,23	0,965	44,23	0,965	44,18	0,962	44,16	0,961
18,0	44,51	0,980	44,55	0,982	44,48	0,978	44,48	0,978	44,46	0,977
20,0	44,66	0,988	44,70	0,990	44,70	0,990	44,65	0,987	44,63	0,986
25,0	44,80	0,995	44,83	0,997	44,85	0,998	44,76	0,993	44,72	0,991
30,0	44,89	1,000	44,89	1,000	44,89	1,000	44,80	0,995	44,81	0,996
50,0							44,89	1,000	44,89	1,000

EXPERIMENT : IX

T_w = 25,95°C u_∞ = 5,01 m/s

T_∞ = 44,95°C v_w = 0,045 m/s

T_0 = 25,5 °C F = 0,00898

y (mm)	STATION 1		STATION 2		STATION 3		STATION 4		STATION 5	
	T(°C)	$\frac{T-T_w}{T_g-T_w}$	T(°C)	$\frac{T-T_w}{T_g-T_w}$	T(°C)	$\frac{T-T_w}{T_g-T_w}$	T(°C)	$\frac{T-T_w}{T_g-T_w}$	T(°C)	$\frac{T-T_w}{T_g-T_w}$
0,0	25,96	0,000	25,95	0,000	25,95	0,000	25,95	0,000	25,95	0,000
1,0	35,36	0,495	35,34	0,494	35,26	0,490	35,11	0,482	35,05	0,479
2,0	37,92	0,630	38,00	0,634	38,03	0,636	38,13	0,641	38,09	0,639
2,5	38,59	0,665	38,57	0,664	38,53	0,662	38,49	0,660	38,66	0,669
3,0	39,31	0,703	39,25	0,700	39,27	0,701	39,16	0,695	39,46	0,711
3,5	39,73	0,725	39,69	0,723	39,71	0,724	39,61	0,719	39,71	0,724
4,0	39,97	0,738	39,93	0,736	39,92	0,735	39,86	0,732	39,92	0,735
4,5	40,33	0,757	40,30	0,755	40,18	0,749	40,11	0,745	40,03	0,741
5,0	40,73	0,778	40,71	0,777	40,77	0,780	40,69	0,776	40,56	0,769
6,0	41,15	0,800	41,11	0,798	41,17	0,801	41,06	0,795	41,00	0,792
7,0	41,76	0,832	41,74	0,831	41,70	0,829	41,72	0,830	41,66	0,827
8,0	42,18	0,854	42,20	0,855	42,12	0,851	42,12	0,851	42,04	0,847
9,0	42,52	0,872	42,50	0,871	42,48	0,870	42,44	0,868	42,39	0,865
10,0	42,96	0,895	43,03	0,899	43,03	0,899	42,90	0,892	42,86	0,890
12,0	43,26	0,911	43,22	0,909	43,28	0,912	43,20	0,908	43,15	0,905
14,0	43,89	0,944	43,79	0,939	43,79	0,939	43,83	0,941	43,81	0,940
16,0	44,32	0,967	44,29	0,965	44,30	0,966	44,23	0,962	44,17	0,959
18,0	44,53	0,978	44,48	0,975	44,46	0,974	44,44	0,973	44,40	0,971
20,0	44,67	0,985	44,68	0,986	44,65	0,984	44,57	0,980	44,53	0,978
25,0	44,91	0,998	44,86	0,995	44,84	0,994	44,80	0,992	44,76	0,990
30,0			44,95	1,000	44,95	1,000	44,91	0,998	44,93	0,999
50,0									44,95	1,000

APPENDIX E

E1 COMPARISON OF MICKLEY ET AL (17) RESULTS

Unsuccessful comparison of data as presented for run H-19b

TEMPERATURE PROFILES MICK 2

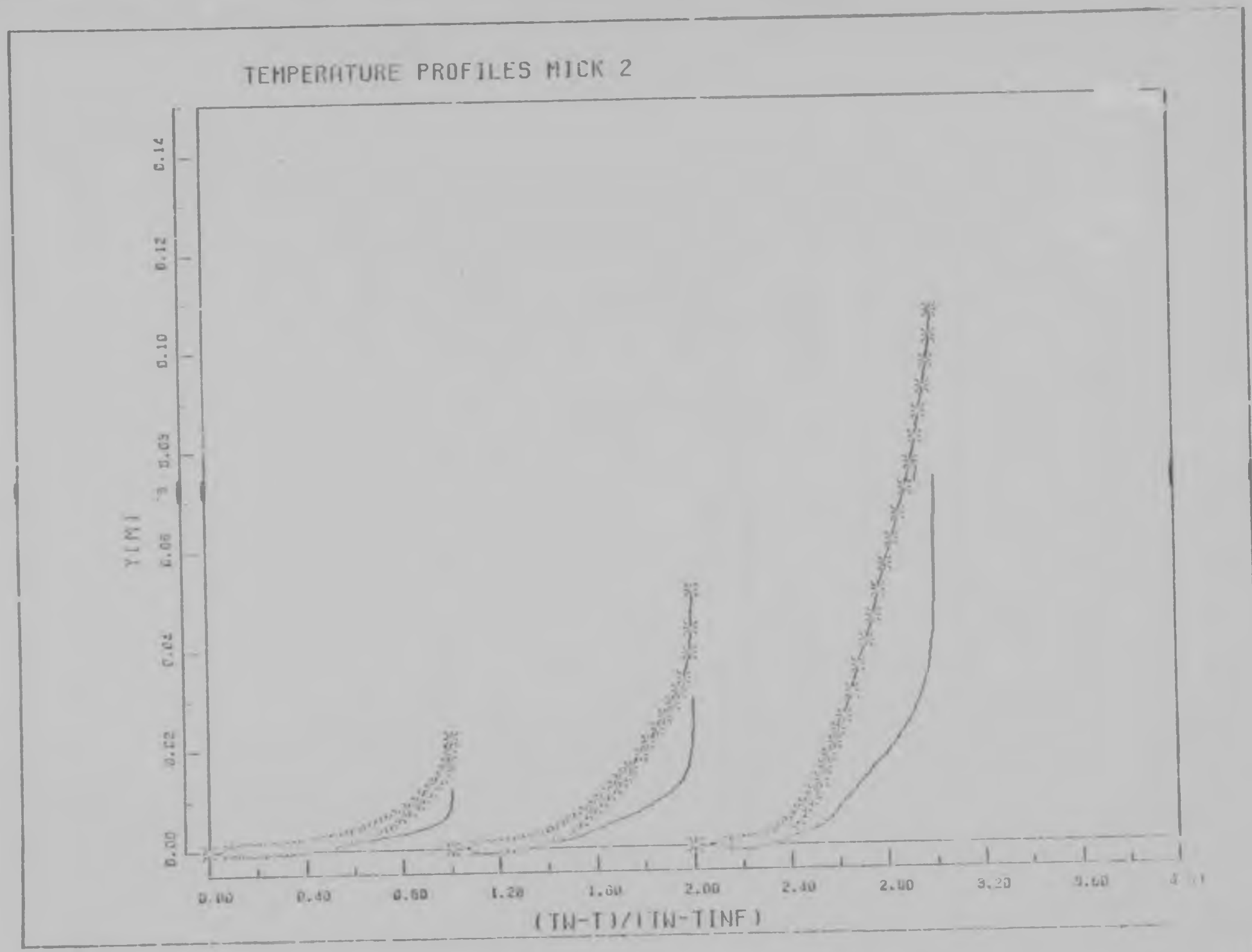

APPENDIX F

F1 INITIAL PROFILES

Presentation of initial two profiles to start the solution of the energy equation. Equation 5.5.9 is used to generate these profiles.

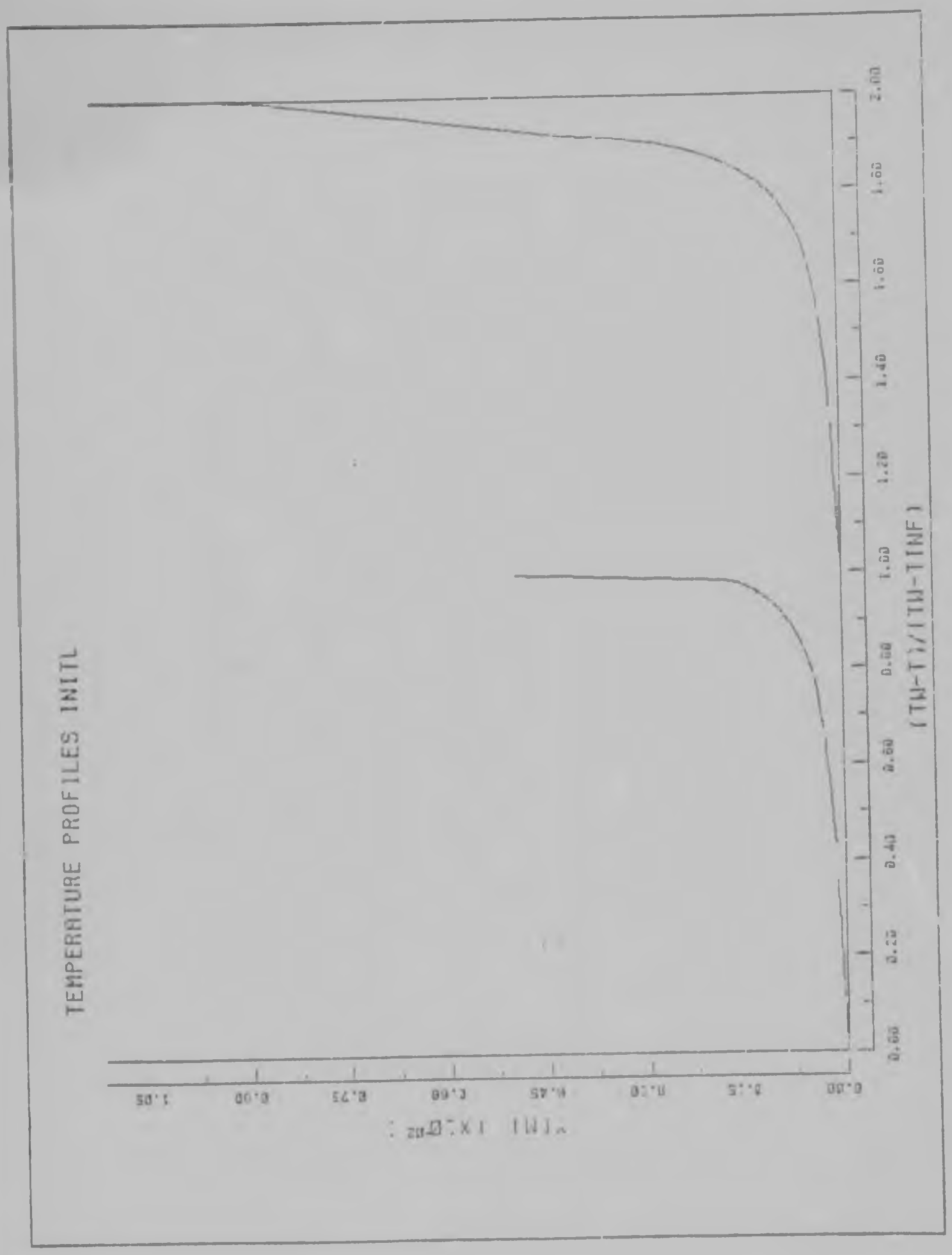
TEMPERATURE PROFILES INITL
(TW-T)/(TW-TINF)
0.00
0.20
0.40
0.60
0.80
1.00
1.20
1.40
1.60
1.80
2.00
0.00
0.15
0.30
0.45
0.60
0.75
0.90
1.05

APPENDIX G

G1 COMPUTER PROGRAM

Inputs to the grogram:

XTR - value of x at which blowing begins
IY - number of η grid points
NX - number of computing stations
DX - step length in ξ direction
X(1) - initial station, in m
H - first η step
K - ratio of adjacent steps
UINF - free stream flow velocity, m/s
TW - wall temperature, °C
TINF - free stream flow temperature, °C
DUDX - pressure gradient, in s^{-1}
PSTAT - static pressure, in Pa
VW1 - injection velocity, m/s
KL - universal mixing length constant

```
      PROGRAM DUEXI(MAINOU=401B,MAINFL=401B,TAPE6=MAINOU,TAPE7=MAINFL,
     *STCFUS=401B,TAPE8=STCFUS)
C     PROGRAM TO SOLVE THE MOMENTUM AND ENERGY EQUATIONS FOR
C     COMPRESSIBLE LAMINAR OR TURBULENT BOUNDARY LAYER FLOW
C     WITH SUCTION OR INJECTION AT THE WALL AND PRESSURE GRADIENT
C
C     AN EDDY VISCOSITY FORMULATION IS USED FOR THE REYNOLDS STRESS
C     A CORRELATION EQUATION IS USED FOR THE TURBULENT PRANDTL NO.
C
C     CALCULATION OF EXPERIMENTAL HOBSON DATA RUN 2
C
      REAL IL,FX,FX1,PTAMP,EP1,PWR,M12
      REAL A(98,5),B(98,1)
      REAL Y(100),ETA(100),YODEL(100),YOTTA(100)
      REAL F(4,100),FD(4,100),FDD(4,100),UV(100),FDC(100)
      REAL EF(100),G(98,1),R(98,3),CDV(100),ST,QW,QHD
      REAL X(60),XI(60)
      REAL I,H,DX,FXI,MU(100),RHO(100)
      REAL PR(100),CP(100),LAMBDA(100),T(100),THETAR(100),PRT(100)
      REAL G(4,100),YODELT(100),PRT,TO(100),THETA(100)
      REAL TW,TINF,TINFS,DELT
      REAL DSTR(4),NU
      REAL DEL,EDEL,CF,USTR,UE,UEQ,UINF,TAU,PP,AP
      REAL BETA,DUDX,TTA,RX,RDEL,RTTA,PSTAT
      REAL T,VW,VWO,VW1,VWP,FDD
      REAL DIFS1,DIFS2
      REAL A1,B1,C1,D1,E1,F1,G1,H1,I1,J1,I1,J2,K2
      REAL XX(102),YY(102)
      DIMENSION NINCH(2),TITLE(2),TITLEX(2)
      REAL X1,X2,X3,X4,X5,X6,XITR,XTR
      TAUF(RHO,MU,X,DUDX,UEQ,NC,IY)=0.02975*RHO(IY)*(X(NC)*DU  UEQ)**2.0
     */((RHO(IY)*(X(NC)*DUDX+UEQ)*X(NC)/MU(IY))**0.20)
C     DATA
      XTR=0.25000
      IY=100
      NX=11
      WRITE(7,800)NX
      WRITE(8,800)NX
  800 FORMAT(3X,I4)
      DX=0.0750
      H=0.0100
      X(1)=0.147
      X(2)=0.297
      X(3)=0.347
      X(4)=0.  7
      X(5)=0.547
      X(6)=0.697
      X(7)=0.847
      X(8)=0.897
      X(9)=0.947
      X(10)=0.997
      X(11)=1.047
      I=1.030
      UINF=14.95
      TW=95.00
      TINF=33.00
      DUDX=0.00
      PSTAT=14  .4
      VWI=0.024000
      IL=0.4
      NC=1.00
C
```

```
      VWU=VW1/UINF
      UEQ=UINF*0.99

      WRITE(6,999)
  999 FORMAT(T6,"SOLUTION OR BOUNDARY LAYER EQUATIO  FOR FLOW OVER A
     * SURFACE WITH SUCTION OR INJECTION AT THE WALL",/T6,100("-")//)
      WRITE(6,1000)UINF,DUDX,VWU
 1000 FORMAT(//T10,"UINF=",D13.6,"  M/S"//T10,"DUDX=",D13.6,"  1/S"
     *,//T10,"VW/UINF=",D13.6)

C      CALCULATION OF  INITIAL FREE STREAM FLUID PROPERTIES
      TW=TW+273.16
      TINF=TINF+273.16
      CP(IY)=(2.4E-7*(TINF-300.0)**2.0+5.0E-5*(TINF-300.0)+1.0049)*
     *1.0E3
      TINFS=TINF-UEQ*UEQ/(2.00*CP(IY))
      LAMBDA(IY)=(-3.2E-04*(TINFS-300.0)**2.0+3.8E-3*(TINFS-300.0)+
     *2.562)*1.0E-2
      RHO(IY)=(PSTAT+8513.6)*9.809/(287.1*TINFS)
      RHO(1)=(PSTAT+8513.6)*9.809/(287.1*TW)

C     CALCULATE MU


      MU(IY)=(1.846*((TINFS/300.0)**1.50)*(410.00/(TINFS+110.0)))*1.0E-5
C     CALCULATE TAU

      TAU=TAUF(RHO,MU,X,DUDX,UEQ,NC,IY)

      WRITE(6,911)TAU,RHO(IY),MU(IY),CP(IY),LAMBDA(IY)
  911 FORMAT(/T5,"TAU=",D13.5,5X,"RHO=",D13.5,6X,"MU=",D13.5,5X,
     *"CP=",D13.6,5X,"LAMBDA=",D13.5)

C     DEFINE PARAMETERS

      N=IY-4.00
C
C
      GO TO 21
      DO 1 I=2,NX
      X(I)=X(I-1)+DX
    1 CONTINUE
   21 CONTINUE
      DO 2 J=1,NX
      XI(J)=MU(IY)*RHO(IY)*X(J)*(X(J)*DUDX/2.00+UEQ)
    2 CONTINUE
      XITR=MU(IY)*RHO(IY)*XTR*(XTR*DUDX/2.0+UEQ)
C     GENERATE ETA POINTS
      CALL GVHO1(H,J,IY,ETA)

C
C     CALCULATE CONSTANTS FOR MATRIX A
      CALL GVHO2(H,J,A1,B1,C1,D1,E1,F1,X1,X2,X3,X4,X5,X6)
C
      NC=1
   85 CALL GVHO3(X,DUDX,UEQ,UE,BETA,NC,PP,AF,TAU,RHO,MU,VW1,USTR,VWP,VW,
     *IY)
      IF(X(NC).LT.0.00)GO TO 3000
      IF(X(NC).LT.0.797)TW=300.16
      IF(X(NC).GE.0.797)TW=296.16
      IF(NC.LT.1)GO TO 1
      GO TO 1*
   10 FDD=TAU*(2.00*XI(NC))**0.50/(RHO(IY)*UE*UE*MU(IY))
   19 CONTINUE
```

```
C
      CALL GVH04(ETA,TAU,FL,MU,RHO,P,PD,IY,DUDX,VW,NC,FDD,NDEL,UE,PP,
     *AP,XI,USTR,DSTR,EDEL,DEL,FD)
C
      CALL GVH05(FD,FDD,K,H,IY,NC,ETA)
      NITER=0.
      NCA=NC
      NCA1=NC
      NCA2=NC
      IF(NC.EQ.2)GO TO 9
      DO 15 I=1,IY
      MU(I)=MU(IY)
      RHO(I)=RHO(IY)
   15 CONTINUE
      GO TO 20
    9 CONTINUE
      DO 16 I=1,IY
      MU(I)=(1.346*((T(I)/300.0)**1.5)*(410.0/(T(I)+110.0)))*1.0E-5
      RHO(I)=(FSTAT*[illegible]13.6)*9.809/(287.1*T(I))
   16 CONTINUE
   20 CONTINUE
      CALL GVH06(XI,ETA,FDD,RHO,MU,AP,DEL,EP,NC,NCA,DSTR,KL,NCA1,NCA2,
     *UE,NITER,IY,X,TAU,FRT)
C     CALCULATION OF INITIAL TURBULENT TEMPERATURE PROFILE
      CALL GVH07(ETA,X,XI,TAU,FL,MU,RHO,FD,IY,NC,NDEL,UE,T,G,CP,

     *LAMBDA,NDELT,DELT,FRT,EP,TW,TINF,TINFS,TO)
            EQ.2)GO TO 82
            I
            IF(RHO,MU,X,DUDX,UEQ,NC,IY)
            *SQRT(2.0*XI(NC))/(RHO(IY)*UE*UE*MU(IY))
            *
 3000
            [illegible]ETA,X,XI,NC,IY,MU,RHO,P,PD,PDD,DUDX,DEL,UE,UINF,K
     *    [illegible]TR,NC[illegible])
      CALL GVH0[illegible](ETA,X,XI,NC,IY,MU,RHO,DEL,TW,TINF,UE,DELT,T,G,
     *NDELT,CP,LAMBDA,TINFS,TO)
      DO 14 I=1,IY
      RHO(I)=( STAT*8513.6)*9.809/(287.1*T(I))
   14 CONTINUE
      IF(NC.EQ.2)GO TO 82
      NC=NC+1
      TAU=TAUF(RHO,MU,X,DUDX,UEQ,NC,IY)
      GO TO 35
   82 CONTINUE
C
C     SET UP DO LOOP IN X DIRECTION
C
      IE=IY-4
      GR=0
      NXI=NX+1
   95 NITER=0
      IF(X(NC).LT.0.797)TW=300.16
      IF(X(NC).GE.0.797)TW=[illegible].16
      NC=NC+1
      IF(NC.EQ.NXI)STOP
      NCA=NC-[illegible]*GR
      NDIF=[illegible]-NCA
      IF(NDIF)3,4,5
    3 NCA1=2
      NCA2=1
      GO TO 6
    4 NCA1=1
```

```
      NCA2=3
      GO TO 6
    5 NCA1=3
      NCA2=2
    6 CONTINUE
      IF(NCA.NE.3)GO TO 17
      GR=GR+1
   17 CONTINUE
C     CALCULATE UE,BETA,B+ AND A+
C
C     CALCULATE TAU FOR NEW STATION
C
      FXI=2.0*XI(NC)
      FX=SQRT(FXI)
      NAT=NCA
      IF(NITER.EQ.0)NAT=NCA1
      TAU=MU(IY)*RHO(IY)*UE*UE*FDD(NAT,1)/FX
C
      CALL GVHO5(X,DUDX,UEQ,UE,BETA,NC,PF,AP,TAU,RHO,MU,VW1,UETR,VWF,VW,
     *IY)
C
C     CALCULATE BOUNDARY CONDITIONS
C
      P(4,1)=-(VW/UE*MU(IY))*(XI(NC)-XITR)/FX
      KP1=K+1.0
      PTAMP=P(4,1)*K*(KP1+1.0)+P(NCA1,3)*K*NCA1
      P(4,2)=PTAMP/(KP1*KP1)
      WRITE(6,9991)P(4,1),P(4,2)
 9991 FORMAT(//T6," P(4,1)=",D13.6,6X," P(4,2)=",D13.6,//)
C     CALCULATE VISCOSITY DENSITY PARAMETERS
      DO 10 I=1,IY
      CDV(I)=((T(I)/T(IY))**0.5)*((T(IY)+110.0)/(T(I)+110.0))
      RHO(I)=(PSTAT+8513.6)*9.809/(287.1*T(I))
      MU(I)=(1.846*((T(I)/300.0)**1.5)*(410.0/(T(I)+110.0)))*1.0E-5
      CP(I)=(2.4E-7*(TO(I)-300.0)**2.0+5.0E-5*(TO(I)-300.0)+[illegible]0049)*
     *1.0E3
      LAMBDA(I)=(-3.2E-5*(T(I)-300.0)**2.0+3.8E-3*(T(I)[illegible])+[illegible])
     **1.0E-2
      PR(I)=MU(I)*CP(I)/LAMBDA(I)
   10 CONTINUE
      GO TO 55
      WRITE(6,13)
   13 FORMAT(/T6,"CDV",T24,"RHO",T40,"MU",T55,"CP",T70,"LAMBDA",
     *T85,"PR",/)
      DO 11 I=1,IY
      WRITE(6,12)CDV(I),RHO(I),MU(I),CP(I),LAMBDA(I),PR(I)
   11 CONTINUE
   12 FORMAT(6(3X,D13.6))
   55 CONTINUE
C     CALCULATE EBS1
   90 CALL GVHO6(XI,ETA,FDD,RHO,MU,AP,DEL,EP,NC,NCA,DSTR,EL,NCA1,NCA2,
     *UE,NITER,IY,X,TAU,PRT)
      IF(NITER.GT.10)GO TO 8
      G(4,1)=(CP(1)*TW)/(CP(IY)*TINF)
      WRITE(6,9992)G(4,1)
 9992 FORMAT(/T6,"G(4,1)=",D13.6,)
C
C      CALCULATE EBS1 DASH
C
C      GENERATE A
      CALL GVHO8(A,A1,B1,C1,D1,E1,F1,X1,X2,X3,X4,X5,X6,XI,NC,K,IY,P,
     *FD,FDD,NCA,NCA1,NITER,BETA,ETA,EP,CDV)
C     GENERATE B
```

```
      CALL GVH07(X1,F,FD,FDD,NCA,NCA1,NCA2,NC,IY,NITER,B,RHO,BETA)
C
C     MODIFY A AND B
      B(1,1)=B(1,1)-A(1,1)*F(4,1)-A(1,2)*F(4,2)
      B(2,1)=B(2,1)-A(2,1)*F(4,2)
      A(IE-1,4)=A(IE-1,4)+A(IE-1,5)
      A(IE,3)=A(IE,3)+A(IE,4)+A(IE,5)
      A(1,1)=0.00
      A(2,1)=0.00
      A(1,2)=0.00
      A(IE,4)=0.00
      A(IE-1,5)=0.00
      A(IE,5)=0.00
      CALL AAZM(A,B,N)
C     CONVERT B TO PHI(F)
      CALL GVH10(B,F,IY)
      CALL GVH11(F,FD,1,H,IY)
      CALL GVH12(F,ETA,FD,FDD,1,H,IY)
C
C     ESTABLISH EDGE OF BOUNDARY LAYER
      CALL GVH13(FD,NDEL,ETA,EDEL,IY)
C     CALCULATE DEL STAR
      CALL GVH14(FD,X1,RHO,UE,NDEL,1,H,DSTR,NC,ETA,IY)
C
C     TEST FOR CONVERGENCE
      NT1=NCA
      IF(NITER.EQ.0)NT1=NCA1
C
C
      WRITE(6,5555)FDD(4,1),FDD(NT1,1)
 5555 FORMAT(15,"FDD(4,1)=",D13.6,"  AND FDD(NT1,1)=",D13.6)
   51 DIFS1=FDD(4,1)-FDD(NT1,1)
      DIFS2=DSTR(4)-DSTR(NT1)
      DIFS1=ABS(DIFS1)
    7 DIFS2=ABS(DIFS2)
      CALL GVH15(F,FD,FDD,DSTR,NCA,IY)
      WRITE(6,7777)DIFS1,DIFS2,NITER
 7777 FORMAT(/15,"DIFS1=",D13.6,'    AND DIFS2=",D13.6,5X,I4,"TH ITER
     *ATION",)
      IF(DIFS1.LT.0.05 .AND.DIFS2.LT.0.01)GO TO 8
      NITER=NITER+1
      GO TO 90
    8 CONTINUE
C
C     THE SOLUTION HAS NOW CONVERGED

C     CALCULATE THETA
      CALL GVH16(FD,X1,RHO,UE,NDEL,1,H,DSTR,TTA,NC,ETA,NCA,IY)
C     SUBROUTINE TO CALCULATE THE VARIABLES REQUIRED FOR PRINTIN
      CALL GVH17(F,FD,FDD,IY,NCA,NDEL,CF,UV,FD,USTR,UE,TAU,RX,RTTA,

     *NDEL,Y,YOTTA,YODEL,RHO,MU,X1,ETA,X,NC,EDEL,DEL,TTA)
C     GENERATE R AND G
      CALL GVH18(R,A1,B1,C1,D1,E1,F1,X1,NC,1,IY,F,FD,NCA,NCA1,
     *EP,FR,FRT,CDV,NCA2,ETA)
      CALL GVH19(X1,FD,FDD,NCA,NCA1,NCA2,NC,IY,0,G,A1,B1,C1,
     *CDV,UE,1,NF,1,R,1,1)
C     MODIFY R AND G
      G(1,1)=G(1,1)-G(4,1)*R(1,1)
      IF=IY-2
      NM=IY-2
      R(1,1)=0.00
      G(IF,1)=G(IF,1)-R(IF,3)
```

```
      R(IF,3)=0.00
      CALL RRGO(R,Q,NM)
      CALL GVH20(Q,G,IY,NCA)
      CALL GVH21(TO,G,IY,T,UV,CP,TINF,THETA,TW)
      CALL GVH22(THETA,NDELT,ETA,EDELT,IY)
      CALL GVH23(G,MU,UV,TO,RHO,CDV,PR,XI,QW,ST,A1,B1,C1,GWD,K,IY,
     *NC,CP)
      H12=DSTR(NCA)/TTA
      NNW=NDEL
      WRITE(6,1001)N
 1001 FORMAT(/////T10,"STATION",I4,/T10,11("="),/)
      WRITE(6,1010)X(NC)
 1010 FORMAT(//T10,"X=",D13.6)
      WRITE(6,1011)XI(NC)
 1011 FORMAT(/T10,"XI=",D13.6)
      WRITE(6,1012)NITER
 1012 FORMAT(/T10,"NO OF ITERATIONS",I4,//)
      WRITE(6,1002)DEL,EDEL,DSTR(NCA),TTA
 1002 FORMAT(//T5,"DEL=",D13.6,5X,"ETADEL=",D13.6,5X,"DELSTR=",
     *D13.6,5X,"THETA=",D13.6,"    (M)")
      WRITE(6,1003)TAU,USTR,CF,PF,AP
 1003 FORMAT(/T5,"TAU=",D13.6,5X,"USTAR=",D13.6,5X,"CF=",D13.6,
     *9X,"PPLUS=",D13.6,9X,"APLUS=",D13.6)
      WRITE(6,1004)RX,RDEL,RTTA,H12
 1004 FORMAT(/T5,"REX=",D13.6,5X,"REDEL=",D13.6,5X,"RETHETA=",
     *D13.6,5X,"H12=",D13.6)
      WRITE(6,1005)UE
 1005 FORMAT(/T5,"UE=",D13.6,"    M/S")
 1006 FORMAT(//T6,"Y(M)",T24,"P",T40,"PD",T55,"PDD",T69,"U/UE",
     *T34,"Y/TTA",T98,"EP",/)
 1007 FORMAT(7(3X,D13.6))
C
C
      WRITE(6,1006)
      DO 1250 I=1,10
      WRITE(6,1007)Y(I),P(NCA,I),PD(NCA,I),PDD(NCA,I),FD(I),YOTTA(I)
     *,EP(I)
 1250 CONTINUE
      DO 1251 I=11,NNW,5
      WRITE(6,1007)Y(I),P(NCA,I),PD(NCA,I),PDD(NCA,I),
     *FD(I),YOTTA(I),EP(I)
 1251 CONTINUE
      GO TO 4004
      DO 1243 I=1,10
      WRITE(6,10400)YOTTA(I),FD(I)
 1243 CONTINUE
      DO 1252 I=11,49,2
      WRITE(6,10400)YOTTA(I),FD(I)
 1252 CONTINUE
      DO 1253 I=50,NNW,5
      WRITE(6,10400)YOTTA(I),FD(I)
 1253 CONTINUE
 4004 CONTINUE
10400 FORMAT(F8.4,F7.4)
      WRITE(6,4000)
 4000 FORMAT(//T6,"Y(M)",T24,"G",T40,"TEMP",T55,"TEMPO",T70,"THETA",/)
      DO 4001 I=1,10
      WRITE(6,4002)Y(I),G(NCA,I),T(I),TO(I)   ,THETA(I)
 4001 CONTINUE
      DO 4003 I=11,NDELT,5
      WRITE(6,4002)Y(I),G(NCA,I),T(I),TO(I),THETA(I)
 4003 CONTINUE
 4002 FORMAT(5(3X,D13.6))
```

```
      IF(THETA(I).LT.0.00)THETA(I)=0.00
      WRITE(7,801)NC,NDELT
  801 FORMAT(2(3X,I4))
      DO 802 I=1,NDELT
      WRITE(7,803)Y(I),THETA(I)
  802 CONTINUE
  803 FORMAT(2(3X,E13.6))
      RNU=MU(IY)/RHO(IY)
      WRITE(8,850)ST,CF,USTR,NU
  850 FORMAT(4(3X,E1 .6))
C
C     STEP TO NEXT X STATION
 2003 CONTINUE
      GO TO 99
 2000 WRITE(6,2001)
 2001 FORMAT(//T5,"PROGRAM STOPPED BECAUSE IER=129",/)
      STOP
      END
C
C     ------------------------------------------------------------------
      SUBROUTINE GVHOIL(ETA,X,XI,NC,IY,MU,RHO,P,FD,FDD,DUDX,DEL,UE,UINF,
     *H,DSTR,NDEL)
C     ------------------------------------------------------------------
C     PROGRAM TO CALCULATE INITIAL PROFILES FOR LAMINAR FLOW.
C     DEL IS DETERMINED FROM A EQUATION AND FROM THE PROFILE
C     AN ITERATIVE PROCESS IS USED
C
C
      REAL ETD(100),F(100),FDD(100),YODEL(100)
      REAL ETA(100),F(4,100),FD(4,100),FDD(4,100),FD(100),Y(100)
      REAL MU(100),RHO(100),DUDX(1),H
      REAL X(2),XI(2),EP1,ET1,ET2
      REAL DEL,UF,DEL2,DEL1,EDEL,TE,FF
      REAL FXI,HF,DF,CF,NF,UINF,EF,LAM,FA,GA,E2
      REAL E3,DIFS2,DIFS1,A1,A2,A3,AFXI
      REAL DSTR(4)
C
   11 AF=2.0*XI(NC)
      NITER=0
      FXI=SQRT(AF)
C     |
      DEL2=2.0*MU(IY)*X(NC)/(RHO(IY)*UINF)
      DEL=SQRT(DEL2)
    6 LAM=DEL2*DUDX*RHO(IY)/MU(IY)
      DF=FXI/(RHO(IY)*UE*DEL)
      DO 1 J=1,IY
      ETD(J)=ETA(J)*DF
    1 CONTINUE
      NITER=NITER+1
      WRITE(6,103)NITER,NC,DEL
  103 FORMAT(/T5,"NITER=",I4,3X,"NC=",I4,5X,"DEL=",D13.6,/)
C
      DO 2 I=1,IY
      E2=ETD(I)*ETD(I)
      E3=E2*ETD(I)
      FA=FTD(I)*(2.0-2.0*E2+E3)
      GA=FTD(I)*(1.0-4.0*ETD(I)+3.0*E2-E3)
      FD(I)=FA+LAM*GA/6.0
    2 CONTINUE
C
C     DETERMINE EDGE OF BOUNDARY LAYER
      NDEL=0
    4 NDEL=NDEL+1
```

```
      DIFS1=1.0-FD(NDEL)
      DIFS1=ABS(DIFS1)
      IF(DIFS1.LT.0.0001)GO TO 3
      IF(NDEL.EQ.IY)GO TO 3
      GO TO 4
    3 EDEL=ETA(NDEL)
      DEL1=FXI*EDEL/(RHO(IY)*UE)
      DIFS2=DEL-DEL1
      DIFS2=ABS(DIFS2)
      DEL=DEL1
      DEL2=DEL*DEL
      IF(DIFS2.LT.0.001)GO TO 5

      IF(NITER.GT.6)GO TO 5
      GO TO 6
C
    5 CONTINUE
      DO 16 J=NDEL,IY
      FD(J)=1.0
   16 CONTINUE
      AFXI=FXI/(RHO(IY)*UE*DEL)
      DO 15 I=1,IY
      YDEL(I)=AFXI*ETA(I)
   15 CONTINUE
      F(1)=0.00
      DO 7 I=2,IY
      J=I-1
      F(I)=(FD(I)+FD(J))*(ETA(I)-ETA(J))/2.0+F(J)
    7 CONTINUE
      A1=-1.*3.0/(H*(1.0+K))
      A2=(K-1.0)*K/H
      A3=K/(H*(1.0+K))
      IYM1=IY-1
      DO 8 I=2,IYM1
      FDD(I)=(A1*FD(I-1)+A2*FD(I)+A3*FD(I+1))/FK**I
    8 CONTINUE
      KF1=K+1.0
      FT1=-FD(1)*K**(K+2.0)
      FT2=FD(2)*KF1*KF1-FD(3)
      FDD(1)=(FT1+FT2)/(H*K*P1)
      IYM2=IY-2
      KF=K**IYM2
      FDD(IY)=(FD(IY)-FD(IYM1))/(KF*H)
      DO 9 I=1,IY
      F(NC,I)=F(I)-ETA(I)
      FD(NC,I)=FD(I)-1.0
      FDD(NC,I)=FDD(I)
    9 CONTINUE
      VU=0.00

      I=NC
      TE=0.00
      DO 13 J=2,NDEL
      JJ=J-1
      IF(NC.EQ.1)GO TO 10
      TE=TE+((RHO(IY)*FD(I,JJ)/RHO(JJ)+(RHO(IY)*FD(I,JJ)/RHO(J,I)))*
     *(ETA(J)-ETA(JJ))/2.0
   10 TE=TE+(FD(I,JJ)+FD(I,J))*(ETA(J)-ETA(JJ))/2.00
   13 CONTINUE
      DELK(I)=FXI*TE/(RHO(IY)*UE)
      GO TO 509
      WRITE(6,510)
  510 FORMAT(//16,"Y(M)",T24,"F",T40,"FD",T55,"FDD",T69,"U/UE",/)
```

```
      DO 509 I=1,NDEL
      Y(I)=FXI*ETA(I)/(RHO(IY)*UE)
      WRITE(6,511)Y(I),P(NC,I),FD(NC,I),FDD(NC,I),FD(I)
  509 CONTINUE
  511 FORMAT(5(3X,D13.6))
  508 CONTINUE
      RETURN
      END
C      ***********************************************************************
      SUBROUTINE GVHO(ETA,X,[illegible],NC,IY,MU,RHO,DEL,TW,TINF,UE,DELT,T,G,
     *NDEL,CP,LAMBDA,TINF)
C      ***********************************************************************
C      SUBROUTINE TO CALCULATE THE INITIAL TEMPERATURE PROFILES FOR
C      LAMINAR FLOW
C      DELT IS CALCULATED FROM THE EQUATION DELT/DEL=(PR)**-0.33
C      THEN AN ITERATIVE PROCESS IS USED
C
      REAL RHO(100),MU(100),PR(100),CP(100),LAMBDA(100)
      REAL X(60),XI(60),DEL,TW,TINF,UE,ETA(100)
      REAL E1,E3,E4,THETAR(100),ETDT(100)
      REAL FXI,AF,DELT,DIFS1,AFXI,DIFS2,DELT1
      REAL T(100),G(4,100),EDELT,YODELT(100),Y(100),TO(100),TINFS
C
      NITER=0
      PR(IY)=MU(IY)*CP(IY)/LAMBDA(IY)
      DELT=DEL/(PR(IY)**0.33)
      AF=2.0*XI(NC)
      FXI=SQRT(AF)
    6 DF=FXI/(RHO(IY)*UE*DELT)
      NITER=NITER+1
      WRITE(6,300)NITER,DELT,PR(IY)
  300 FORMAT(/T5 "NITER=",I4,6X,"DELT=",D13.6,5X,"PR=",D13.6,/)
      DO 1 J=1,IY
      ETDT(J)=ETA(J)*DF
    1 CONTINUE
      DO 2 I=1,IY
      E1=ETDT(I)
      E3=ETDT(I)*ETDT(I)*E1
      E4=ETDT(I)*E3
      THETAR(I)=1.00-2.00*E1+2.[illegible]*E3-E4
    2 CONTINUE
      DO 3 J=1,IY
      T(J)=THETAR(J)*(TW-TINFS)+TINFS
      TO(J)=T(J)+UE*UE/(2.00*CP(IY))
      G(NC,J)=TO(J)/TINF
    3 CONTINUE
      T(IY)=TINFS
      TO(IY)=TINF
      T(1)=TW
      TO(1)=TW
C     DETERMINE EDGE OF BOUNDARY LAYER
      NDELT=0
    4 NDELT=NDELT+1
      DIFS1=1.0-G(NC,NDELT)
      DIFS1=ABS(DIFS1)
      IF(DIFS1.LT.0.001)GO TO 10
      IF(NDELT.EQ.IY)GO TO 10
      GO TO 4
   10 EDELT=ETA(NDELT)
      DELT1=FXI*EDELT/(RHO(IY)*UE)
      DIFS2=DELT-DELT1
      DIFS2=ABS(DIFS2)
      IF(DIFS2.LT.0.001)GO TO 5
```

```
      IF(NITER.GT.5)GO TO 5
      GO TO 6
    5 CONTINUE
C
      DO 9 I=1,NDELT,IY
      G(NC,I)=1.00
      T(I)=TINF
      TO(I)=TINF
    9 CONTINUE
      AFXI=1.0/(RHO(IY)*UE*DELT)
      DO 11 I=1,IY
      YDELT(I)=AFXI*ETA(I)
   11 CONTINUE
      WRITE(7,805)NC,NDELT
  805 FORMAT(2(5X,I4))
      DO 806 I=1,NDELT
      Y(I)=AFXI*ETA(I)/(RHO(IY)*UE)
      THETAR(I)=(TO(I)-TW)/(TINF-TW)
      WRITE(7,807)Y(I),THETAR(I)
  806 CONTINUE
  807 FORMAT(2(5X,E13.6))
      GO TO 399
      WRITE(6,400)
  400 FORMAT(/T5,"Y(M)",T24,"THETA",T36,"T/TINF",T51,"TEMP",T50,
     *"TEMPO",/)
      DO 401 I=1,IY
      Y(I)=FXI*ETA(I)/(RHO(IY)*UE)
      WRITE(6,402)Y(I),THETAR(I),G(NC,I),T(I),TO(I)
  401 CONTINUE
  402 FORMAT(5(3X,D13.6))
  399 CONTINUE
      RETURN
      END
C
C     ******************************************************************
      SUBROUTINE GVHO1(H,K,IY,ETA)
C     ******************************************************************

C     PROGRAM TO CALCULATE ETA FOR MAIN
      REAL H,F,FM1,S
      REAL ETA(100)
      IM1=I-1
      ETA(1)=0.00
      IF(I.EQ.1.00)GO TO 20
      DO 1 I=2,IY
      J=I-1
      S=F**J-1.00
      ETA(I)=H*S/FM1
    1 CONTINUE
      GO TO 30
   20 DO 40 I=2,IY
      J=I-1
      ETA(I)=ETA(J)+H
   40 CONTINUE
   30 CONTINUE
      RETURN
      END
C
C     ******************************************************************
      SUBROUTINE GVHO2(H,I,G1,B1,C1,D1,E1,F1,X1,X2,X3,X4,X5,X6)
C     ******************************************************************
C     PROGRAM TO CALCULATE THE CONSTANTS REQUIRED IN SETTING UP THE
C     MATRIX A
```

```
      REAL M,K,A1,B1,C1,D1,E1,F1,G1,H1,I1,J1,F1,K1M,KP1,H2,H3
      REAL X1,X2,X3,X4,X5,X6
C
      K1M=1.0-K
      KP1=1.0+K
      H2=KP1**2.00
      H3=H**3.00
C
      A1=-1.0/(H*KP1)
      B1=(1.0M*K)/H
      C1=K/(H*KP1)
C
      D1=2.00*(1.0**4.0)/(H2*KP1)
      E1=-4.00*(1.0**3.0)/H2
      F1=2.00*(1.0**3.0)/(H2*KP1)
C
      G1=-3.00*K**3.00/(H3*K.2)
      H1=2.00*(1.0**3.00+K**3.00-1.00)*K**5.00/(H3*KP1)
      I1=-3.0**5.00/K.2+(1.0M*1.00/K2
      I1=2.00*I1**3.00/H3
      J1=2.00*(-1.0M*K**2.00-1.00)*K**2.00/(H3*KP1)
      F1=2.00*K**2.00/(H2*K2)
      X1=2.00*K**6.00/(H2*KP1)
      X2=-2.00*K**5.00/H2
      X3=2.00*K**5.00/(H2*KP1)
      X4=2.00*K**4/(H2*KP1)
      X5=-2.00*K**4/H2
      X6=2.00*K**4/(H2*KP1)
      RETURN
      END
C
C     ******************************************************************
      SUBROUTINE OVHOS(X,DUDX,UEQ,UE,BETA,NC,PP,AF,TAU,RHO,MU,VW1,USTR,
     *VWP,VW,IY)
C     ******************************************************************
C     PROGRAM TO CALCULATE UE,BETA,VW,PP,AF,USTR,AND VWP
C
      REAL DUDX,UEQ,UE,BETA,PP,AF,TAU,VW1,VW,USTR,NU,USTR3,
     *VWP,PEW
      REAL X(60)
      REAL RHO(100),MU(100)
      REAL AP1,AP2
      UE=X(NC)*DUDX+UEQ
      BETA=1.0-(UE/UEQ)**2.0
      USTR=SQRT(TAU/RHO(IY))**0.50
      PP=UE*DUDX*MU(IY)/(RHO(IY)*USTR**3.0)
      IF(X(NC).GE.0.727.AND.X(NC).LT.1.08)GO TO 1
      VW=0.00
      VWP=0.00
      AP1=1.00-11.80*PP
      AF=25.0/SQRT(AP1)
      WRITE(6,100)M,PP,AF,USTR UE
  100 FORMAT(/5X,"M=",I4,2X,"PP=",D13.6,2X,"AF=",D13.6,2X,"USTR=",
     *D13.6,2X,"UE=",D13.6,/5X,"FROM OVHOS",)
      GO TO 2
    1 VW VW1
      VWP=VW/USTR
      PEW=EXP(11.80*VWP)
      AP2=-PP*(1.M 1.00)/VWP+PEW
      AF=25.00/SQRT(AP2)
    2 RETURN
      END
```

```
C
C     ******************************************************************
      SUBROUTINE GVHO4(ETA,TAU,FL,MU,RHO,P,FD,IY,DUDX,VW,NC,FDD,NDEL,
     *UE,PP,AP,XI,USTR,DSTR,EDEL,DEL,FD)
C     ******************************************************************
C     PROGRAM TO GENERATE INITIAL VELOCITY PROFILES
C
      REAL SR4
      REAL TAU,FL,DUDX,VW,USTR,UE,PP,AP,NU,FXI,AFXI,SR2,SR1,
     *SR3,UE,FDD,DSTR(4),DIFS1,TEMP,EDEL
      REAL MU(100),RHO(100)
      REAL ETA(100),YP(100),UP(100),FD(100),P(4,100),PD(4,100),
     *G(100),P(100),Y(100)
      REAL XI(50)
      REAL PEW
      REAL DEL
C
      USTR=MU(IY)*FDD*UE*UE*0.50*(2.00/XI(NC))**0.50
      USTR=USTR**0.50
      NUINF=MU(IY)/RHO(IY)
      FXI=(2.0*XI(NC))**0.50
      AFXI=FXI*USTR/(MU(IY)*UE)
      DO 1 I=1,IY
      YP(I)=AFXI*ETA(I)
    1 CONTINUE
C
      G(1)=1.00
      DO 2 I=2,IY
      SR2=YP(I)/AP
      IF(SR2.LT.0.01)GO TO 300
      PEW=0.00
      IF(SR2.LT.100)PEW=1.0/EXP(SR2)
      SR4=1.0-PEW
      GO TO 301
  300 SR4=0.00
  301 SR1=2.0*FL*YP(I)*SR4
      SR3=SR1**2.00
      G(I)=2.00/(1.00+SQRT(1.00+SR3))
    2 CONTINUE
C
C
C     INTEGRATION
      UP(1)=0.00
      DO 3 I=2,IY
      J=I-1
      UP(I)=(G(I)+G(J))*(YP(I)-YP(J))/2.00 UP(J)
    3 CONTINUE
      USE=USTR/UE
      DO 4 I=1,IY
      FD(I)=UP(I)*USE
    4 CONTINUE
C     DETERMINE EDGE OF BOUNDARY LAYER
      NDEL=0
    8 NDEL=NDEL+1
      DIFS1=1.00-FD(NDEL)
      IF(DIFS1.LT.0.0001)GO TO 9
      IF(NDEL.EQ.IY)GO TO 9
      GO TO 8
    9 ND2=NDEL
      DO 41 I=ND2,IY
      FD(I)=1.00
   41 CONTINUE
```

```
C
C     INTEGRATE TO OBTAIN F
      F(1)=0.00
      DO 5 I=2,IY
      J=I-1
      F(I)=(FD(I)+FD(J))*(ETA(I)-ETA(J))/2.00+F(J)
    5 CONTINUE
C
C     GENERATE P AND PD
      DO 6 I=1,IY
      P(NC,I)=F(I)-ETA(I)
    6 CONTINUE
      DO 7 I=1,IY
      PD(NC,I)=FD(I)-1.00
    7 CONTINUE
C
C     CALCULATE DSTR
      TEMP=0.00
      DO 10 I=2,NDEL
      J=I-1
      TEMP=TEMP+(FD(NC,I)+PD(NC,J))*(ETA(I)-ETA(J))/2.00
   10 CONTINUE
      DSTR(NC)=-FXI*TEMP/(RHO(IY)*UE)
      EDEL=ETA(NDEL)
      DEL=FXI*EDEL/(RHO(IY)*UE)
      WRITE(6,500)
  500 FORMAT(//T6,"Y(M)",T24,"F",T40,"PD",T55,"U/UE",/)
      DO 502 I=1,NDEL
      Y(I)=FXI*ETA(I)/(RHO(IY)*UE)
      WRITE(6,501)Y(I),P(NC,I),FD(NC,I),FD(I)
  502 CONTINUE
  501 FORMAT(4(3X,D13.6))
  499 CONTINUE
      RETURN
      END
C
C     ******************************************************************
      SUBROUTINE GVHOS(G,GD,K,H,IY,NC,ETA)
C     ******************************************************************
C     GENERAL DIFFERENTIATION PROGRAM
      REAL G(4,100),GD(4,100),I
      REAL ETA(100)
      REAL H,KIM,FP1,AS,BS,CS
C
      N1=NC
      KIM=1.00-K
      FP1=K+1.00
      IYM1=IY-1
      AS=-1.**3.00/(H*FP1)
      BS=(1.-KIM)/H
      CS=-1./(H*FP1)
C
      DO 1 I=2,IYM1
      GD(N1,I)=(AS*G(N1,I-1)+BS*G(N1,I)+CS*G(N1,I+1))/(1.**[
    1 CONTINUE
C     TO OBTAIN GD(N1,1) AND GD(N1,IY) A FIRST ORDER POLYNOMIAL FIT IS
C     USED
C
      GD(N1,1)=-G(N1,1)*(1.+2.00)+G(N1,2)*FP1*FP1-G(N1,3)
      GD(N1,I)=GD(N1,1)/(H*(FP1)
C
      IYM2=IY-2
      GD(N1,IY)=FP1*GD(N1,IYM1)-1.*GD(N1,IYM2)
```

```
C
C     INTEGRATE TO OBTAIN F
      F(1)=0.00
      DO 5 I=2,IY
      J=I-1
      F(I)=(FD(I)+FD(J))*(ETA(I)-ETA(J))/2.00+F(J)
    5 CONTINUE
C
C     GENERATE F AND FD
      DO 6 I=1,IY
      F(NC,I)=F(I)-ETA(I)
    6 CONTINUE
      DO 7 I=1,IY
      FD(NC,I)=FD(I)-1.00
    7 CONTINUE
C
C     CALCULATE DSTR
      TEMP=0.00
      DO 10 I=2,NDEL
      J=I-1
      TEMP=TEMP+(FD(NC,I)+FD(NC,J))*(ETA(I)-ETA(J))/2.00
   10 CONTINUE
      DSTR(NC)=-FXI*TEMP/(RHO(IY)*UE)
      EDEL=ETA(NDEL)
      DEL=FXI*EDEL/(RHO(IY)*UE)
      WRITE(6,500)
  500 FORMAT(//T6,"Y(M)",T24,"F",T40,"PD",T55,"U/UE",/)
      DO 502 I=1,NDEL
      Y(I)=FXI*ETA(I)/(RHO(IY)*UE)
      WRITE(6,501)Y(I),F(NC,I),FD(NC,I),FD(I)
  502 CONTINUE
  501 FORMAT(4(3X,D13.6))
  499 CONTINUE
      RETURN
      END
C
C     ******************************************************************
      SUBROUTINE GVH05(G,GD,K,H,IY,NC,ETA)
C     ******************************************************************
C     GENERAL DIFFERENTIATION PROGRAM
      REAL G(4,100),GD(4,100),K
      REAL ETA(100)
      REAL H,KIM,KP1,AS,BS,CS
C
      N1=NC
      KIM=1.00-K
      KP1=K+1.00
      IYM1=IY-1
      AS=-K**3.00/(H*KP1)
      BS=-KIM*K/H
      CS=K/(H*KP1)
C
      DO 1 I=2,IYM1
      GD(N1,I)=(AS*G(N1,I-1)+BS*G(N1,I)+CS*G(N1,I+1))/K**I
    1 CONTINUE
C     TO OBTAIN GD(N1,1) AND GD(N1,IY) A FIRST ORDER POLYNOMIAL FIT IS
C     USED
C
      GD(N1,1)=-G(N1,1)*K*(K+2.00)+G(N1,2)*KP1*KP1-G(N1,3)
      GD(N1,1)=GD(N1,1)/(H*K*KP1)
C
      IYM2=IY-2
      GD(N1,IY)=KP1*GD(N1,IYM1)-K*GD(N1,IYM2)
```

```
      THETA(J)=(TO(J)-TW)/(TINF-TW)
    7 CONTINUE
      T(1)=TW
      TO(1)=TW
      T(IY)=TINFS
      TO(IY)=TINF
C     DETERMINE EDGE OF BOUNDARY LAYER
      NDELT=0
    8 NDELT=NDELT+1
      DIFS1=1.00-THETA(NDELT)
      DIFS1=ABS(DIFS1)
      IF(DIFS1.LT.0.001)GO TO 9
      IF(NDELT.EQ.IY)GO TO 9
      GO TO 8
    9 CONTINUE
      DO 10 I=NDELT,IY
      G(NC,I)=1.00
      T(I)=TINF
      TO(I)=TINF
   10 CONTINUE
      AF=2.0*XI(NC)
      FXI=SQRT(AF)
      EDELT=ETA(NDELT)
      DELT=FXI*EDELT/(RHO(IY)*UE)

      AFXI=FXI/(RHO(IY)*UE*DELT)
      WRITE(7,810)NC,NDELT
  810 FORMAT(2(3X,I4))
      DO 811 I=1,NDELT
      Y(I)=FXI*ETA(I)/(RHO(IY)*UE)
      WRITE(7,812)Y(I),THETA(I)
  811 CONTINUE
  812 FORMAT(2(3X,E13.6))
      WRITE(6,   )
      DO 11 J=1,NDELT
      YDELT(J)=FXI*ETA(J)
      Y(J)=FXI*ETA(J)/(RHO(IY)*UE)
      WRITE(6,201)Y(J),G(NC,J),T(J),TO(J)
   11 CONTINUE
  200 FORMAT(/T6,"Y(M)",T24,"T/TINF",T40,"TEMF",T55,"TEMFO",/)
  201 FORMAT(4(3X,D13.6))
  199 CONTINUE
      RETURN
      END
C
C     ******************************************************************
      SUBROUTINE GVHOS(A,A1,B1,C1,D1,E1,F1,X1,X2,X3,X4,X5,X6,XI,NC,K,
     *IY,F,FD,FDD,NEA,NEA1,NITER,BETA,ETA,EP,CDV)
C     ******************************************************************
C     PROGRAM TO CALCULATE THE COEFFICIENT MATRIX A
      REAL  XI(60)
      REAL  A1,B1,C1,D1,E1,F1,X1,X2,X3,X4,X5,X6
      REAL  A(96,5),F(4,100),FD(4,100),FDD(4,100),EP(100)
      REAL  NN,DH1,DH2
      REAL  ,CDV(100)
      REAL  Z1,Z2,Z3,Z4,Z5,Z6,Z7
      REAL  ETA(100)
      REAL  BETA
C
C

      DH1=XI(NC-1)-XI(NC-2)
      DH2=XI(NC  )-XI(NC-1)
      NN=(DH1+2.00*DH2)/(DH2*(DH1+DH2))
```

```
      NT=NCA
      IF(NITER.GT.0)GO TO 10
      NT=NCA1
   10 IE=IY-4

      DO 1 J=1,IE
      I=J+2
      I3=3*I
      A(J,1)=A1*X1*CDV(I-1)*(1.00+EP(I-1))/K**I3
    1 CONTINUE
      DO 2 J=1,IE
      I=J+2
      I3=3*I
      I2=2*I
      Z1=A1*2*CDV(I-1)*(1.00+EP(I-1))/K**I3
      Z2=B1*D1*CDV(I)*(1.00+EP(I))/K**I3
      Z3=D1*(P(NT,I)+ETA(I))/K**I2
      Z4=BETA*A1*(PD(NT,I)+2.00)/K**I
      Z5=2.00*X1(NC)*NN*A1*(PD(NT,I)+1.00)/K**I
      A(J,2)=Z1+Z2+Z3-Z4-Z5
    2 CONTINUE
      DO 3 J=1,IE
      I=J+2
      I3=3*I
      I2=2*I
      Z1=A1*X3*CDV(I-1)*(1.00+EP(I-1))/K**I3
      Z2=B1*E1*CDV(I)*(1.00+EP(I))/K**I3
      Z3=C1*X4*CDV(I+1)*(1.00+EP(I+1))/K**I3
      Z4=E1*(P(NT,I)+ETA(I))/K**I2
      Z5=BETA*D1*(PD(NT,I)+2.00)/K**I
      Z6=2.00*X1(NC)*(PD(NT,I)+1.00)*NN*B1/K**I
      Z7=2.00*X1(NC)*PD(NT,I)*NN
      A(J,3)=Z1+Z2+Z3+Z4-Z5-Z6+Z7
    3 CONTINUE
      DO 4 I=1,IE
      I=J+2
      I3=3*I
      I2=2*I
      Z1=B1*F1*CDV(I)*(1.00+EP(I))/K**I3
      Z2=C1*X5*CDV(I+1)*(1.00+EP(I+1))/K**I3
      Z3=F1*(P(NT,I)+ETA(I))/K**I2
      Z4=BETA*C1*(PD(NT,I)+2.00)/K**I
      Z5=2.00*X1(NC)*C1*NN*(PD(NT,I)+1.00)/K**I
      A(J,4)=Z1+Z2+Z3-Z4-Z5
    4 CONTINUE
      DO 5 I=1,IE
      I=J+2
      I3=3*I
      A(J,5)=C1*X6*CDV(I+1)*(1.00+EP(I+1))/K**I3
    5 CONTINUE
      RETURN
      END
C
C     ******************************************************************
      SUBROUTINE GVARS(XI,ETA,PDD,KNO,MU,AP,DEL,EF,NC,NCA,DSTR,II,NCA1,
     *NCA2,NE,NITER,IY,X,TAU,FRT)
C     ******************************************************************
C     PROGRAM TO CALCULATE EPSI THROUGHOUT ETA RANGE
C
      REAL II,FUNC1,FUNC2,FUNC3,FUNC4,FUNC5
      REAL TAU,FRT(100),YF(100)
      REAL X(60)
      REAL EFXI
```

```
      REAL EDEL
      REAL XI(60)
      REAL ETA(100),FDD(4,100),EPI(100),EF(100)
      REAL MU(100),MP(100),AF,DEL,DSTR(4),UE,T1,DIFS1,FXI,T2
      NT=NCA
      FXI=(2.00*XI(NC))**0.50
      IF(NITER.GT.0)GO TO 1
      NT=NCA1
    1 EDEL=FRO(IY)*UE*DEL/FXI
      IF(X(NC).LT.0.0)GO TO 300
      FUNC3=0.0
      DO 10 I=2,IY
      FUNC1=(RHO(IY)/RHO(I)+RHO(IY)/RHO(I-1))/2.0
      FUNC2=ETA(I)-ETA(I-1)
      FUNC3=FUNC3+FUNC1*FUNC2
   10 CONTINUE
      FUNC4=0.0
      DO 2 I=1,IY
      IF(ETA(I).LE.0.000001)GO TO 400
      FUNC4=FUNC4+((RHO(IY)/RHO(I)+RHO(IY)/RHO(I-1))/2.0)*(ETA(I)-
     *ETA(I-1))
      T1=1.00+5.5*(FUNC4/FUNC3)**6
      GO TO 401
  400 T1=1.00
  401 FDD(I)=((0.0168*UE*DSTR(NT))/T1)*(RHO(I)/MU(I))
    2 CONTINUE
      EPI(1)=0.00
      WRITE(6,9999)FDD(NT,1),NITER,DSTR(NT)
      IF(FDD(NT,1).LT.0.00)STOP
 9999 FORMAT(/T5,"FDD(NT,1)=",D13.6,"  AND NITER=",I4," AND DSTR(NT)="
     *,D13.6,/)
      I=1
      FUNC5=0.0
    3 I=I+1
      FUNC5=FUNC5+((RHO(IY)/RHO(I)+RHO(IY)/RHO(I-1))/2.0)*
     *(ETA(I)-ETA(I-1))
      BFXI=((FXI*FDD(NT,1)*RHO(1)*MU(1)/RHO(I))**0.5)/AF
      T1=-(RHO(I)*FUNC5*BFXI)/(MU(IY)*RHO(IY))
      T2=1.00
      IF(T1.GT.-50.00)T2=1.00-EXP(T1)
      EPI(I)=(0.4*FUNC5*T2)**2.0*(RHO(IY)/RHO(I))*FXI*FDD(NT,I)/MU(I)
      DIFS1=EP(I)-EPI(I)
      IF(DIFS1.LT.0.00)GO TO 4
      IF(I.EQ.IY)GO TO 4
      GO TO 3
    4 DO 5 J=1,I
      EP(J)=EPI(J)
    5 CONTINUE
      WRITE(6,10000)I

10000 FORMAT(/T10,"THE MATCHING POINT FOR EPSI WAS AT",I4,)
      GO TO 301
  300 DO 6 I=1,
      EP(I)=0.00
    6 CONTINUE
  301 CONTINUE
C     CALCULATION OF TURBULENT PRANDTL NO.
      DO 7 I=1,IY
      YP(I)=(FXI*ETA(I)*((TAU/RHO(I))**0.5))/(RHO(IY)*UE*MU(IY))
      PRT(I)=1.43-0.17*(YP(I)**0.25)
      IF(PRT(I).LT.0.86)PRT(I)=0.86
    7 CONTINUE
      RETURN
```

```
      END
C
C     ******************************************************************
      SUBROUTINE GVH09(X1,F,FD,FDD,NCA,NCA1,NCA2,NC,IY,NITER,B,RHO,
     *BETA)
C     ******************************************************************
C     PROGRAM TO CALCULATE VECTOR B
C
      REAL LL,MM,DH1,DH2,T1,T2,T3,FX,T4,BETA
      REAL X1(60)
      REAL F(4,100),FD(4,100),FDD(4,100),B(96,1),RHO(100)
      FX=2.00*X1(NC)
      NT=NCA
      IF(NITER.GT.0)GO TO 10
      NT=NCA1
   10 IE=IY-4
      DH1=X1(NC-1)-X1(NC-2)
      DH2=X1(NC)-X1(NC-1)
      LL=DH2/(DH1*(DH1+DH2))
      MM=-(DH1+DH2)/(DH1*DH2)
      DO 1 J=1,IE
      I=J+2
      T1=LL*FD(NCA2,I)+MM*FD(NCA1,I)
      T2=(FD(NT,I)+1.00)*T1
      T3=LL*F(NCA2,I)+MM*F(NCA1,I)
      T4=FDD(NT,I)*T3
      B(J,1)=FX*(T2-T4)-BETA*(RHO(IY)/RHO(I)-1.0)
    1 CONTINUE
      RETURN
      END
C
C     ******************************************************************
      SUBROUTINE GVH10(B,F,IY)
C     ******************************************************************
C     PROGRAM TO WRITE B AS F
      REAL B(96,1),F(4,100)
      IE=IY-4
      DO 1 J=1,IE
      I=J+2
      F(4,I)=B(J,1)
    1 CONTINUE
C
C     FIND F(4,IY-1) AND F(4,IY)
      F(4,IY-1)=F(4,IY-2)
      F(4,IY)=F(4,IY-2)
C
      RETURN
      END
C
C     ******************************************************************
      SUBROUTINE GVH11(F,FD,I,H,IY)
C     ******************************************************************
C     PROGRAM TO CALCULATE FD, WITH BOUNDARY CONDITIONS
      REAL F(4,100),FD(4,100)
      REAL I,H,TA,TB,TC,I1,FI,IM
      FD(4,1)=-1.00
      FI=I+1.00
      IM=1.00 I
      IYM1=IY-1
      TA=-1.**3.00/(H*FI)
      TB=-(IM*I/H
      TC=F/(H*FI)
      DO 1 I=2,IYM1
```

```
      I1=I+1
      FD(4,I)=P(4,I-1)*TA/(1+P(4,I)*TB/K1+P(4,I+1)*TC/(1
    1 CONTINUE
      FD(4,IY)=0.00
      RETURN
      END
C
C     ******************************************************************
      SUBROUTINE GVH12(P,ETA,FD,FDD,H,IY)
C     ******************************************************************
C     PROGRAM TO CALCULATE FDD FROM P
C
      REAL P(4,100),H2,D1,D2,D3,D4,D5,D6,D7
      REAL FD(4,100),FDD(4,100),ETA(100),I
      REAL H,T1A,T2A,T3A,I1,F
      REAL KP1,K1M
      IYM1=IY-1
      KP1=1.00+1
      K1M=1.00-1
      T1A=-1.**3.00/(H*KP1)
      T2A=-K1M*KP1/H
      T3A=1./(H*KP1)
      DO 1 I=2,IYM1
      I1=I+1
      FDD(4,I)=(FD(4,I-1)*T1A+FD(4,I)*T2A+FD(4,I+1)*T3A)/K1
    1 CONTINUE
      D1=(FD(4,1)-FD(4,2))/(ETA(1)-ETA(2))
      D2=(FD(4,2)-FD(4,3))/(ETA(2)-ETA(3))
      D3=(D1-D2)/(ETA(1)-ETA(3))
      FDD(4,1)=D1+D3*(ETA(1)-ETA(2))
      IYM2=IY-2
      KF=K**IYM2
      FDD(4,IY)=(FD(4,IY)-FD(4,IYM1))/(KF*H)
      RETURN
      END
C     ******************************************************************
      SUBROUTINE GVH13(FD,NDEL,ETA,EDEL,IY)
C     ******************************************************************
C     PROGRAM TO ESTABLISH EDGE OF BOUNDARY LAYER
C     !
      REAL FD(4,100),ETA(100)
      REAL DIFS3,EDEL
      NDEL=0
    1 NDEL=NDEL+1
      DIFS3=ABS(FD(4,NDEL))
      IF(DIFS3.LT.0.0001)GO TO 2
      IF(NDEL.EQ.IY)GO TO 2
      GO TO 1
    2 EDEL=ETA(NDEL)
      WRITE(6,100)EDEL,NDEL
  100 FORMAT(/T5,"FROM GVH13, EDEL=",D13.6,"       AND NDEL=",I4,/)
      RETURN
      END
C
C     ******************************************************************
      SUBROUTINE GVH14(FD,XI,RHO,UE,NDEL,K,H,DSTR,MC,ETA,IY)
C     ********** ******************************************************
C     PROGRAM TO CALCULATE DEL STAR
      REAL FD(4,100),ETA(100)
      REAL RHO(100),UE,I,H,DSTR(4),ATP,FXI
      REAL XI(60)
C
      ATP=0.00
```

```
      DO 1 I=2,NDEL
      JM1=I-1
      ATP=ATP+((RHO(IY)*FD(4,I)/RHO(I))+(RHO(IY)*FD(4,J)/RHO(J)))*
     *(ETA(I)-ETA(J))/2.00
    1 CONTINUE
      FXI=(2.00*X(NC))**0.50
      DSTR(4)=-FXI*ATP/(RHO(IY)*UE)
      RETURN
      END
C
C     ******************************************************************

      SUBROUTINE GVH15(F,FD,FDD,DSTR,NCA,IY)
C     ******************************************************************
C     PROGRAM TO WRITE THE PRESENT ITERATION INTO THE PRESENT STATION
C     ******************************************************************
      REAL F(4,100),FD(4,100),FDD(4,100),DSTR(4)
      DO 1 I=1,IY
      F(NCA,I)=F(4,I)
    1 CONTINUE
      DO 2 I=1,IY
      FD(NCA,I)=FD(4,I)
    2 CONTINUE
      DO 3 I=1,IY
      FDD(NCA,I)=FDD(4,I)
    3 CONTINUE
      DSTR(NCA)=DSTR(4)
      RETURN
      END
C     ******************************************************************
      SUBROUTINE GVH16(FD,XI,RHO,UE,NDEL,IY,DSTR,TTA,NC,ETA,NCA,IY)
C     ******************************************************************
C     PROGRAM TO CALCULATE THETA
      REAL XI(60)
      REAL RHO(100),UE(100),H,DSTR(4),TTA,ATP,T1,T2,FXI
      REAL FD(4,100),ETA(100)
      ATP=0.00
      DO 1 I=2,NDEL
      JM1=I-1
      T1=FD(NCA,I)*(1.00+FD(NCA,I))
      T2=FD(NCA,J)*(1.00+FD(NCA,J))
      ATP=ATP+(T1+T2)*(ETA(I)-ETA(J))/2.00
    1 CONTINUE
      FXI=(XI(NC)*2.00)**0.50
      TTA=FXI*ATP/(RHO(IY)*UE)
      RETURN
      END
C     ******************************************************************
      SUBROUTINE GVH17(F,FD,FDD,IY,NCA,NDEL,CF,UV,FD,USTR,UE,TAU,RX,
     *RTTA,EDEL,Y,YOTTA,YODEL,RHO,MU,XI,ETA,X,NC,EDEL,DEL,TTA)
C     ******************************************************************
C     PROGRAM TO CALCULATE VARIABLES PRIOR TO PRINTING
      REAL F(4,100),FD(4,100),FDD(4,100),UV(100),Y(100),
     *YOTTA(100),YODEL(100),XI(60),X(20)
      REAL CF,USTR,DSTR(4),UE,TAU,RX,RTTA,RDEL,EDEL,DEL,TTA,FXI
      REAL ETA(100),FD(100),RHO(100),MU(100)
      FXI=(XI(NC)*2.00)**0.5
      CF=MU(IY)*(2.00/XI(NC))**0.50*FDD(NCA,1)
      TAU=CF*RHO(IY)*UE*UE/2.00
      USTR=SQRT(TAU/RHO(IY))**0.50
      DO 1 I=1,IY
      Y(I)=FXI*ETA(I)/(RHO(IY)*UE)
```

```
    1 CONTINUE
      DEL=Y(IY)/DEL
      RX=RHO(IY)*UE*X(NC)/MU(IY)
      RDEL=RHO(IY)*UE*DEL/MU(IY)
      RTTA=RHO(IY)*UE*TTA/MU(IY)
C
      DO 2 I=1,IY
      FD(I)=FD(NCA,I)*1.00
    2 CONTINUE
      DO 3 I=1,IY
      UV(I)=FD(I)*UE
    3 CONTINUE
      IF(DEL.LT.0.1E-5)GO TO 6
      DO 4 I=1,IY
      YODEL(I)=Y(I)/DEL
    4 CONTINUE
    6 CONTINUE
      DO 5 I=1,IY
      YOTA(I)=Y(I)/TTA
    5 CONTINUE
      RETURN
      END
C     ***************************************************************
      SUBROUTINE AAZM(AA,B,N)
C     ***************************************************************
      IMPLICIT REAL (A-H,O-Z)
      DIMENSION A(96,97),X(96),AA(96,5),B(96,1)
      JJJ=N+1
      NP1=N+1
      DO 1 I=1,N
      DO 2 J=1,N
      A(I,J)=0.00
    2 CONTINUE
    1 CONTINUE
      J=3
      DO 1000 I=1,3
      A(I,1)=AA(I,J)
      J=J-1
 1000 CONTINUE
C
      J=4
      DO 1001 I=1,4
      A(I,2)=AA(I,J)
      J=J-1
 1001 CONTINUE
C
      NM4=N-4
      DO 1002 IS=1,NM4
      J=5
      JJ=IS+2
      IT=IS+4
      DO 1003 I=IS,IT
      A(I,JJ)=AA(I,J)
      J=J-1
 1003 CONTINUE
 1002 CONTINUE
C
      J=5
      NM3=N-3
      NM1=N-1
      DO 1004 I=NM3,N
      A(I,NM1)=AA(I,J)
      J=J-1
```

```
 1001 CONTINUE
      N=5
      NM2=N-2
      DO 1005 I=NM2,N
      A(I,N)=AA(I,J)
      J=J+1
 1005 CONTINUE
      DO 1006 I=1,N
      A(I,NP1)=B(I,1)
 1006 CONTINUE
      M7=1
      N=JJ1-1
      IF(N.LE.0)STOP
      DET=1.00
      L=N-1
      NP=N+1
      DO 36 I=1,L
      M=I+1
      ADD=ABS(A(I,I))
      IR=I
      DO 38 I=M,N
      ATT=ABS(A(I,I))
      IF(ADD-ATT)37,38,38
   37 ADD=ATT
      IR=I
   38 CONTINUE
      IF(IR-I)39,41,39
   39 DET=-DET
      DO 40 J=I,NP
      S=A(IR,J)
      A(IR,J)=A(K,J)
   40 A(K,J)=S
   41 DO 44 I=M,N
      IF(A(I,I),EQ.0.00)GO TO 36
      S=A(I,K)/A(K,K)
      DO 45 J=M,NP
77
      A(I,J)=A(I,J)-S*A(K,J)
   45 CONTINUE
   44 CONTINUE
   36 CONTINUE
      X(N)=A(N,NP)/A(N,N)
      DO 43 I=1,L
      K=N-I
      M=K+1
      S=0.00
      DO 42 J=M,N
   42 S=S+A(K,J)*X(J)
      X(K)=(A(K,NP)-S)/A(K,K)
   43 CONTINUE
      IF(M7.LE.0)GO TO 30
   30 CONTINUE
      DO 1007 I=1,N
      B(I,1)=X(I)
 1007 CONTINUE
      RETURN
      END
C
C     ******************************************************************
      SUBROUTINE GVNIB(R,A1,B1,C1,D1,E1,F1,X1,NP,N,IY,F,PD,NCA,NCA1,
     *FF,FR,FRT,CDV,NCAC,ETA)
C     ******************************************************************
C     PROGRAM TO CALCULATE THE COEFFICIENT MATRIX R
```

```
C
      REAL X1(60)
      REAL A1,B1,C1,D1,E1,F1
      REAL R(300,3),P(4,100),PD(4,100),EP(100),PR(100),CDV(100)
      REAL I,PRT
      REAL Z1,Z2,Z3,Z4,Z5,Z6
      REAL ETA(100)
      REAL DH1,DH2,LL,MM,NN
C
      DH1=X1(NA-1)-X1(NA-2)
      DH2=X1(NC)-X1(NC-1)
      LL=DH2/(DH1*(DH1+DH2))
      MM=-(DH1+DH2)/(DH1*DH2)
      NN=((DH1+2.0*DH2)/(DH2*(DH1+DH2))
      NT=NA-1
    1 IF=IY-2
      DO 2 J=1,IF
      I=J+1
      I2=2*I
      Z1=(CDV(I)/PR(I))*(1.0+(EP(I)*PR(I))/PRT)*(D1+A1*B1)/K**I2
      Z2=(CDV(I-1)/PR(I-1))*(1.0+(EP(I-1)*PR(I-1))/PRT)*A1*A1/K**I2
      Z3=(CDV(I+1)/PR(I+1))*(1.0+(EP(I+1)*PR(I+1))/PRT)*B1*C1/K**I2
      Z4=(P(NT,I)+ETA(I))*A1/K**I
      Z5=(LL*P(NCA2,I)+MM*P(NCA1,I)+NN*P(NT,I))*A1*2.0*X1(NC)/K**I
      R(J,1)=Z1+Z2+Z3+Z4+Z5
    2 CONTINUE
      DO 3 J=1,IF
      I=J+1
      I2=2*I
      Z1=(CDV(I)/PR(I))*(1.0+(EP(I)*PR(I))/PRT)*(E1+B1*D1)/K**I2
      Z2=(CDV(I-1)/PR(I-1))*(1.0+(EP(I-1)*PR(I-1))/PRT)*B1*A1/K**I2
      Z3=(CDV(I+1)/PR(I+1))*(1.0+(EP(I+1)*PR(I+1))/PRT)*B1*C1/K**I2
      Z4=(P(NT,I)+ETA(I))*B1/K**I
      Z5=(LL*P(NCA2,I)+MM*P(NCA1,I)+NN*P(NT,I))*B1*2.0*X1(NC)/K**I
      Z6=2.00*X1(NC)*NN*(P1(NT,I)+1.00)
      R(J,2)=Z1+Z2+Z3+Z4+Z5-Z6
    3 CONTINUE
      DO 4 J=1,IF
      I=J+1
      I2=2*I
      Z1=(CDV(I)/PR(I))*(1.0+(EP(I)*PR(I))/PRT)*(F1+C1*B1)/K**I2
      Z2=(CDV(I-1)/PR(I-1))*(1.0+(EP(I-1)*PR(I-1))/PRT)*C1*A1/K**I2
      Z3=(CDV(I+1)/PR(I+1))*(1.0+(EP(I+1)*PR(I+1))/PRT)*C1*C1/K**I2
      Z4=(P(NT,I)+ETA(I))*C1/K**I
      Z5=(LL*P(NCA2,I)+MM*P(NCA1,I)+NN*P(NT,I))*C1*2.0*X1(NC)/K**I
      R(J,3)=Z1+Z2+Z3+Z4+Z5
    4 CONTINUE
      RETURN
      END
C
C     ******************************************************************
      SUBROUTINE GVH19(X1,PD,PDD,NCA,NCA1,NCA2,NC,IY,G,G,A1,B1,F1,CDV,
     *DE,TINF,PR,I,CF)
C     ******************************************************************
C     PROGRAM TO CALCULATE VECTOR G
C
      REAL X1(60),CP(100)
      REAL G(4,100),G(9a,1),PDD(4,100),PD(4,100),CDV(100),PR(100)
      REAL LL,MM,A1,B1,C1,K
      REAL NC,TINF,I1,I2,T3,T4,HINF,FX,DH1,DH2
C
      FX=2.00*X1(NC)
      NT=NCA
```

```
    1 IF(IY-
      DH1=X(NC-1)-X(NC-2)
      DH2=X(NC)-X(NC-1)
      LL=DH2/(DH1*(DH1+DH2))
      MM=-(DH1+DH2)/(DH1*DH2)
      NINF=IP(IY)*INF
      DO 2 J=1,IP
      I=I+1
      T1=(FD(NT,I)+1.0)*(LL*G(NCA2,I)+MM*G(NCA1,I))
      T2=A1*CDV(I-1)*(1.0-(1.0/PR(I-1)))*(PD(NT,I-1)+1.0)*PDD(NT,I-1)
      T3=B1*CDV(I)*(1.0-(1.0/PR(I)))*(PD(NT,I)+1.0)*PDD(NT,I)
      T4=C1*CDV(I+1)*(1.0-(1.0/PR(I+1)))*(PD(NT,I+1)+1.0)*PDD(NT,I+1)
      Q(J,1)=EX*(1-((UE*UE)/NINF)*(T2+T3+T4)/I**I
    2 CONTINUE
      RETURN
      END
C
C     ******************************************************************
      SUBROUTINE RRGG(RR,Q,NM)
C     ******************************************************************
C
      IMPLICIT REAL (A-H,O-Z)
      DIMENSION R(98,99),X(98),RR(98,3),Q(98,1)
C
      JJ1=NM+1
      NP1=NM+1
      DO 1 J=1,NM
      DO 2 I=1,NM
      R(I,J)=0.00
    2 CONTINUE
    1 CONTINUE
      J=2
      DO 1000 I=1,2
      R(I,1)=RR(I,J)
      J=J-1
 1000 CONTINUE
C
      NM2=NM-2
      DO 1001 IS=1,NM2
      J=3
      JJ=IS+1
      IT=IS+2
      DO 1002 I=IS,IT
      R(I,JJ)=RR(I,J)
      J=J-1
 1002 CONTINUE
 1001 CONTINUE
      J=3
      NM1=NM-1
      DO 1003 I=NM1,NM
      R(I,NM)=RR(I,J)
      J=J-1
 1003 CONTINUE
C
      DO 1004 I=1,NM
      R(I,NP1)=Q(I,1)
 1004 CONTINUE
C
      GO TO 100
      NM1=NM-1
      DO 10 I=1,NM1

      IP1=I+1
```

```
      IF(R(I,I).EQ.0.00)GO TO 11
      IF(R(IP1,I).EQ.0.00)GO TO 10
      S=R(IP1,I)/R(I,I)
      DO 12 J=I,NP1
      R(IP1,J)=R(IP1,J)-S*R(I,J)
   12 CONTINUE
      GO TO 10
   11 IF(R(IP1,I).EQ.0.00)GO TO 10
      DO 13 J=1,NP1
      S=R(IP1,J)
      R(IP1,J)=R(I,J)
      R(I,J)=S
   13 CONTINUE
   10 CONTINUE
      DO 51 I=1,NM
      IF(R(I,I).EQ.0.00)DET=0.00
   51 CONTINUE
      WRITE(6,52)DET
   52 FORMAT(1X,"DET= ",D13.6)
      X(NM)=R(NM,NP1)/R(NM,NM)
      DO 14 I=1,NM1
      J=NM-I
      IP1=J+1
      S=0.00
      DO 15 L=IP1,NM
      S=S+R(J,L)*X(L)
   15 CONTINUE
      X(J)=(R(J,NP1)-S)/R(J,J)
   14 CONTINUE
      DO 15 I=1,NM
      Q(I,1)=X(I)
   16 CONTINUE
  100 CONTINUE
      DET=1.00
      L=NM-1
      MP=NM+1
      DO 36 I=1,L
      M=I+1
      ADD=ABS(R(I,I))
      IR=I
      DO 38 J=M,NM
      ATT=ABS(R(J,I))
      IF(ADD-ATT)37,38,38
   37 ADD=ATT
      IR=J
   38 CONTINUE
      IF(IR-I)39,41,39
   39 DET=-DET
      DO 40 J=I,NP
      S=R(IR,J)
      R(IR,J)=R(I,J)
   40 R(I,J)=S
   41 DO 44 J=M,NM
      IF(R(I,I).EQ.0.00)GO TO 36
      S=R(J,I)/R(I,I)
      DO 45 K=M,NP
      R(J,K)=R(J,K)-S*R(I,K)
   45 CONTINUE
   44 CONTINUE
   36 CONTINUE
      X(NM)=R(NM,NP)/R(NM,NM)
      DO 47 I=1,L
      J=NM-I
```

```
      M=I+1
      S=0.00
      DO 42 J=M,NM
   42 S=S+R(I,J)*X(J)
      X(I)=(R(I,NP1)-S)/R(I,I)
   43 CONTINUE
      DO 1007 I=1,NM
      Q(I,1)=X(I)
 1007 CONTINUE
      RETURN
      END

C     ******************************************************************
      SUBROUTINE GVH3Q(Q,G,IY,NCA)
C     ******************************************************************
C     PROGRAM TO WRITE Q AS G
C
      REAL Q(98,1),G(4,100)

      IF=IY-1
      DO 1 J=1,IF
      I=J+1
      G(4,I)=Q(J,1)
      G(NCA,I)=G(4,1)
    1 CONTINUE

      G(4,IY)=G(4,IY-1)
      G(NCA,1)=G(4,1)
      RETURN
      END
C
C     ******************************************************************
      SUBROUTINE GVH21(TO,G,IY,T,UV,CP,TINF,THETA,TW)
C     ******************************************************************
C     PROGRAM TO CALCULATE STATIC AND STAGNATION TEMPERATURES
C
      REAL TO(100),T(100),G(4,100),UV(100),CP(100)
      REAL TINF,THETA(100),TW

      DO 1 I=1,IY
      TO(I)=G(4,I)*TINF*CP(IY)/CP(I)
      THETA(I)=(TO(I)-TW)/(TINF-TW)
      T(I)=TO(I)-(UV(I)**2.0)/(2.0*CP(I))
    1 CONTINUE
      RETURN
      END

C     ******************************************************************
      SUBROUTINE GVH22(THETA,NDELT,ETA,EDELT,IY)
C     ******************************************************************
C     PROGRAM TO ESTABLISH EDGE OF BOUNDARY LAYER
C
      REAL THETA(100),ETA(100),DIFS3,EDELT

      NDELT=0
    1 NDELT=NDELT+1
      DIFS3=1.0-ABS(THETA(NDELT))
      IF(DIFS3.LT.0.0001)GO TO 2
      IF(NDELT.EQ.IY)GO TO 2
      GO TO 1
    2 EDELT=ETA(NDELT)
      WRITE(6,101)EDELT,NDELT
  101 FORMAT(/T5,"EDELT=",D13.6,"     AND NDELT=",I4,)
```

```
      RETURN
      END
C
C     ******************************************************************
      SUBROUTINE GVH23(G,MU,UV,TO,RHO,CDV,FR,XI,GW,ST,A1,B1,C1,GWD,K,IY,
     *NC,CF)
C     ******************************************************************
C     PROGRAM TO CALCULATE HEAT TRANSFER RATE TO T . WALL AND
C     DETERMINE THE FLOW STANTON NUMBER
C
      REAL G(4,100),MU(100),UV(100),TO(100),RHO(100),CDV(100),PR(100)
      REAL XI(60),GW,ST,GWD,A1,B1,C1,I,AFXI
      REAL CP(100)
C
      AFXI=SQRT(2.0*XI(NC))
      I=2
      GWD=(A1*G(4,I-1)+B1*G(4,I)+C1*G(4,I+1))/(K**I)
      GW=-(CDV(1)*RHO(IY)*MU(,Y)*UV(IY)*TO(IY)*CP(IY)*GWD)/(FR(1)*AFXI)
      ST=-GW/(RHO(IY)*UV(!Y)*(CF(IY)*TO(IY)-CF(1)*TO(1)))
      WRITE(6,800)GWD,GW,ST
  800 FORMAT(/T6,"GDASHW=",D13.6,"   GW=",D13.6,"  AND ST=",D13.6,/)
      RETURN
      END
```

APPENDIX H

H1 EXPERIMENTAL ERROR ANALYSIS

Table H.1 Experimental Apparatus Accuracy

Apparatus	Accuracy
Hewlett Packard Digital Voltmeter	± 0,001 volt
Disa 55D01 Anemometer Unit (Connected to thermistor)	± 0,01 Ω
Disa 55D01 Anemometer Unit (Connected to hot wire)	Output read on DVM
Disa 55D10 Linearizer Unit	Output read on DVM
NKC Thermometer Unit	± 0,5°C
Furness Digital Manometer	± 0,01 mm H_2O
Van Essen Manometer Model 6750	± 0,002" H_2O
Mercury Manometer	± 0,5 mm Hg

APPENDIX H

H1 EXPERIMENTAL ERROR ANALYSIS

Table H.1 Experimental Apparatus Accuracy

Apparatus	Accuracy
Hewlett Packard Digital Voltmeter	± 0,001 volt
Disa 55D01 Anemometer Unit (Connected to thermistor)	± 0,01 Ω
Disa 55D01 Anemometer Unit (Connected to hot wire)	Output read on DVM
Disa 55D10 Linearizer Unit	Output read on DVM
NKC Thermometer Unit	± 0,5°C
Furness Digital Manometer	± 0,01 mm H_2O
Van Essen Manometer Model 6750	± 0,002" H_2O
Mercury Manometer	± 0,5 mm Hg

Table H.2 Calibration Apparatus Accuracy

Apparatus	Accuracy
Disa 55D44 Pressure Control Unit	± 0,1 mbar
Disa 55D46 Pressure Converter	± 0,1 bar

For the velocity calibration of the hot wire probe use was made of the Disa Calibration rig and the velocity read on the Pressure Converter. The error in velocity can be estimated from the following relationship. (Ref 13)

$$\frac{dv}{v} = \frac{1}{2}\left(\frac{dp}{p} - \frac{d\rho}{\rho}\right) \qquad \ldots \text{ H.1.1}$$

Assuming no error in ρ

V (m/s)	ΔP (bar)	% error
2,0	1,0	5,0
10,0	3,43	1,5
20,0	6,48	0,8

The mainstream velocity measured with the anemometer varied from approximately 5 to 15 m/s giving respective errors of 2,6% and 1%. When considering King's Law which gives the heat flux relationship for the hot wire

$$I^2 R_w = \frac{E_o^2}{R_w} + KU^n \left(T_{hw} - T_a\right) \qquad \ldots \text{ H.1.2}$$

it is noted that the heat flux is proportional to both the flow velocity and temperature. During the velocity calibration the anemometer output is linearized thus accounting for the exponent to the velocity term in the equation above.

The error in temperature can be estimated to be linear as it was calibrated with respect to the thermocouple in the wind tunnel.

V (m/s)	T (°C)	% Error Temp	% Error Vel	Total Error
5,0	45,0	1,1	2,6	3,7
15,0	33,0	1,5	1,0	2,5

Thus the total error, which is estimated to be the sum of the velocity and temperature errors (as indicated by the product of the velocity and temperature terms in H.1.2) is 3,7% for the low velocity which is considered acceptable.

LIST OF REFERENCES

1 BAYLEY F.J., CORNFORTH J.W. and TURNER A.B.
Experiments on a Transpiration Cooled Combustion Chamber.
Journal of Heat and Fluid Flow, Volume 3, No 2, 1973.

2 BAYLEY F.J.and TURNER A.B.
The Transpiration-Cooled Gas Turbine.
Journal of Engineering for Power, October 1970, pp 351 - 358.

3 BRADSHAW P., FERRIS D.H. and ATWELL N.P.
Calculation of Boundary-layer Development using the Turbulent Energy Equation
J Fluid Mechanics 28 part 3, 1967, pp 593 - 616.

4 BUNKER W.W., MOGUL J.M. and WOLF J.C. (Curtis Wright Corporation)
A High Temperature Turbine for Operation on Coal-Derived Fuel.
ASME, 79-GT-173 , 1979.

5 CEBECI T.
Behaviour of Turbulent Flow Near a Porous Wall with Pressure Gradient.
AIAA Journal V8, 12 , 1970, pp 2152 - 2156.

6 CEBECI T. and SMITH A.M.O.
Analysis of Turbulent Boundary Layers.
Academic Press, New York, 1974.

7 CEBECI T. and SMITH A.M.O.
A Finite Difference Method for Calculating Compressible Laminar and Turbulent Boundary Layers.
J of Basic Engineering, Sept. 1970,pp 523 - 535.

8 DUWEZ P. and WHEELER H.L.
Experimental Study of Cooling by Injection of a Fluid Through a Porous Material.
Journal of the Aeronautical Sciences, Vol 15, No. 9.
Sept. 1948.

9 GRIMSON J.
Fluid Dynamics and Heat Transfer.
McGraw - Hill Brook Co., Maidenhead, 1971.

10 HINZE J.O.
Turbulence.
McGraw Hill, New York, 1959 .

11 JENKINS R.
Variation of the Eddy Conductivity with Prandtl Modulus and its use in Prediction of Turbulent Heat Transfer Coefficients.
Inst. Heat Transfer Fluid Mechanics, 1951, pp 147 - 158.

12 KAYS W.M., and MOFFAT R.J.
"Behaviour of Transpired Turbulent Boundary Layers".
Studies in Convection, Theory, Measurement and Applications
Edited by B.E. Launder, Academic Press, 1975.

13 KRIEG M.
An Investigation into Practical Aspects of Transpiration Flows.
Master of Science Dissertation in Engineering, University of the Witwatersrand,1978.

14 KUTATELADZE S.S. and LEONTEV A.J.
Turbulent Boundary Layers in Compressible Gasses.
(Translated by Spalding D.B.)
Edward Arnold Publishers Ltd. London, 1964.

15 MANNING G.B., MOSKOWITZ S. and WOLF J.C. (Curtis Wright Corporation)
Development of a High Temperature Turbine for Operation on Coal-Derived Fuel.
ASME, 80-GT-188, 1980.

16 MICKLEY H.S. and DAVIS R.S.
Momentum Transfer for Flow Over a Flat Plate with Blowing.
NACA TN 4017, 1957.

17 MICKLEY H.S., ROSS R.C., SQUYERS A.C., STEWART W.E.
Heat Mass and Momentum Transfer for Flow Over a Flat Plate with Blowing or Suction.
NACA Technical Note 3208, July 1956.

18 J.C. ROTTA
Temperaturverteilungen in Der Turbulenten Grenzschicht an der Elenen Plate.
Int. Journal of Heat and Mass Transfer, Vol. 7, 1964, pp 215 - 228.

19 RUBESIN M.W.
An Analytical Estimation of the Effect of Transpiration Cooling on the Heat-Transfer and Skin-Friction Characteristics of a Compressible Turbulent Boundary Layer.
NACA TN 3341, 1954.

20 SCHLICHTING H.
Boundary Layer Theory.
Pergamon Press, Oxford, 1979.

21 SIMPSON R.L., WHITTEN D.G. and MOFFAT R.J.
An Experimental Study of the Turbulent Prandtl Number of Air with Injection and Suction.
Int Journal Heat Mass Transfer, Vol. 13, 1970. pp 125 - 143.

22 VAN DRIEST E.R.
Convective Heat Transfer in Gases - Section F -
Turbulent Flows and Heat Transfer - High Speed Aerodynamics
and Jet Propulsion - Volume V (Editor C.C: Lin)
Princeton University Press, 1959.

23 VAN DRIEST E.R.
On Turbulent Flow near a Wall.
J of the Aerospaces Sciences, V. 23,11 1956, pp 1007 - 1011.

24 YUAN S.W. (Editon LIN C.C.)
Cooling by Protective Fluid Films - Section G -
Turbulent Flows and Heat Transfer High Speed Aerodynamics
and Jet Propulsion - Volume V.
Princeton University Press, 1959.

Author Hobson G V
Name of thesis An Investigation into the heat transfer of Transpiration cooling 1982

PUBLISHER:
University of the Witwatersrand, Johannesburg
©2013

LEGAL NOTICES:

Copyright Notice: All materials on the University of the Witwatersrand, Johannesburg Library website are protected by South African copyright law and may not be distributed, transmitted, displayed, or otherwise published in any format, without the prior written permission of the copyright owner.

Disclaimer and Terms of Use: Provided that you maintain all copyright and other notices contained therein, you may download material (one machine readable copy and one print copy per page) for your personal and/or educational non-commercial use only.

The University of the Witwatersrand, Johannesburg, is not responsible for any errors or omissions and excludes any and all liability for any errors in or omissions from the information on the Library website.